Epigenetic Regulation of Muscle Stem and Progenitor Cells

Gregory Charles Addicks

This thesis is submitted as a partial fulfillment of the Ph.D. program in Cellular and Molecular Medicine.

Submitted August 31st 2017

Department of Cellular and Molecular Medicine

Faculty of Medicine

University of Ottawa

Authorization

Regarding the use of material from "Iain W. McKinnell, Jeff Ishibashi, Fabien Le Grand, Vincent J. G. Punch, Gregory C. Addicks, Jack F. Greenblatt, F. Jeffrey Dilworth, and Michael A. Rudnicki. Pax7 activates myogenic genes by recruitment of a histone methyltransferase complex" in Appendix B of this thesis: **No permission is required from the authors or the publishers.**

Author Requests

If you are the author of this content (or his/her designated agent) please read the following. Since 2003, ownership of copyright in in original research articles remains with the Authors*, and provided that, when reproducing the Contribution or extracts from it, the Authors acknowledge first and reference publication in the Journal, the Authors retain the following non-exclusive rights:

a. To reproduce the Contribution in whole or in part in any printed volume (book or thesis) of which they are the author(s).
b. They and any academic institution where they work at the time may reproduce the Contribution for the purpose of course teaching.
c. To reuse figures or tables created by them and contained in the Contribution in other works created by them.
d. To post a copy of the Contribution as accepted for publication after peer review (in Word or Tex format) on the Author's own web site, or the Author's institutional repository, or the Author's funding body's archive, six months after publication of the printed or online edition of the Journal, provided that they also link to the Journal article on Nature Research's web site (eg through the DOI).

Nature Research encourages the self-archiving of the accepted version of your manuscript in your funding agency's or institution's repository, six months after publication. This policy complements the recently announced policies of the US National Institutes of Health, Wellcome Trust and other research funding bodies around the world. Nature Research recognizes the efforts of funding bodies to increase access to the research they fund, and we strongly encourage authors to participate in such efforts.

Authors wishing to use the published version of their article for promotional use or on a web site must request in the normal way.

If you require further assistance please read Nature Research's online author reuse guidelines.

Note: *British Journal of Cancer* maintains copyright polices of its own that are different from the general Nature Research policies. Please consult this journal to learn more.

* Commissioned material is still subject to copyright transfer conditions

Abstract

Epigenetic mechanisms are of fundamental importance for resolving and maintaining cellular identity. The mechanisms regulating muscle stem and progenitor cell identity have ramifications for understanding all aspects of myogenesis. The epigenetic mechanisms regulating muscle stem cells are therefore important aspects for understanding the regulation of muscle regeneration and maintenance.

Important roles for the trithorax H3K4 histone methyltransferase (HMT) MLL1 have been established for early embryogenesis, and for hematopoietic and neural identity. Here, using a conditional *Mll1* knockout (KO), we find that *in vivo*, MLL1 is necessary for efficient muscle regeneration, and for maintenance and proliferation of muscle stem and progenitor cells. Loss of *Mll1* in cultured myoblasts reveals an essential role for expression of the myogenic specification gene Pax7.

Mll1 KO results in a minor decrease in Pax7 mRNA and a strong decrease of Pax7 protein. While MLL1 was found to bind the *Pax7* promoter, *Mll1* KO results in a minor decrease of H3K4me3 at *Pax7*, supporting a recognized non-HMT role for *Mll1* at *Pax7*. Microarray analysis of mRNA expression in *Mll1* KO myoblasts finds that *Myf5* is the most strongly downregulated of all genes, unexpectedly, mRNA expression of previously identified MLL1 targets are unaffected by loss of MLL1 in myoblasts. Pax7 activates *Myf5* expression through recruitment of a H3K4 HMT, and in *Mll1* KO myoblasts expression of, and H3K4me3 at Myf5 is lost. Exogenous Pax7 rescues *Myf5* expression and H3K4me3 at *Myf5* in the absence of MLL1, indicating that *Myf5* expression is conditional on Pax7, but not MLL1.

We also show that *Myf5* DNA is methylated in non-myogenic cells, and in satellite stem cells that have never expressed *Myf5*, but is not methylated in satellite cells that are committed to the myogenic lineage, indicating that demethylation of *Myf5* may be a fundamental step in myogenic commitment. Intriguingly, *Myf5* promoter DNA becomes remethylated in *Mll1* KO myoblasts.

This work finds that *Pax7* expression and myogenic identity is partly dependent on MLL1 expression. Further, evidence is uncovered that myogenic commitment is initiated by demethylation of *Myf5*. These findings add to the understanding of the epigenetic mechanisms that regulate and define muscle stem cells.

Acknowledgements

A long list of mentors has contributed to my development as a scientist. I thank Susan K. Donaldson who, through privilege of association, gave me my first experience in formal science. I especially thank Meg Titus who taught me everything I needed to know to be a “real scientist”. I thank Ren-He Xu and James Thompson for an incredible experience in cutting edge biology. I thank Robert Haché and Ella Atlas for giving me my first opportunity in Canada.

Specifically to this thesis, I especially thank Michael Rudnicki for giving me the opportunity to formally progress beyond technical assistance, and for providing an extraordinary environment within which to do so. Michael also gave me essential insight into many of the things that go into being a remarkably successful scientist, and was always willing to hear my ideas and to share his. Much thanks also to my thesis advisory committee members Jeff Dilworth, David Lohnes, and David Picketts for insightful comments and recommendations.

I want to thank the technical staff of the Rudnicki lab for doing your best at a thankless job, and all of the Rudnicki lab members for existential grounding among other things. I also especially thank Caroline Brun and Marie-Cloud Sincennes for providing an *in vivo* foundation for the role of MLL1 in myogenesis.

Finally, I would like to thank my wife, Jennifer Phillips for her patience, encouragement, and support, and my son, Soren for being a really great little guy.

Table of Contents

Authorization ... ii
Abstract ... iii
Acknowledgements ... v
Table of Contents ... vi
List of Figures ... viii
List of Tables ... ix
List of Abbreviations ... x
Chapter 1. Introduction ... 1
1.1. Skeletal Muscle ... 2
1.2. Embryonic Myogenesis ... 3
1.3. Satellite Cells and Muscle Regeneration ... 6
1.4. Molecular Regulation of Muscle Determination ... 10
1.5. Regulation of Myogenic Regulatory Factor Expression ... 11
1.6. Myogenic Specification by Pax3 and Pax7 ... 13
1.7. Epigenetic Specification of Cellular Identity ... 16
1.8. Regulation of Transcription by Histone Modifications ... 17
1.9. Repressive Histone Modifications ... 20
1.10. Role of DNA Methylation in Regulating Gene Expression ... 21
1.11. Activating or Permissive Histone Modifications ... 22
1.12. Role of MLL1 in Cellular Identity Regulation ... 23
1.13. Role of DNA Methylation in Cell Identity Specification and Differentiation 25
1.14. Epigenetic Regulation of Satellite Cells and Myogenesis ... 27
1.15. Rationale and Objectives ... 29
Chapter 2. Methods ... 30
2.1. Mice and Muscle Injury ... 31
2.2. Image Acquisition ... 31
2.3. Myoblast Isolation and Culture ... 32
2.4. siRNA Knockdown ... 33
2.5. RNA Isolation and Reverse Transcriptase Reaction ... 34
2.6. Real-Time Quantitative PCR of cDNA ... 34
2.7. Microarray Analysis ... 35
2.8. Proliferation Assays ... 36
2.9. Western Blots ... 36
2.10. Western Blot Quantification ... 37
2.11. Immunostaining ... 38
2.12. Chromatin Immunoprecipitation ... 38
2.13. Methyl DNA Immunoprecipitation ... 40
2.14. RT-qPCR and qPCR of ChIP and meDIP DNA ... 41
2.15. Plasmids ... 41
2.16. Virus Production, Infection and Selection ... 42
2.17. Transfection and Selection of Stable Tet-ON Cell Lines ... 43
2.18. Isolation of Satellite Cells with Florescence Activated Cell Sorting ... 43
2.19. Statistical Analysis ... 44

Chapter 3 - Results 45
3.1. siRNA Knockdown of MLL1 Dysregulates *Myf5* and *Pax7* Expression 46
3.2. *Mll1* KO Results in a Regeneration Defect After Muscle Injury 49
3.3. Loss of MLL1 Deters Muscle Fibre Regeneration After Injury 51
3.4. *Mll1* KO Results in Loss of Satellite Cells After Injury 53
3.5. Loss of MLL1 Results in a Strong Proliferation Defect in Primary Myoblasts 54
3.6. *Mll1* KO Results in Specific Changes to Gene Expression 57
3.7. *Mll1* KO Does Not Induce or Effect Induction of Myogenic Differentiation .. 62
3.8. *Mll1* KO Results in Loss of Pax7 Protein Expression 64
3.9. Epigenetic Regulation of *Pax7* in *Mll1* KO Myoblasts 66
3.10. Epigenetic Regulation of *Myf5* in *Mll1* KO Myoblasts 67
3.11. Exogenous Pax7 Rescues *Myf5* Expression in *Mll1* KO Myoblasts 70
3.12. Inducible Pax7 Rescues *Myf5* Expression After Loss of MLL1 71
3.13. Exogenous Pax7 Expression Down-Regulates and Epigenetically Represses Endogenous Pax7 74
3.14. Exogenous Pax7 Rescues Fgfr4 but Not Other Genes in *Mll1* KO 76
3.15. Exogenous Pax7 Rescues *Myf5* Expression in *Mll1*/*Mll2* KO Myoblasts 78
3.16. *Myf5* is Repressed by DNA Methylation in ES Cells and Other Non-Myogenic Cell Types and is Not Methylated in Myoblasts or Myotubes. 80
3.17. Demethylation of the *Myf5* Promoter Marks the Transition from Satellite Stem Cell to Committed Myogenic Cell and Methylation at *Myf5* is Re-Established in *Mll1* KO Myoblasts 83
3.18. Exogenous Pax7 Induces Sub-Physiological *Myf5* Expression in Non-Myogenic Cells, but does not Demethylate *Myf5* DNA. 86
3.19. Tet3 Interacts with Dvl3 88
Chapter 4. Discussion 89
4.1.0. Overview of Regulation of *Pax7* expression by MLL1. 90
4.1.1. MLL1 is Required for Efficient Myogenic Regeneration 91
4.1.2. MLL1 is Required for Proliferation of Myogenic Cells. 91
4.1.3. Role of MLL1 in Pax7 Expression 93
4.1.4. MLL1 does Not Regulate Hox or Dlx2 Gene Expression in Myoblasts 94
4.1.5. MLL1 is Not Required for Myogenic Differentiation 97
4.1.6. MLL1 is Not Required for Activation of *Myf5* by Pax7 98
4.1.7. Role of MLL1 in Myogenic Cell Identity 99
4.1.8. Biomedical Implications of the Regulation of Pax7 by MLL1 100
4.1.9. Future Directions Regarding the Role of MLL1 in Myogenesis 101
4.2.0. Overview of Demethylation of *Myf5* Proximal Promoter 103
4.2.1. H3K4 Methylation and Promoter DNA Demethylation at *Myf5* 105
4.2.2. Inhibition of DNA Demethylation by Non-Canonical Wnt Signaling 106
4.2.3. The Role of Metabolism in Epigenetic Regulation 107
4.2.4. The Role of Metabolism in Stem Cells and Myogenesis 109
4.2.5. Hypothetical Mechanism for Regulation of *Myf5* Demethylation 110
4.2.6. Future Directions Regarding the Role of *Myf5* DNA Methylation in Regulation of Satellite Stem Cell Identity 112
4.3 Conclusion and Significance 114

References **117**
Appendix A **140**
Appendix B **154**

List of Figures

Figure 1. Developmental origin of muscle **5**
Figure 2. Muscle regeneration **9**
Figure 3. Overview of epigenetics **19**
Figure 4. siRNA knockdown of MLL1 dysregulates *Myf5* and *Pax7* expression. **48**
Figure 5. *Mll1* KO results in regeneration defect after muscle injury **50**
Figure 6. Loss of MLL1 deters muscle fibre regeneration after injury **52**
Figure 7. *Mll1* KO results in loss of satellite cells after injury **54**
Figure 8. Loss of MLL1 results in a strong proliferation defect in primary myoblasts **57**
Figure 9. *Mll1* KO results in specific changes to gene expression **60**
Figure 10. *Mll1* KO does not induce or effect induction of myogenic differentiation **63**
Figure 11. *Mll1* KO results in loss of Pax7 protein **65**
Figure 12. Epigenetic regulation of *Pax7* in *Mll1* KO myoblasts **68**
Figure 13. Epigenetic regulation of *Myf5* in *Mll1* KO myoblasts **69**
Figure 14. Exogenous Pax7 rescues *Myf5* expression in *Mll1* KO myoblasts **71**
Figure 15. Inducible Pax7 rescues *Myf5* expression after loss of MLL1 ..... **73**
Figure 16. Exogenous Pax7 expression downregulates and epigenetically represses endogenous Pax7 ..... **75**
Figure 17. Exogenous Pax7 rescues Fgfr4 but not other genes in *Mll1* KO **77**
Figure 18. Exogenous Pax7 rescues *Myf5* expression in *Mll1*/*Mll2* KO myoblasts **79**
Figure 19. *Myf5* is repressed by DNA methylation in ES cells and other non-myogenic cell types and unmethylated in committed myogenic cells **82**
Figure 20. *Myf5* is unmethylated in committed myogenic cells and methylation at *Myf5* is reestablished in *Mll1* KO myoblasts **85**
Figure 21. Exogenous Pax7 induces sub-physiological *Myf5* expression, but does not demethylate *Myf5* DNA. **87**
Figure 22. Reciprocal co-immunoprecipitation of Tet3 with Dvl3 supports possible role for Wnt signaling in regulation of DNA demethylation **88**

List of Tables

Table 1. Gene expression microarray comparison of control and *Mll1* KO myoblasts 61
Table S1. Primers for gene expression analysis 140
Table S2. Primers for ChIP qPCR 142
Table S3. Primers for meDIP qPCR 142
Table S4. Cloning and subcloning primers 143
Table S5. List of small interfering RNAs 144
Table S6. List of antibodies 145
Table S7. Affymetrix data for all probes with greater than two fold change 146

List of Abbreviations

4-OHT	4-hydroxy tamoxifen
Asb4	Ankyrin repeat and SOCS box containing 4
ATP	Adenosine triphosphate
bHLH	Basic helix loop helix transcription factor
BM	Bone marrow
BPTF	Bromodomain PHD Finger Transcription Factor
BSA	Bovine serum albumin
c-met	MET Proto-Oncogene, Receptor Tyrosine Kinase
Carm1	Coactivator Associated Arginine Methyltransferase 1
cDNA	Complementary DNA
Cdx4	Caudal Type Homeobox 4
CE	CreER
Cfp1	CXXC Finger Protein 1
CG	Cytosine guanine dinucleotide
ChIP	Chromatin immunoprecipitation
CMV	Cytomegalovirus
CpG	Cytosine-phosphate-guanine GC dinucleotide
Cre	Cre recombinase
CreER	Cre recombinase-Estrogen receptor (tamoxifen activated nuclear localization domain) fusion
Ct	Cycle threshold
CTX	Cardiotoxin
CXXC4	CXXC domain containing 4
Dlx2	Distal-Less Homeobox 2
DML	dorsomedial lip
DMNT1	DNA methyltransferase 1
DMNT3A	DNA methyltransferase 3A
DMNT3B	DNA methyltransferase 3B
DNA	Deoxyribonucleic acid
Dox	Doxycycline
Dvl3	Dishevelled Segment Polarity Protein 3
EB	Estrogen receptor (tamoxifen activated nuclear localization domain)
ER	Estrogen receptor
ERMS	Embryonal rhabdomyosarcoma
ERT2	Estrogen receptor (tamoxifen activated nuclear localization domain)
EtOH	Ethanol
Eya1	Eyes absent transcriptional coactivator and phosphatase 4
Eya4	Eyes absent transcriptional coactivator and phosphatase 2
EzH2	Enhancer of Zeste 2 Polycomb Repressive Complex 2 Subunit
FACS	Florescence activated cell sorting
Fgfr4	Fibroblast Growth Factor Receptor 4
fl	Flanked by LoxP
GDF11	Growth Differentiation Factor 11

GOI	Gene of interest
H1B	Histone subunit 1B
H2A	Histone subunit 2A
H2AK119	Histone H2A lysine 119
H2B	Histone subunit 2B
H3	Histone subunit 3
H3K20	Histone H3 lysine 20
H3K27	Histone H3 lysine 27
H3K36	Histone H3 lysine 36
H3K4	Histone H3 lysine 4
H3K4	Histone H3 lysine 4
H3K9	Histone H3 lysine 9
H4	Histone subunit 4
HAT	Histone acetyltransferases
HDAC	Histone deacetylase
hGFAP	Human glial fibrillary acidic protein (transgenic promoter)
Hif1a	Hypoxia-inducible factor 1-alpha
HMT	Histone methyl transferase
Hox	Hox gene
Hoxa9	Homeobox protein Hox-A9
HSC	Hematopoietic Stem Cell
IDAX	CXXC4
IDH1/2	Isocitrate Dehydrogenase 1/2
IgG	Immunoglobulin G
IgH	Immunoglobulin heavy chain
IP	Immuno-precipitation
K	Lysine
Ki67	Antigen KI-67
KO	Knockout
loxP	Locus of X-over P1
MBD	Methyl DNA binding protein
me3	Trimethyl
meCpG	Methylcytosine-phosphate-guanine CG dinucleotide
meDIP	Methyl DNA immuno-precipitation
MEF	Mouse embryonic fibroblasts
Mef2	Myocyte enhancer factor-2
MLL1	Mixed lineage leukemia 1, Lysine Methyltransferase 2A
MLL2	Mixed lineage leukemia 2, Lysine Methyltransferase 2B, Trx2
MLL3	Mixed lineage leukemia 3, Lysine Methyltransferase 2C
MLL4	Mixed lineage leukemia 4, Lysine Methyltransferase 2D, ALR
mpc	Myogenic progenitor cell
MRF	Myogenic regulatory factor
mrf4	Myogenic regulatory factor 4
mRNA	Messenger RNA
Msx1	Msh Homeobox 1
Myf5	Myogenic factor 5

MyHC	Myosin heavy chain 2a
MyoD	Myogenic differentiation 1
NAD+	Oxidized nicotinamide adenine dinucleotide
NeuroD6	Neuronal Differentiation 6
NURF	Nucleosome remodeling factor
p38	Mitogen-Activated Protein Kinase P38 Alpha
Pax3	Paired box protein Pax-3
Pax7	Paired box protein Pax-7
PBS	Phosphate buffered saline
Pbx1	Pre-B-cell leukemia homeobox 1
PCP	Plainer cell polarity pathway
PCR	Polymerase chain reaction
PDB	Protein Data Bank
PolII	RNA polymerase II
PRC2	Polycomb repressive complex 2
Prdm16	PR domain containing 16
RMA	Robust multi-array average
RMS	Rhabdomyosarcoma
RNA	Ribonucleic acid
RT-qPCR	Real-time quantitative PCR
S	Serine
SEM	Standard error of the mean
Set	Su(var)3-9, Enhancer-of-zeste and Trithorax domain
Set1A	SET domain containing 1A
Set1B	SET domain containing 1B
Set2	SET domain containing 2
siRNA	Small interfering RNA
Six1	Sine oculis homeobox homolog 1
Six4	Sine oculis homeobox homolog 4
Suv4-20h1	Suppressor of Variegation 4-20 Homolog 1
SVZ	Subventricular zone
T	Threonine
TA	Tibialis anterior muscle
TE	Tris buffered EDTA
Tet	Ten-eleven translocation methylcytosine dioxygenase gene family protein
Tet-ON	Tetracycline activated gene expression
Tet2	Ten-eleven translocation methylcytosine dioxygenase protein 2
Tet3	Ten-eleven translocation methylcytosine dioxygenase protein 3
TNF	Tumor necrosis factor
Trx2	MLL2
TSS	Transcription start site
TUNEL	Terminal deoxynucleotidyl transferase dUTP Nick-end labeling
VLL	Ventrolateral lip
YFP	Yellow florescent protein
YFP–	Lineage negative (Myf5) conditional YFP (non-expresser)
YFP+	Lineage positive (Myf5) conditional YFP (expresser)

> And he will be unable to see the realities of which in his former state he had seen the shadows; and then conceive some one saying to him, that what he saw before was an illusion, but that now, when he is approaching nearer to being and his eye is turned towards more real existence, he has a clearer vision, –what will be his reply? And you may further imagine that his instructor is pointing to the objects as they pass and requiring him to name them, –will he not be perplexed? Will he not fancy that the shadows which he formerly saw are truer than the objects which are now shown to him?

— Plato. The Republic, Book VII, The Allegory of the Cave, 380 BC (B. Jowett translation, 1871)

> On the papers were written thoughts, ends of thoughts, beginnings of thoughts.
>
> One by one the mind of Doctor Reefy had made the thoughts. Out of many of them he formed a truth that arose gigantic in his mind. The truth clouded the world. It became terrible and then faded away and the little thoughts began again.

— Sherwood Anderson. Winesburg, Ohio; a group of tales of Ohio small town life, 1919

Chapter 1. Introduction

1.1. Skeletal Muscle

Skeletal muscle makes up approximately 40% of the mass of a typical human body (Rolfe and Brown, 1997). Skeletal muscle is responsible for voluntary movement, posture and respiration and is attached via tendons to the skeletal system, which acts as levers, to translate muscle contraction to forceful movement (Descartes, 1630). Skeletal muscle contraction is stimulated by lower motor neurons at neuromuscular junctions within the muscle, and this stimulation is controlled and coordinated at several levels within the central nervous system resulting in coordinated movement and maintenance of posture (Sherrington, 1922).

Skeletal muscles are composed of bundles of individual multinucleated muscle fibres surrounded by connective tissue which scale through repetition of small subunits to form muscles of highly variable size (Leeuwenhoek and Sprengell, 1720). Skeletal muscle fibres consist of an elongated syncytium primarily composed of contractual elements arranged into myofibrils of repeating sarcomeres, and which can contain hundreds or thousands of myonuclei (Rollet, 1884, 1885; Veratti, 1902; Jordan, 1920).

The contraction apparatus of the muscle are made up of bundles of myosin-motor-protein thick filaments terminating in motor heads which bind to and exert a power stroke upon static actin thin filaments in an ATP dependent process (Huxley, 1969). The myosin protein bundles extend bi-directionally from the center of the sarcomere. During contraction, the myosin proteins proceed stepwise along the actin filaments, which are anchored at z discs at the ends of the sarcomere. This process ultimately results in forceful shorting of the sarcomere and when individual fibres contract in synchrony, a forceful shorting of the muscle (Huxley and Niedergerke, 1954).

Contraction is stimulated when motor neuron signals, propagated through t-tubules localized around the z bands, trigger the opening of calcium channels in calcium sequestering sarcoplasmic reticulum (Donaldson, 1985). In relaxed muscle, myosin binding sites on actin are blocked allowing movement of actin and myosin filaments. When calcium is released, it binds to troponin C ultimately resulting in unblocking of myosin binding sites on actin and thereby allowing myosin to bind thereby initiating power strokes on the actin, and muscle contraction (Squire, 1975).

Adult muscle has a remarkable regenerative ability and can respond to stimuli triggering its anabolic growth (Chargé and Rudnicki, 2004), thereby providing adequate strength to cope with changing needs. Muscle may also be catabolized or otherwise lost during normal aging and in periods of disuse, extreme caloric deficit or muscle wasting disease (McKinnell and Rudnicki, 2004). Understanding of the mechanisms by which muscle is maintained, grows or is lost is essential for combating muscle disease and may be useful for aiding muscle maintenance, allowing for better mobility and independence during later stages of life.

1.2. Embryonic Myogenesis

During embryonic development muscle is derived from the somites which coalesce from the paraxial mesoderm starting around embryonic day 8 in the mouse or 25 days after fertilization in humans. The somites are induced through oscillations in morphogen gradients resulting in gene expression changes and formation of a sequence of somite pairs lateral to the neural tube and notochord (Hofmann et al., 2004; Pourquié, 2003). The somites are formed progressively from anterior to posterior with the anterior

somites progressively developing while succeeding somites continue to form (Buckingham et al., 2003). The somites will give rise to the axial skeleton, dermis and all muscle, apart from the muscle of the face and head.

The somites gain dorsal-ventral polarity when sonic hedgehog signals from the notochord induce formation of the sclerotome which will form the axial skeleton and cartilage (Chiang et al., 1996). The remaining somite is termed the dermomyotome and is flanked by a dorsomedial lip (DML) adjacent to the neutral tube and ventrolateral lip (VLL) at its opposing end (Kaufman, 1992). Muscle progenitor cells form at the VLL and DML, migrate to form a myotome layer under the dermomyotome that will develop into the muscles of the trunk and back (Parker et al., 2003; Tajbakhsh and Buckingham, 1999). The limb muscles are formed by cells which migrate away from the VLL of the dermomyotome into the limb buds (Vasyutina and Birchmeier, 2006). The cells of the dermomyotome are marked by expression of paired box transcription factors Pax3 and Pax7 (Buckingham and Relaix, 2007; Buckingham et al., 2003; Goulding et al., 1994). As development progresses, the cells of the dermomyotome differentiate or are dispersed as Pax3 and/or Pax7 expressing precursors that are interspersed into the myotome and myogenic tissues of the limbs and give rise to muscle satellite cells (Gros et al., 2005; Kassar-Duchossoy et al., 2005; Relaix et al., 2005).

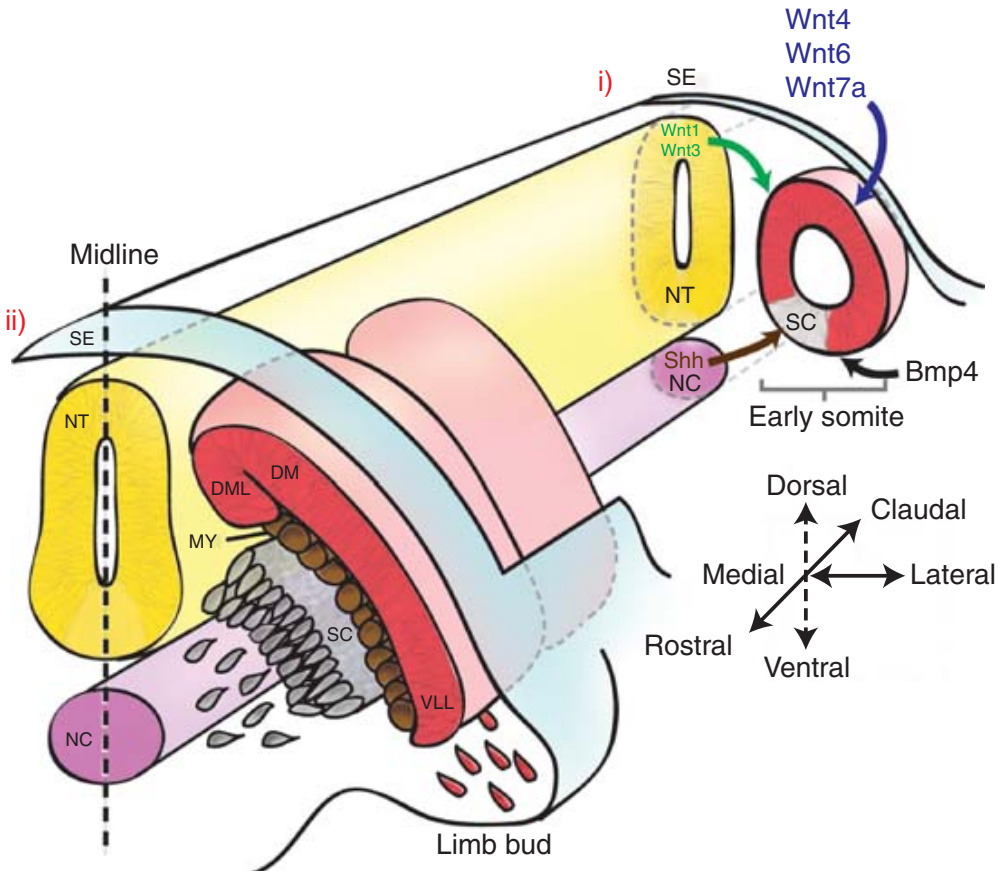

Figure 1. Developmental origin of muscle
All muscle, with the exception of that of the head and neck, is derived from cells originating from the somites, which are formed progressively via segmentation of the presomitic paraxial mesoderm. As the somites mature, the ventral portion becomes sclerotome (SC, grey), which will form the bones and cartilage of the spine and ribs. The dorsal-lateral somite becomes dermomyotome (DM, red). As the dermomyotome matures Pax3 expressing cells migrate over the dorsal medial lip (DML) and the ventrolateral lip (VLL) to form the epaxial and hypaxial myotome (MY, brown) where they begin expressing myogenic regulatory factors and will give rise to the muscles of the trunk. Pax3 expressing cells from the VLL (red) will migrate to the limb buds where they will become the muscles of the limbs. Undifferentiated Pax3/Pax7 cells are retained throughout development, residing in the satellite cell niche after muscle formation is complete. Reproduced with permission from Bentzinger et al., 2012.

1.3. Satellite Cells and Muscle Regeneration

In mammals, the nuclei of muscle fibres are post mitotic and do not re-enter the cell or contribute to muscle regeneration (Snow, 1977, 1978). The anabolic and regenerative capacity of muscle has long been recognized, and when satellite cells, so named due to their localization peripheral to muscle fibers, were first observed, it was quickly hypothesized that they might be the solution to the "muscle regeneration problem" (Mauro, 1961). It has since been determined that satellite cells are muscle stem cells, the source for postnatal muscle growth and muscle regeneration (Church et al., 1966; Bischoff, 1974; Snow, 1978).

In early postnatal mice, satellite cells and progenitors comprise up to 30% of nuclei in the muscle. This percentage drops to around 5% during adulthood (Bischoff, 1994). In adult muscle, satellite cells are generally quiescent and have transcriptional profiles reflecting low metabolic activity and cell cycle progression but active signaling and regulatory mechanisms (Cheung and Rando, 2013). Upon injury, satellite cells enter the cell cycle and can proliferate extensively prior to differentiation and regeneration of the muscle (Snow, 1978). In the adult, satellite cells are also the primary, and are likely the only source for muscle regeneration, and loss of Pax7 expressing cells results in loss of muscle regeneration (Seale et al., 2000; Lepper et al., 2011; Sambasivan et al., 2011a; von Maltzahn et al., 2013a).

While satellite cells are important for maintaining muscle homeostasis under normal physiological conditions, most of our *in vivo* understanding of satellite cell regulation and function comes from regeneration experiments induced by severe injury in laboratory conditions. Upon injury, a phase of muscle degeneration occurs during which

injured fibres undergo necrosis, and inflammatory signals recruit macrophages to clear damaged tissue (Arnold et al., 2007). Some satellite cells enter a proliferation phase in which they are termed muscle progenitor cells (mpc) and activate a cascade of myogenic basic helix loop helix regulatory (transcription) factor (MRF) expression, resulting in activation of the differentiation program. During differentiation, expression of functional muscle components is upregulated, and myocytes elongate and fuse with remaining muscle fibres or with each other forming new muscle fibres to replace and repair lost and damaged muscle tissue (Rudnicki et al., 2009).

During regeneration, some satellite cells are reserved and are available to contribute to regeneration in subsequent rounds injury/regeneration (Collins et al., 2005; Montarras et al., 2005; Sacco et al., 2008; Porpiglia et al., 2017). It is not clear how the decision to differentiate or to remain a satellite cell niche is determined, however differences in signaling and other micro-environmental differences may result in differences in satellite cell response to injury. Differing expression of MRFs, or differences in progression down the myogenic pathway, likely make some cells more apt to respond to differentiation cues while others remain recalcitrant to differentiation signals (Shea et al., 2010; Zammit et al., 2004).

Satellite cells lacking a history of Myf5 expression are an example of myogenic cells that resist differentiation signals. Lineage tracing for *Myf5* expression finds that 90% of satellite cells have expressed *Myf5* (Kuang et al., 2007). Satellite cells which have never expressed *Myf5* (satellite stem cells) have long-term stem cell characteristics and contribute more robustly to both regenerating muscle fibres and to the satellite cell pool after transplant, than cells which have expressed Myf5. This finding indicates that

satellite stem cells remain proliferative for a longer time after transplant prior to differentiation of a portion of their progeny. Satellite stem cells can divide symmetrically to make two stem cells which have never expressed *Myf5*, or asymmetrically with one daughter cell expressing *Myf5* (Kuang et al., 2007; Le Grand et al., 2009). This asymmetric division is a clear example of generation of myogenic cell heterogeneity and results in cell populations with distinctive responses to differentiation cues.

Satellite cell-derived myoblasts can be isolated and grown *in vitro* under mitogenic culture conditions. *Ex vivo*, myoblasts have extensive proliferative capacity, and can be induced to undergo myogenic differentiation by withdrawal of mitogenic factors (Rando and Blau, 1994). While cultured myoblasts are an excellent system for study of myogenesis and myogenic regeneration, they are functionally and molecularly distinct from quiescent satellite cells (Fukada et al., 2007; Montarras et al., 2005), and are also distinct from activated satellite cells *in vivo* (Pallafacchina et al., 2010). Compared to cultured myoblasts, *in vivo* muscle damage results in activated satellite cells and other distinct types of mpcs (Porpiglia et al., 2017), residing within a complex microenvironment which may contribute to heterogeneity, thereby accounting for differences in function and gene expression. *Ex vivo* cultured myoblasts provide an example of myogenic cells which easily respond to differentiation cues and when transplanted after *ex vivo* culture have low contribution to myogenesis or the satellite cell pool after transplant (Montarras et al., 2005).

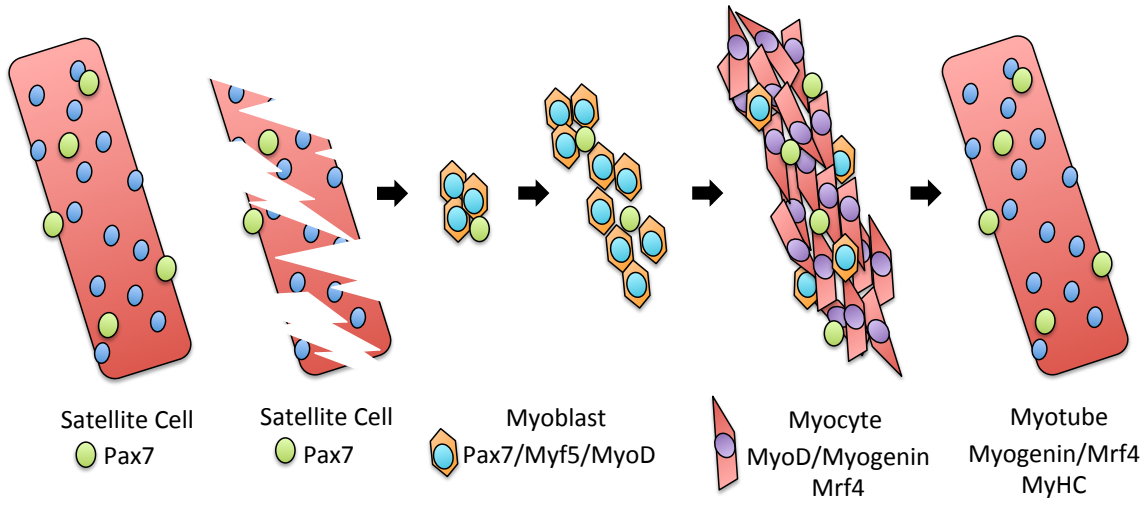

Figure 2. Muscle regeneration
The regenerative potential of muscle is derived from Pax7 expressing satellite cells residing under the basal lamina of muscle fibres. When muscle is damaged, satellite cells proliferate with some myogenic progenitor cells (mpcs), myoblasts, committing to myogenesis by expressing myogenic regulatory factors Myf5 and MyoD. As regeneration progresses mpcs may enter the differentiation program, becoming myocytes through expression of myogenin and Mrf4 and downregulation of Pax7 and Myf5. As terminal differentiation progresses, myocytes upregulate functional muscle gene expression, such as myosin heavy chain (MyHC) and fuse to form new myotubes thereby regenerating lost muscle. During this process, not all cells with myogenic potential proceed through the differentiation program and some cells are reserved to repopulate the satellite cell niche.

1.4. Molecular Regulation of Muscle Determination

Myogenesis, like all morphogenic or differentiation pathways, is highly regulated through extracellular signals and intracellular regulation of gene expression. Myogenesis is a stepwise process arguably, and in most cases, starting with expression of the paired box transcription factors *Pax3* or *Pax7* in stem or progenitor cells (Relaix et al., 2005). While expression of *Pax3* or *Pax7* does not signal commitment to myogenic differentiation, both factors target *Myf5* for expression (Bajard et al., 2006; McKinnell et al., 2008; Kawabe et al., 2012; Soleimani et al., 2012; Daubas and Buckingham, 2013; Himeda et al., 2013). Not all *Pax3* or *Pax7* expressing cells have expressed *Myf5* however and the activation of *Myf5* occurs through a process involving Pax3/7 signals myogenic commitment (Kuang et al., 2007; Le Grand et al., 2009).

Myf5, together with other basic helix-loop-helix type transcription factors MyoD, myogenin and Mrf4 comprise the myogenic regulatory factors. The MRFs were discovered through a series of experiments exploring the finding that treatment of 10T1/2 cells with 5-azacytadine, a DNA methyltransferase inhibitor, resulted in adoption of the myogenic fate in a fraction of cells (Constantinides et al., 1977; Taylor and Jones, 1979), presumably through de-repression of a factor involved in myogenic fate determination (Konieczny and Emerson, 1984). The key to these discoveries was that exogenous expression of any of the MRFs is capable of converting 10T1/2 cells to the myogenic lineage. The first MRF was isolated using a cDNA/mRNA subtraction technique to find cDNAs that were present in both 5-azacytadine derived 10T1/2-myoblasts and C2C12 myoblasts (an immortalized mouse myoblast line (Blau et al., 1983; Yaffe and Saxel, 1977)), but not in untreated 10T1/2 cells. Through functional screening the selected

cDNAs, a specific cDNA (that coding for MyoD) which was capable of converting 10T1/2 cells was discovered (Davis et al., 1987). The remaining MRFs, which have high homology, were then found through hybridization of cDNA libraries to the *MyoD* cDNA (Braun et al., 1989a, 1990; Miner and Wold, 1990; Rhodes and Konieczny, 1989; Wright et al., 1989).

The *in vivo* importance of the MRFs was confirmed with the development of knockout (KO) mice which showed distinct roles for each MRF. Loss of Myogenin was found the have the strongest effect on development of muscle, resulting in profound muscle deficiency and neonatal death (Hasty et al., 1993; Nabeshima et al., 1993). It was found that single knockout of *MyoD*, *Myf5* or *Mrf4* had more subtle effects with perturbations of myogenesis at specific developmental stages ultimately resulting largely normal muscle (Braun and Arnold, 1995; Braun et al., 1992; Patapoutian et al., 1995; Rudnicki et al., 1992; Zhang et al., 1995). Double or triple knockouts resulted in a severe muscle defect for *MyoD*/*Mrf4* KO, to complete loss of muscle for *MyoD*/*Myf5* KO, indicating that there is incomplete functional overlap between *Myf5*, *MyoD* and *Mrf4* (Rawls et al., 1998; Rudnicki et al., 1993). Cis-interactions influencing expression of the adjacent genes *Myf5* and *Mrf4* have complicated the use of genetic knockouts for understanding of the unique roles for each (Braun and Arnold, 1995; Kassar-Duchossoy et al., 2004).

1.5. Regulation of Myogenic Regulatory Factor Expression

The expression of MRFs during satellite cell activation and differentiation occurs in a step-wise fashion with myogenic cells first expressing *Myf5*, which is expressed

slightly earlier than *MyoD* (Ott et al., 1991). *Myf5* is expressed in the majority of quiescent satellite cells (Beauchamp et al., 2000) while *MyoD* is not. Both *Myf5* and *MyoD* are expressed concurrently in activated satellite cells. At the initiation of differentiation, *myogenin* is upregulated. *Mrf4* expression is activated as differentiation proceeds. *MyoD*, *myogenin* and *Mrf4* are expressed throughout differentiation but *Myf5* expression is lost in early differentiation concurrently with loss of *Pax3/7* expression.

The expression of *Myf5* is tightly correlated with expression of *Pax3* and/or *Pax7* and both Pax3 and Pax7 have been shown to bind enhancers near *Myf5* (Bajard et al., 2006; Himeda et al., 2013; Maroto et al., 1997; McKinnell et al., 2008; Soleimani et al., 2012). In some circumstances, such as in the muscles of the face and during early embryogenesis, *Myf5* expression may also be regulated by other factors such as Pitx2 (Zacharias et al., 2011), and has a complex system of enhancers regulating its expression during early development depending on location and developmental stage (Carvajal et al., 2008). The regulation of *MyoD* expression is less clearly understood. Compound mutants for *Pax3*/*Myf5*(*Mrf4*) or *Six1*/*Six4*/*Myf5*(*Mrf4*) do not activate *MyoD* expression during early myogenesis (Relaix et al., 2013; Tajbakhsh et al., 1997), however this effect may be due to loss of myogenic cell identity, cell death, or cell cycle exit, rather than direct regulation of *MyoD* by these factors.

It is also possible that expression of *MyoD* is downstream of but indirectly regulated by Pax3, Myf5, Mrf4 or Six1/4. Ectopic Pax3 expression can induce *Myf5* and *MyoD* expression in a number of permissive early embryonic tissues (Maroto et al., 1997), and ectopic Myf5 can induce *MyoD* expression (Braun et al., 1989b), however

during myogenic differentiation *Myf5* expression is downregulated with *Pax3*/*7* while *MyoD* expression continues (Bentzinger et al., 2012).

Myogenin and *Mrf4* expression are activated after *Myf5* and *MyoD* as terminal differentiation and expression of *myosin heavy chain* (*MHC*) begins. *Myogenin* is regulated by a set of DNA binding elements on which MyoD-Six1/4-Mef2-Pbx1 and other factors can act to stimulate or repress its transcription (Faralli and Dilworth, 2012). The *Mrf4* gene is located adjacent (about 8.5 kb upstream) to *Myf5* and regulatory interactions between *Myf5* and *Mrf4* may have a role in their expression. Some evidence suggests that activation of either *Myf5* or *Mrf4* results in excluding the activation of the other (Carvajal et al., 2008).

1.6. Myogenic Specification by Pax3 and Pax7

The homeodomain containing paired-box transcription factors Pax3 and Pax7 have important roles in myogenesis. Pax3 and Pax7 have high homology, with higher homology to each other than to other Pax gene products. Both contain an amino terminal paired domain, which is common among several Pax genes, and has several DNA binding sequences that bind the major and minor grove of DNA (Xu et al., 1999). Pax3 and Pax7 also contain a homeodomain which has further DNA binding motifs (Birrane et al., 2009). The paired domain and homeodomain each bind DNA in a sequence-specific fashion (Soleimani et al., 2012). The carboxyl-terminal of both Pax7 and Pax3 contain transactivation domains (Schafer et al., 1994).

The Splotch mutant, a spontaneous *Pax3* mutation, forms axial muscle (Bober et al., 1994), but is devoid of limb and diaphragm muscles due to a role of Pax3 in

migration of myogenic cells from the somites (Daston et al., 1996; Tremblay et al., 1998). *Pax7* KO results in viable mice which are born at a similar size to littermates but fail to thrive with most dying at 2 to 3 weeks of age due to respiratory failure with few surviving into adulthood (Mansouri et al., 1996; Seale et al., 2000). Postnatal muscle growth and muscle regeneration are absolutely dependent on expression of *Pax7* which is expressed in most or all satellite cells and continues to be expressed in mpcs during regeneration and is also expressed in myoblasts *ex vivo* (Kuang et al., 2006; von Maltzahn et al., 2013a; Seale et al., 2000).

In the absence of *Pax7*, the satellite cell pool is lost, muscle growth is deficient and regeneration fails (Seale et al., 2000). *Ex vivo* Pax7 KO myoblasts exit the cell cycle and precociously differentiate (von Maltzahn et al., 2013a; Günther et al., 2013). *Pax3* and *Pax7* double mutants form some muscle in the early myotome during development, but continued myogenesis is not maintained (Relaix et al., 2005), likely reflecting the roles for Pax7 and Pax7 in proliferation and inhibition of differentiation.

The muscles of the head are derived from the pharyngeal arches and have a distinct origin from the muscles of the trunk and limbs. Genetic ablation studies show that head muscles are not derived from *Pax3/7* expressing cells (Hutcheson et al., 2009). Factors including Pitx2, Tbx1, Six1/4 and Eya1/4 may contribute to direct activation of myogenic genes or to maintaining survival, proliferation, and myogenic permissiveness in the head and in the precursors for the small amount of trunk muscle occurring in *Pax7*/*Pax3* double knockout (Buckingham and Rigby, 2014; Sambasivan et al., 2011b).

As described above, both *Pax3* and *Pax7* are expressed in the dermomyotome. *Pax3* is specifically expressed in, and is required for, myogenic cells during migration

into the limb bud through activation of c-met (Epstein et al., 1996). Despite their high homology, genetic substitution of *Pax3* with *Pax7* can rescue trunk musculature, but cannot rescue c-met expression and migration of myogenic cells to the limb buds (Relaix et al., 2004). Genetic ablation of *Pax3* expressing cells results in total loss of *Pax7* expressing cells (Hutcheson et al., 2009), and genetic labeling of *Pax3* expressing cells labels all *Pax7* expressing satellite cells (Gros et al., 2005; Schienda et al., 2006), suggesting that *Pax3* expression occurs concurrently or prior to *Pax7* expression.

As suggested by knockout phenotypes, both Pax3 and Pax7 have roles in proliferation and their loss results in apoptosis (Borycki et al., 1999; Relaix et al., 2006), or differentiation (von Maltzahn et al., 2013a). The loss of cells that are dependent on Pax3 or Pax7 is the predominant effect of knockout models (Seale et al., 2000; Relaix et al., 2005). Because *Pax3* and *Pax7* knockouts results in loss of myogenic precursors, genetic KO *in vivo* obscures their direct roles in expression of myogenic genes.

Using *in vitro* cell culture models, a clear role has been established for Pax7 in transcriptional activation of the myogenic regulatory factor (MRF) gene *Myf5* (McKinnell et al., 2008; Soleimani et al., 2012; Kawabe et al., 2012). Pax7 acts as a transcriptional activator through recruitment of a histone methyltransferase complex (HMT) to write a permissive histone 3 lysine 4 tri-methyl epigenetic mark (H3K4me3) at target genes, and interactions of Pax7 with HMTs MLL1 and MLL2 have been identified through co-immunoprecipitation and *in vitro* binding assays (Kawabe et al., 2012; McKinnell et al., 2008). The possibility that Pax7 can interact with other H3K4 HMTs has not been excluded. Others have found the related transcription factor Pax6 interacts

with HMTs MLL1, MLL2 and Set1a to activate its target genes (Sun et al., 2016), suggesting possible promiscuity among Pax-HMT interactions.

As mentioned above, satellite stem cells which have never expressed *Myf5* express *Pax7*, but paradoxically Pax7 does not initiate *Myf5* expression in these cells (Kuang et al., 2007). It was found that loss of Carm1, or mutation of arginine residues that are methylated by Carm1 on Pax7, decreases the ability of Pax7 to activate *Myf5* expression, thereby providing a mechanism to regulate Pax7 activity (Kawabe et al., 2012).

1.7. Epigenetic Specification of Cellular Identity

The concept of epigenetic regulation was developed by Conrad Waddington during the mid 1900s (Waddington, 1947, 1956), and was formed in a period before DNA was understood to be the genetic material, and before histones or any kind of genetic packaging was discovered. His epigenetics was based on the early embryology experiments examining the induction potential of the Spemann-Mangold organizer, the organizers of birds and mammals and other experiments in which specific changes to cellular or tissue identity can be induced by exposure to signaling molecules from tissues or tissue extracts. The focus of the epigenetics concept was the variant potential of tissues, both temporally; at different stages of development, and regionally; at different areas in the developing embryo, to respond to induction signals. What Waddington was trying to reconcile with the epigenetics concept is that “the genetic control of particular kinds of substances” is specific to developmental stage and location and therefore

developmental stage and location must confer some kind of change to genes such that induction with a substance has differing effects.

The modern conception of epigenetics focuses on non-genetic changes to DNA and its local environment, specifically methylation of DNA at CpG residues and post-translational modifications to the histones which package DNA, and the direct mechanisms by which these changes occur, or are maintained. It is important to stress that, while the modern field of epigenetics and Waddington's concept of epigenetics have some functional overlap, the extent that DNA methylation and specific histone modifications are important pertaining to Waddington's epigenetics seems to be variable. Many histone modifications seem to be a requirement for transcription rather than being a regulator of potential. Similarly, DNA methylation has multiple roles specified by its location, and the role of DNA methylation in regulating potential seems to be case-specific rather than general. A modern concept of what Waddington was referring to with the term epigenetics can probably only be described with a largely holistic description of developmental regulators including transcription factor expression, cell surface receptor expression, messenger availability, etc., in addition to a subset of histone and DNA modifications.

1.8. Regulation of Transcription by Histone Modifications

Nuclear DNA is highly organized and is packed into nucleosomes comprised of the histone octamer with two each of histone proteins H2A, H2B, H3 and H4 which form a small core, and about 146 base pairs of DNA (Bentley et al., 1984; Luger et al., 1997), that wraps around the histone octamer. There is one nucleosome for approximately every

200 base pairs of DNA, allowing for a short span of DNA between each nucleosome coil (Kornberg, 1974; Bentley et al., 1984). This arrangement is often compared to beads on a string, however the overall mass ratio of DNA to histone is heavily weighted to the DNA (Luger et al., 1997), and histones serve as a minimal substrate allowing for a generic but specifically tailorable regulator of DNA as well as an organizational tool.

Transcription of DNA to RNA is highly regulated, but ultimately requires two basic steps, recruitment of RNA polymerase, and unpacking of DNA from histones to allow access to DNA and transcriptional elongation. Both of these steps rely on specific modifications to histones which result in re-configuration histone proteins and histone-DNA interactions, and/or serve as adhesion points for binding of various components of the RNA polymerase and nucleosome remodeling apparatuses (Bannister and Kouzarides, 2011; Lawrence et al., 2016).

After each round of transcription DNA needs to be repackaged on histones to prevent spurious transcriptional initiation, and to maintain genome integrity and organization (Carrozza et al., 2005; Joshi and Struhl, 2005; Keogh et al., 2005; Wang et al., 2009b). The histone modifications required for transcription can ostensibly be blocked by repressive modifications which in some cases are incompatible with active modifications (for example, a methylated lysine cannot be acetylated) or which otherwise prevent recruitment of active modification writers. The histone modifications which are required for active transcription, and those which repress transcription, appear to be progressive such that step-wise accumulation of activating modifications results in active transcription and repressive modifications increasingly constrain opportunities for activating modifications to be deposited and inhibit access to DNA and histones.

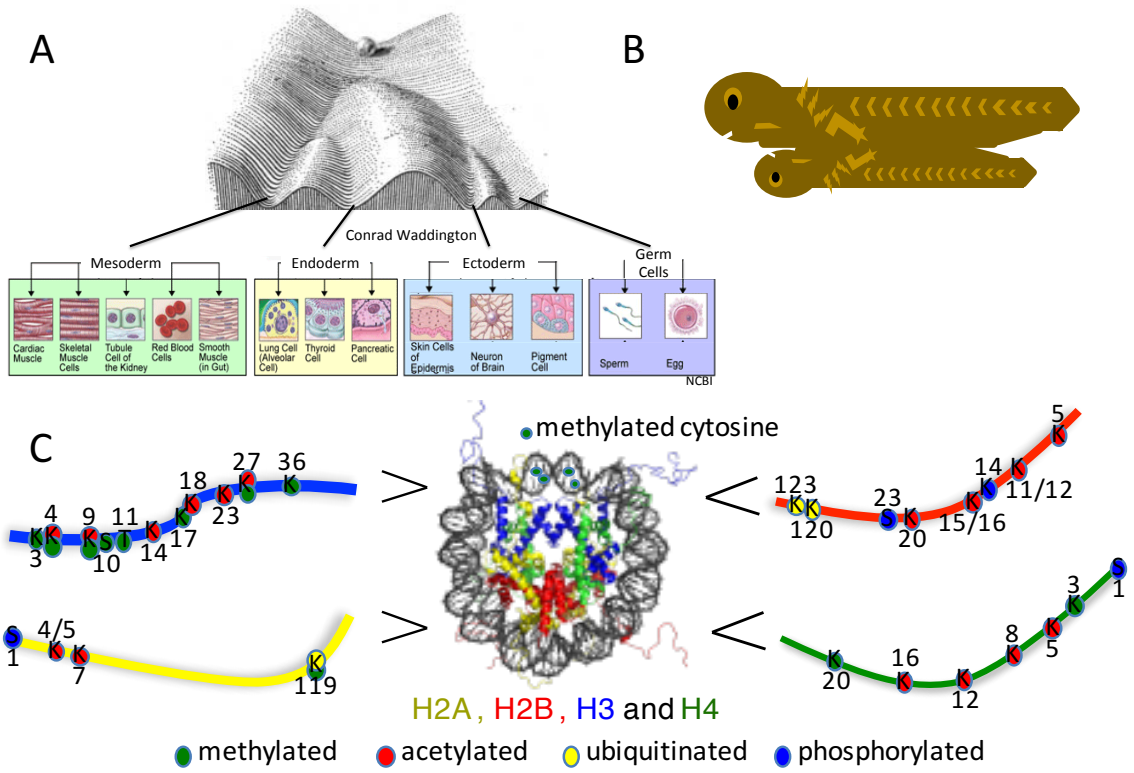

Figure 3. Overview of epigenetics

(A) Waddington's epigenetics describes progressively diminishing developmental potential of tissues. Early in development tissues have potential to form all parts of the body, as development progresses, potential becomes limited due to progressive epigenetic changes overlaying the genetic mechanism. (Adapted from Waddington, 1956 and NCBI, unattributed)

(B) Waddington's epigenetics is based on the transient ability of tissues to react to inducing signals throughout development. Here the xenopus body plan has been doubled through transplantation of Spemann/Mangold organizer at the blastocyst stage. (based upon Spemann and Mangold, 1923)

(C) Post-translational epigenetic modifications of octameric histones regulate histone-DNA and histone-protein binding resulting in regulation of DNA. DNA is organized onto histones with 146 base pairs wound ~ 660˚ around each octamer, entering and exiting near histone H3 (blue) tails. Histones have extensive potential modifications; examples of possible tail modifications are shown. The globular domains of histones are also modified. DNA may also be modified by methylation of cytosine residues at GpG dinucleotides resulting in differing effects depending on localization. meCpG at the proximal promoter represses gene expression. (PDB rendering based on Luger et al., 1997 ((Wheeler, 2007) with permission), histone modification selection from Lawrence et al, 2016).

1.9. Repressive Histone Modifications

Methylation of the protruding N-terminal tails of histone H3 at lysines K9 (H3K9) and K27 (H3K27) are both associated with silent DNA. H3K27 methylation is written by polycomb repressive complex PRC2 by the catalytic enzyme EzH2 (Cao et al., 2002; Czermin et al., 2002; Müller et al., 2002). H3K27 trimethylation (me3) has been found in some cases to co-localize with the permissive mark H3K4me3 in bivalent chromatin where transcription is initiated resulting in short 3' transcripts, but does not continue to make protein coding mRNA (Bernstein et al., 2006). The H3K27me3 mark is often found in conjunction with H2AK119ubiquitin (ub) which is written by the PRC1 complex, and it has been found that both PRC2 and PRC1 can bind to H3K27me3 to propagate silencing (Cao et al., 2002; Müller et al., 2002; Czermin et al., 2002; Hansen et al., 2008; Margueron et al., 2009). Several methods for recruitment of PRC2 to genes for initiation of repression have been reported (Beisel and Paro, 2011) and the necessary complexity of gene regulation has likely resulted in numerous ways to regulate gene silencing through polycomb.

An alternative, but not mutually exclusive, mode of gene silencing is through H3K9 and DNA methylation (Beisel and Paro, 2011). H3K9 methylation is incompatible with H3K9 acetylation, a mark associated with active transcription and recruitment of RNA polymerase, and is likely incompatible with transcription initiation for this reason. H3K9 methylation also recruits de-novo DNA methyltransferases DNMT3A/B resulting in methylation of adjacent DNA, but DNMT3A/B are only active in the presence of unmethylated H3K4 (Epsztejn-Litman et al., 2008; Ooi et al., 2007; Smith and Meissner, 2013). DNA methyltransferases DMNT1 and DNMT3A also bind and recruit H3K9

methyltransferases (Fuks et al., 2003; Smallwood et al., 2007) thereby creating a reinforcing loop.

1.10. Role of DNA Methylation in Regulating Gene Expression

Vertebrate DNA is methylated specifically on cytosine moieties at CpG dinucleotides and is copied to the cytosines of complementary strands by DNMT1 (Hermann et al., 2004). Several mechanism have been proposed for targeting of CpG sites for de-novo methylation, which occurs through DNMT3A and DNMT3B (Okano et al., 1999), including recruitment through unmethylated H3K4 (Ooi et al., 2007; Otani et al., 2009). DNA has a much lower CpG content than would be statistically predicted, as chance deamination of methylated cytosine converts it to thymine and this mutation is not always corrected with mismatch repair (Sved and Bird, 1990). Because of this chance mechanism, CpG dinucleotides that are not lost to mutation are apt to have functional significance.

DNA methylation has evolved to have many functions depending on location. As CpG methylation results in a change to the DNA structure, CpG methylation status can affect sequence specific DNA binding either by preventing or enabling sequence recognition, thereby enabling or inhibiting downstream effects of factor binding (Schübeler, 2015; Zhu et al., 2016). DNA methylation at or near the transcription start site inhibits transcription through methyl-DNA binding proteins, which bind to methylated DNA in a non-sequence specific manner and recruit histone deacetylase (HDAC) containing complexes to inhibit transcription (Boyes and Bird, 1991; Jones et al., 1998; Nan et al., 1998). During transcription RNA polymerase II (Pol II) recruits a

H3K36 methyltransferase to the gene body (Krogan et al., 2003). While H3K36me3 is associated with active transcription, it recruits DNMT3B to methylate the intragenic region and acts to prevent transcription initiation away from the transcription start site (Baubec et al., 2015; Morselli et al., 2015; Neri et al., 2017).

DNA methylation and H3K9me3 are also associated with heterochromatin in which the DNA and nucleosomes are tightly packed, resulting in limited access to DNA, which further inhibits transcription and transcription factor binding, and possibly acts as a protective layer against epigenetic changes (Toit, 2012). Together, the repressive epigenetic marks perhaps most closely resemble Waddington's epigenetic restriction, however all of these marks can be specifically erased by catalytic enzymes and so technically do not result in permanent inhibition. While the methods for depositing repressive marks often allow for spreading and are somewhat promiscuous (Talbert and Henikoff, 2006), the erasure of repressive marks seems to be tightly regulated. Therefore, a cell's potential for removal of repressive marks, through its current expressed gene products may be the factor that most closely relates to Waddington's epigenetics.

1.11. Activating or Permissive Histone Modifications

Several posttranslational histone modifications are correlated with active transcription. The H3K4me3 mark is almost always found near the TSS of active genes (Bernstein et al., 2002; Liang et al., 2004), however it can also be found in conjunction with H3K27me3 at inactive genes (Bernstein et al., 2006). There are six H3K4 methyltransferases Set1A and Set1B which are responsible for writing the majority of H3K4me3 (Ardehali et al., 2011; Wu et al., 2008), MLL1 and MLL2 which have been

found to have specific roles for H3K4me3 at Hox genes (Wang et al., 2009a), and MLL3 and MLL4 which have specific roles at enhancers (Herz et al., 2012; Hu et al., 2013).

Numerous acetylated lysines on histone H3 and H4 are strongly associated with transcription initiation and elongation. Histone acetylation is written by a diverse set of proteins in the histone acetyltransferases (HAT) family (Marmorstein and Zhou, 2014). Histone lysine acetylation in the globular region of histones is thought to relax the interaction of DNA with histones, thus allowing access of DNA to the transcription mechanism (Kebede et al., 2015; Lawrence et al., 2016). Acetylation also serves as a binding site for bromodomain containing enzymes such at BPTF which is part of the nucleosome remodeling factor (NURF) complex which is also necessary for allowing access to DNA during transcription (Li et al., 2006).

H3K36me3 is specifically associated with transcriptional elongation. One of several H3K36 HMTs, Set2, associates with active PolII during elongation (Kizer et al., 2005). H3K36me3 specifically marks transcriptionally active exons (Kolasinska-Zwierz et al., 2009) internal from the transcription start site and, as mentioned above, has a role in inhibiting transcription initiation away from the TSS through recruitment of DNA methyltransferases (Baubec et al., 2015; Morselli et al., 2015; Neri et al., 2017), HDACs (Carrozza et al., 2005; Keogh et al., 2005), and other factors (Wen et al., 2014).

1.12. Role of MLL1 in Cellular Identity Regulation

MLL1 is a H3K4 methyltransferase that together with MLL2 has been found to have a specific role at Hox genes, and loss of MLL1/2 function in cultured cells largely affects H3K4me3 at *Hox* genes and does not affect H3K4me3 at most other genes (Wang

et al., 2009a). *MLL1* knockout has been found to result in loss of transcription of, and the H3K4me3 mark at, a more specific set of Hox genes than MLL1/2 loss of function (Wang et al., 2009a). These results were obtained from heterogeneous MEF cells and confounding effects on cell fate decisions and/or intrinsic Hox cluster regulation may obscure the specific roles for MLL1 for this study. Due to numerous MLL1 translocations in hematopoietic malignancies, a major focus to understanding the role of H3K4 methylation has been on MLL1 (Hess, 2004; Shilatifard, 2012). Loss of MLL1 is embryonic lethal due to hematopoietic deficiency (Hess et al., 1997; Yagi et al., 1998), and also results in defects in neurodevelopment (Ayton et al., 2001; Yu et al., 1998). *Mll1* haplodeficiency causes homeotic transformation resulting in malformation of the spine and ribs due to disregulation of *Hox* gene expression (Yu et al., 1995).

Conditional knockout of *Mll1* in hematopoietic and neurogenic cells has shed insight into specific roles in regulation of cellular identity. *Mll1* KO in hematopoietic stem cells results in disregulation and loss of expression of several *Hox* genes and *Cdx4*, a closely related homeodomain containing transcription factor, leading to hematopoietic failure (Ernst et al., 2004a; Jude et al., 2007). Exogenous expression of any of the affected Hox genes or Cdx4 results in partial rescue of hematopoietic colony formation in vitro. Loss of MLL1 in neural precursors *in vivo* results in accumulation of precursor cells in the subventricular zone and failure to initiate neurogenesis and migrate due to loss of expression of the homeodomain transcription factor Dlx2 (Lim et al., 2009). *In-vitro Mll1* KO neural precursors can only differentiate to glial lineages, however exogenous Dlx2 expression can rescue neural differentiation.

While *Mll1* KO is embryonic lethal, deletion of the C-terminal methyltransferase Set domain results in viable mice with homeotic defects resembling *Mll1* haploinsufficiency (Terranova et al., 2006). Loss of the MLL1 Set domain in hematopoietic cells also results in normal hematopoiesis (Mishra et al., 2014). These results have been interpreted to suggest that MLL1 has a role in gene expression beyond its HMT activity. Indeed, examination of H3K4me3 at direct MLL1 targets *Dlx2* and *Hoxa9* in neural and hematopoietic *Mll1* KO finds no change to H3K4me3 at these genes (Lim et al., 2009; Mishra et al., 2014). The functional, non-HMT, role of MLL1 continues to be investigated. Changes to H3K4me1, DNA methylation, H3K27 methylation and histone acetylation have been reported at MLL1 target genes in *Mll1* KO cells to explain decreased gene expression in the absence of changes to H3K4me3 (Lim et al., 2009; Mishra et al., 2014; Terranova et al., 2006), however a consensus mechanism has not yet emerged.

1.13. Role of DNA Methylation in Cell Identity Specification and Differentiation

Until recently, it was thought that DNA methylation was gained with developmental progress and with age and faithfully maintained by DNMT1 during mitosis. Through identification of mammalian enzymes with homology to the enzyme producing base J in Trypanosomes, the role of Tet proteins in hydroxylation of methylated DNA, which was previously thought to be an accident of oxidative insult, was discovered (Tahiliani et al., 2009). When methylated cytosine is hydroxylated, it is no longer bound by methyl DNA binding (MBD) proteins which repress transcription

(Valinluck et al., 2004), or by DNMT1, and may be removed by subsequent oxidation steps and DNA excision repair, or by dilution through DNA replication during motisos (Rasmussen and Helin, 2016; Valinluck et al., 2004; Wu and Zhang, 2014).

While DNA methylation has a clear mechanism for propagation through the cell cycle through DNMT1 (Hermann et al., 2004), its specific roles in regulating epigenetic identity has been unclear. With the recent discovery of Tet based DNA demethylation, a fundamental change in the role of DNA methylation has emerged and necessitated reassessment of previous work and previous conceptions regarding DNA methylation. Out of this, a new role for DNA methylation has emerged in which DNA methylation maintains gene repression until specific triggers activate demethylation thus facilitating gene expression. The strongest evidence for this role are mutations of Tet genes in myeloid malignancies (Abdel-Wahab et al., 2009; Delhommeau et al., 2008) and mutation of IHD1/2 genes resulting in aberrant proteins which convert the Tet substrate alpha-ketoglutarate to a Tet inhibitor 2-hydroxygluterate (Figueroa et al., 2010). Presumably the loss of Tet function in these malignancies results in inefficient demethylation (and derepression) of genes required to initiate differentiation thereby resulting in excess proliferating progenitors (Song et al., 2013a, 2013b)..

The dynamic regulation of global DNA methylation has been intensely studied in early development and in germ cells. Gain of methylation at specific genes that are only expressed in early development has also been determined (Meissner et al., 2008). Globally, 70 to 80% of CpGs are methylated and during development, only about 22% of CpGs exhibit changes to their methylation status, and most changes occur in regulatory regions rather than proximal to transcription start sites (Ziller et al., 2013). While specific

demethylation events during development and differentiation are hypothesized, determination of stage specific demethylation events at specific genes and regulatory regions, and how these demethylation events are triggered require further characterization.

1.14. Epigenetic Regulation of Satellite Cells and Myogenesis

In quiescent satellite cells a majority of the DNA is tightly packed in facultative heterochromatin in a H3K20me3/Suv4-20h1 dependent manner. (Boonsanay et al., 2016). Upon activation satellite cell nuclei expand as chromatin condensation is relaxed, thereby allowing further epigenetic changes and activation of MRF and myogenic gene expression. In the absence of Suv4-20h1 global H3K27me3 levels are also decreased and MyoD expression is upregulated in satellite cells (Boonsanay et al., 2016), however it has not been determined if MyoD is directly repressed by H3K20me3 or H3K27me3 in quiescent satellite cells. MyoD expression is also repressed by histone H1B recruitment by Msx1 (Lee et al., 2004), and deposition of H3.3 is associated with its activation (Yang et al., 2011).

Myogenin and other genes required for myogenic function such as *creatine kinase* (*ckm*) and *MHCIIb* have been determined to be repressed by Ezh2/H3K27me3 in C2C12 satellite cells (Caretti et al., 2004; Juan et al., 2009; Seenundun et al., 2010). After initiation of differentiation, expression of *Ezh2* is lost as myogenic gene expression is upregulated. Coinciding with loss of Ezh2 is recruitment of UTX to myogenic genes resulting in demethylation of H3K27 (Seenundun et al., 2010). A requirement for Ezh2 has also been established for repression of myogenic genes *in vivo*, thereby preventing

loss of satellite cells (Caretti et al., 2004; Juan et al., 2011). These results are however partially contradicted by a report finding that *myogenin*, *ckm* and *MHCIIb* are not marked by H3K27me3 in satellite cells *in vivo* and loss of Ezh2 does not result in up regulation of these genes (Woodhouse et al., 2013). The *myogenin* proximal promoter has also been determined to be methylated prior to its activation and unmethylated when expressed (Lucarelli et al., 2001; Fuso et al., 2010; Palacios et al., 2010a; Oikawa et al., 2011; Miyata et al., 2015; Naito et al., 2016; Zhong et al., 2017). *Myogenin* has a non-GC rich promoter, which are often repressed by DNA methylation and are not consistently repressed by H3K27me3, which is usually found at promoters with high CG content (Smith and Meissner, 2013). H3K9me3, which is often found along with DNA methylation, is also found at the myogenin promoter and this mark is replaced with H3K9ac upon activation (Gillespie et al., 2009; Mal and Harter, 2003; Zhang et al., 2002).

Pax7 expression is repressed by H3K27me3 in embryonic stem cells (Boyer et al., 2006; Bracken et al., 2006; Lee et al., 2006) and is also H3K4 trimethylated (Zhao et al., 2007). This bivalent status is presumably resolved with loss of H3K27me3 as Pax7 is activated in myogenic precursors during early development. After terminal myogenic differentiation is initiated Pax7 expression is lost and it has been proposed that *in vivo*, inflammatory TNF alpha-activated p38 signaling promotes downregulation of Pax7 through PRC2/H3K27me3 (Palacios et al., 2010b).

1.15. Rationale and Objectives

While investigating whether there is a requirement for Pax7 to act through a specific HMT for transcriptional activation (McKinnell et al., 2008), we found that knockdown of MLL1 results in rapid loss of expression of both the Pax7 target *Myf5*, and *Pax7* itself. Considering the importance of Pax7 in regulation of satellite cells and regenerative myogenesis we hypothesized that MLL1 plays an important role in regulating *Pax7* transcription and hence myogenic regeneration. Because MLL1 and MLL2 have been implicated in activation of *Myf5* expression by Pax7 (Kawabe et al., 2012; McKinnell et al., 2008), we also aimed to determine the role and requirement for MLL1/2 in activation of *Myf5* by Pax7.

Chapter 2. Methods

2.1. Mice and Muscle Injury

Pax7$^{+/CreERT2}$-MLL1$^{fl/fl}$ mice were bred by crossing *Pax7*$^{+/CreERT2}$ mice kindly provided by Chen-Ming Fan (Lepper et al., 2009) with *Mll1* floxed mice kindly provided by Patricia Ernst (Ernst et al., 2004b). For excision of *Mll1*, mice were treated with 4 x IP injections of 100ul tamoxifen (Sigma, T5648) solution dissolved at 10mg/ml in corn oil, followed by maintenance on tamoxifen chow 500mg/kg (Envigo, TD.130857). Muscle injury was induced by longitudinal injection of 50µl of 10mg/ml cardiotoxin from *Naja mossambica mossambica* (Sigma, C9759) into TA muscles of to anesthetized animals. Mice were maintained for the designated times and sacrificed to harvest regenerating TA muscles. TA muscles were weighed and frozen with liquid nitrogen in embedding media (Sakura Finetek USA Inc., 4853) for sectioning.

Mice used for experiments and for generation of myoblast lines were males and females on a mixed 129/B6 genetic background. Mouse colonies were maintained in a certified animal facility in accordance with institutional guidelines as regulated by the Canadian Council of Animal Care. Protocols were approved by Animal Research Ethics Board at the University of Ottawa and are reviewed on an annual basis.

2.2. Image Acquisition

Imaging was performed on a Zeiss Axio Observer.D1 (EC Plan-Neofluar 20×/0.50 NA M27, EC Plan-Neofluar 40×/1.30 NA oil DIC M27, and Plan Apochromat 63×/1.40 NA oil DIC M27 objectives) with Zeiss Axiocam HR using Zen. Images were cropped and adjusted for brightness using Zen version 2.3 (Carl Zeiss AG). Images were

also cropped and assembled into figures using Microsoft PowerPoint and Adobe Illustrator.

For fibre Feret diameter determination, several images were combined to generate an image of the entire muscle section, borders of the muscle fibres were highlighted, the minimal inner diameter was determined and recorded. For histograms, Feret diameters were binned and quantified for each size category. Ferets for each muscle were averaged to generate an average Feret diameter for each muscle. Average fibre Feret diameter for muscles from each experimental condition was used for calculating average fibre Feret and as input for statistical analysis quantifying differences in muscles from each experimental condition.

2.3. Myoblast Isolation and Culture

For siRNA knockdown, myoblasts were isolated from C57BL/6J mice (Jackson Labs). For in-vitro analysis of loss of MLL1, MLL2 or MLL1 and MLL2 myoblasts were isolated from *Mll1*$^{fl/fl}$ mice (Jude et al., 2007) kindly provided by Patricia Ernst, *Mll2*$^{fl/fl}$ mice kindly provided by Francis Stewart (Glaser et al., 2006), or *Mll1*$^{fl/fl}$/*Mll2*$^{fl/fl}$, each crossed with *Rosa26*-CreER^{T2} mice (Seibler et al., 2003). Control myoblasts were isolated from littermates without *Rosa26*-CreER^{T2}.

Myoblasts were isolated from hind limb muscles from 3 to 4 week old mice essentially as previously described (Rando and Blau, 1994), muscles were minced with razor blades, enzymatically digested in serum free DMEM at 37C for 20 minutes with 1% w/v collagenase (Roche cat no. 11088831001), 0.4% w/v dispase II (Roche cat no. 04942078001). Muscle tissue digest was triturated by pipetting half way through

digestion. After digestion cells were filtered through a 100uM cell strainer (Fisher, 22363549) and brought to 10mls in PBS, collected by centrifugation, suspended in myoblasts medium and pre-plated to remove fibroblasts. After one week of culture with pre-plating, myoblast cultures were over 99% Pax7 positive.

Myoblast were cultured on collagen-coated dishes in Ham's F10 medium (Wisent, 318-051-CL) supplemented with 20% FBS and 5ng/ml of basic FGF (Millipore, GF003AFMG). Myoblasts were maintained by passaging every 2 to 3 days by washing once with PBS, adding 1 ml 0.05% Trypsin (Wisent, 325-044-EL) with 0.02% EDTA in PBS and incubating at room temperature until cells become detached, and replating at approximately 1/3 to 1/6. For in-vitro knockouts and non-Cre expressing controls, myoblasts were treated with 500nM (Z)-4-Hydroxytamoxifen (4-OHT, (Sigma, H7904-5MG)) for 7 days followed by 3 days culture in the absence of 4-OHT prior to collection of cells for analysis. Control cells were treated with EtOH vehicle; final EtOH concentration was 0.005%. Differentiation was triggered in DMEM (Wisent 319-016-CL) supplemented with 5% horse serum.

2.4. siRNA Knockdown

Myoblasts isolated from C57BL/6J mice were seeded in 6 well dishes. Wells were transfected with siRNAs consisting of three unique duplexes targeting each gene that were pooled in equal concentrations, or non-targeting siRNAs using Lipofectamine RNAimax (ThermoFisher, 13778150) using supplied protocol with 7.5ul Lipofectamine RNAimax per well with a final total siRNA concentration of 5nM. Media was changed 6 hours after transfection, after 24 hours cells were transfected again as above and media

was changed after 6 hours. Cells were harvested by trypsinization 48 hours after first transfection, or harvested or fixed for immunostaining at time points indicated during time course. siRNA sequences are listed in Table S5

2.5. RNA Isolation and Reverse Transcriptase Reaction

Cells were harvested by trypsinization, washed with PBS and directly subjected to RNA isolation. RNA was isolated by precipitation with chaotropic salts and purification on silica columns using Nucleospin RNA kit (Macherey-Nagel, 740955), according to manufacturer's instructions and including DNAse treatment. RNA was quantified using NanoDrop 1000 Spectrophotometer (ThermoFisher). 250ng to 1ug of RNA (for individual experiments, equal RNA was used for all samples) was used per 20ul reverse transcription reaction using SuperScript III Reverse Transcriptase (ThermoFisher, 18080044) according to manufacturers instructions using random heximers and running reverse transcriptase reaction at 50˚C for 1 hour.

2.6. Real-Time Quantitative PCR of cDNA

Reverse transcription product was used directly for qPCR reactions using 0.5ul to 1ul per qPCR reaction. iQ SYBR Green Supermix (Bio-Rad, 1708886) was used for PCR reactions according to manufacturers instructions, with SYBR-DNA-complex florescence serving to indicate generation of reaction product. qPCR data was generated on a real-time thermocycler with inbuilt florescent plate reader (Agilent Stratagene Mx3005P) during 40 cycles (15s at 95˚C, 30s at 60˚C, and 30s at 72˚C). Primer specificity was determined by denaturation curve.

For gene expression experiments, cycle threshold (Ct) values were converted to relative fold change in Excel (Microsoft) by the following formulas. For RT-qPCR relative quantification of reverse transcript cDNAs, fold change = 1.9^(eCt/cCt), where eCt = gene of interest (GOI) Ct for cDNA from experimental condition and cCt = control GOI Ct for control condition, and the 1.9 value assumes a 90% PCR efficiency. For individual gene expression experiments all samples were generated concurrently, RNA was quantified and quality confirmed by NanoDrop analysis, and equal RNA input was used for reverse transcription reactions. For all experiments each technical replicate (n) represents a single qPCR reaction for a individual sample generated from an RNA isolation and RT reaction. Primers for specific mRNAs are listed in Table S1.

2.7. Microarray Analysis

Total RNA was purified as described above. Samples were hybridized to Affymetrix MoGene 1.0 ST chipsets (Affymetrix, Santa Clara, CA) at StemCore Laboratories at the Ottawa Hospital Research Institute (Ontario, Canada). Raw data were RMA normalized using with the Bioconductor R package.

The RMA normalized data was log2 transformed to determine fold change in gene expression. Criteria used to derive Table 1: For downregulated genes, log-fold change of greater than one (that is, 2-fold cut-off), Affymetrix signal greater than 7 for the higher signal; For upregulated genes, 13 most highly upregulated genes with Affymetrix signal greater than 8 for the higher signal; For myogenic genes, selected genes with known roles in myogenesis with emphasis on homeodomain containing transcription factors, not listed in other sections of table; for MLL1 Targets, Hox genes

with Affymetrix signal greater than 7 and other select genes previously purported to be regulated by MLL1. Criteria used to derive Table S7: all Affymetrix probes with absolute log-fold change of greater than one (2-fold cut-off).

Microarray data are available from the Gene Expression Omnibus, National Center for Biotechnology Information (http://www.ncbi.nlm.nih.gov /geo/) under series accession no. GSE108339.

2.8. Proliferation Assays

For each control and experimental condition (n), cells from discrete plates were trypsinized as above, suspended in a total volume of 1.5mls and counted. 2 x 10^5 cells were seeded into 1 x 10 cm dishes for each (n). At indicated time points, cells were trypsinized and counted and fold proliferation was calculated by dividing total cells by total plated cells. Cells were diluted and replated as above at each time point and fold proliferation for secondary and tertiary time points were calculated by multiplying the reciprocal dilutions for prior time points by fold proliferation for current time point.

2.9. Western Blots

Cells were harvested by trypsinization, washed 1 x with cell culture medium and 1 x with PBS and frozen or used directly. Fresh or frozen cells were suspended in lysis buffer (10mM Tris Ph7.6/0.5% triton-x/150mM NaCl) with EDTA-free protease inhibitors (Roche, 05 892 791 001) on ice and quantified using Bio-Rad Protein Assay Dye Reagent Concentrate (Bio-Rad, 5000006). 10 to 25 ug protein was diluted into 10 to 20 ul total volume in SDS-PAGE loading buffer (final concentration 50mM Tris pH 6.8,

2% SDS, 6% (v/v) Glycerol, 2mM DTT, 0.01% (w/v) Bromophenol Blue). Samples were heated to 99˚C for 5 minutes and vortexed twice during incubation. Samples were loaded into SDS-PAGE acrylamide gels, electrophoresed and transferred to Immobilon-P membrane (Fisher, IPVH00010) using standard protocols. All blots were blocked with 20% powdered skimmed-milk in PBS for 1 hour, incubated for 1 hour with primary antibodies in PBS with 10% powdered skimmed-milk, washed 3x 10 minutes with 0.5% Tween-20 in PBS, incubated with isotype appropriate HRP conjugated secondary antibodies, in PBS with in 10% powdered skimmed-milk, washed 3x 10 minutes with 0.5% Tween-20 in PBS, enveloped with chemiluminescent substrate and exposed to film or imaged with FluorChem HD2 imaging system (Alpha Innotech). Film was scanned to JPEG using an EPSON perfection 4990 desktop scanner. Images were cropped and rotated in Preview (Macintosh OS), and were assembled into figures using PowerPoint (Microsoft). Antibodies are listed in Table S6.

2.10. Western Blot Quantification

Western blot bands for the protein of interest (Pax7) and standard (tubulin) were quantified using image J (https://imagej.nih.gov/ij/docs/menus/analyze.html#gels) by generating a density histogram of the lanes and determining the area under the curve for bands of interest. For each sample set (n) the Pax7 value was normalized to the standard value and a ratio of control Pax7 to experimental (*Mll1* KO) Pax7 was determined. Each (n) represents a separate experiment using conditional knockout myoblasts isolated from individual mice.

2.11. Immunostaining

Sections were cut to 12µm cross sections for immunostaining. Sections or cultured cells were fixed with 2% paraformaldehyde (Electron Microscopy Sciences, 51710) for 20 minutes at room temperature, washed with PBS, remaining paraformaldehyde was quenched with 100mM glycine for 5 minutes, and washed 2 x with PBS. Fixed cells were blocked in blocking buffer (2% BSA, 5% horse serum, 0.5% triton-x in PBS) for 1 hour at room temperature or ON at 4C. Blocked cells were incubated with primary antibodies for 1 hour at room temperature, washed with PBS, incubated with secondary antibody for 1 hour at room temperature, washed with PBS, and mounted using PermaFluor Aqueous Mounting Medium (ThermoFisher, TA-006-FM) with 1ug/ml Hoechst 33258 (Invitrogen H3569).

2.12. Chromatin Immunoprecipitation

6 x 100 mm plates of myoblasts at 20% confluence were trypsinized and suspended in myoblast culture media, pelleted at 1000 x g for 5 minutes, washed 1x with media, pelleted, and washed 1 x with PBS. Cells were suspended in 1 ml of 1% formaldehyde (Electron Microscopy Sciences) and crosslinked for 20 minutes at room temperature with mixing by inversion every 5 minutes. Cells were washed 3 x in PBS with 20% horse serum, and suspended in 250ul 10mM Tris Ph7.6/0.5% triton-x/150mM NaCl with protease inhibitors in ice. Protein concentration was determined by Bradford assay, and samples were diluted to equal protein concentration and volume was reduced to 250ul where necessary. Cells were sonicated in 1.5ml tubes using a Bioruptor sonicator (Diagenode) at 4C using 100% power 30 seconds on 1 minute off for 1 hour.

Sonicated samples were centrifuged at 20,000g at 4C for 20 minutes and supernatant was transferred to a new tube.

100ul of sonicated sample was transferred to 1 well of an 8 well PCR strip tube with 2ug antibody for each triplicate immuno precipitation (IP) (rabbit anti H3K4me3 (Millipore, ab8580), rabbit anti-H3K27me3 (Millipore, ab6002), or normal Rabbit IGG (Millipore, 12-370), or mouse anti-MLL1 N-terminal (Millipore, 05-764), or normal Mouse IGG (Millipore, 12-371)), and rotated at room temperature for 1 hour. For mouse anti-MLL1 IP and normal mouse IgG IP control, 2ug of rabbit anti mouse antibody (Jackson, 315-005-008) was added to amplify protein A/G binding, and samples were rotated for an additional 30 minutes. 25ul of washed magnetic protein A/G beads were added to each well and samples were rotated for and additional 30 minutes. Beads were isolated using a custom built 8 well strip magnetic separator (Gregory C. Addicks) and washed 5 x with 100 ul of 150mM NaCl with 10mM Tris Ph7.6, 0.5% Triton X-100.

Bound DNA was eluted in 100ul elution buffer (TE (10mM Tris, pH 8.0, 0.1mM EDTA)(IDT 11-05-01-13)) with 0.25% SDS and 10ug/ml proteinase K (New England BioLabs, P8107S) at 50˚C for 2 hours with rotation, inputs were diluted 1/20 into 100ul elution buffer and treated as IPs. Magnetic beads were magnetically separated from elution and supernatants were transferred to new strip tubes. 4ul of 5M NaCl was added to each supernatant and samples were reverse-crosslinked at 56˚C overnight. Eluted DNA was purified with NucleoSpin Gel and PCR Clean-up (Macherey-Nagel, 740609) using a protocol for samples containing SDS with buffer NTB (Macherey-Nagel, 740595) and eluted in 50ul for assessment by qPCR.

2.13. Methyl DNA Immunoprecipitation

2 x 100 mm plates of myoblasts at 20% confluence were trypsinized and suspended in myoblast culture media, pelleted at 1000 x g for 5 minutes, washed 1x with PBS and pelleted. DNA was isolated from cells using NucleoSpin Tissue kit (Macherey-Nagel, 740952) and quantified using a NanoDrop 1000 Spectrophotometer (ThermoFisher). 3ug DNA was diluted into 130ul TE and sheared to 500bp using a Covaris S220 Focused-ultrasonicator in microTUBE AFA Fiber Snap-Cap tubes (Covaris, PN 520045) using the recommended settings for purified DNA shearing. Sheared DNA was re-purified using NucleoSpin Gel and PCR Clean-up (Macherey-Nagel, 740609) using buffer NTI diluted 3 x with water to remove low MW DNA. Purified sonicated DNA was quantified using NanoDrop.

1ug purified sonicated DNA was added to 1 well of a 8 well PCR strip tube in a total of 50ul binding buffer (10mM Tris Ph7.6, 0.5% Triton X-100, 150mM NaCl). DNA was denatured at 95C for 5 minutes and transferred directly to ice. 1ug mouse anti-5-methylcytosine antibody clone 33D3 (Millipore, MABE146) was added to each well and samples were rotated at room temperature for 1 hour. To amplify binding to protein A/G beads, 2ug of rabbit anti-mouse antibody (Jackson, 315-005-008) was added and samples were rotated for an additional 30 minutes. 25ul of washed magnetic protein A/G beads were added to each well and samples were rotated for 30 minutes. Beads were isolated using a custom built magnetic apparatus (Gregory C. Addicks) and washed 5 x with 100ul of binding buffer.

Bound DNA was eluted in 100ul elution buffer (TE (10mM Tris, pH 8.0, 0.1mM EDTA)(IDT 11-05-01-13)) with 0.25% SDS and 10ug/ml proteinase K (New England

BioLabs, P8107S) at 50˚C for 2 hours with rotation. Magnetic beads were magnetically separated from elution and supernatants were transferred 1.5ml tubes. Eluted DNA was purified with NucleoSpin Gel and PCR Clean-up (Macherey-Nagel, 740609) using a protocol for samples containing SDS with buffer NTB (Macherey-Nagel, 740595) and eluted in 50ul for assessment by qPCR.

2.14. RT-qPCR and qPCR of ChIP and meDIP DNA

2.5 to 5 ul of ChIP or meDIP DNA was used per PCR reaction, input DNA for ChIP and meDIP was diluted 1/20 and a corresponding volume was used per reaction. iQ SYBR Green Supermix (Bio-Rad, 1708886) was used for PCR reactions according to manufacturers instructions, with SYBR-DNA-complex florescence serving to indicate generation of reaction product. qPCR data was generated on a real-time thermocycler (Agilent Stratagene Mx3005P) during 40 cycles (15s at 95˚C, 30s at 60˚C, and 30s at 72˚C). Primer specificity was determined by a denaturation curve.

ChIP and MeDIP percent input values were calculated in Excel by the following formula. Percent input = (1.9^(pCt/iCt))*5 where pCt = Ct value for IP DNA, iCt = Ct value for 1/20 diluted input DNA, and 1.9 value assumes a 90% PCR efficiency. For ChIP and MeDIP experiments each replicate (n) represents individual IPs of individually isolated and sonicated samples followed by single qPCR reactions for each IP.

2.15. Plasmids

All plasmids have been deposited to Addgene. CMV-Pax7d and CMV-Myf5 were expressed from pHAN-Pax7d(puro) and pHAN-Myf5(puro) retroviral vectors described

previously (Seale et al., 2004; Ishibashi et al., 2005) which are based on the pHIT retroviral system (Soneoka et al., 1995). CMV-Asb4, CMV-Fgfr4, CMV-Lbx1, CMV-Six2 and CMV-Dlx1 were all expressed from pHAN vectors, pHAN-Asb4(puro), pHAN-Fgfr4(puro), pHAN-Lbx1(puro), pHAN-Six2(puro), pHAN-Dlx1(puro), which were created for this project. New plasmids were created by amplifying respective cDNAs from total myoblast RNA reverse transcriptase reaction products that were produced as described above. cDNAs were cloned using PCR primers flanked with restriction sites, restriction digesting PCR products, and ligating restriction enzyme cut cDNAs into like cut plasmids or plasmids cut to make complementary ends. Plasmids were verified by sequencing to contain in-frame cDNAs matching mouse NCBI sequences. Tet-ON Pax7 was created by amplifying Pax7d from pHAN-Pax7d(puro) via PCR with primers containing appropriate Gateway sequences flanking PCR product and sub-cloning Pax7d into pCLX-pTF-DEST-EBR (Giry-Laterrière et al., 2011) using the Gateway system (Invitrogen).

2.16. Virus Production, Infection and Selection

Adenovirus was produced by transfection of Phoenix-ECO cells (ATCC CRL-3214) with Lipofectamine 2000 (ThermoFisher 11668019) according to manufacturers instructions. After 48 hours, media was collected and passed through a 0.45 um filter. Myoblasts, plated in 10 cm dishes were infected with 1 ml of virus supernatant. After 48 hours cells were selected with 3ug/ml puromycin for 5 days and maintained on 0.5ug/ml puromycin.

2.17. Transfection and Selection of Stable Tet-ON Cell Lines

Myoblasts were plated into 10 cm dishes and transfected with linearized plasmid with FuGENE HD (Promega, E2311) according to manufacturers instructions. After 24 hours cells were split to 10 x 10 cm dishes and selected with 2ug/ml blasticidin (ThermoFisher, R21001). After 1-2 weeks, well separated colonies were aspirated with wide bore pipette and plated in 6 well dishes. Cells were trypsinized and a portion was frozen at -80 in 10% DMSO in myoblast medium. Remaining cells were treated with 4-OHT for 1 week and a portion collected for western blot. Further remaining cells were treated with 3ug/ml Doxycycline (Dox) for 1 week to activate Tet-ON Pax7 and cells collected for western blot. Western blot was used to ensure that the Tet-ON plasmid was silent in the absence of Dox and activated with Dox. About 5% of colonies showed no Pax7 expression after *Mll1* KO and strong Pax7 expression with Dox.

2.18. Isolation of Satellite Cells with Florescence Activated Cell Sorting

Hind limb muscles from *Myf5*-Cre/Rosa-YFP mice were enzymatically digested, filtered and pelleted as for myoblast isolation and culture above. Cell pellets were suspended in 20% FBS in PBS and re-pelleted. The pellet was suspended in 1ml FACS buffer (5% FBS in PBS with 1mM EDTA) with 3 ul APC-conjugated mouse anti-integrin-alpha7 (clone R2F2) (University of British Colombia AbLab, 67-0010-10) and 2ul each of phycoerythrin (PE)-conjugated mouse anti-Sca-1 (clone D7) (BD Biosciences, 553108), mouse anti-CD45 (clone 30-F11) (BD Biosciences, 12-0451-83), mouse anti-CD31 (clone 390) (BD Biosciences, 12-0311-81), and mouse anti-CD11b (clone M1/70) (BD Biosciences, 12-0112-81), and with 1ug/ml Hoechst 33342. Cells were incubated in the

dark at 4˚C for 20 minutes. 9mls FACS buffer was added, mixed, and cells pelleted. Cells were suspended in 1.5mls, transferred to FBS coated FACS tubes and APC positive, PE negative cells were divided into YFP+ and YFP– fractions using a MoFlo XDP (Beckman Coulter) cell sorter at StemCore Laboratories, Ottawa Hospital Research Institute. Isolated cells were transferred to a FBS coated 1.5ml tube, pelleted and stored at –80 for meDIP.

2.19. Statistical Analysis

All quantitative data are expressed as mean standard error of the mean ± SEM, represented as error bars. Statistical analysis was performed on at least three biological replicates (for *in-vitro* myoblasts derived data, biological replicates are separately treated cells from the same animal) and significance was determined by Student's t test. P-values for relevant comparisons, which achieve statistical significance, are indicated in figures. Non-significance for relevant comparisons is also indicated. P-values of < 0.05 were considered statistically significant. All *in-vitro* myoblasts derived data is representative of at minimum two separate experiments using cells isolated from individual mice.

Chapter 3 - Results

All experiments were performed in their entirety by the author except for the following. Those presented in figures 5, 6 and 7, which were performed by Caroline Brun with assistance by Natasha Mercier and the author. Affymetrix data was generated by our in-house microarray facility StemCore Laboratories from mRNA samples submitted by the author.

3.1. siRNA Knockdown of MLL1 Dysregulates *Myf5* and *Pax7* Expression

Pax7 is critical for specification of muscle stem and progenitor cells, and is required for postnatal muscle growth and regeneration (von Maltzahn et al., 2013a; Seale et al., 2000). It was previously determined that Pax7 acts to activate gene expression through interactions with MLL1/2 (Kawabe et al., 2012; McKinnell et al., 2008). Our first aim was to determine if there was a specific H3K4 methyltransferase upon which Pax7 was dependent upon for deposition of the H3K4me3 mark at, and activation of, *Myf5* expression.

To determine if there is a requirement for a specific H3K4 HMT for Pax7 to activate target genes, individual H3K4 HMTs (*Mll1*, *Mll2*, *Mll3*, *Mll4*, *Setd1a* and *Setd1b*) were knocked down with siRNA in cultured primary myoblasts. Pax7 has previously been determined to activate *Myf5* expression (McKinnell et al., 2008) and *Myf5* expression was therefore used as a readout for Pax7-HMT activity. We found that knockdown of *Mll1* results in decreased *Myf5* mRNA expression while knockdown of other individual H3K4 HMTs had no significant effect (Figure 4A, 4B and 4C).

Previously, it was found that MLL1 regulates expression of *Hox* genes and other homeodomain containing transcription factors (Ernst et al., 2004a; Jude et al., 2007; Lim

et al., 2009; Terranova et al., 2006; Wang et al., 2009a; Yu et al., 1995). Therefore, because the paired box homeodomain containing transcription factor Pax7 has a role of importance in myogenesis (von Maltzahn et al., 2013a; Seale et al., 2000), we also aimed to determine whether *Pax7* expression was effected by *Mll1* KD. In addition to decreased *Myf5* expression, our knockdown of *Mll1* also resulted in decreased *Pax7* mRNA and protein expression as determined by RT-qPCR, western blot, and immunostaining (Figure 4A, 4D and 4E). A time course of *Mll1* knockdown indicated that *Pax7* and *Myf5* expression may decrease concurrently (Figure 4F), because Pax7 regulates *Myf5* expression the decrease in *Pax7* precludes establishment of a specific requirement for MLL1 in activation of *Myf5* by Pax7. Together these preliminary results suggested that a more rigorous examination of the role of MLL1 in myogenesis was warranted.

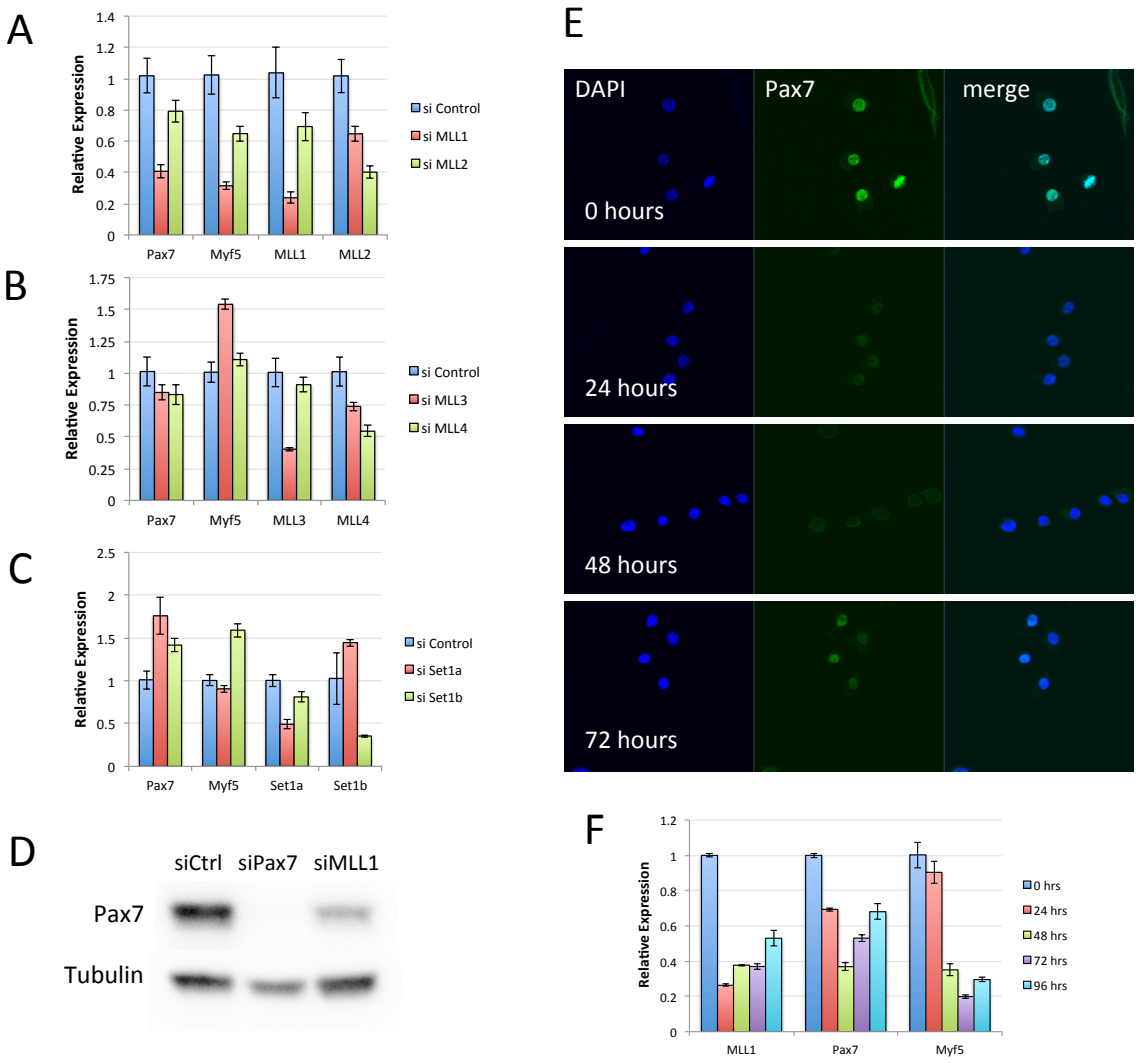

Figure 4. siRNA knockdown of MLL1 dysregulates *Myf5* and *Pax7* expression.

(A) RT-qPCR analysis of primary myoblasts with siRNA knockdown of MLL1 or MLL2 relative to control siRNA treated myoblasts. (n=3)

(B) As in (A) but with siRNA knockdown of *MLL3* or *MLL4*. (n=3)

(C) As in (A) but with siRNA knockdown of *Set1a* or *Set1b*. (n=3)

(D) Western blot of primary myoblasts treated with nonspecific siRNA or siRNA targeting *Pax7* or *MLL1*.

(E) Florescence microscopy showing DAPI (blue) and Anti-Pax7 immunostaining (green) of primary myoblasts treated with siRNA targeting *MLL1* for 0, 24, 48 or 72 hours.

(F) RT-qPCR analysis of primary myoblasts subjected to siRNA knockdown of *MLL1* after 0,24,48,72 or 96 hours. (n=3)

3.2. *Mll1* KO Results in a Regeneration Defect After Muscle Injury

Because MLL1 knockdown resulted in decreased expression of Pax7, which is critical for postnatal myogenesis (Seale et al., 2000; von Maltzahn et al., 2013a), we further investigated the role of MLL1 in adult myogenesis. To this end, conditional *Mll1* knockout (KO) mice with loxP sites flanking exon 2 of *Mll1* (Jude et al., 2007), $Mll1^{fl/fl}$, were crossed with mice expressing tamoxifen activated $CreER^{T2}$ from the *Pax7* locus (Lepper et al., 2009), $Pax7^{CE/+}$, to drive *MLL1* KO in satellite cells. Conditional *Mll1* KO was induced in Pax7 expressing cells by intraperitoneal injection of tamoxifen for 4 days. Because Pax7 is critical for myoblast proliferation (von Maltzahn et al., 2013a), mice were maintained on tamoxifen diet in order to ensure full recombination, as cells which escape recombination might out-proliferate *Mll1* KO cells, and eclipse the effects of *Mll1* KO.

One week after the first tamoxifen injection, control and tamoxifen treated tibialis anterior (TA) muscles were injected with cardiotoxin (CTX), PBS vehicle was injected into contralateral muscles as controls. Muscle regeneration and satellite cell content was assessed 7 or 21 days after CTX injection (Figure 5A).

Seven days post TA injections, CTX injected TA muscles had similar weight per body weight in control and tamoxifen treated mice (Figure 5B and 5C). 21 days after CTX injection, TA muscles in control mice exhibited regeneration-induced hypertrophy as compared to contralateral TA muscles. CTX injected TA muscles in mice with satellite cell *Mll1* KO were significantly smaller compared to uninjured contralateral muscles and showed scant growth from 7 to 21 days (Figure 5B and 5D). Tamoxifen had no effect on regeneration of control $MLL1^{fl/fl}$ mice (data not shown). These results indicate that loss of

MLL1 in Pax7 expressing satellite cells results in a gross regeneration defect, supporting a role for MLL1 in postnatal muscle regeneration.

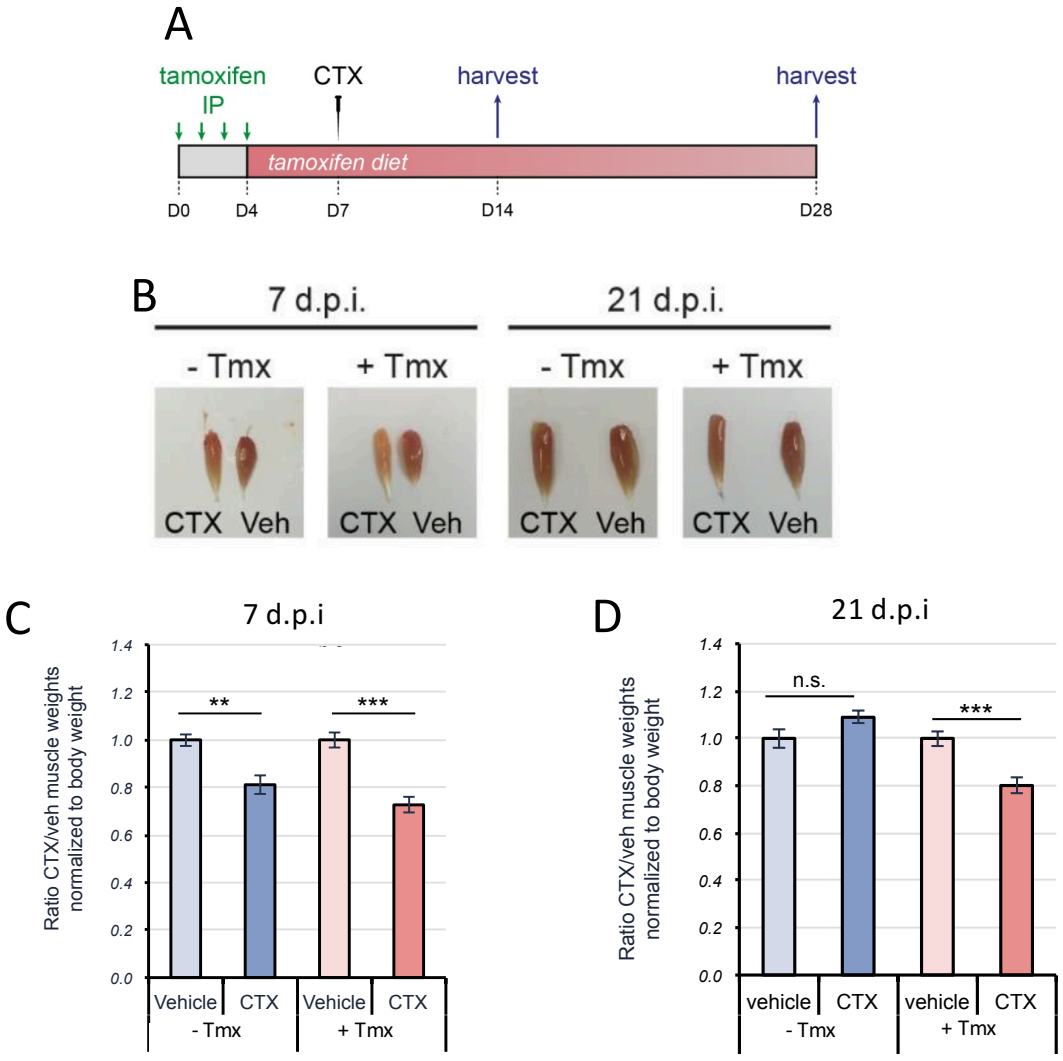

Figure 5. *Mll1* KO results in regeneration defect after muscle injury
(A) Schematic of time line for tamoxifen injections and muscle injury.
(B) Cardiotoxin (CTX) or vehicle (Veh) injected tibialis anterior (TA) muscles isolated from tamoxifen treated (+Tam) or untreated (-Tam) $Pax7^{CE}/Mll1^{fl/fl}$ mice either 7 days or 21 days after cardiotoxin or vehicle injections. (representative examples)
(C) Relative mass for vehicle or cardiotoxin injected TA muscles normalized to body weight from tamoxifen treated or untreated $Pax7^{CE}/Mll1^{fl/fl}$ mice either 7 days or 21 days after cardiotoxin or vehicle injections. (n=7)
(D) As in (C) but for 21 days after cardiotoxin or vehicle injections. (n=7)
*p<0.05, **p<0.01, ***p<0.001

3.3. Loss of MLL1 Deters Muscle Fibre Regeneration After Injury

To further determine the underlying effects resulting in the gross regeneration defect seen after CTX induced degeneration/regeneration when MLL1 is lost in Pax7 expressing satellite cells, isolated TA muscles were sectioned and stained. Regenerating muscle have nuclei located to the center of the muscle fibres which re-localize to the periphery of the muscle as fibres mature (Kelly and Zacks, 1969), therefore sections were stained with 4',6-diamidino-2-phenylindole (DAPI) which stains DNA, thereby marking the nucleus, to identify regenerating fibres. During muscle regeneration damaged areas are infiltrated with extracellular matrix proteins until replaced by regenerated muscle fibres therefore sections were also stained with wheat germ agglutinin (WGA) to show damaged areas of the muscle.

Sectioning of injured muscles 7 days post CTX injections revealed robust regeneration in TA muscles from control mice, while TA muscles from tamoxifen treated satellite cell *Mll1* KO mice were found to have substantial wheat gluten agglutinate (WGA) stained infiltrate between fibres, and fibres with smaller average Feret (Figure 6A and 6C). 21 days after CTX injections, *Mll1* KO TA muscles had decreased inter-fibre infiltrate, had fibres with centrally located nuclei and looked similar to control muscles. Regenerating *Mll1* KO muscles continued to have smaller fiber Ferets compared to regenerating control muscles (Figure 6B and 6D) indicating a continuing regeneration defect 21 days post CTX injection. Tamoxifen treatment of control $Mll1^{fl/fl}$ mice lacking Cre resulted in cardiotoxin induced regeneration similar to untreated $Pax7^{CE}/Mll1^{fl/fl}$ mice (data not shown). Together these results show that there is a marked delay and reduction in muscle regeneration when MLL1 expression is lost in satellite cells.

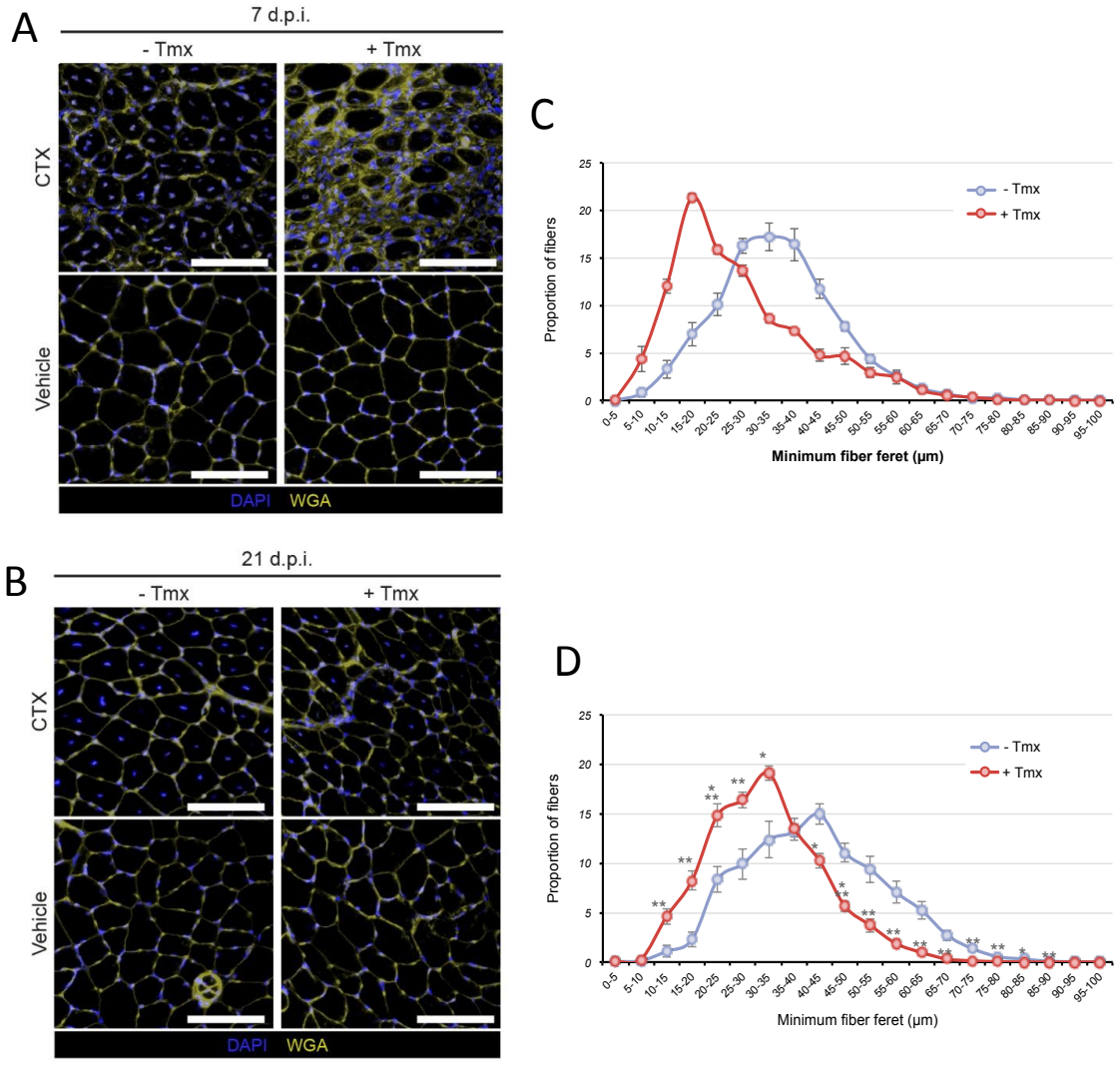

Figure 6. Loss of MLL1 deters muscle fibre regeneration after injury
(A) Sections of vehicle or cardiotoxin (CTX) injected TA muscles from tamoxifen treated (+Tam) or untreated (-Tam) $Pax7^{CE}/Mll1^{fl/fl}$ mice 7 days after cardiotoxin or vehicle injections. Wheat germ agglutinin (WGA), yellow. Nuclei stained with DAPI, blue. (representative images, bar=100µm)
(B) As in (A) except 21 days after muscle injury or sham.
(C) Fibre Ferets of cardiotoxin injected TA muscles from tamoxifen treated or untreated $Pax7^{CE}/Mll1^{fl/fl}$ mice 7 days after cardiotoxin. (n=7)
(D) As in (C) except 21 days after muscle injury or sham. (n=7)
*p<0.05, **p<0.01, ***p<0.001

3.4. *Mll1* KO Results in Loss of Satellite Cells After Injury

As knockout of *Mll1* in Pax7 expressing satellite cells resulted in a regeneration defect and siRNA knockdown of MLL1 resulted in decreased Pax7, which is necessary for myogenic proliferation, we next aimed to determine if the regeneration defect seen in *Mll1* KO in satellite cells was associated with decreased satellite and myogenic progenitor cells (mpcs) in regenerating muscle. During muscle regeneration, satellite cells and mpcs continue to express Pax7 prior to the initiation of differentiation. After differentiation is initiated, Pax7 is downregulated while myogenin is upregulated leading to terminal differentiation and fusion to form new muscle. Because regeneration is reliant upon Pax7 and myogenin expressing cells, sections were stained for Pax7 and myogenin to assess the quantity of myogenic progenitors.

Staining of sections of 7-day post CTX regenerating muscles for Pax7 or myogenin resulted in staining of cells located at the periphery of muscle fibres for both control mice and tamoxifen treated mice in which MLL1 is lost in satellite cells (Figure 7A). Both Pax7 expressing and myogenin expressing cells were greatly reduced in tamoxifen treated mice as compared to untreated mice (Figure 7B and 7C). While loss of Pax7 expression, and thus loss of Pax7-expressing cells might be expected with the loss of MLL1, the finding that there are also reduced myogenin-expressing cells, suggests that mpcs are indeed reduced with loss of MLL1. These results indicate that loss of MLL1 results in a reduction of myogenic progenitors during regeneration and suggests that the *Mll1* KO regeneration defect may be at least partly due a proliferation defect in the cells which directly contribute to the regenerating muscle.

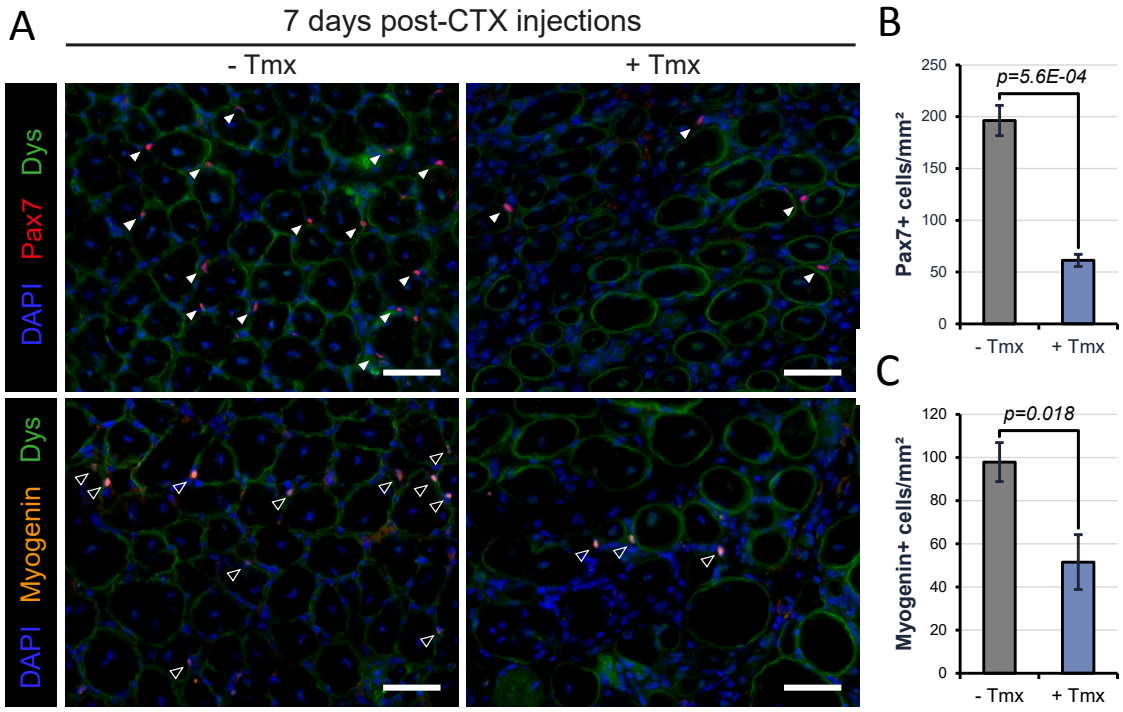

Figure 7. *Mll1* KO results in loss of satellite cells after injury
(A) Sections of CTX injected TA muscles from tamoxifen treated (+Tam) or untreated (-Tam) $Pax7^{CE}/Mll1^{fl/fl}$ mice 7 days after injury stained for Pax7, top panels (red, marked with solid white arrows) or Myogenin, bottom panels (orange, marked with open white arrows). Dystrophin (Dys, green) delineates the muscle fibres, and DAPI marks nuclei (blue). (representative images, bar=50µm).
(B) Pax7 positive satellite cells per square mm in TA muscle sections from tamoxifen treated (+Tam) or untreated (-Tam) $Pax7^{CE}/Mll1^{fl/fl}$ mice 7 days after injury. (n=5)
(C) Myogenin positive satellite cells per square mm in TA muscle sections from tamoxifen treated (+Tam) or untreated (-Tam) $Pax7^{CE}/Mll1^{fl/fl}$ mice 7 days after injury. (n=5).

3.5. Loss of MLL1 Results in a Strong Proliferation Defect in Primary Myoblasts

To more clearly define the role of MLL1 in myogenic cells, conditional *Mll1* KO myoblasts were derived from mice with tamoxifen activated $CreER^{T2}$ expression from the Rosa locus (Seibler et al., 2003). To knockout MLL1 in myoblast cultures, cells were treated with 4-hydroxy tamoxifen (4-OHT) for 7 days followed by a three-day wash out

(Figure 8A). Due to a strong proliferation defect in myoblasts lacking MLL1, 4-OHT treatment of myoblasts from *Pax7*^{CE}/*Mll1*$^{fl/fl}$ failed to produce cultures with > 80% *Mll1* KO. Greater Cre expression from the Rosa locus allowed for a rate of recombination over time that was faster than the rate of DNA replication during proliferation and resulted in > 99% recombination (data not shown).

4-OHT induced knockout of *Mll1* in cultured myoblasts resulted in an overt decrease in proliferation. While EtOH vehicle treated myoblasts doubled in population approximately every 24 to 36 hours, *Mll1* KO myoblasts took around 3 times as long per population doubling (Figure 8B). No difference in proliferation rate was seen in 4-OHT treated compared to EtOH vehicle treated myoblasts lacking CreER expression (Figure 8C), indicating that 4-OHT treatment alone had no effect on proliferation.

Previously it was found that *Pax7* KO results in loss of proliferation and precocious differentiation (von Maltzahn et al., 2013a). It may be that low levels of Pax7 expressed in *Mll1* KO cells may allow for slow, but ongoing, proliferation while maintaining the undifferentiated state. Overall, our results in myoblasts coincide with *in vivo* results showing that loss of MLL1 in Pax7 expressing satellite cells results in delayed regeneration and indicates that the observed regeneration defect *in vivo* is likely due to a proliferation defect in *Mll1* KO satellite cells.

To further assess proliferation in *Mll1* KO myoblasts, control and *Mll1* KO myoblasts were stained with antibody for the proliferation marker Ki67. *Mll1* KO resulted in a significant decrease in cells positively stained for Ki67 (Figure 8D and 8E), further supporting a role for MLL1 in proliferation of primary myoblasts. To determine if *Mll1* KO myoblasts were being lost through apoptosis cells were stained by terminal

deoxynucleotidyl transferase dUTP Nick-end labeling (TUNEL). Both control and *Mll1* KO myoblasts had ~2.5% of cells labeled with TUNEL indicating that the apparent decrease in proliferation in *Mll1* KO myoblasts is not the result of a loss of cells through an increase in apoptosis (Figure 8F and 8G).

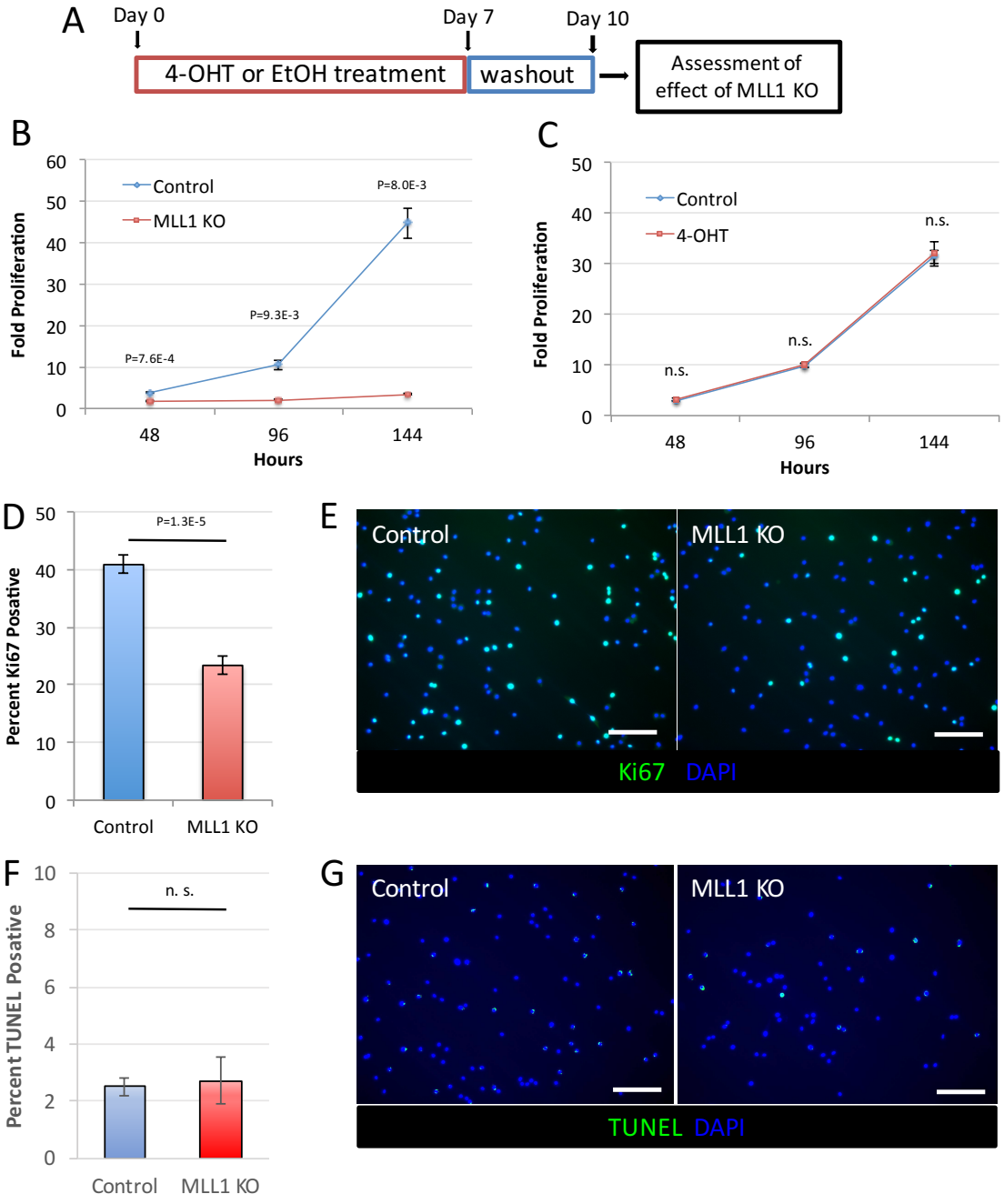

Figure 8. Loss of MLL1 results in a strong proliferation defect in primary myoblasts
(A) Schematic of in-vitro 4-OHT treatment used for Control and *Mll1* KO myoblasts.
(B) Proliferation of 4-OHT (*Mll1* KO) or ethanol (Control) treated $Mll1^{fl/fl}$/*Rosa*$CreER^{T2}$ myoblasts. Fold proliferation is cell count at each time point per cells plated at T=0. (n=3)
(C) As in (B) except myoblasts are derived from $Mll1^{fl/fl}$ mice without *Rosa*$CreER^{T2}$.
(D) Percent Ki67 positive for Control and *Mll1* KO myoblasts. (n=6)
(E) Representative fields of anti Ki67 stained Control and *Mll1* KO myoblasts.
(F) Percent TUNEL positive for Control and *Mll1* KO myoblasts. (n=3)
(G) Representative fields of TUNEL stained Control and *Mll1* KO myoblasts.

3.6. *Mll1* KO Results in Specific Changes to Gene Expression

To confirm and expand upon our previous results obtained using siRNA targeting *Mll1*, RT-qPCR was used to quantify mRNA expression for *Mll1*, *Pax7*, *Myf5*, *MyoD* and myogenin in *Mll1* KO myoblasts (Figure 9A). As was seen with *Mll1* siRNA, *Mll1* KO resulted in a decrease in *Pax7* mRNA expression to about 60% of control *Pax7* expression. Three *Mll1* conditional KO cell lines were assessed at least once for each cell line and *Pax7* mRNA expression in *Mll1* KO myoblasts was consistently ~ 60% of control *Pax7* expression levels (Figure 9A, 10A, 11E, 15B, 16A, 17B). This finding, that Pax7 expression always decreases by near exactly 60%, suggests a direct, rather than secondary or tertiary, change to the regulation of *Pax7* mRNA expression occurs with *Mll1* KO. A stronger decrease in mRNA expression was seen for *Myf5*, which was consistently expressed below 5% of control levels. Across all experiments *MyoD* and *myogenin* expression were not significantly affected by loss of MLL1.

To better understand what other gene expression changes occur with *Mll1* KO, microarray was used to broadly determine differences in mRNA expression between control and *Mll1* KO myoblasts (Table 1, Table S7 and Figure 9B). As with the *in vitro*

Mll1 KO experiments above, to avoid confounding variability, paired samples were obtained by treating conditional *Mll1* KO myoblasts with 4-OHT for 7 days followed by 3 days washout, while control cells were treated with EtOH vehicle. Cells were maintained at comparable density to avoid variability in paracrine signaling, which might also influence gene expression. RT-qPCR was used to confirm *Mll1* KO and a greater than 98% loss of *Mll1* mRNA was found at exon 2.

Previous comparisons of *Mll1* KO mouse embryonic fibroblasts (MEF) to control MEF found wide changes in gene expression (Wang et al., 2009a). Our samples generated fewer changes to gene expression than had previously been seen when gene expression had been compared between control and *Mll1* KO samples. The specificity of our results may be due to the relatively homogeneous nature of cultured myoblasts and possibly also due to our paired samples. Because H3K4 trimethylation is associated with active gene expression, it was expected that loss of MLL1 would result in decreased expression of genes specifically targeted by MLL1 and other secondary changes. Unexpectedly, less than 0.22% of probes (78 out of 35,557, of which only 15 were for protein coding mRNAs) showed a greater than 2-fold decrease in expression (Figure 9B, Table 1 and Table S7). Likely due to secondary effects of loss of MLL1, 2.6% of probes had a greater that 2-fold increase in expression (929 out of 35557). Confirming our RT-qPCR results, microarray indicated a modest 0.27% decrease in Pax7 mRNA expression in *Mll1* KO myoblasts (Table 1). Remarkably, the effect of *Mll1* KO was highly specific to *Myf5*. Among all genes, *Myf5* has largest decrease in expression and was the only gene with expression decreasing by more than 10-fold (Figure 9B and Table 1 and Table S7). Ankyrin repeat and SOCS box containing 4 (*Asb4*), was also strongly affected.

Microarray also found little change in expression for several genes involved in myogenesis, including homeodomain containing transcription factors with known roles in myogenesis (Table 1).

Previously, genes coding for Hox and homeodomain containing transcription factors were identified as targets of MLL1 (Ernst et al., 2004a; Lim et al., 2009; Wang et al., 2009a). Homeodomain containing transcription factors *Six2*, *Dlx1* and *Lbx1* were also among the few genes found to have a greater than 2-fold decrease in expression (Figure 9A and 9B and Table 1 and Table S7). Importantly, expression of other homeodomain containing genes which had previously been reported to be MLL1 targets that were downregulated with *Mll1* KO, such as some Hoxa group and Hoxc group genes (Ernst et al., 2004a; Wang et al., 2009a), and Dlx2 (Lim et al., 2009) were unchanged in our microarray results (Table 1). The finding that there was no change in expression of *Hoxc10* or *Dlx2* was confirmed by qPCR (Figure 9A). These results indicate a more specific role for MLL1 than was anticipated based on previous work.

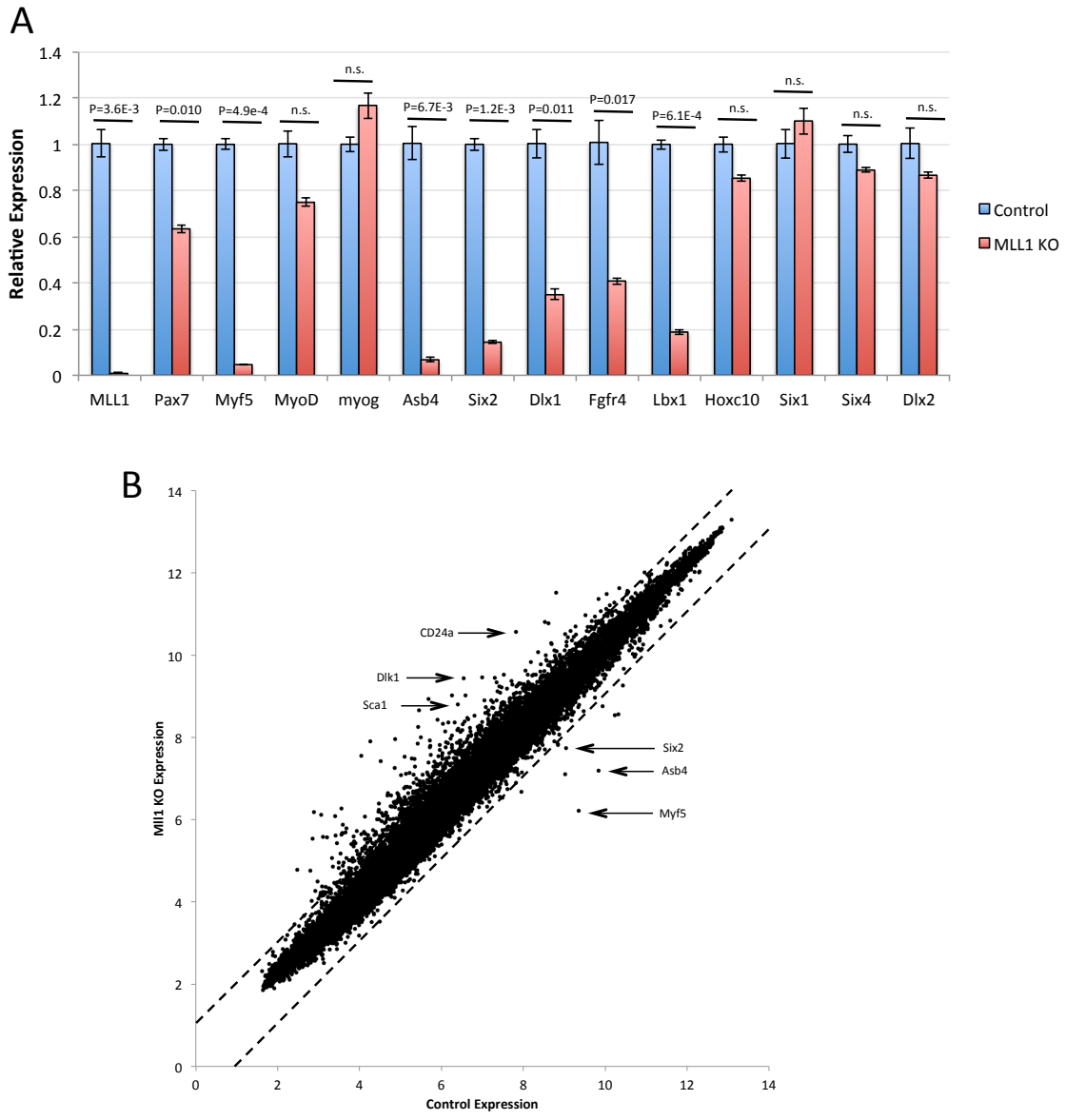

Figure 9. *Mll1* KO results in specific changes to gene expression
(A) RT-qPCR analysis of control and *Mll1* KO myoblasts treated as in Figure 8A. (n=3) (B) Dot blot of gene expression Affymetrix values as determined by microarray contrasting gene expression in control myoblasts to *Mll1* KO myoblasts. Upper and lower dashed lines mark 2 fold increase and decrease in expression.

Down in MLL1 KO

	Array Signal				Fold Change	
	Control	MLL1 KO			Array	qPCR
1	9.51	6.14	Myf5	–	10.33	20
2	9.99	7.12	Asb4	–	7.31	14.28
3	9.20	7.67	Six2	–	2.89	7.14
4	9.00	7.74	Dlx1	–	2.40	2.85
5	9.00	7.77	Fgfr4	–	2.34	2.43
6	7.64	6.46	Olfr767	–	2.27	
7	7.97	6.82	Lbx1	–	2.22	5.26
8	8.91	7.84	Lmnb1	–	2.11	
9	8.69	7.64	Cdc42ep3	–	2.07	
10	9.04	8.00	Lbr	–	2.05	
11	8.03	7.02	Cdkn2c	–	2.01	
12	10.61	9.61	Hist1h2bb	–	2.00	
13	9.90	8.90	Anp32a	–	2.00	

Up in MLL1 KO

	Array Signal				Fold Change	
	Control	MLL1 KO			Array	qPCR
1	5.84	8.87	Slc40a1	+	8.16	
2	5.60	8.59	Timp3	+	7.94	
3	5.02	7.89	Stmn2	+	7.33	
4	6.70	9.37	Dlk1	+	6.37	18.25
5	6.41	8.95	Sfrp2	+	5.83	4.64
6	7.97	10.50	Cd24a	+	5.76	4.96
7	7.15	9.40	Nnat	+	4.75	
8	6.75	8.95	RbEST47	+	4.62	
9	6.55	8.73	Ly6a (Ska1)	+	4.54	2.89
10	6.19	8.26	Krt18	+	4.22	
11	8.68	10.75	Nptx1	+	4.19	
12	7.68	9.46	Grem1	+	3.44	
13	7.51	9.28	Pgf	+	3.41	

Myogenic genes - Low / no change

Array Signal				Fold Change	
Control	MLL1 KO			Array	qPCR
12.15	12.27	Myod1	+	1.08	1.33
7.30	7.94	Myog	+	1.56	1.17
5.40	5.07	Myf6	–	1.26	1.70
6.44	6.42	Mef2b	–	1.01	
11.08	11.12	Mef2a	+	1.03	
6.25	7.69	Mef2c	+	2.71	
6.62	7.86	Myh1	+	2.36	
6.44	6.99	Pax3	+	1.47	
10.29	10.02	Pax7	–	1.21	1.58
6.97	6.53	Pitx2	–	1.36	
9.58	9.35	Tbx1	–	1.17	
11.02	11.13	Six1	+	1.08	
9.81	10.11	Six4	+	1.23	

MLL1 Targets

Array Signal				Fold Change	
Control	MLL1 KO			Array	qPCR
7.44	7.47	Hoxa6	+	1.024	
7.64	7.88	Hoxa7	+	1.18	
8.29	8.17	Hoxa9	–	1.085	
7.74	7.65	Hoxa10	–	1.062	
8.28	7.81	Hoxa11	–	1.381	
7.02	7.16	Hoxc5	+	1.099	
7.84	8.06	Hoxc6	+	1.164	
8.03	7.59	Hoxc8	–	1.36	
8.44	8.69	Hoxc9	+	1.189	
8.51	8.65	Hoxc10	+	1.102	0.854
10.44	10.79	Dlx2	+	1.269	0.867
6.41	5.85	Prdm16	–	1.468	
4.52	5.32	Evi1	+	1.742	

Table 1. Gene expression microarray comparison of control and *Mll1* KO myoblasts

Microarray data for control and *Mll1* KO myoblasts for genes downregulated by more than 2 fold in *Mll1* KO (top left), the top upregulated genes in *Mll1* KO (top right), myogenic genes and homeodomain containing transcription factor genes with known roles in myogenesis (bottom left), and for putative MLL1 targets (bottom right). Housekeeping genes *Gapdh*, *Hrpt1*, and *Actb* had fold change of less than +/– 1.01 (data not shown). Fold change Array is the log2 transformation of the absolute difference in microarray signal between control and *Mll1* KO. "+" or "–" indicates fold upregulation or downregulation respectively. Fold change by qPCR was obtained from independent samples. For *Hoxc10* and *Dlx2*, expression was slightly upregulated in microarray data samples, and downregulated in qPCR data therefore + fold change was used to indicate the microarray result and the less-than-1-value to indicate reciprocal ($fold^{-1}$) downregulation as determined by qPCR.

3.7. *Mll1* KO Does Not Induce or Effect Induction of Myogenic Differentiation

Previously it was found that *Pax7* KO in myoblasts results in precocious differentiation (von Maltzahn et al., 2013a). While Pax7 expression is decreased with *Mll1* KO, there was no increase in *myogenin* or myosin heavy chain 2a (*MyHC*), which are upregulated during myogenic differentiation (Bentzinger et al., 2012), in proliferating *Mll1* KO myoblasts (Figure 9A,10A and 10B), indicating that loss of MLL1 does not initiate differentiation.

Either Myf5 or MyoD are capable of activating of the myogenic program (Davis et al., 1987; Lassar et al., 1986; Rudnicki et al., 1993). While *Myf5* expression is lost in *Mll1* KO myoblasts, *MyoD* expression is maintained, so it would be expected that the ability to undergo myogenic differentiation would also be retained upon loss of MLL1, unless MLL1 is required for activation of genes necessary for progression through myogenic differentiation. In order to determine if *Mll1* KO myoblasts are indeed capable of normal activation of the myogenic program, control and *Mll1* KO myoblasts were cultured in low mitogen conditions which promote differentiation (Rando and Blau, 1994). Western blot and qPCR found little difference between control and *Mll1* KO myoblasts when genes that are up and down regulated during differentiation were assessed (Figure 10A and 10B), indicating that myogenic differentiation capability is retained. Immunostaining of differentiating myoblasts also showed similar expression of myosin heavy chain and myoblast fusion in control and *Mll1* KO (Figure 10C). Expression of *Mll1* is downregulated by ~80% in control myoblasts when placed in

differentiation conditions (Figure 10A), suggesting that decreased *Mll1* expression may partly contribute to downregulation of *Pax7* during normal myogenic differentiation.

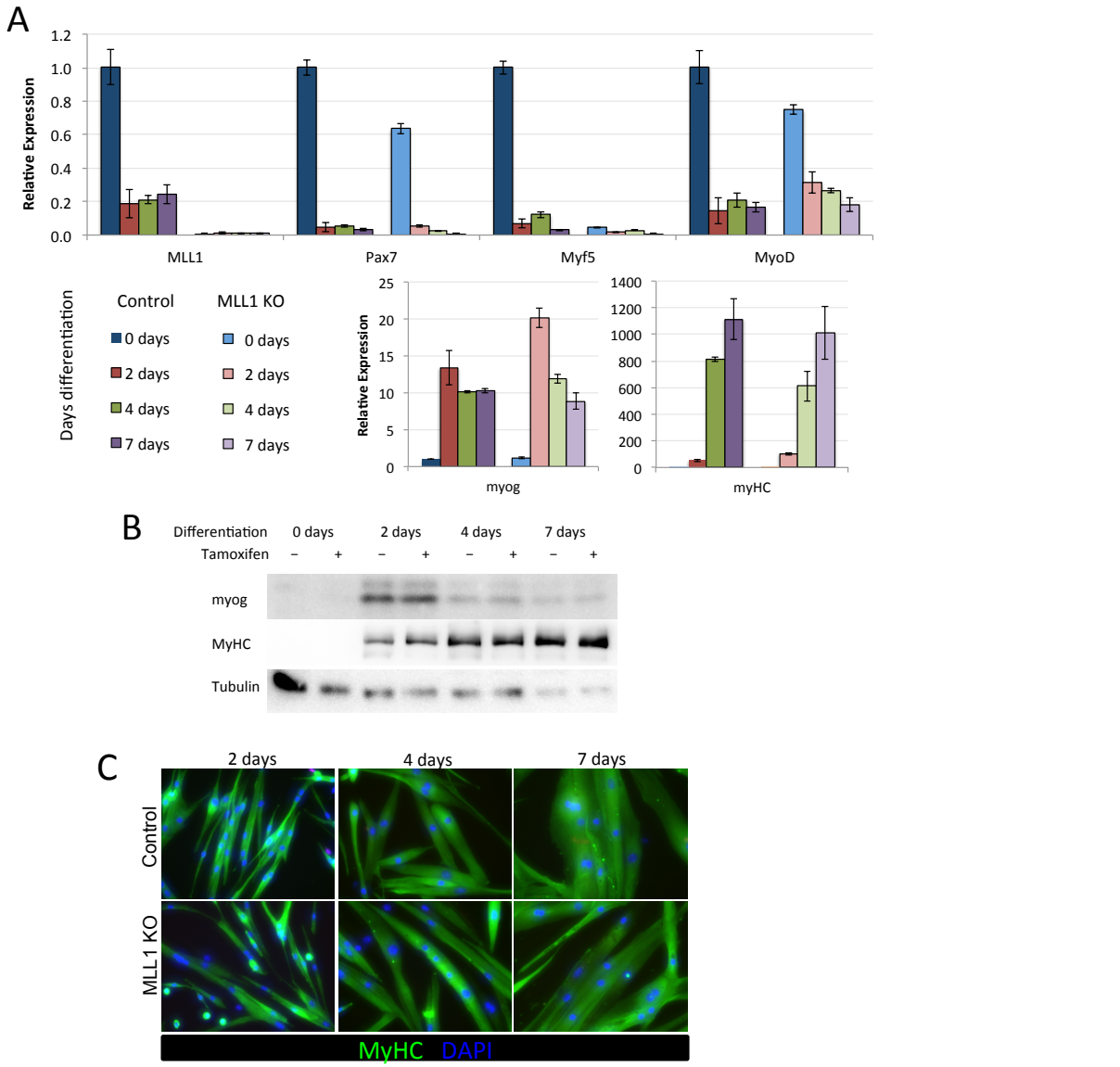

Figure 10. *Mll1* KO does not induce or effect induction of myogenic differentiation

(A) RT-qPCR analysis of control and *Mll1* KO myoblasts 0, 24, 48 and 72 hours after induction of differentiation. (n=3)

(B) Western blot of total cell lysate from control and *Mll1* KO myoblasts 0, 24, 48 and 72 hours after induction of differentiation using indicated antibodies.

(C) Differentiating control and *Mll1* KO myoblasts stained with DAPI (blue) and immunostained with anti-myosin heavy chain (green) 24, 28 and 72 hours after induction of differentiation.

3.8. *Mll1* KO Results in Loss of Pax7 Protein Expression

A clear role for Pax7 in activation of *Myf5* expression has been established (McKinnell et al., 2008). Because *Myf5* expression is lost in *Mll1* KO myoblasts, *Pax7* expression was assessed further to determine if changes to *Pax7* expression could account for the change in *Myf5* expression. While 4-OHT induced knockout of *Mll1* in cultured myoblasts consistently resulted in a 40% decrease of *Pax7* mRNA expression (Figure 9A), a greater effect was found for Pax7 protein expression, which was reduced by 83.6% as compared to vehicle control myoblasts (Figure 11A and 11B). 4-OHT treated myoblasts derived from siblings lacking Cre had no change in *Pax7* expression (Figure 11C). Immunostaining for Pax7 confirmed that Pax7 protein is lost upon *Mll1* KO (Figure 11D). Because of the discrepancy between the change in *Pax7* transcript and protein expression, primers targeting across the *Pax7* mRNA were used for RT-qPCR to confirm that the full *Pax7* transcript was being expressed. A consistent decrease in *Pax7* mRNA expression was found across the transcript suggesting normal transcription (Figure 11E). These results suggest that the change in *Myf5* expression found with loss of MLL1 may be due to loss of Pax7 and preclude establishing a requirement for Pax7 to activate *Myf5* expression through MLL1.

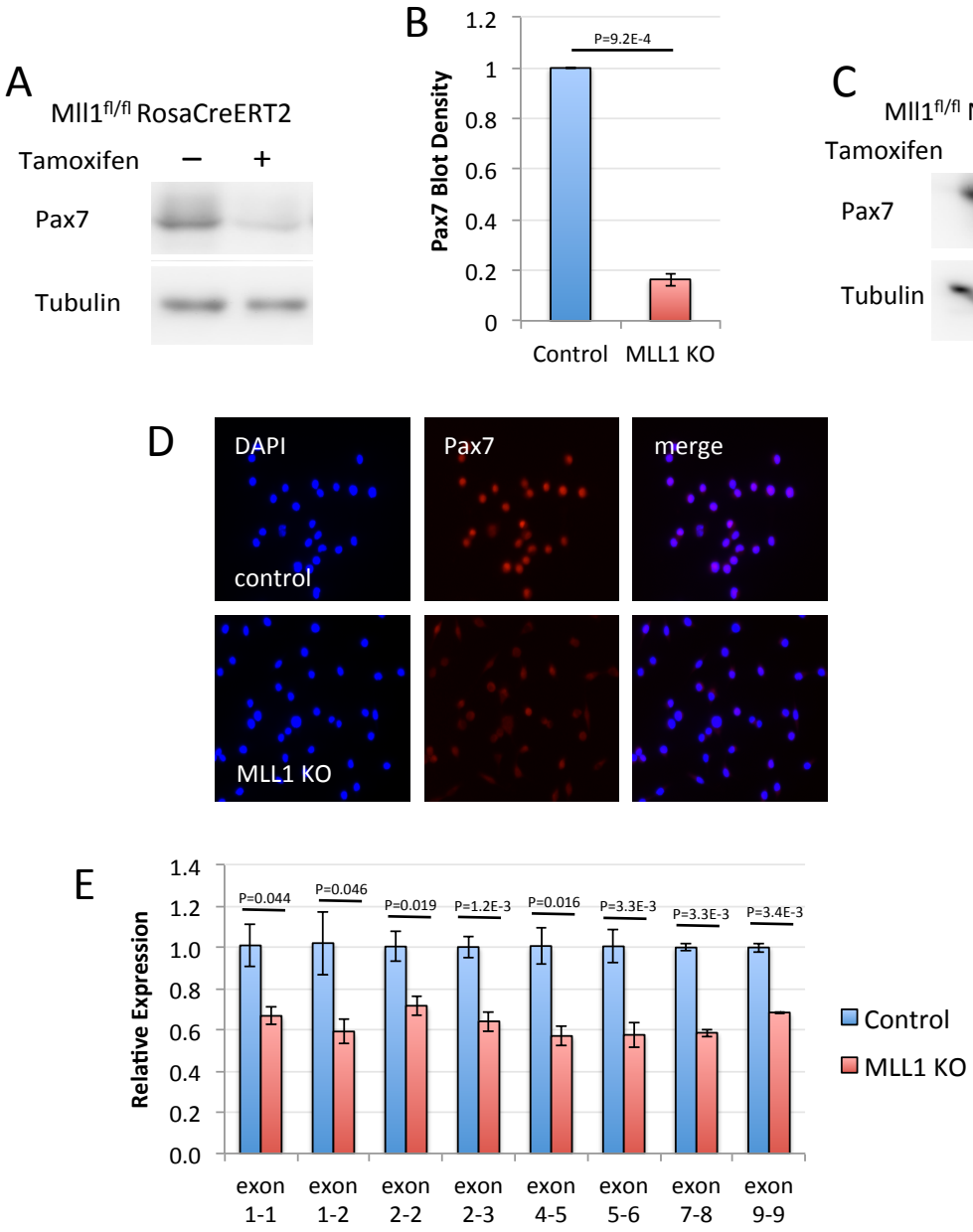

Figure 11. *Mll1* KO results in loss of Pax7 protein
(A) Western blot of control (tamoxifen –) and *Mll1* KO (tamoxifen +) myoblasts from *Rosa*^{CE}/*Mll1*$^{fl/fl}$ mice treated as in Figure 8A. (representative blots).
(B) Quantification of Pax7 protein expression by western blot intensity in *Mll1* KO myoblasts relative to control myoblasts (n=3).
(C) Western blot of tamoxifen (4-OHT) and EtOH control treated *Mll1*$^{fl/fl}$/Cre^{-} myoblasts.
(D) Immunostaining for Pax7 (red) in control and *Mll1* KO myoblasts, nuclei are stained with DAPI (blue).
(E) RT-qPCR of control and *Mll1* KO myoblasts using primers amplifying sites across the Pax7 mRNA.

3.9. Epigenetic Regulation of *Pax7* in *Mll1* KO Myoblasts

To determine if loss of MLL1 results in loss of H3K4 trimethylation at *Pax7*, we performed chromatin immunoprecipitation (ChIP) using anti-H3K4me3 antibody. qPCR of anti-H3K4me3 ChIP DNA found a ~ 25% decrease in H3K4 trimethylation near the *Pax7* transcription start site (TSS) (Figure 12B). In embryonic stem cells *Pax7* and several other *Pax* genes have two peaks of H3K4 trimethylation, one near the TSS and one in an area of high sequence conservation located between exons 3 and 4 (Figure 12A and data not shown), ((Marson et al., 2008) GEO accession GSE11724). Interestingly *Mll1* KO had a stronger effect on the second H3K4me3 peak located ~ 11.7 kb downstream from the *Pax7* TSS than on H3K4me3 near the TSS, with a greater than 50% decrease in H3K4me3 in this region (Figure 12B). The role of this internal H3K4 trimethylation site is unclear.

Many developmentally important genes have so-called bivalent epigenetic marks with both H3K4 trimethylation and H3K27 trimethylation found near the TSS and in which the H3K27me3 mark is thought to represses transcription in the presence of H3K4me3 (Bernstein et al., 2006). Previously it was found that loss of MLL1 in neural progenitors resulted in an increase in H3K27me3 at *Dlx2* (Lim et al., 2009). To determine if there is an increase in H3K27me3 at *Pax7* with *Mll1* KO we performed anti-H3K27me3 ChIP and assessed bound DNA with qPCR. Consistent with continued expression of *Pax7* mRNA, increased H3K27me3 was not found at *Pax7* after *Mll1* KO (Figure 12C), indicating that loss of MLL1 does not result in epigenetic repression of *Pax7* expression via deposition of H3K27me3. To determine if MLL1 is specifically targeted to *Pax7*, anti-MLL1 ChIP was performed. MLL1 was found to bind both near

the *Pax7* TSS and at the internal H3K4me3 locus and this binding was abolished in *Mll1* KO myoblasts (Figure 12D), confirming specific localization of MLL1 to *Pax7*.

While *Mll1* KO is embryonically lethal (Ayton et al., 2001; Yu et al., 1995), deletion of the C-terminal catalytic domain of MLL1 results in viable mice, suggesting a role of MLL1 beyond HMT activity (Terranova et al., 2006). These results suggest that H3K4me3 found at *Pax7* after *Mll1* KO is maintained by a HMT other than MLL1. The finding that MLL1 binds at *Pax7* suggests that MLL1 has a role in Pax7 expression which is additional to or other than histone methylation or activation of general transcription.

3.10. Epigenetic Regulation of *Myf5* in *Mll1* KO Myoblasts

Pax7 has been determined to activate *Myf5* expression through recruitment of a H3K4 methyltransferase (Kawabe et al., 2012; McKinnell et al., 2008). Because *Myf5* expression is lost in *Mll1* KO myoblasts, we also assessed H3K4me3 at *Myf5* to determine if loss of MLL1 results in loss of the activating H3K4me3 mark. When MLL1 expression is lost in primary myoblasts this indeed results in a loss of H3K4me3 at *Myf5* (Figure 13B). Interestingly, and despite *Myf5* expression being downregulated, we found no increase in H3K27me3 at *Myf5* with *Mll1* KO (Figure 13C). These results suggest that loss of *Myf5* expression in *Mll1* KO myoblasts is due to loss of the H3K4me3 at *Myf5* and not due to repression by H3K27me3.

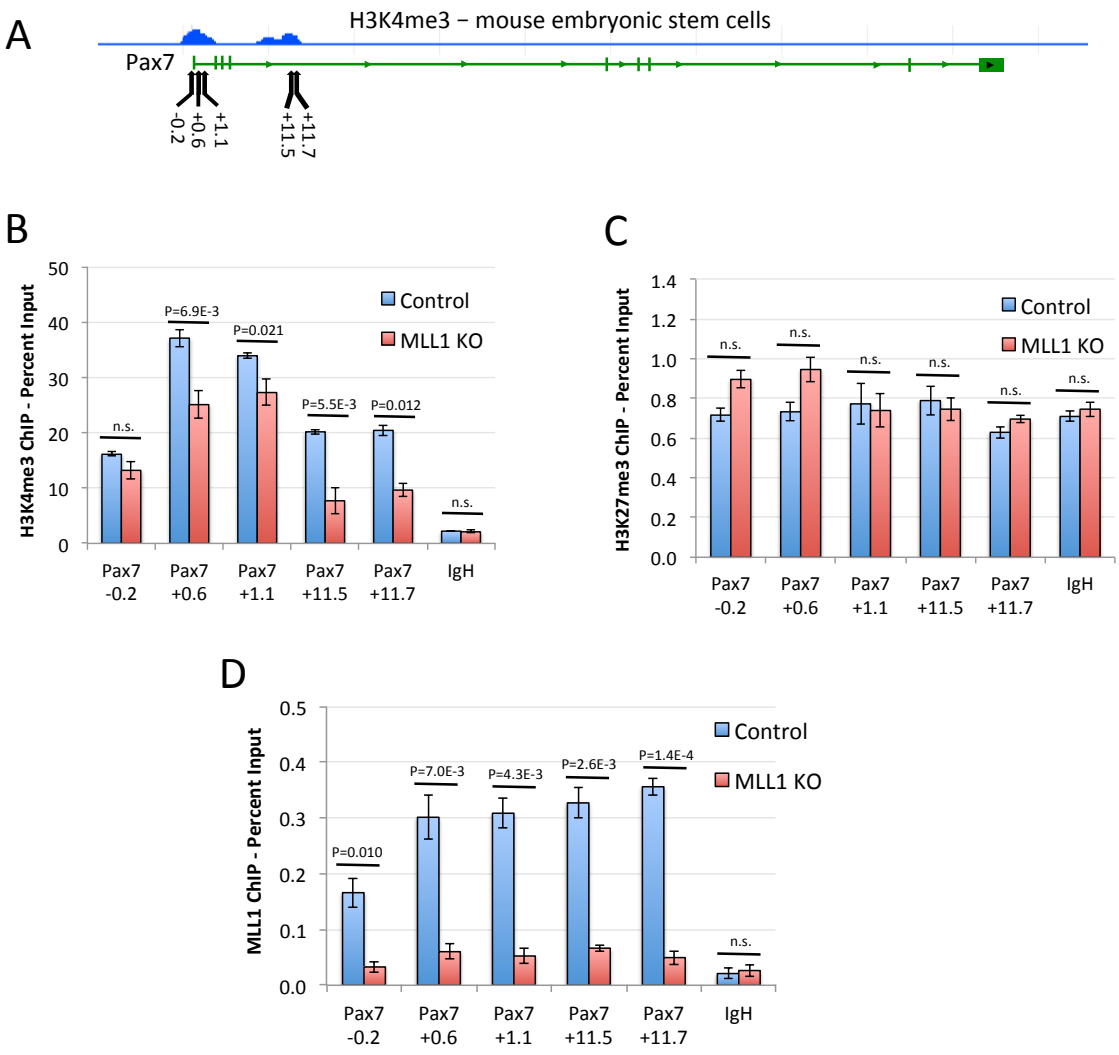

Figure 12. Epigenetic regulation of *Pax7* in *Mll1* KO myoblasts
(A) Anti-H3K4me3 ChIP-seq of mouse embryonic stem cells (GSM307164) at *Pax7* and primer sites relative to *Pax7* TSS for ChIP qPCR
(B) Anti-H3K4me3 ChIP qPCR of control and *Mll1* KO myoblasts prepared as in Figure 8A at *Pax7* and control *IgH* locus. (n=3)
(C) Anti-H3K27me3 ChIP qPCR as in (B). (n=3)
(D) Anti-MLL1 ChIP qPCR as in (B). (n=4)

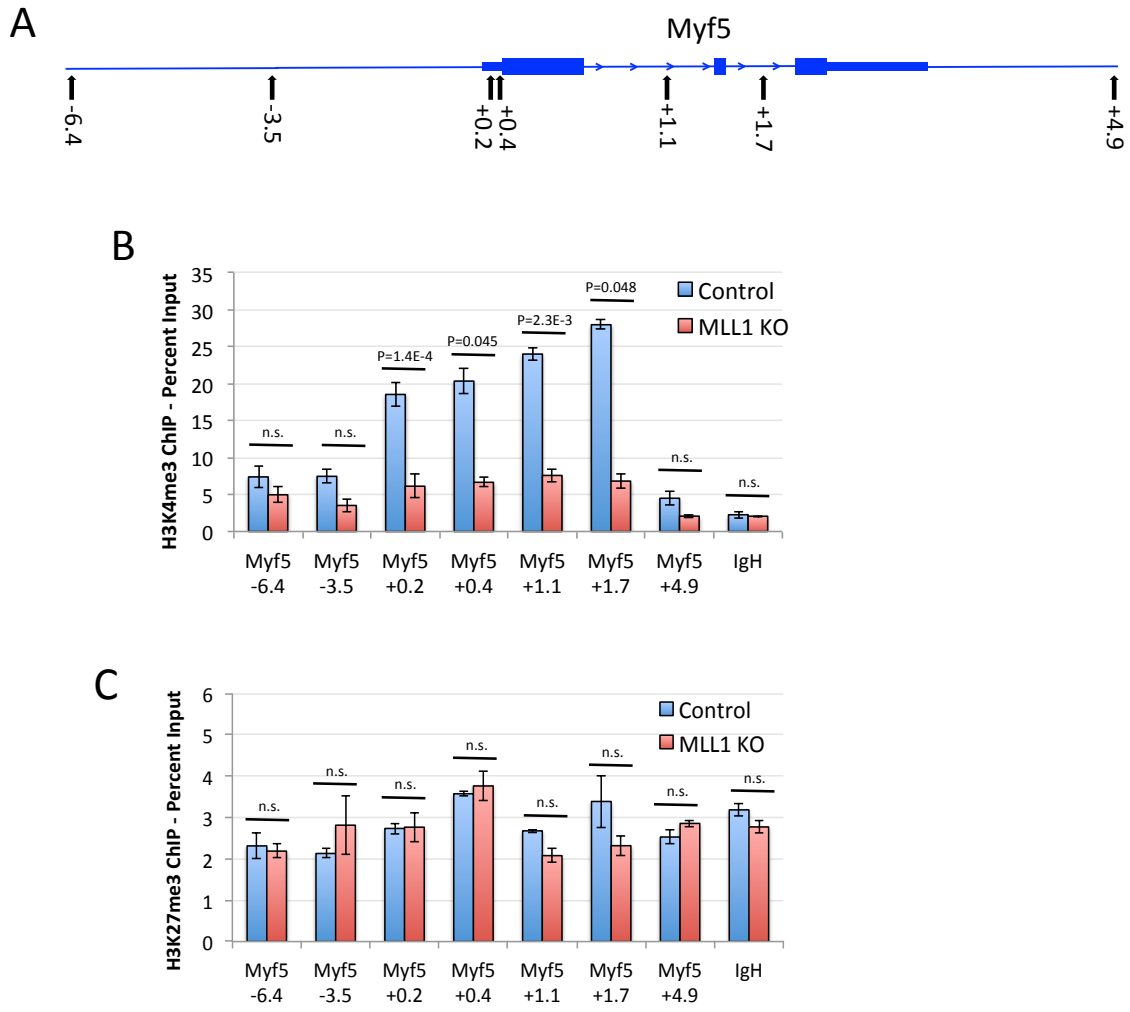

Figure 13. Epigenetic regulation of *Myf5* in *Mll1* KO myoblasts
(A) Primer sites relative to *Myf5* TSS for ChIP qPCR
(B) Anti-H3K4me3 ChIP qPCR of control and *Mll1* KO myoblasts at loci relative to the *Myf5* TSS and at control *IgH* locus. (n=3)
(C) Anti-H3K27me3 ChIP qPCR of control and *Mll1* KO myoblasts at loci relative to the *Myf5* TSS and the control locus *IgH*. (n=3)

3.11. Exogenous Pax7 Rescues *Myf5* Expression in *Mll1* KO Myoblasts

Because *Mll1* KO results in loss of Pax7 protein, we questioned if the loss of *Myf5* expression, and loss of H3K4me3 at *Myf5*, was a secondary effect to loss of Pax7, and not a direct result of loss of MLL1 activity at *Myf5*. To address whether loss of *Myf5* is secondary to loss of Pax7 in *Mll1* KO myoblasts, conditional *Mll1* KO myoblasts were stably transduced via adenoviral vector with a construct expressing Pax7 from the CMV promoter, which we reasoned would not be affected by changes to MLL1 expression.

Exogenous expression of Pax7 caused an increase in *Myf5* expression compared to control myoblasts infected with virus containing empty vector (Figure 14A). When *Mll1* was knocked out in CMV-Pax7 expressing myoblasts no effect was seen on *Myf5* expression (Figure 14A), indicating that in *Mll1* KO myoblasts, loss of *Myf5* expression is secondary to loss of Pax7, rather than being a direct result of loss of MLL1. Because CMV-Pax7 was expressed ~ 6 fold over endogenous *Pax7*, *Mll1* KO had little effect on expression of total Pax7 in CMV-Pax7 expressing myoblasts (Figure 14A). H3K4me3 at *Myf5* was also unaffected in *Mll1* KO myoblasts expressing CMV-Pax7 (Figure 14B), indicating that MLL1 is not required for maintenance of H3K4me3 at *Myf5*.

Exogenous Pax7 expression also resulted in increased proliferation compared to empty vector control myoblasts (Figure 14C). When *Mll1* was knocked, out a proportional decrease in proliferation was seen in CMV-Pax7 expressing cells compared to control cells (Figure 14C). While CMV-Pax7 expressing *Mll1* KO myoblasts maintain a proliferation rate similar to empty vector *Mll1* positive myoblasts, because MLL1 KO results in a decrease in proliferation in the absence of a change in Pax7 expression, these

results suggest that the proliferation defect seen with *Mll1* KO is partially independent of Pax7.

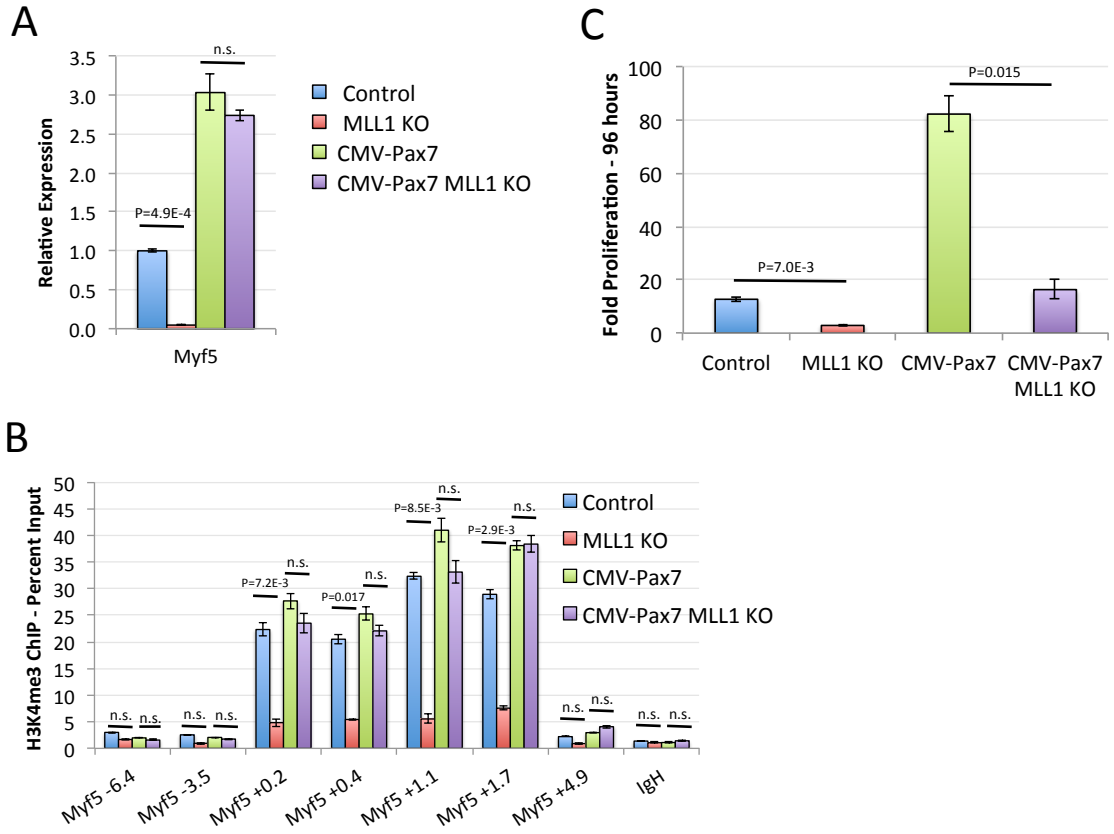

Figure 14. Exogenous Pax7 rescues *Myf5* expression in *Mll1* KO myoblasts
(A) RT-qPCR analysis of *Myf5* expression in empty vector (Control), empty vector *Mll1* KO (MLL1 KO), CMV-Pax7 expressing *Mll1*+ (CMV-Pax7) and CMV-Pax7 expressing *Mll1* KO (CMV-Pax7 MLL1 KO) myoblasts. Empty vector and CMV-Pax7 expressing *Rosa*^{CE}/MLL1$^{fl/fl}$ myoblasts treated with 4-OHT or ethanol as in Figure 8A. (n=3)
(B) Anti-H3K4me3 ChIP qPCR of myoblasts as in (A) at loci relative to the *Myf5* TSS as in Figure 13A and at control *IgH* locus. (n=3)
(C) Fold proliferation of myoblasts as in (A) 96 hours after seeding (n=3).

3.12. Inducible Pax7 Rescues *Myf5* Expression After Loss of MLL1

In order to determine if exogenous Pax7 expressed at physiological levels can rescue *Myf5* expression and restore H3K4me3 to *Myf5* after *Myf5* expression is lost in

Mll1 KO, conditional *Mll1* KO myoblasts were stably transfected with a construct expressing Pax7 from a doxycycline (Dox) inducible promoter (Tet-ON Pax7).

When myoblasts were treated with 4-OHT and assessed 14 days after the initial 4-OHT treatment, *Myf5* expression and H3K4me3 at *Myf5* were lost; induction of Pax7 expression by addition of Dox for 7 days restored *Myf5* expression and H3K4me3 to *Myf5* (Figure 15B and 15C). Importantly, unlike CMV-Pax7, Tet-ON Pax7 mRNA and protein expression were at a similar level to endogenous *Pax7* (Figure 15B and 15C) showing that super-physiological Pax7 expression is not necessary to initiate or drive *Myf5* expression in the absence of MLL1. Additionally, western blot of Pax7 expressed via the Tet-ON-Pax7 system showed a similar level of Pax7 protein compared to control cells (Figure 15D) indicating that the loss of Pax7 protein in *Mll1* KO cells is not due to activation of a Pax7 targeting protein degradation pathway. These results confirm that Pax7 is able to activate *Myf5* expression in the absence of MLL1, and reject the possibility of a Pax7 degradation pathway that is specifically activated through *Mll1* KO.

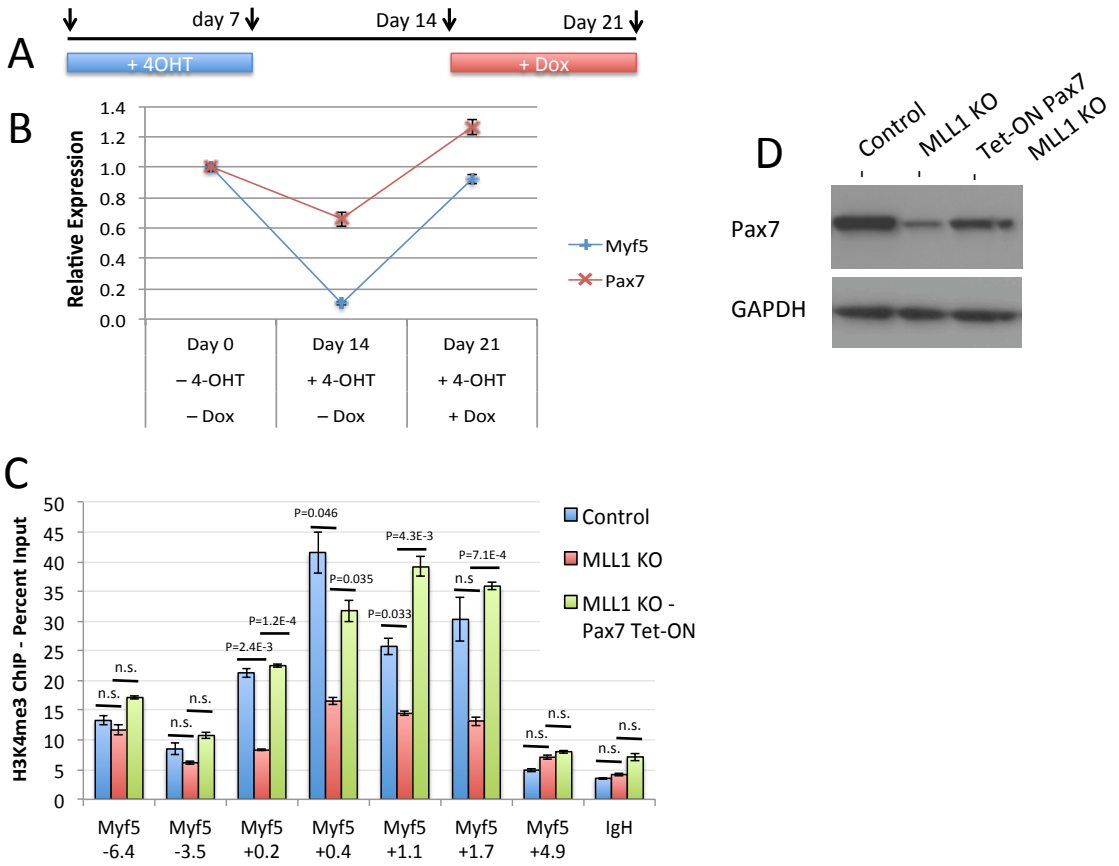

Figure 15. Inducible Pax7 rescues *Myf5* expression after loss of MLL1
(A) Schematic of tamoxifen (4-OHT) and doxycycline (Dox) treatment of myoblasts used for Figures 15B, 15C, and 15D. Cells treated with 4-OHT from day 0 to day 7 (blue bar) to induce recombination resulting in *Mll1* KO, and treated with doxycycline from day 14 to day 21 (red bar) to induce expression of Tet-ON Pax7. Samples collected at day 0 for control, day 14 for *Mll1* KO and day 21 for *Mll1* KO Pax7 Tet-ON.
(B) RT-qPCR analysis of control, *Mll1* KO and *Mll1* KO Pax7 Tet-ON induced myoblasts collected at day 0, day 14 and day 21 as indicated in (A). (n=3)
(C) Anti-H3K4me3 ChIP qPCR of control, *Mll1* KO and *Mll1* KO Pax7 Tet-ON induced myoblasts collected at day 0, day 14 and day 21 as indicated in (A). (n=3)
(D) Western blot of control, *Mll1* KO and *Mll1* KO Pax7 Tet-ON myoblasts collected at day 0, day 14, and day 21 as in (A) using indicated antibodies.

3.13. Exogenous Pax7 Expression Down-Regulates and Epigenetically Represses Endogenous Pax7

Some previous work using *Mll1* KO in hematopoietic stem cells and MEF suggests that MLL1 directly regulates H3K4me3 at target genes (Milne et al., 2002; Wang et al., 2009a). Because *Mll1* KO resulted in moderate change to H3K4me3 or H3K27me3 at Pax7, a positive control where Pax7 is epigenetically repressed would be useful to confirm the validity of our ChIP results.

Interestingly, when CMV-Pax7 was exogenously over-expressed this resulted in downregulation of endogenous Pax7 expression by more than 20-fold, a ~ 10-fold decrease in H3K4me3, and a ~ 7-fold gain of H3K27me3 at *Pax7* (Figure 16A, 16B and 16C). This is in contrast to the loss of MLL1, which resulted in less than one-fold decrease of H3K4me3 at *Pax7* and no change to H3K27me3 in both untransfected *Mll1* KO myoblasts (Figure 12B, 12C), and in empty vector control *Mll1* KO myoblasts (Figure 16B and 16C). These results highlight the mild effect of loss of MLL1 on epigenetic regulation of *Pax7* via H3K4me3 and H3K27me3, and support a more cryptic role for MLL1 in Pax7 expression, seemingly through a mechanism other than deposition of the H3K4me3 mark.

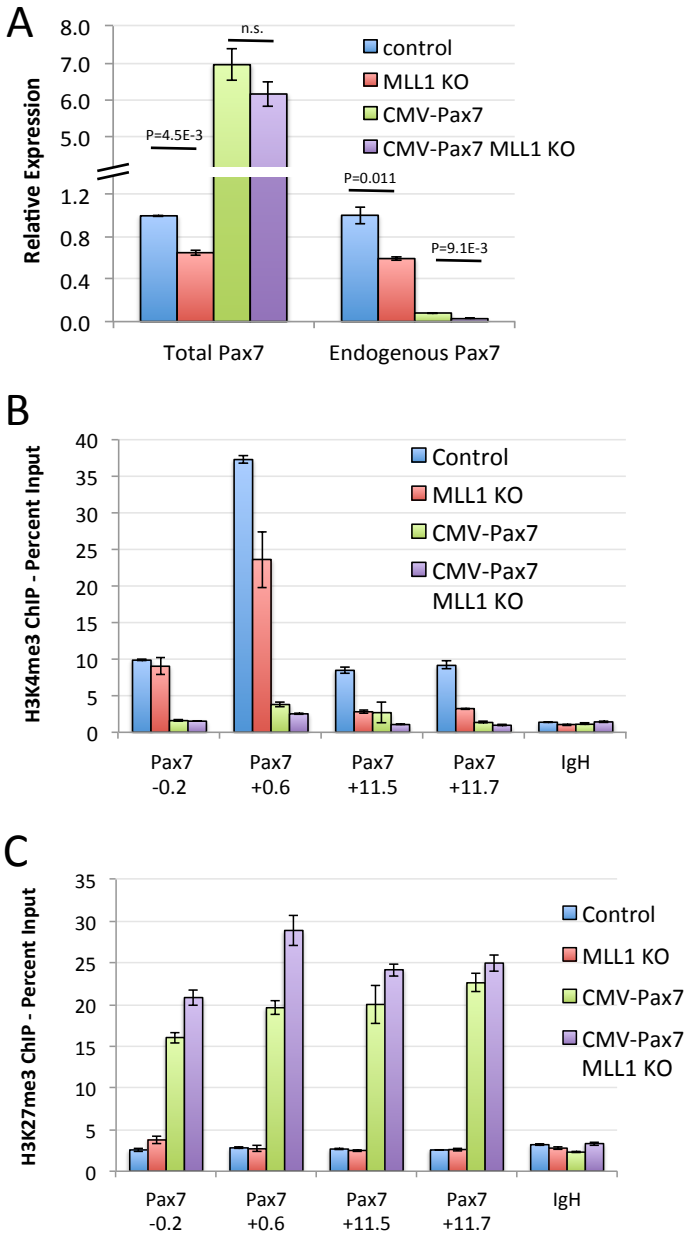

Figure 16. Exogenous Pax7 expression downregulates and epigenetically represses endogenous Pax7

(A) RT-qPCR analysis of expression of total and endogenous *Pax7* mRNA, using primers specific for the coding sequence and 5' UTR respectively, in empty vector (Control), empty vector *Mll1* KO (MLL1 KO), CMV-Pax7 expressing *Mll1*+ (CMV-Pax7) and CMV-Pax7 expressing *Mll1* KO (CMV-Pax7 MLL1 KO) myoblasts. Empty vector and CMV-Pax7 expressing MLL1$^{fl/fl}$RosaCreER^{T2} myoblasts treated with 4-OHT or ethanol as in Figure 8A. (n=3)

(B) Anti-H3K4me3 ChIP qPCR of samples as in (A). (n=3)

(C) Anti-H3K27me3 ChIP qPCR of samples as in (A). (n=3)

3.14. Exogenous Pax7 Rescues Fgfr4 but Not Other Genes in *Mll1* KO

Expression of additional genes that were identified by microarray as being strongly affected by loss of MLL1 were also assessed in CMV-Pax7 *Mll1* KO myoblasts. Unlike its rescue effect on *Myf5*, CMV-Pax7 failed to rescue expression of several other genes (*Six2*, *Dlx1*, *Lbx1*, and *Asb4*) that were downregulated with *Mll1* KO (Figure 17A). This indicates that many genes downregulated in *Mll1* KO myoblasts are directly regulated by MLL1, or that changes to their expression are secondary to other effects caused by loss of MLL1, and are independent of Pax7. Exogenous Pax7 did prevent decreased *Fgfr4* expression in *Mll1* KO myoblasts indicating that *Fgfr4* expression may be linked to Pax7 rather than MLL1 and confirming previous findings that Pax7 regulates *Fgfr4* expression (Soleimani et al., 2012). Exogenous expression of Asb4, Six2, Dlx1, Lbx1 or Fgfr4 failed to rescue expression of *Myf5*, *Pax7* or other genes in *Mll1* KO myoblasts (data not shown). Exogenous Asb4 expression had a similar effect on proliferation as was seen with exogenous Pax7 above (data not shown), possibly suggesting a combinatorial effect on proliferation between Pax7 and Asb4. Exogenous expression of Six2, Dlx1, Lbx1 or Fgfr4 had no overt effect on proliferation in control or *Mll1* KO myoblasts. Exogenous Myf5 expression also failed to rescue *Pax7* expression, *Six2* expression or proliferation in *Mll1* KO myoblasts (Figure 17B and data not shown), indicating that loss of *Myf5* expression in *Mll1* KO myoblasts does not drive changes to *Pax7* expression or proliferation rate.

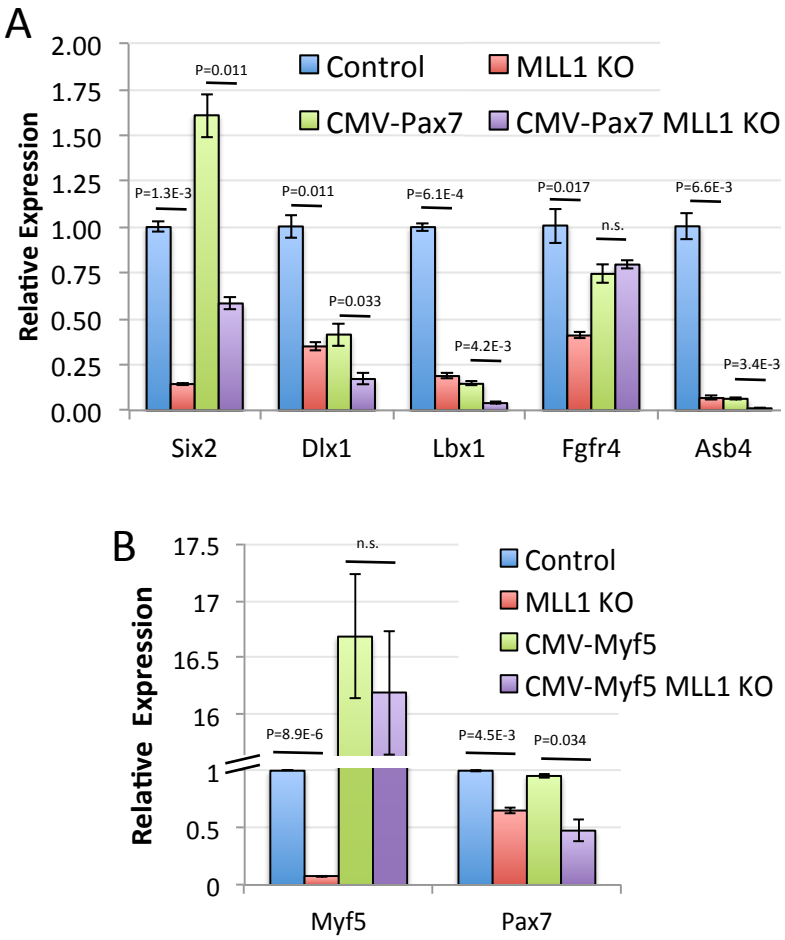

Figure 17. Exogenous Pax7 rescues Fgfr4 but not other genes in *Mll1* KO
(A) RT-qPCR of mRNA from control empty vector (Control), *Mll1* KO empty vector (MLL1 KO), CMV-Pax7 and CMV-Pax7 *Mll1* KO (CMV-Pax7 MLL1 KO) myoblasts; relative expression levels to control empty vector myoblasts. (n=3)
(B) RT-qPCR of mRNA from control empty vector (Control), *Mll1* KO empty vector (MLL1 KO), CMV-Myf5 and CMV-Myf5 *Mll1* KO (Myf5-Pax7 MLL1 KO) myoblasts; relative expression levels to control empty vector myoblasts. (n=3)

3.15. Exogenous Pax7 Rescues *Myf5* Expression in *Mll1*/*Mll2* KO Myoblasts

Previously it was suggested that Pax7 interacts with MLL2 (Trx2) to activate target genes (McKinnell et al., 2008) or acts through MLL1/2 (Kawabe et al., 2012). To determine the effect of loss of MLL2 on regulation of *Myf5* expression via Pax7, myoblasts were derived from $Mll2^{fl/fl}$ mice expressing Rosa-CreER^{T2} (Glaser et al., 2006).

Knockout of *Mll2* in cultured myoblasts had no significant effect on expression of *Myf5* or *Pax7* (Figure 18A). To test the possibility that, in the absence of MLL1, Pax7 may be activating *Myf5* expression via MLL2, $Mll1^{fl/fl}$ /$Mll2^{fl/fl}$ myoblasts were made as above. *Mll1*/*Mll2* KO resulted in similar effects to expression of *Pax7* and *Myf5* as were seen in *Mll1* KO myoblasts (Figure 18B). When Pax7 was exogenously expressed in $Mll1^{fl/fl}$ /$Mll2^{fl/fl}$ myoblasts, no loss of *Myf5* expression was found after 4-OHT treatment (Figure 18C).

Therefore, while epigenetic regulation of *Myf5* via Pax7 may occur via MLL1 and MLL2, neither MLL1 nor MLL2 are required for activation of *Myf5* by Pax7, and Pax7 is likely able to also act through H3K4 HMTs other than MLL1 or MLL2.

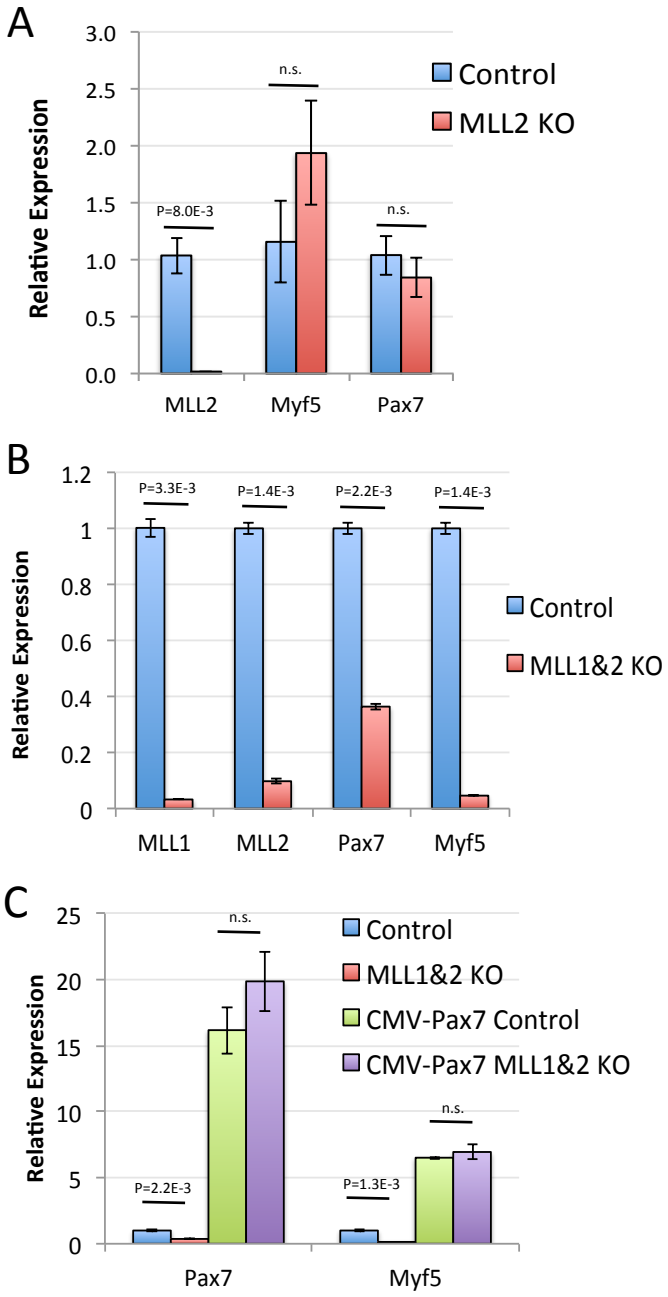

Figure 18. Exogenous Pax7 rescues *Myf5* expression in *Mll1*/*Mll2* KO myoblasts

(A) RT-qPCR analysis of control and *Mll2* KO myoblasts treated as in Figure 8A. (n=3)
(B) RT-qPCR analysis of control and *Mll1*/*Mll2* double KO myoblasts treated as in Figure 8A. (n=3)
(C) RT-qPCR analysis of control and *Mll1*/*Mll2* double KO myoblasts, exogenous CMV-Pax7 expressing *Mll1*+/*Mll2*+ myoblasts, and CMV-Pax7 expressing *Mll1*/*Mll2* double KO myoblasts treated as in Figure 8A. (n=3).

3.16. *Myf5* is Repressed by DNA Methylation in ES Cells and Other Non-Myogenic Cell Types and is Not Methylated in Myoblasts or Myotubes.

Inactive genes are often marked by the repressive H3K27me3 mark, however after *Mll1* KO and downregulation of *Myf5* (Figure 9A), no increase in H3K27me3 is seen at *Myf5* (Figure 13B). Rather than being repressed by the H3K27me3 mark, some genes are repressed by DNA methylation which is widely accepted to inhibit gene expression when localized to the proximal promotor. (Boyes and Bird, 1991; Schübeler, 2015; Smith and Meissner, 2013). We questioned if the mode by which *Myf5* expression is repressed is through DNA methylation.

To determine if *Myf5* is repressed by DNA methylation in non-myogenic cells we queried published methyl DNA immunoprecipitation (meDIP) sequencing data sets. Our analysis of published meDIP sequencing data sets show DNA methylation at *Myf5* in cultured human embryonic stem cells and in several other human tissues and cell types (Figure 19A), (Bernstein et al., 2010; Gascard et al., 2015); GEO accession GSE16368). A separate study also found that *Myf5* is in a group of about 2% of genes which are specifically marked by promoter DNA CpG methylation in the inner cell mass at the implantation stage (Borgel et al., 2010).

Because *Myf5* is negatively regulated by CpG methylation in most non-myogenic cell types, we aimed to determine if CpG methylation at *Myf5* is removed in myoblasts which express *Myf5*. Our meDIP-qPCR experiments found that *Myf5*-expressing mouse myoblasts have less than 1% of CpG methylation at the *Myf5* TSS relative to that found in mouse embryonic fibroblasts (MEF) (Figure 19B). In order to determine if *Myf5* expression is required to maintain the *Myf5* promoter in a unmethylated state, meDIP was

also used to assess DNA methylation in *in-vitro* differentiated myotubes, which no longer express *Myf5*. DNA methylation was not found at *Myf5* in differentiated myotubes (Figure 19B), indicating that expression of *Myf5* is not specifically required for maintenance of unmethylated DNA at *Myf5*. Our results support the contention that *Myf5* is repressed by promoter DNA methylation in most lineages, and that methylation at *Myf5* is specifically lost during developmental progress leading to the myogenic lineage.

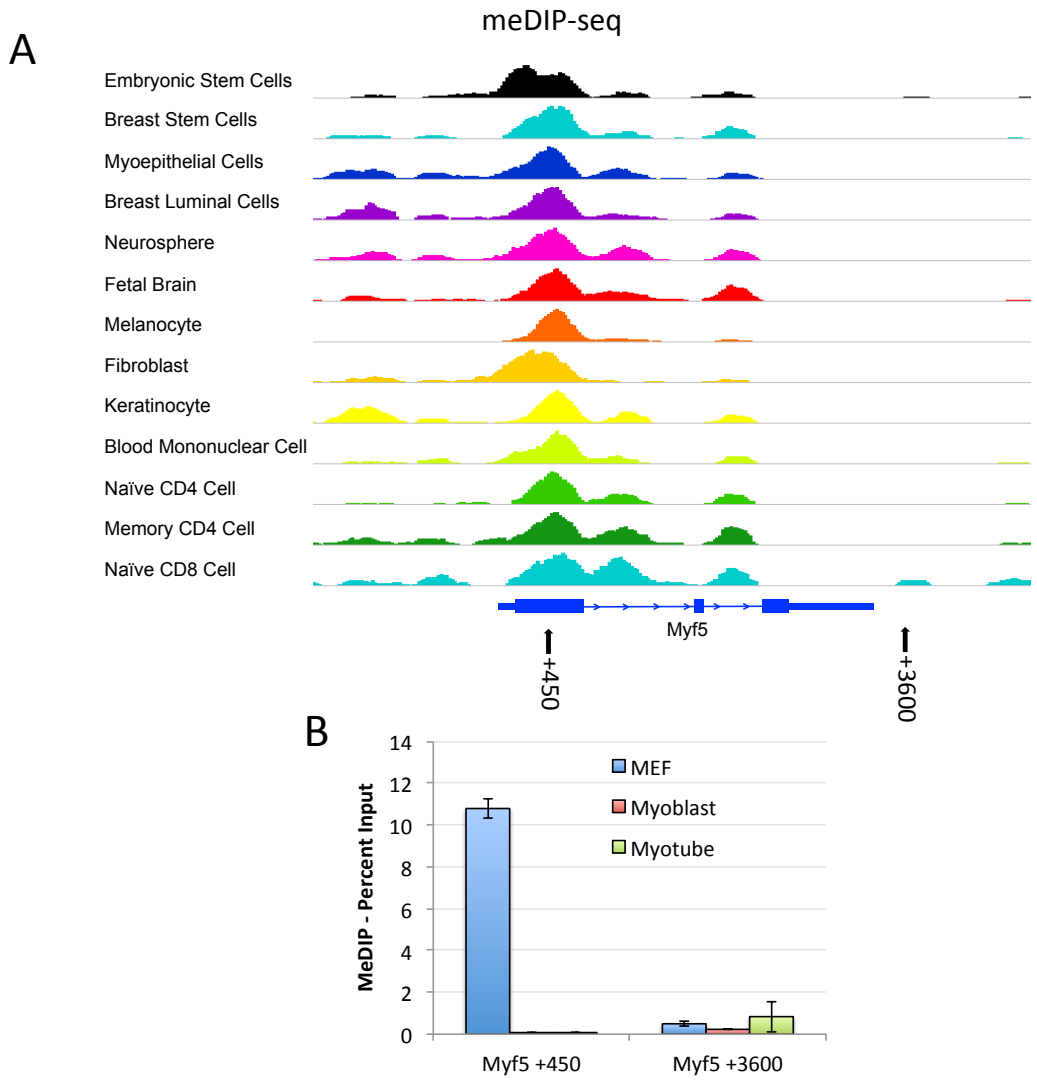

Figure 19. *Myf5* is repressed by DNA methylation in ES cells and other non-myogenic cell types and unmethylated in committed myogenic cells.
(A) MeDIP-seq trace data at *Myf5* in human embryonic stem cells and other human cell types. WIG data for; Embryonic Stem Cells - GSM534016, Breast Stem Cells - GSM543019, Myoepithelial Cells - GSM1517154, Breast Luminal Cells - GSM1517153, Neurosphere - GSM669612, Fetal Brain - GSM669614, Melanocyte -GSM941727, Fibroblast - GSM958182, Keratinocyte - GSM941726 Blood Mononuclear Cell - GSM543023, Naïve CD4 Cell - GSM613913, Memory CD4 Cell - GSM669608, Naïve CD8 Cell - GSM669609, was mapped to *Myf5* using the integrated genomics viewer from the Broad Institute
(B) MeDIP qPCR of MEF, myoblasts and in-vitro differentiated myotubes at loci relative to the *Myf5* TSS. (n=3)

3.17. Demethylation of the *Myf5* Promoter Marks the Transition from Satellite Stem Cell to Committed Myogenic Cell and Methylation at *Myf5* is Re-Established in *Mll1* KO Myoblasts

Previous work has established that satellite cells are heterogeneous and that there are at least two populations of satellite cells, committed satellite cells, which have previously expressed *Myf5*, and satellite stem cells, which have no history of *Myf5* expression (Kuang et al., 2007). The finding that many adult cell types have methylation at the *Myf5* promoter, and that *Myf5* promoter methylation is lost in myogenic cells suggests that *Myf5* promoter methylation may be lost specifically at the transition from satellite stem cell to committed satellite cell.

To determine if there is a difference in methylation status between satellite stem cells and committed satellite cells, satellite cells were isolated from *Myf5*-Cre/*Rosa*-YFP (expressing Cre recombinase from the *Myf5* locus containing EYFP at the *Rosa* locus for which expression is blocked by a floxed stop sequence, (Kuang et al., 2007)), lineage tracing mice using florescence activated cell sorting (FACS). Freshly isolated satellite cells (Pasut et al., 2012), were separated into committed satellite cell (YFP+) and satellite stem cell (YFP–) populations and DNA methylation status was determined by meDIP qPCR. MeDIP of DNA from YFP+ and YFP– fractions shows that YFP+ satellite cells have little DNA methylation compared to YFP– satellite stem cells (Figure 20B). For both YFP+ and YFP– cell populations DNA methylation was found at *Sohlh2* promoter, which is unmethylated in the germline (Pan et al., 2011). For both YFP+ and YFP– cell populations no methylation was found at the *Pax7* promoter or at the promoter for the neural bHLH factor *NeuroD6*.

This finding suggests that DNA methylation at *Myf5* blocks activation of *Myf5* expression by Pax7 in satellite stem cells, and that during commitment to the myogenic lineage loss of methylation at *Myf5* allows Pax7 mediated activation of *Myf5* expression.

Previously it was shown that inhibition of MLL1 facilitates the reconversion of epiblast stem cells to naive pluripotency (Zhang et al., 2016a), implying that loss of MLL1 may to some extent facilitate cellular reprogramming through relaxation of cell type rigidity. We therefore questioned if loss of MLL1 would also result in loss of myogenic cell type identity. Unexpectedly, *Mll1* KO myoblasts not only lose *Myf5* expression but DNA methylation at *Myf5* DNA is re-established (Figure 20C), indicating partial conversion of cultured myoblasts to a state resembling a satellite stem cell which has never expressed *Myf5*. Importantly, *MyoD* continues to be expressed in *Mll1* KO myoblasts therefore myogenic progenitor identity is maintained through *MyoD*.

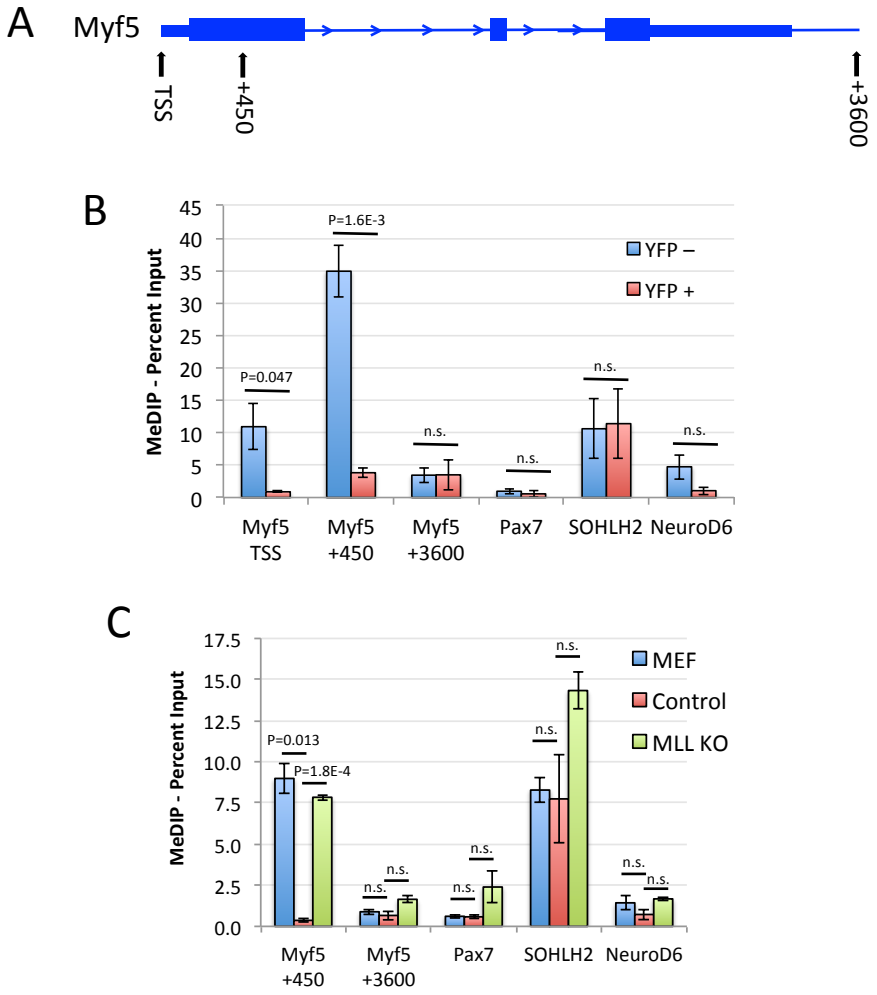

Figure 20. *Myf5* is unmethylated in committed myogenic cells and methylation at *Myf5* is reestablished in *Mll1* KO myoblasts

(A) Schematic of loci relative to the *Myf5* transcription start site (TSS) for MeDIP qPCR
(B) MeDIP qPCR of freshly isolated YFP+ satellite stem cells and YFP– committed satellite cells isolated via FACS from *Myf5*-Cre/RosaYFP mice (n=3)
(C) MeDIP qPCR of MEF, myoblasts (Control) and *Mll1* KO myoblasts (MLL1 KO) at indicated loci. (n=3)

3.18. Exogenous Pax7 Induces Sub-Physiological *Myf5* Expression in Non-Myogenic Cells, but does not Demethylate *Myf5* DNA.

Previously it was shown that transfection of 10T1/2 cells with Pax7 is able to induce *Myf5* expression (McKinnell et al., 2008). Because it is difficult to collect sufficient samples of satellite stem cells from mice to be able to interrogate the mechanism by which *Myf5* DNA is demethylated, we aimed to determine if *Myf5* DNA is methylated in 10T1/2 cells and if viral transfection of 10T1/2 cells with a construct expressing exogenous Pax7 results in demethylation of *Myf5*.

Comparing primary myoblast and 10T1/2 cell DNA methylation using MeDIP, we found that *Myf5* DNA is highly methylated in 10T1/2 cells compared to primary myoblasts (Figure 21A). While transfection of 10T1/2 cells with virus expressing exogenous Pax7 does upregulate *Myf5* expression by ~60 fold compared to 10T1/2 cells transfected with empty vector, *Myf5* expression remains about 20-fold lower in exogenous Pax7 expressing 10T1/2 cells than in primary myoblasts (Figure 21B). MeDIP analysis of exogenous Pax7 expressing 10T1/2 cells found no change in DNA methylation at *Myf5* compared to 10T1/2 cells transfected with empty vector (Figure 21A).

These results suggest that Pax7 expression alone is not sufficient to fully activate *Myf5* expression and that additional steps are required for *Myf5* DNA to become demethylated thereby allowing *Myf5* expression at a physiological level.

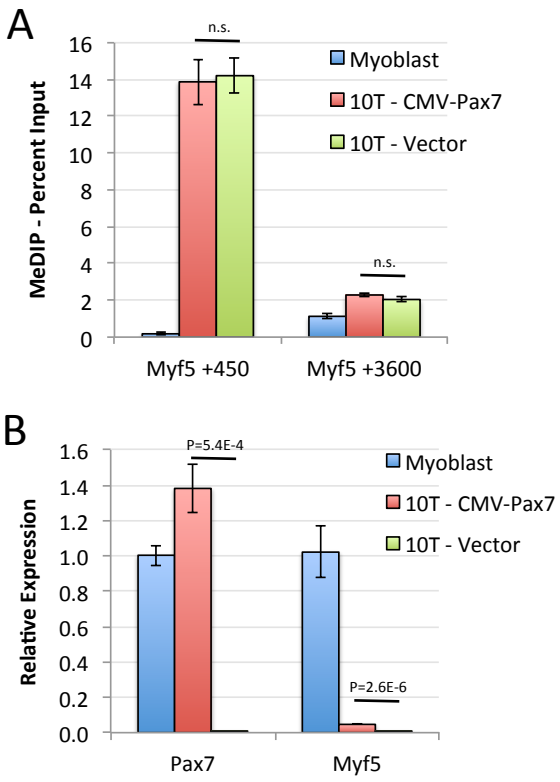

Figure 21. Exogenous Pax7 induces sub-physiological *Myf5* expression, but does not demethylate *Myf5* DNA.
(A) MeDIP qPCR of myoblasts, CMV-Pax7 expressing 10T1/2 cells and vector control 10T1/2 cells at loci relative to the *Myf5* TSS. (n=3).
(B) RT-qPCR of Pax7 and *Myf5* expression in myoblasts, CMV-Pax7 expressing 10T1/2 cells and vector control 10T1/2 cells. (n=3)

3.19. Tet3 Interacts with Dvl3

Previously, an interaction between IDAX (CXXC4), which contains a vestigial CXXC domain of Tet2 and the Wnt pathway protein dishevelled was found (Hino et al., 2001). Our lab has found that Wnt7a/Fzd7 signaling blocks asymmetric division and activation of *Myf5* expression in satellite stem cells (Le Grand et al., 2009), therefore, we questioned whether dishevelled might also interact with Tet proteins which retain their CXXC domains. Reciprocal immunoprecipitation of exogenously expressed Dvl3 and Tet3 confirmed an interaction between these two proteins. These results may point to a direct role for Wnt7a/Fzd7 signaling in regulation of Tet proteins that are likely required for demethylation of *Myf5*.

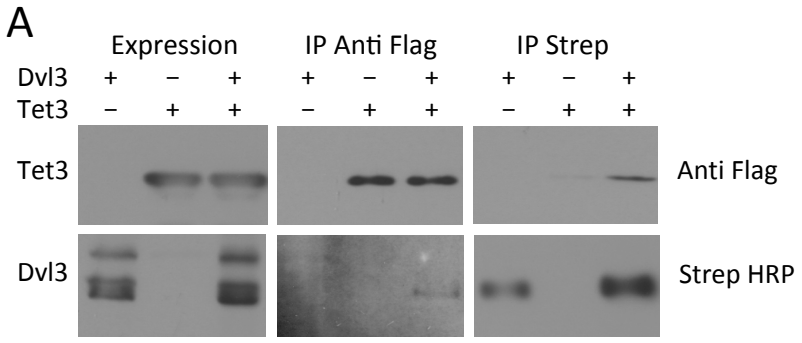

Figure 22. Reciprocal co-immunoprecipitation of Tet3 with Dvl3 supports possible role for Wnt signaling in regulation of DNA demethylation
(A) Western blots of whole cell lysate, anti-FLAG IP precipitate, or Streptavidin precipitate from 293T cells transfected with constructs expressing SBP tagged Dvl3 or Flag tagged Tet3 as indicated and detected with Anti-Flag antibody or Streptavidin-HRP.

Chapter 4. Discussion

This work offers new insights into the role of MLL1 in myogenesis, specifically regarding its role in proliferation and regulation of Pax7 and challenges previous conceptions about the role of MLL1 in Hox gene expression. Further this work uncovers a role for DNA methylation in regulation of *Myf5* expression and suggests demethylation of *Myf5* is a key step in myogenic commitment of satellite stem cells.

4.1.0. Overview of Regulation of *Pax7* expression by MLL1.

In this study, we examined the role of MLL1 in myogenic stem and progenitor cells. MLL1 was found to be required for efficient *in vivo* myogenic regeneration. The regeneration defect appears to be largely due to loss of proliferation of *Mll1* KO satellite cells and mpcs which is partially caused by loss of Pax7 expression. *Mll1* KO results in a consistent ~40% decrease in Pax7 mRNA expression, and a strong ~85% decrease in Pax7 protein. Molecular analysis via anti-MLL1 ChIP determined that MLL1 directly targets Pax7, however loss of MLL1 does not result in epigenetic repression of *Pax7* or a strong loss of H3K4me3 at *Pax7*. Microarray comparing mRNA from control and *Mll1* KO myoblasts found remarkably little change in gene expression even among Hox genes or Dlx2 which have been previously determined to be *Mll1* targets (Ernst et al., 2004a; Lim et al., 2009; Milne et al., 2002; Wang et al., 2009a; Yu et al., 1995). Intriguingly, *Myf5* was the gene most strongly downregulated by *Mll1* KO. While MLL1/2 have been purported to have a role in activation of *Myf5* by Pax7 (Kawabe et al., 2012; McKinnell et al., 2008) the effects of the loss of MLL1 on *Myf5* expression are dependent on loss of Pax7 but independent of MLL1, as exogenous Pax7 rescues *Myf5* expression and H3K4me3 at *Myf5* in *Mll1* KO myoblasts. *Mll1* KO resulted in loss of H3K4me3 and,

exceptionally, gain of DNA methylation at the *Myf5* promoter, both of which are the result of low Pax7 protein expression rather than direct effects of loss of MLL1.

4.1.1. MLL1 is Required for Efficient Myogenic Regeneration

Our finding that muscle regeneration in *Mll1* KO mice is deficient due to loss of satellite cells is redolent of the effect of loss of MLL1 in hematopoiesis and neurogenesis. Conditional knockout of *Mll1* exons 3-4 (the conditional *Mll1* allele used for this work) using polyinosinic:polycytidylic acid activated Mx1-Cre results in a depletion of cells in the bone marrow (Jude et al., 2007), which results in severe anemia. Another conditional *Mll1* KO, with exons 8-9 deleted, results in a weaker hematopoietic defect in which adult hematopoiesis is normal, however HSC from these mice are unable to reconstitute hematopoiesis after transplant (McMahon et al., 2007). Conditional *Mll1* KO (exon 3-4 mutant) using a hGFAP-Cre transgene, which is active in neural precursors during postnatal neurogenesis, results in mice which exhibit progressive neurological deterioration after birth (Lim et al., 2009). These findings, and ours, point to similar important roles for MLL1 in diverse types of stem and progenitor cells with loss of MLL1 resulting in critical defects for tissues derived from these progenitors.

4.1.2. MLL1 is Required for Proliferation of Myogenic Cells

We found that MLL1 has a clear role in proliferation of satellite cells and myoblasts, however previous work indicates that the role of MLL1 in proliferation may be cell-type specific. *Mll1* KO embryos are of normal size until death at around embryonic day 11.5 to 13.5 (Hess et al., 1997; Yagi et al., 1998; Yu et al., 1995). MLL1

is not required for proliferation of embryonic stem cells (Ernst et al., 2004a), neural stem cells (NSC) (Lim et al., 2009), or for proliferation during formation of embryoid bodies from embryonic stem cells (Ernst et al., 2004a). MLL1 is required for maintenance of quiescence in hematopoietic stem cells and proliferation of hematopoietic progenitor cells (Jude et al., 2007; McMahon et al., 2007). The effect of *Mll1* KO on *in vitro* proliferation of hematopoietic progenitors is partially restored by exogenous expression of several Hox proteins (Hoxa9, Hoxa10, Hoxb3, Hoxb4) or Cdx4 (Ernst et al., 2004a).

We have previously shown that *Pax7* KO results in cell cycle arrest and precocious differentiation (von Maltzahn et al., 2013a). Perhaps because a low amount of Pax7 continues to be expressed, *Mll1* KO myoblasts maintain slow proliferation and do not spontaneously differentiate in mitogen culture conditions. Since exogenous over-expression of Pax7 only partly rescues proliferation in *Mll1* KO myoblasts, the proliferation defect seen with loss of *Mll1* is likely due to both loss of Pax7, and other Pax7-independent effects. An analysis of the effect of exogenous expression of other genes which were downregulated after *Mll1* KO found that exogenous expression of Asb4, an ankyrin repeat and suppressor of cytokine signalling box-containing protein, which targets proteins for degradation and may be involved in oxygen or carbohydrate sensing (Bode et al., 2011; Li et al., 2011), had a partial rescue effect on proliferation similar to that of Pax7, however, the significance of this finding is unclear. Exogenously expressed Six2, Dlx1, Lbx1 or Fgfr4 had no effect on proliferation. Our findings, combined with conflicting effects of loss of *Mll1* on proliferation in other cell types, suggests that the resultant loss of proliferation with *Mll1* KO is a secondary effect resulting from cell-type specific changes to gene expression or cell identity.

Notably, it has been determined that Prdm16 is a target of MLL1, and that rescue of Prdm16 expression in *Mll1* KO HSC is able to rescue proliferation and gene expression (Artinger et al., 2013). Prdm16 also has a role in regulation of satellite cells with high Prdm16 levels promoting brown fat differentiation (Seale et al., 2008). By microarray, Prdm16 expression was decreased by ~33% in *Mll1* KO myoblasts, however, in control myoblasts Prdm16 expression was below cut-off level for physiological relevance, and was previously determined to be expressed more than 65 fold lower in myoblasts than in brown fat (Yin et al., 2013a). While Prdm16 may have a role in HSC proliferation, changes in Prdm16 expression in *Mll1* KO myoblasts likely do not account for their decreased proliferation.

4.1.3. Role of MLL1 in Pax7 Expression

Because of our previous work showing the tight linkage between Pax7 and *Myf5* expression (McKinnell et al., 2008) we looked at Pax7 expression in *Mll1* KO myoblasts using RT-qPCR and found a consistent ~40% decrease in Pax7 mRNA suggesting a specific change to the regulation of *Pax7* transcription. Although the ~40% decrease in Pax7 expression did not seem to account for the near total loss of expression of the Pax7 target *Myf5*, we also found a disproportionate ~85% decrease in Pax7 protein. While MLL1 was found to bind at *Pax7, Mll1* KO resulted in a modest decrease of H3K4me3 and no gain of H3K27me3 at *Pax7*. These results are possibly explained by previous work suggesting the role of MLL1 is partly or largely independent of its H3K4 methyltransferase activity (Terranova et al., 2006; Mishra et al., 2014), and confirms previous findings that loss of MLL1 may not result in changes to H3K4me3 at its target

genes (Lim et al., 2009; Mishra et al., 2014). Because loss of MLL1 seems to result in *Pax7* mRNA which is not efficiently translated, a role for MLL1 in regulating mRNA activity through a translational regulatory mechanism, such as recruitment of mRNA binding proteins (Shi and Barna, 2015), might be suggested.

Of particular importance, the relatively small decrease in *Pax7* mRNA expression found by microarray in *Mll1* KO myoblasts would not have never been deemed significant for further examination without our *a priori* understanding of the role of Pax7 in myogenesis and *Myf5* expression. It is therefore likely that there may be additional undetected changes to protein expression of MLL1 targets occurring with *Mll1* KO in myogenic cells and in other cell types.

4.1.4. MLL1 does Not Regulate Hox or Dlx2 Gene Expression in Myoblasts

Based on gene expression analysis of *Mll1* KO cells from mouse embryo fibroblasts (MEF) (Wang et al., 2009a), embryoid bodies (EBs) (Ernst et al., 2004a; Terranova et al., 2006), bone marrow (BM) (Jude et al., 2007), and whole embryos (Yu et al., 1995), MLL1 is thought to be required for expression of specific *Hox* genes. In *Mll1* KO MEF, *Hoxc6-10*, which were among the most highly expressed *Hox* genes in control MEF, were all downregulated by several fold (Wang et al., 2009a). In EBs and BM, several *Hox* genes including *Hoxa9-10* were also found to have a multi-fold decrease in expression when MLL1 is lost (Ernst et al., 2004a; Jude et al., 2007).

Surprisingly, our microarray data from control and *Mll1* KO myoblasts found little change in expression of any *Hox* gene. *Hoxa6-10* and *Hoxc5-10,* which were among the most highly expressed *Hox* genes in myoblasts, had no greater change in expression

than 25% up or down with MLL1 KO. Among all *Hox* genes, only *Hoxa11* had a change greater than 25%, with its expression decreased by ~27.5% in *Mll1* KO relative to control myoblasts. Microarray data was partially confirmed using qPCR for *Hoxc10*, the *Hox* gene with highest expression in myoblasts. *Hoxc10* was increased by ~10% by microarray and decreased by ~18% by qPCR in *Mll1* KO relative to control myoblasts, suggesting that no clear disregulation of *Hoxc10* transcription occurs when MLL1 is lost in myoblasts.

During post-natal neurogenesis, *Mll1* KO in NSC in the sub-ventricular zone (SVZ) results in loss of *Dlx2* mRNA expression, and loss of *Dlx2* expression was purported to directly result in the inability to differentiate to neurons (Lim et al., 2009). Similar to our findings for Hox genes, our microarray and qPCR data showed no difference in *Dlx2* mRNA expression between control and *Mll1* KO myoblasts. By microarray, and based on qPCR Ct values (data not shown), *Dlx2* is expressed at a level similar to or higher than *Pax7*, thus *Dlx2* is seemingly expressed at a physiologically relevant level in myoblasts but is unaffected by loss of MLL1.

An explanation for the different effects we found on Hox gene expression in *Mll1* KO myoblasts, compared to previously published reports, may be due to the heterogeneity of cell populations used for earlier work. In MEF, or the embryos from which the MEF were derived, and in EBs, *Mll1* KO may result in a shift in cell identities, fate choices or developmental progression, or in cell-type specific proliferation defects within these cell populations. Similarly, BM and SVZ cells are non-specifically isolated from their respective tissues (Jude et al., 2007; Lim et al., 2009), and as with whole embryos, it is likely that the specific cellular makeup of BM and the SVZ is transformed

when MLL1 is lost. The resulting changes in cell-type populations of embryos, embryo derived *Mll1* KO MEF and EBs, BM and SVZ may then result in cell populations that intrinsically do not expresses *Hox*/*Dlx2* genes, express *Hox*/*Dlx2* genes at a lower level, or expresses a different subset of *Hox*/homeobox containing genes. Thus, rather than being required for expression of *Hox*/*Dlx2*, MLL1 may be required for maintenance or proliferation of the specific cell types which express these genes. As cultured myoblasts are homogeneous (Rando and Blau, 1994) and have limited cell-type plasticity under standard growth conditions (Yin et al., 2013b), *Mll1* KO may not effect *Hox* or *Dlx2* gene expression in myoblasts because *Mll1* KO cannot result in a major change to cell types or cell populations. It may be that a subtle change in myoblast type does occur which results in our findings that *Six2*, *Lbx1*, and *Dlx2* expression are downregulated. For example, in early development a subset of muscle precursors migrate into the limb bud (Vasyutina and Birchmeier, 2006); it has been found that *Lbx1* expression is required for muscle precursor migration (Schafer and Braun, 1999), therefore loss of *Lbx1* may signify a shift to a non-migratory muscle progenitor type.

MLL1 has been shown to specifically bind to a subset of expressed *Hox* genes (Guenther et al., 2005; Milne et al., 2002, 2005) and to *Dlx2* (Lim et al., 2009) and may indeed have a role in expression of these genes. If MLL1 is required for formation of translation competent *Hox*/*Dlx2* mRNA, as it seems to be for *Pax7*, loss of MLL1 may result in changes to cell fate due to loss of translation of these factors. Rather than MLL1 being directly required for *Hox*/*Dlx2* gene mRNA expression, the resulting changes to cell types may account for the loss of *Hox* and *Dlx2* mRNA expression. If this is true, and MLL1 is not directly necessary for expression of specific mRNAs, it may be that all

changes in mRNA expression, including loss of *Six2*, *Dlx1* and *Lbx1*, in *Mll1* KO myoblasts are secondary effects due to changes in translation of transcription factors driving their expression.

4.1.5. MLL1 is Not Required for Myogenic Differentiation

It has been reported that loss of MLL1 results in impaired differentiation to the neural but not glial lineage (Lim et al., 2009). Loss MLL1 in the hematopoietic lineage causes hematopoietic stem and progenitor cells to exit quiescence, after which they are lost, however, there is no apparent effect on the progress of progenitors through hematopoietic differentiation (Ernst et al., 2004a; Jude et al., 2007; McMahon et al., 2007). Loss of MLL1 in primary myoblasts also has no apparent effect on myoblast differentiation with *Mll1* KO and control myoblasts showing similar changes to gene expression while differentiating under low mitogen conditions *in vitro*. While MLL1 may write the H3K4me3 mark at specific loci (Milne et al., 2002) and also contributes to gene expression through non-HMT activity (Mishra et al., 2014; Terranova et al., 2006), MLL1 is thought to act at a subset of genes (Wang et al., 2009a), and as was found for hematopoietic differentiation (Jude et al., 2007), MLL1 is dispensable for activation of genes required for myogenic differentiation. Importantly, either Myf5 or MyoD are required for activation of the myogenic program (Rudnicki et al., 1993). While Myf5 expression is lost in *Mll1* KO myoblasts, MyoD expression is unaffected and therefore *Mll1* KO myoblasts are able to initiate myogenic differentiation through MyoD in the absence of Myf5.

The effect of loss of MLL1 in satellite cells seems to be similar to loss of MLL1 *ex vivo*. In injured muscle from tamoxifen injected Pax7-Cre/MLL1$^{fl/fl}$ mice a portion of satellite cells express myogenin indicating that differentiation is initiated. Additionally, centrally located nuclei are found in regenerating muscle from tamoxifen injected Pax7-Cre/MLL1$^{fl/fl}$ mice, indicating that fusion of new nuclei derived from *Mll1* KO satellite cells occurs.

4.1.6. MLL1 is Not Required for Activation of *Myf5* by Pax7

Previous work has identified MLL1 and MLL2 as HMTs which interact with Pax7 to activate target genes including *Myf5* (Kawabe et al., 2012; McKinnell et al., 2008). We found that *Mll2* KO in primary myoblasts had no effect on *Myf5* expression, indicating that MLL2 is not required for Myf5 expression. *Mll1* KO resulted in loss of *Myf5* mRNA expression and loss of H3K4me3 at *Myf5*, but also resulted in loss of Pax7 protein. Because Pax7 protein was lost with *Mll1* KO, loss of Pax7 precluded determining if MLL1 is required for Pax7 to activate *Myf5*.

Exogenous expression of Pax7 at super-physiological levels was able to maintain *Myf5* expression after *Mll1* KO or *Mll1*/*Mll2* double KO in myoblasts, indicating that Pax7 can maintain *Myf5* expression in the absence of MLL1 and MLL2. Inducible Pax7, expressed at physiological levels, was able to re-establish Myf5 expression and H3K4me3 at *Myf5* subsequent to loss of MLL1 and loss of H3K4me3 at *Myf5*. It has been proposed that the majority of H3K4me3 is written by Set1A/B (Ardehali et al., 2011; Wu et al., 2008), and it is likely Pax7 may also interact with Set1A/B or other H3K4 HMTs to activate *Myf5* expression.

4.1.7. Role of MLL1 in Myogenic Cell Identity

In this work, we report our analysis of previously published date showing that *Myf5* is repressed by CpG methylation early in development, at the inner cell mass (Borgel et al., 2010), and embryonic stem cell stage, and in many cell types in later stages of development (Bernstein et al., 2010; Gascard et al., 2015). We further determined that CpG methylation at the *Myf5* TSS is absent in myoblasts and committed satellite cells that have expressed *Myf5*, and find evidence that satellite stem cells that have never expressed *Myf5* retain DNA methylation at Myf5. These findings suggest that *Myf5* may not be expressed in Pax7 expressing satellite stem cells due to CpG methylation at *Myf5*. When MLL1 expression is lost in cultured myoblasts, DNA methylation is gained at *Myf5* suggesting a pivotal shift in cellular identity away from a committed myogenic cell towards a more stem cell like state.

The basis for re-methylation of *Myf5* in *Mll1* KO myoblasts is unclear. Re-methylation of *Myf5* may be directly related to loss of *Myf5* transcription, however we did not see DNA methylation of *Myf5* in *in vitro* differentiated myotubes that do not express *Myf5*. Re-methylation of *Myf5* may require both loss of *Myf5* transcription and continued proliferation. Proliferation, which does not occur during myogenic differentiation, may remove or dilute epigenetic marks preventing methylation of *Myf5*. Importantly, *Pax7* KO also results in exit from the cell cycle but partially spares *Myf5* expression, with *Myf5* expression deceasing by ~ 40% (Maltzahn et al., 2013, and data not shown). The partial maintenance of *Myf5* expression in *Pax7* KO perhaps indicates that activating epigenetic marks at *Myf5* are retained in the absence of Pax7, and suggests

that proliferation is required for activating H3K4ms3 marks to be lost. Because exogenous Pax7 rescues expression of *Myf5* in *Mll1* KO myoblasts it is assumed that exogenous Pax7 also maintains *Myf5* in a unmethylated state, it seems unlikely that loss of MLL1 triggers a fundamental change in regulation of methylation directly resulting in re-methylation of *Myf5*.

4.1.8. Biomedical Implications of the Regulation of Pax7 by MLL1

This work may potentially be used at address two matters of clinical importance. First, recent work has identified specific inhibitors for MLL1 (Cao et al., 2014; Zhang et al., 2016a), or the obligate MLL1/2 cofactor menin (Grembecka et al., 2012). An intriguing possibility is that inhibition of MLL1 in cultured myoblasts would result in cells which have *Myf5* repressed by DNA methylation, and which may possibly have greater potential to repopulate the satellite niche after transplant. While MyoD expression is found in *Mll1* KO myoblasts, *MyoD* mRNA is also expressed in satellite cell progenitors and activated satellite cells, and is downregulated in quiescent satellite cells (Bentzinger et al., 2012; Kanisicak et al., 2009; Wood et al., 2013). Because MyoD expression might trigger differentiation prior to a transplanted myogenic cell embedding to a satellite cell niche, a combination of MLL1 inhibition, and *MyoD* inhibition through siRNA, TNF alpha (Guttridge et al., 2000) or hypoxia (Yun et al., 2005) might result in conversion of myoblasts, which can be vastly expanded *in vitro*, into therapeutically useful cells with myogenic stem cell potential. This therapeutic potential would also depend upon maintenance of myogenic lineage specification or identity, and restoration of *Pax7* expression after the MLL1 inhibitor had been removed during transplant.

Second, rhabdomyosarcoma (RMS), a poor prognosis childhood malignancy is often associated with translocations resulting in fusions between 5' PAX3 or PAX7 and 3' FOXO1A (FKHR) (Barr, 2001). In the absence of Pax3/7-FKHR fusions, PAX7 expression is also often upregulated in the embryonal RMS subtype (ERMS) (Tiffin et al., 2003). Importantly, in some RMS and in most ERMS, MLL1 likely regulates PAX7-FKHR and PAX7 expression. Because PAX7-FKHR or PAX7 expression seems to be integral for some RMS or ERMS tumors, our work suggests that MLL1 inhibitors may be useful therapeutic tools. Hypothetically, MLL1 inhibitors would result in downregulation of PAX7-FKHR or PAX7 expression in RMS or ERMS and result in decreased cancer cells proliferation or differentiation. Because MLL1 is required for HSC and NSC, and is likely required for other stem cell types, use of MLL1 inhibitors, like other chemotherapeutic agents, would need to be carefully administrated to avoid excess off-target toxicity.

4.1.9. Future Directions Regarding the Role of MLL1 in Myogenesis

This work raises several unresolved questions regarding the role of MLL1 in gene regulation. First, while MLL1 causes a decrease in Pax7 mRNA expression, there is a disproportional drop in Pax7 protein relative to the change in Pax7 mRNA. Further, this work also finds that in *Mll1* KO myoblasts, mRNA expression levels of other putative MLL1 targets are not affected by loss of MLL1. Our data suggest that MLL1 localizes to Pax7, and that Pax7 protein is not specifically degraded in *Mll1* KO myoblasts. Previously published work has also confirmed recruitment of MLL1 to target Hox genes (Wang et al., 2009a). Our findings suggest that the major role of MLL1 at Pax7 is neither

as a H3K4 HMT nor as a transcription regulator. The finding that Pax7 mRNA is produced while Pax7 protein expression is disproportionally downregulated points to a novel role for MLL1 in preparing Pax7 mRNA for translation. It may also be that MLL1 also has a role for translation of Hox genes rather that for their transcription.

All previous work analyzing the effect of *Mll1* KO on transcription was done using mRNA isolated from heterogeneous cell populations consisting of whole embryos (Yu et al., 1995; Hess et al., 1997; Yokoyama et al., 2013), heterogeneous tissues (Yagi et al., 1998; Terranova et al., 2006; Jude et al., 2007; Lim et al., 2009), or heterogeneous cell cultures (Milne et al., 2002; Ernst et al., 2004a; Wang et al., 2009a; Milne et al., 2010). Because homogeneous cell types were not used, a causality problem arises and it cannot be determined from these experiments whether loss of MLL1 results in loss of target gene mRNA expression, or loss of cells that are dependent upon translation products of MLL1 target gene mRNAs. As an example of cell specific MLL1 dependence, as we have shown, loss of MLL1 in regenerating muscle results in loss of Pax7 expressing satellite cells. Transcriptional analysis of *Mll1* KO whole muscle would therefore show that Pax7 mRNA is lost, not because Pax7 is not being transcribed in satellite cells, but because the satellite cells, which express Pax7, are lost. Much of the previous work with *Mll1* KO models also suggests that loss of MLL1 results in defects to specific cell types resulting in changes to the cellular composition of complex tissues. Further work using purified homogenous cell populations is necessary to address this causality problem and to determine if the general role of MLL1 is a conventional facilitation-of-transcription role, or if the role of MLL1 is to prepare mRNAs of its target genes for translation.

While we endeavored to show that full length Pax7 mRNA was being produced in *Mll1* KO myoblasts, it may be that there is a subtle change to Pax7 transcription that results in a change in translation rate. The mechanism by which MLL1 might prepare target gene mRNAs for translation is unclear and as the field of translational regulation matures, additional likely mechanisms may emerge. Promisingly, recent work has determine that the ribosomal protein L38 (Rpl38) has a specific role in translation of Hox mRNAs and loss of Rpl38 function results in homeotic transformations (Kondrashov et al., 2011; Xue et al., 2015), which are also found in *Mll1* mutant embryos (Yu et al., 1995). While nothing specifically suggests that MLL1 prepares mRNAs for interaction with Rpl38, it may not be a coincidence that *Mll1* KO seems to result in Pax7 mRNA that is inefficiently translated, and that other MLL1 target genes are included in a group for which transcription product mRNAs seem to require a special process for translation. The coincidental requirement for both MLL1 and Rpl38 for expression of overlapping targets suggests that further work may be justified to clarify whether MLL1 contributes to targeting of mRNAs to Rpl38 or to other ribosomal proteins.

4.2.0. Overview of Demethylation of *Myf5* Proximal Promoter

There are two types of muscle satellite cells, satellite stem cells, that have never expressed the MRF *Myf5*, or committed satellite cells, which have expressed *Myf5* (Kuang et al., 2007). Satellite stem cells and committed satellite cells both express Pax7, which activates *Myf5* expression (McKinnell et al., 2008; Kawabe et al., 2012). Since Pax7 activates *Myf5*, and *Pax7* is expressed in satellite stem cells, an ongoing question is why Pax7 does not activate *Myf5* expression in satellite stem cells. Recent work has

determined that Pax7 is activated when methylated by Carm1, and that Carm1 specifically methylates Pax7 in committed satellite cells (Kawabe et al., 2012). The mechanism by which the Pax7-Carm1 interaction is regulated is unclear and other mechanisms, beyond methylation of Pax7, may also contribute to maintenance of satellite stem cells.

Assessment of human methyl DNA immune precipitation (meDIP) data found that in embryonic stem cells, and many somatic cell types, the *Myf5* gene DNA is methylated in the 5'coding region proximal to its transcription start site (*Myf5* TSS) ((Bernstein et al., 2010; Gascard et al., 2015); GEO accession GSE16368). Here, we determined that *Myf5* TSS DNA methylation is found in MEF but not in cultured myoblasts, indicating that *Myf5* DNA methylation is lost or specifically removed in the myogenic lineage. Because methylation located in 5' transcribed DNA is associated with gene silencing (Klose and Bird, 2006), we questioned if *Myf5* TSS methylation may function to silence *Myf5* expression in satellite stem cells which express *Pax7* but not *Myf5*. We determined that the *Myf5* TSS is unmethylated in satellite cells directly isolated from mice that are marked by Myf5 activated lineage tracing. Satellite stem cells which are not marked by *Myf5* expression were found to have over 10-fold more DNA methylation than the *Myf5* positive lineage, indicating that the transition from satellite stem cell to committed satellite cell likely involves specific demethylation of the *Myf5* TSS.

We further explored possible mechanisms that may regulate demethylation of *Myf5*. Based on previous work (Hino et al., 2001; Ko et al., 2013), we found that Dvl3 co-precipitates with Tet3, suggesting a possible mechanism in which Wnt7a signaling,

which promotes symmetric satellite stem cell divisions (Le Grand et al., 2009), acts to inhibit activation of *Myf5* expression through negative regulation of Tet demethylation. We also found that exogenous Pax7 expression, while sufficient to upregulate *Myf5* expression in non-myogenic cells, does not automatically result in demethylation of *Myf5* DNA and results in sub-physiological *Myf5* expression.

4.2.1. H3K4 Methylation and Promoter DNA Demethylation at *Myf5*

An important consideration regarding the finding that *Myf5* is likely demethylated at the point of myogenic commitment are the mechanisms by which DNA demethylation at *Myf5* may be regulated. Exogenous Pax7 expression is sufficient to upregulate *Myf5* mRNA expression in non-myogenic 10T1/2 cells (McKinnell et al., 2008). However, we found the level of *Myf5* mRNA expression is more than 10 fold lower in exogenous Pax7 expressing 10T1/2 cells than in normal primary myoblasts, confirming previous findings showing that Myf5 protein expression is expressed at a lower level in exogenous Pax7 expressing 10T1/2 cells than in myoblasts (McKinnell et al., 2008). We also found that in 10T1/2 cells expressing exogenous Pax7, the *Myf5* proximal promoter remains methylated. These results suggest that while Pax7 expression is able to act by depositing H3K4me3 at *Myf5* in non-myogenic 10T1/2 cells (McKinnell et al., 2008), Pax7 is unable to demethylate *Myf5* and DNA methylation at *Myf5* prevents its efficient expression.

It has previously been reported that many developmental genes have bivalent epigenetic marks with activating H3K4me3 and repressive H3K27me3 (Bernstein et al., 2006). At these bivalent domains, the repressive H3K27me3 is able to prevent mRNA elongation and gene expression despite initiation of transcription through H4K3me3. No

bivalent domain containing H3K4me3 and DNA methylation has been reported, however, to our knowledge bivalence with DNA methylation is not contradicted by published research. In some cases H3K4me3 and DNA methylation may be conflicted, for instance methylation of H3K4 inhibits de-novo DNA methylation by DNMT3A through DNMT3L (Ooi et al., 2007; Otani et al., 2009), however, no effect for H3K4 methylation status has been reported for maintenance of DNA methylation by DNMT1. CXXC domains in MLL1/2 and the SetD1A/B accessory protein Cfp1 bind to unmethylated CpGs, and target H3K4me3 to unmethylated CpG islands (Allen et al., 2006; Ayton et al., 2004; Birke et al., 2002; Clouaire et al., 2012; Thomson et al., 2010), however, it is unclear if CpG methylation excludes H3K4 HMTs during their recruitment by transcription factors, as occurs at *Myf5* through Pax7. It may be that an uncharacterized bivalent domain with H3K4me3 and methylated DNA exists in some conditions, and that this bivalent domain is found at *Myf5* in exogenous Pax7 expressing 10T1/2 cells and in satellite stem cells that express Pax7 but have never expressed *Myf5*.

4.2.2. Inhibition of DNA Demethylation by Non-Canonical Wnt Signaling

Non-canonical Wnt signaling through Wnt7a/Frizzled7 has an inhibitory role regulating the satellite stem cell to myogenic satellite cell transition. Wnt7a/Frizzled7 signaling blocks asymmetric satellite stem cell division and initiation of *Myf5* expression by activating the plainer cell polarity (PCP) pathway (Le Grand et al., 2009). The precise mechanism by which Wnt7a/Frizzled7/PCP blocks activation of *Myf5* and asymmetric division is unclear. Wnt7a/Frizzled7/PCP may act to directly block the pathway leading

to *Myf5* expression, act indirectly to maintain stem cell niche localization required for repression of *Myf5*, or both.

Prior to the discovery of the role of Tet family enzymes in DNA demethylation, an interaction between IDAX (also known as CXXC4), and dishevelled, a downstream effector of Wnt signaling, was determined (Hino et al., 2001). IDAX is a ancestral domain of Tet2, which post-translationally complexes with Tet2. Tet1 and Tet3 retain their CXXC domain (Ko et al., 2013). The interaction between IDAX, Wnt signaling/dishevelled, and Tet-based DNA demethylation has not been explored since the discovery of the function of Tet demethylases. Because IDAX interacts with dishevelled, which is linked to the Wnt signaling pathway, this provides a potential mechanism for how Wnt signaling may regulate DNA demethylation at *Myf5*.

Through Co-IP experiments of exogenously expressed proteins we found an interaction between Tet3 and Dvl3, showing that the Tet3 CXXC domain interacts with dishevelled. The Tet-dishevelled interaction supports a hypothesis in which Wnt7a/Frizzled7/PCP signaling inhibits *Myf5* DNA demethylation in satellite stem cells through inhibition of Tet.

4.2.3. The Role of Metabolism in Epigenetic Regulation

Several recent publications have identified roles for metabolism in regulating myogenesis (Cerletti et al., 2012; Liu et al., 2012; Ryall et al., 2015a; Zhang et al., 2016b). Metabolism also has a well-recognized role in regulation of stem cells, and metabolic abnormalities are a hallmark of cancer cells with stem cell like characteristics (Warburg, 1956; Gu et al., 2016; Peng et al., 2016; Sen et al., 2016; Tian et al., 2016).

The role of metabolism in regulation of epigenetic mechanisms is in part through changes in availability of rate limiting substrates, including acetyl-CoA, NAD+, and alpha-ketoglutarate, that are used by epigenetic regulators (Ryall et al., 2015b; Su et al., 2016). Acetyl-CoA is the substrate for acetyltransferases which acetylate histones on active genes, thereby facilitating separation of histones from DNA, and allowing the transcriptional machinery access to DNA (Marmorstein and Zhou, 2014). Nuclear acetyl-CoA and histone acetylation also depend on availability of citrate which is generated through glycolysis (Wellen et al., 2009). NAD+ is a substrate for a class III HDACs, the sirtuins, which deacetylate histones (Janke et al., 2015; Seto and Yoshida, 2014). NAD+ levels and sirtuin activity are increased by caloric restriction and under fatty acid oxidation (Janke et al., 2015; Ryall et al., 2015a), while hypoxia and/or predominance of the glycolytic pathway results in decreased NAD+ levels and sirtuin activity (Ryall et al., 2015a; Su et al., 2016). Importantly, demethylation of histones by JmjC histone demethylases, and DNA by Tet DNA demethylases, both require oxygen as well as alpha-ketoglutarate (Janke et al., 2015; Su et al., 2016). In hypoxic conditions lactate dehydrogenase A converts alpha-ketoglutarate to L-2-hydroxyglutarate which acts as an inhibitor for alpha-ketoglutarate binding by JmjC and Tet enzymes (Intlekofer et al., 2015). A similar molecule, R-2-hyrodxyglutarate, which also inhibits Tet demethylases, is produced by mutations in IDH1/2 that are found in some hematopoietic malignancies (Figueroa et al., 2010). Together, these varied metabolic mechanisms likely have an integral role in epigenetic regulation of cell fate decisions, and may be part of niche based and regional- or spatial-developmental regulation of stem cells.

4.2.4. The Role of Metabolism in Stem Cells and Myogenesis

Multiple studies have found evidence for the presence of, and requirement for, a hypoxic niche for hematopoietic stem cells (HSC) (Chow et al., 2001; Parmar et al., 2007; Simsek et al., 2010; Suda et al., 2011). The role of the hypoxic niche in regulation of DNA methylation/demethylation in HSC has not been examined. Because Tet enzymes are inhibited in hypoxia (Intlekofer et al., 2015; Janke et al., 2015; Su et al., 2016) and mutations resulting in Tet dysfunction cause myeloid malignancies resembling inhibited HSC differentiation (Abdel-Wahab et al., 2009; Figueroa et al., 2010; Ko et al., 2010), it seems likely that the hypoxic niche contributes to HSC maintenance in part through inhibition of DNA demethylation.

The role of metabolism in regulation of myogenesis is an active area of study. Caloric restriction was found to have a positive effect on myogenic regeneration, and satellite cells from caloric restricted mice were found to have higher transplantation efficiency (Cerletti et al., 2012). The growth factor GDF11 has been found to have a beneficial effect on muscle regeneration in aged mice through improved mitochondrial function (Sinha et al., 2014). Analysis of the metabolic change occurring when freshly isolated quiescent satellite cells are cultured *ex vivo* for 48 hours identified a metabolic shift from fatty acid oxidation to glycolysis resulting in decreased NAD+ levels and sirtuin activity in cultured myoblasts (Ryall et al., 2015a). Another study determined that replenishment of NAD+ levels in aged mice resulted in enhanced muscle regeneration and increased lifespan through rescue of mitochondrial function in aged stem cells (Zhang et al., 2016b). Several studies have identified differing effects of atmospheric oxygen and low oxygen on propagation and differentiation of satellite cell derived

myoblasts *in vitro* (Chakravarthy et al., 2001; Csete et al., 2001; Gustafsson et al., 2005; Li et al., 2007; Liu et al., 2012; Urbani et al., 2012; Yun et al., 2005). Roles for Hif1a and Notch signaling (Gustafsson et al., 2005; Yun et al., 2005), and expression of microRNAs (Liu et al., 2012) have also been implicated as effectors of the hypoxic response during myogenesis.

While the role of metabolism in regulation of acetylation and de-acetylation is well recognized, the role of hypoxia and metabolism in regulation of DNA demethylation and its effects are relatively unexplored in any cell type. A critical role for DNA demethylation at *myogenin* during terminal myogenesis has been suggested by several studies (Fuso et al., 2010; Lucarelli et al., 2001; Miyata et al., 2015; Oikawa et al., 2011; Zhong et al., 2017). While works cited above have determined a role for metabolic changes in muscle regeneration and differentiation, a clear consensus regarding the metabolic mechanisms regulating myogenesis has not been delineated. Metabolism and mitochondrial function seem to affect myogenesis *in vivo*, as well as *in vitro*, and metabolic factors have been determined to have a role in regulation of DNA demethylation. Therefore, it seems likely that metabolic programming may have an effect on epigenetic regulation of myogenic commitment through demethylation of *Myf5* DNA, and on myogenic differentiation through demethylation of myogenin and activation of *myogenin* transcription.

4.2.5. Hypothetical Mechanism for Regulation of *Myf5* Demethylation

The importance of a functional stem and progenitor cell population for the regenerative capacity of muscle likely dictates redundancy in negative regulation of

differentiation, thereby ensuring maintenance of a stem and progenitor cell pool. While Wnt7a, through Frizzled7 and non-canonical PCP Wnt signaling, has an established role in inhibiting *Myf5* expression or promoting symmetric satellite stem cell divisions (Le Grand et al., 2009; von Maltzahn et al., 2013b), the specific mechanism linking Wnt7a to repression of *Myf5* expression at the gene is unclear.

Based on the available literature, and assuming that *Myf5* is specifically activated through demethylation via Tet demethylases during myogenic commitment, a potential hypothesis for negative regulation of *Myf5* demethylation is that non-canonical Wnt signaling or hypoxia can each individually, or in combination, inhibit Tet demethylation of *Myf5* thereby sparing satellite stem cells from the effects of pro-differentiation signals. Wnt7a signaling may occur in the satellite cell niche, however, Wnt7a expression increases after muscle damage (Le Grand et al., 2009), suggesting that the Wnt7a inhibitory signal is also released to cells outside of the niche during regeneration. It is unclear if the muscle satellite cell niche is hypoxic, however the oxygen affinity of myoglobin is higher than that of hemoglobin (Wittenberg, 1970), and unsaturated myoglobin may strip blood of oxygen resulting in hypoxic venous blood flow. Hypoxia would also be expected throughout damaged muscle after significant injury prior to re-establishment of the capillary network. If it is also a requirement that *myogenin* is demethylated during terminal differentiation, hypoxia in the injured muscle may also contribute to the delay of differentiation during the proliferative period after injury and until circulation is reestablished. The mechanism by which Tet demethylases are recruited during gene activation is unknown, however it may be that DNA demethylation

is an automatic response at permissive genes marked with H3K4me3 when Tet function is not inhibited by non-canonical Wnt signaling or metabolic inhibition.

4.2.6. Future Directions Regarding the Role of *Myf5* DNA Methylation in Regulation of Satellite Stem Cell Identity

Our evidence strongly suggests that *Myf5* expression is repressed by DNA methylation in non-myogenic cells and in satellite stem cells, and is not repressed in committed satellite cells and other myogenic progenitors. Further work is required to determine if *Myf5* is actively demethylated during the transition from satellite stem cell to myogenic satellite cells. Because hydroxylation through Tet enzymes is the only known mechanism for active demethylation, loss of function experiments targeting Tet enzymes through siRNA, KO or chemical inhibitor are necessary. *Myf5* is activated experimentally during asymmetric satellite stem cell divisions after injury *in vivo,* or in *ex vivo* cultured myofibers. If *Myf5* is activated through active demethylation, loss of Tet function would be expected to result in increased YFP– cells and YFP–/YFP– symmetric divisions in a *Myf5*-Cre/Rosa-YFP context.

The non-canonical Wnt signaling PCP pathway has been clearly shown to block activation of *Myf5* (Le Grand et al., 2009; Maltzahn et al., 2011; Bentzinger et al., 2013; von Maltzahn et al., 2013b; Bentzinger et al., 2014). A previous connection has also been determined between the Tet2 binding partner IDAX and the Wnt signaling protein dishevelled (Hino et al., 2001; Ko et al., 2013), and our own work has also shown a interaction between Dvl3 and Tet3. The link between the Wnt7a/Frizzled pathway and Tet protein inhibition should therefore be explored further. It is currently unclear how the

Tet/dishevelled interaction is regulated; however, because Wnt7a inhibits activation of *Myf5* it might be expected that the non-canonical Wnt7a/PCP pathway results in an inhibitory interaction between dishevelled and Tet. Alternatively, it has been proposed that dishevelled acts as a nuclear cytoplasmic shuttle protein (Itoh et al., 2005), in which case dishevelled may act to import or export Tet from the nucleus depending upon PCP signaling. Ultimately, it would be expected that stimulation of satellite stem cells with Wnt7a would results in a change in interaction of Tet with dishevelled, or a dishevelled dependent change in nuclear/cytoplasmic localization of Tet.

It is currently unclear how Tet proteins are recruited to specific sites on DNA. Some evidence suggests that Tet2 is recruited by sequence specific transcription factors and that Tet1 and Tet3 are recruited to CpG dinucleotides through their CXXC domains (Rasmussen and Helin, 2016). It is possible that Tet proteins are recruited to *Myf5* by Pax7; if so, it is likely there is an additional level of regulation to a Tet-Pax7 interaction. Exogenous Pax7 expression in 10T1/2 cells results in upregulation of *Myf5*, but *Myf5* levels are sub-physiological and *Myf5* DNA remains methylated. Further work will be needed to determine if Pax7 and Tet proteins interact and how this interaction may be regulated. It is possible that the Tet-dishevelled interaction precludes a Tet-Pax7 interaction and release of Tet proteins from dishevelled allows Tet to interact with Pax7 and to be recruited to *Myf5*.

Tet proteins require oxygen and alpha-ketoglutarate to oxidize methylcytosine to hydroxy-methylcytosine (Sharma and Rando, 2017), therefore it would be expected that *Myf5* demethylation cannot occur in a hypoxic niche or under hypoxic conditions during regeneration. Future work will be necessary to determine if satellite stem cells exist in a

hypoxic niche, if oxygen levels are sufficiently deficient to inhibit demethylation of *Myf5*, and if the hypoxic niche therefore acts to maintain the satellite stem cell state through blocking of Tet protein function.

4.3 Conclusion and Significance

This work determines that MLL1 is required for efficient myogenic regeneration. MLL1 is required for proliferation of myogenic cells and for expression of the myogenic specification factor Pax7 at the protein, but not transcript, level. Loss of MLL1 also results in loss of expression of the Pax7 target gene *Myf5*. Exogenous expression of Pax7 in an *Mll1* KO context rescues *Myf5* expression indicating that Pax7 activates genes independent of MLL1. Further, transcription of previously identified MLL1 targets is spared in *Mll1* KO myoblasts, indicating that purported roles for MLL1 in gene expression may need reevaluation.

Pax7 specifies permissive cells to the myogenic lineage (Seale et al., 2004; Darabi et al., 2011, 2012), and its expression is essential for muscle stem cells and myogenic regeneration (von Maltzahn et al., 2013a; Seale et al., 2000). This work provides new understanding into how Pax7 expression is regulated and its findings contribute to our understanding of the regulation and specification of myogenic stem cells and adds to the knowledge base that is required for formulation of therapeutic strategies for myogenic disease. This work also, through experiments disparate to previous work, confirms previous findings that *Myf5* expression is linked to Pax7. Finally, this work suggests that targeting MLL1 activity through chemical inhibitors (Cao et al., 2014; Zhang et al.,

2016a), to disrupt *Pax7* expression may be a useful strategy for combating *Pax7* fusion and *Pax7* expression-related rhabdomyosarcoma.

This work also determines that *Myf5* expression is inhibited by CpG methylation in non-myogenic cell types and that CpG methylation at *Myf5* is lost in the myogenic lineage. The specific demethylation of *Myf5* is a rare clear example of a lineage regulating gene for which DNA methylation is lost during fate commitment. Satellite stem cells which have not expressed *Myf5* are of potential use for restoration of healthy muscle in muscle dystrophies, therefore greater understanding of how *Myf5* is activated will provide further points of intervention for development of satellite stem cell based therapies. Further study of the mechanisms regulating demethylation of *Myf5* may also reveal more detail regarding the general mechanisms for demethylation of genes. While the myogenic pathway may proceed independently of *Myf5* expression (Rudnicki et al., 1993), loss of Tet function is associated with malignancy in non-muscle tissues (Figueroa et al., 2010; Ko et al., 2010), presumably due to failure to initiate differentiation programs. Therefore, understanding of the mechanisms which regulate demethylation of *Myf5* during myogenesis may also be useful for gaining general understanding of malignancies involving Tet loss of function and the resulting interruption of differentiation initiation.

Each of the independent findings of this thesis provide significant new understanding to the field of muscle biology but also have implications for the wider field of epigenetics, development and regenerative medicine. The findings regarding the role of MLL1 in myogenesis provide a specific example of the role of MLL1. This work also provides unique clarity to the role of MLL1 through elimination of effects resulting from

cell-type instability occurring with loss of MLL1 by assessing loss of MLL1 in relatively homogenous and cell-type-stable myoblasts. These findings challenge previous conclusions and suggest that revisions in our understanding of MLL1 biology are necessary. The finding that *Myf5* is likely demethylated during myogenic commitment also has great importance for muscle biology, and also provides a well-defined platform for greater delineation of the mechanisms for and regulation of DNA demethylation.

It is hoped that, like the work preceding it, these findings will be used as the basis for further research, thereby continuing the stepwise progression towards a truer understanding.

References

Abdel-Wahab, O., Mullally, A., Hedvat, C., Garcia-Manero, G., Patel, J., Wadleigh, M., Malinge, S., Yao, J., Kilpivaara, O., Bhat, R., et al. (2009). Genetic characterization of TET1, TET2, and TET3 alterations in myeloid malignancies. Blood *114*, 144–147.

Allen, M.D., Grummitt, C.G., Hilcenko, C., Min, S.Y., Tonkin, L.M., Johnson, C.M., Freund, S.M., Bycroft, M., and Warren, A.J. (2006). Solution structure of the nonmethyl-CpG-binding CXXC domain of the leukaemia-associated MLL histone methyltransferase. EMBO J *25*, 4503–4512.

Ardehali, M.B., Mei, A., Zobeck, K.L., Caron, M., Lis, J.T., and Kusch, T. (2011). Drosophila Set1 is the major histone H3 lysine 4 trimethyltransferase with role in transcription. EMBO J. *30*, 2817–2828.

Arnold, L., Henry, A., Poron, F., Baba-Amer, Y., Rooijen, N. van, Plonquet, A., Gherardi, R.K., and Chazaud, B. (2007). Inflammatory monocytes recruited after skeletal muscle injury switch into antiinflammatory macrophages to support myogenesis. J. Exp. Med. *204*, 1057–1069.

Artinger, E.L., Mishra, B.P., Zaffuto, K.M., Li, B.E., Chung, E.K.Y., Moore, A.W., Chen, Y., Cheng, C., and Ernst, P. (2013). An MLL-dependent network sustains hematopoiesis. Proc. Natl. Acad. Sci. *110*, 12000–12005.

Ayton, P., Sneddon, S.F., Palmer, D.B., Rosewell, I.R., Owen, M.J., Young, B., Presley, R., and Subramanian, V. (2001). Truncation of theMLL gene in exon 5 by gene targeting leads to early preimplantation lethality of homozygous embryos. Genesis *30*, 201–212.

Ayton, P.M., Chen, E.H., and Cleary, M.L. (2004). Binding to Nonmethylated CpG DNA Is Essential for Target Recognition, Transactivation, and Myeloid Transformation by an MLL Oncoprotein. Mol. Cell. Biol. *24*, 10470–10478.

Bajard, L., Relaix, F., Lagha, M., Rocancourt, D., Daubas, P., and Buckingham, M.E. (2006). A novel genetic hierarchy functions during hypaxial myogenesis: Pax3 directly activates Myf5 in muscle progenitor cells in the limb. Genes Dev. *20*, 2450–2464.

Bannister, A.J., and Kouzarides, T. (2011). Regulation of chromatin by histone modifications. Cell Res. *21*, 381–395.

Barr, F.G. (2001). Gene fusions involving PAX and FOX family members in alveolar rhabdomyosarcoma. Oncogene *20*, 5736–5746.

Baubec, T., Colombo, D.F., Wirbelauer, C., Schmidt, J., Burger, L., Krebs, A.R., Akalin, A., and Schübeler, D. (2015). Genomic profiling of DNA methyltransferases reveals a role for DNMT3B in genic methylation. Nature *520*, 243–247.

Beauchamp, J.R., Heslop, L., Yu, D.S.W., Tajbakhsh, S., Kelly, R.G., Wernig, A., Buckingham, M.E., Partridge, T.A., and Zammit, P.S. (2000). Expression of Cd34 and Myf5 Defines the Majority of Quiescent Adult Skeletal Muscle Satellite Cells. J. Cell Biol. *151*, 1221–1234.

Beisel, C., and Paro, R. (2011). Silencing chromatin: comparing modes and mechanisms. Nat Rev Genet *12*, 123–135.

Bentley, G.A., Lewit-Bentley, A., Finch, J.T., Podjarny, A.D., and Roth, M. (1984). Crystal structure of the nucleosome core particle at 16 A resolution. J. Mol. Biol. *176*, 55–75.

Bentzinger, C.F., Wang, Y.X., and Rudnicki, M.A. (2012). Building Muscle: Molecular Regulation of Myogenesis. Cold Spring Harb. Perspect. Biol. *4*, a008342.

Bentzinger, C.F., Wang, Y.X., von Maltzahn, J., Soleimani, V.D., Yin, H., and Rudnicki, M.A. (2013). Fibronectin Regulates Wnt7a Signaling and Satellite Cell Expansion. Cell Stem Cell *12*, 75–87.

Bentzinger, C.F., Maltzahn, J. von, Dumont, N.A., Stark, D.A., Wang, Y.X., Nhan, K., Frenette, J., Cornelison, D.D.W., and Rudnicki, M.A. (2014). Wnt7a stimulates myogenic stem cell motility and engraftment resulting in improved muscle strength. J. Cell Biol. jcb.201310035.

Bernstein, B.E., Humphrey, E.L., Erlich, R.L., Schneider, R., Bouman, P., Liu, J.S., Kouzarides, T., and Schreiber, S.L. (2002). Methylation of histone H3 Lys 4 in coding regions of active genes. Proc. Natl. Acad. Sci. U. S. A. *99*, 8695–8700.

Bernstein, B.E., Mikkelsen, T.S., Xie, X., Kamal, M., Huebert, D.J., Cuff, J., Fry, B., Meissner, A., Wernig, M., and Plath, K. (2006). A bivalent chromatin structure marks key developmental genes in embryonic stem cells. Cell *125*, 315–326.

Bernstein, B.E., Stamatoyannopoulos, J.A., Costello, J.F., Ren, B., Milosavljevic, A., Meissner, A., Kellis, M., Marra, M.A., Beaudet, A.L., Ecker, J.R., et al. (2010). The NIH Roadmap Epigenomics Mapping Consortium. Nat. Biotechnol. *28*, 1045–1048.

Birke, M., Schreiner, S., García-Cuéllar, M.-P., Mahr, K., Titgemeyer, F., and Slany, R.K. (2002). The MT domain of the proto-oncoprotein MLL binds to CpG-containing DNA and discriminates against methylation. Nucleic Acids Res. *30*, 958–965.

Birrane, G., Soni, A., and Ladias, J.A.A. (2009). Structural Basis for DNA Recognition by the Human PAX3 Homeodomain,. Biochemistry (Mosc.) *48*, 1148–1155.

Bischoff, R. (1974). Enzymatic liberation of myogenic cells from adult rat muscle. Anat. Rec. *180*, 645–661.

Bischoff, R. (1994). The satellite cell and muscle regeneration. In Myology, A.G. Engle, and C. Franzini-Armstrong, eds. (New York: McGraw-Hill), pp. 97–118.

Blau, H.M., Chiu, C.-P., and Webster, C. (1983). Cytoplasmic activation of human nuclear genes in stable heterocaryons. Cell *32*, 1171–1180.

Bober, E., Franz, T., Arnold, H.H., Gruss, P., and Tremblay, P. (1994). Pax-3 is required for the development of limb muscles: a possible role for the migration of dermomyotomal muscle progenitor cells. Dev. Camb. Engl. *120*, 603–612.

Bode, M., Wu, Y., Pi, X., Lockyer, P., Dechyapirom, W., Portbury, A.L., and Patterson, C. (2011). Regulation of ankyrin repeat and suppressor of cytokine signalling box protein 4 expression in the immortalized murine endothelial cell lines MS1 and SVR: a role for tumour necrosis factor alpha and oxygen. Cell Biochem. Funct. *29*, 334–341.

Boonsanay, V., Zhang, T., Georgieva, A., Kostin, S., Qi, H., Yuan, X., Zhou, Y., and Braun, T. (2016). Regulation of Skeletal Muscle Stem Cell Quiescence by Suv4-20h1-Dependent Facultative Heterochromatin Formation. Cell Stem Cell *18*, 229–242.

Borgel, J., Guibert, S., Li, Y., Chiba, H., Schübeler, D., Sasaki, H., Forné, T., and Weber, M. (2010). Targets and dynamics of promoter DNA methylation during early mouse development. Nat. Genet. *42*, 1093–1100.

Borycki, A.G., Li, J., Jin, F., Emerson, C.P., and Epstein, J.A. (1999). Pax3 functions in cell survival and in pax7 regulation. Development *126*, 1665–1674.

Boyer, L.A., Plath, K., Zeitlinger, J., Brambrink, T., Medeiros, L.A., Lee, T.I., Levine, S.S., Wernig, M., Tajonar, A., Ray, M.K., et al. (2006). Polycomb complexes repress developmental regulators in murine embryonic stem cells. Nature *441*, 349–353.

Boyes, J., and Bird, A. (1991). DNA methylation inhibits transcription indirectly via a methyl-CpG binding protein. Cell *64*, 1123–1134.

Bracken, A.P., Dietrich, N., Pasini, D., Hansen, K.H., and Helin, K. (2006). Genome-wide mapping of Polycomb target genes unravels their roles in cell fate transitions. Genes Dev. *20*, 1123–1136.

Braun, T., and Arnold, H.H. (1995). Inactivation of Myf-6 and Myf-5 genes in mice leads to alterations in skeletal muscle development. EMBO J. *14*, 1176–1186.

Braun, T., Buschhausen-Denker, G., Bober, E., Tannich, E., and Arnold, H.H. (1989a). A novel human muscle factor related to but distinct from MyoD1 induces myogenic conversion in 10T1/2 fibroblasts. EMBO J. *8*, 701–709.

Braun, T., Bober, E., Buschhausen-Denker, G., Kohtz, S., Grzeschik, K.-H., Arnold, H.H., and Kotz, S. (1989b). Differential expression of myogenic determination genes in muscle cells: possible autoactivation by the Myf gene products. EMBO J. *8*, 3617.

Braun, T., Bober, E., Winter, B., Rosenthal, N., and Arnold, H.H. (1990). Myf-6, a new member of the human gene family of myogenic determination factors: evidence for a gene cluster on chromosome 12. EMBO J. *9*, 821–831.

Braun, T., Rudnicki, M.A., Arnold, H.-H., and Jaenisch, R. (1992). Targeted inactivation of the muscle regulatory gene Myf-5 results in abnormal rib development and perinatal death. Cell *71*, 369–382.

Buckingham, M., and Relaix, F. (2007). The Role of Pax Genes in the Development of Tissues and Organs: Pax3 and Pax7 Regulate Muscle Progenitor Cell Functions. Annu. Rev. Cell Dev. Biol. *23*, 645–673.

Buckingham, M., and Rigby, P.W.J. (2014). Gene Regulatory Networks and Transcriptional Mechanisms that Control Myogenesis. Dev. Cell *28*, 225–238.

Buckingham, M., Bajard, L., Chang, T., Daubas, P., Hadchouel, J., Meilhac, S., Montarras, D., Rocancourt, D., and Relaix, F. (2003). The formation of skeletal muscle: from somite to limb. J. Anat. *202*, 59–68.

Cao, F., Townsend, E.C., Karatas, H., Xu, J., Li, L., Lee, S., Liu, L., Chen, Y., Ouillette, P., Zhu, J., et al. (2014). Targeting MLL1 H3K4 Methyltransferase Activity in Mixed-Lineage Leukemia. Mol. Cell *53*, 247–261.

Cao, R., Wang, L., Wang, H., Xia, L., Erdjument-Bromage, H., Tempst, P., Jones, R.S., and Zhang, Y. (2002). Role of Histone H3 Lysine 27 Methylation in Polycomb-Group Silencing. Science *298*, 1039–1043.

Caretti, G., Di Padova, M., Micales, B., Lyons, G.E., and Sartorelli, V. (2004). The Polycomb Ezh2 methyltransferase regulates muscle gene expression and skeletal muscle differentiation. Genes Dev. *18*, 2627–2638.

Carrozza, M.J., Li, B., Florens, L., Suganuma, T., Swanson, S.K., Lee, K.K., Shia, W.-J., Anderson, S., Yates, J., Washburn, M.P., et al. (2005). Histone H3 Methylation by Set2 Directs Deacetylation of Coding Regions by Rpd3S to Suppress Spurious Intragenic Transcription. Cell *123*, 581–592.

Carvajal, J.J., Keith, A., and Rigby, P.W.J. (2008). Global transcriptional regulation of the locus encoding the skeletal muscle determination genes Mrf4 and Myf5. Genes Dev. *22*, 265–276.

Cerletti, M., Jang, Y.C., Finley, L.W.S., Haigis, M.C., and Wagers, A.J. (2012). Short-Term Calorie Restriction Enhances Skeletal Muscle Stem Cell Function. Cell Stem Cell *10*, 515–519.

Chakravarthy, M.V., Spangenburg, E.E., and Booth, F.W. (2001). Culture in low levels of oxygen enhances in vitro proliferation potential of satellite cells from old skeletal muscles. Cell. Mol. Life Sci. CMLS *58*, 1150–1158.

Chargé, S.B.P., and Rudnicki, M.A. (2004). Cellular and Molecular Regulation of Muscle Regeneration. Physiol. Rev. *84*, 209–238.

Cheung, T.H., and Rando, T.A. (2013). Molecular regulation of stem cell quiescence. Nat. Rev. Mol. Cell Biol. *14*, 329–340.

Chiang, C., Litingtung, Y., Lee, E., Young, K.E., Corden, J.L., Westphal, H., and Beachy, P.A. (1996). Cyclopia and defective axial patterning in mice lacking Sonic hedgehog gene function. Nature *383*, 407–413.

Chow, D.C., Wenning, L.A., Miller, W.M., and Papoutsakis, E.T. (2001). Modeling pO2 Distributions in the Bone Marrow Hematopoietic Compartment. I. Krogh's Model. Biophys. J. *81*, 675–684.

Church, J.C.T., Noronha, R.F.X., and Allbrook, D.B. (1966). Satellite cells and skeletal muscle regeneration. Br. J. Surg. *53*, 638–642.

Clouaire, T., Webb, S., Skene, P., Illingworth, R., Kerr, A., Andrews, R., Lee, J.-H., Skalnik, D., and Bird, A. (2012). Cfp1 integrates both CpG content and gene activity for accurate H3K4me3 deposition in embryonic stem cells. Genes Dev. *26*, 1714–1728.

Collins, C.A., Olsen, I., Zammit, P.S., Heslop, L., Petrie, A., Partridge, T.A., and Morgan, J.E. (2005). Stem Cell Function, Self-Renewal, and Behavioral Heterogeneity of Cells from the Adult Muscle Satellite Cell Niche. Cell *122*, 289–301.

Constantinides, P.G., Jones, P.A., and Gevers, W. (1977). Functional striated muscle cells from non-myoblast precursors following 5-azacytidine treatment. Nature *267*, 364–366.

Csete, M., Walikonis, J., Slawny, N., Wei, Y., Korsnes, S., Doyle, J.C., and Wold, B. (2001). Oxygen-mediated regulation of skeletal muscle satellite cell proliferation and adipogenesis in culture. J. Cell. Physiol. *189*, 189–196.

Czermin, B., Melfi, R., McCabe, D., Seitz, V., Imhof, A., and Pirrotta, V. (2002). Drosophila Enhancer of Zeste/ESC Complexes Have a Histone H3 Methyltransferase Activity that Marks Chromosomal Polycomb Sites. Cell *111*, 185–196.

Darabi, R., Santos, F.N.C., Filareto, A., Pan, W., Koene, R., Rudnicki, M.A., Kyba, M., and Perlingeiro, R.C.R. (2011). Assessment of the Myogenic Stem Cell Compartment Following Transplantation of Pax3/Pax7-Induced Embryonic Stem Cell-Derived Progenitors. STEM CELLS *29*, 777–790.

Darabi, R., Arpke, R.W., Irion, S., Dimos, J.T., Grskovic, M., Kyba, M., and Perlingeiro, R.C.R. (2012). Human ES- and iPS-Derived Myogenic Progenitors Restore DYSTROPHIN and Improve Contractility upon Transplantation in Dystrophic Mice. Cell Stem Cell *10*, 610–619.

Daston, G., Lamar, E., Olivier, M., and Goulding, M. (1996). Pax-3 is necessary for migration but not differentiation of limb muscle precursors in the mouse. Dev. Camb. Engl. *122*, 1017–1027.

Daubas, P., and Buckingham, M.E. (2013). Direct molecular regulation of the myogenic determination gene Myf5 by Pax3, with modulation by Six1/4 factors, is exemplified by the −111 kb-Myf5 enhancer. Dev. Biol. *376*, 236–244.

Davis, R.L., Weintraub, H., and Lassar, A.B. (1987). Expression of a single transfected cDNA converts fibroblasts to myoblasts. Cell *51*, 987–1000.

Delhommeau, F., Dupont, S., James, C., Masse, A., Couedic, J.P. le, Valle, V.D., Alberdi, A., Dessen, P., Fontenay, M., Casadevall, N., et al. (2008). TET2 Is a Novel Tumor Suppressor Gene Inactivated in Myeloproliferative Neoplasms: Identification of a Pre-JAK2 V617F Event. Blood *112*, lba-3-lba-3.

Descartes, R. (1630). L'Homme.

Donaldson, S.K. (1985). Peeled mammalian skeletal muscle fibers. Possible stimulation of Ca2+ release via a transverse tubule-sarcoplasmic reticulum mechanism. J. Gen. Physiol. *86*, 501–525.

Epstein, J.A., Shapiro, D.N., Cheng, J., Lam, P.Y., and Maas, R.L. (1996). Pax3 modulates expression of the c-Met receptor during limb muscle development. Proc. Natl. Acad. Sci. *93*, 4213–4218.

Epsztejn-Litman, S., Feldman, N., Abu-Remaileh, M., Shufaro, Y., Gerson, A., Ueda, J., Deplus, R., Fuks, F., Shinkai, Y., Cedar, H., et al. (2008). De novo DNA methylation promoted by G9a prevents reprogramming of embryonically silenced genes. Nat. Struct. Mol. Biol. *15*, 1176–1183.

Ernst, P., Mabon, M., Davidson, A.J., Zon, L.I., and Korsmeyer, S.J. (2004a). An Mll-dependent Hox program drives hematopoietic progenitor expansion. Curr. Biol. *14*, 2063–2069.

Ernst, P., Fisher, J.K., Avery, W., Wade, S., Foy, D., and Korsmeyer, S.J. (2004b). Definitive hematopoiesis requires the mixed-lineage leukemia gene. Dev. Cell *6*, 437–443.

Faralli, H., and Dilworth, F.J. (2012). Turning on Myogenin in Muscle: A Paradigm for Understanding Mechanisms of Tissue-Specific Gene Expression. Comp. Funct. Genomics *2012*, 1–10.

Figueroa, M.E., Abdel-Wahab, O., Lu, C., Ward, P.S., Patel, J., Shih, A., Li, Y., Bhagwat, N., Vasanthakumar, A., Fernandez, H.F., et al. (2010). Leukemic IDH1 and IDH2 Mutations Result in a Hypermethylation Phenotype, Disrupt TET2 Function, and Impair Hematopoietic Differentiation. Cancer Cell *18*, 553–567.

Fukada, S., Uezumi, A., Ikemoto, M., Masuda, S., Segawa, M., Tanimura, N., Yamamoto, H., Miyagoe-Suzuki, Y., and Takeda, S. (2007). Molecular Signature of Quiescent Satellite Cells in Adult Skeletal Muscle. STEM CELLS *25*, 2448–2459.

Fuks, F., Hurd, P.J., Deplus, R., and Kouzarides, T. (2003). The DNA methyltransferases associate with HP1 and the SUV39H1 histone methyltransferase. Nucleic Acids Res. *31*, 2305–2312.

Fuso, A., Ferraguti, G., Grandoni, F., Ruggeri, R., Scarpa, S., Strom, R., and Lucarelli, M. (2010). Early Demethylation of non-CpG, CpC-rich, elements in the myogenin 5'-flanking region: A priming effect on the spreading of active demethylation. Cell Cycle *9*, 3965–3976.

Gascard, P., Bilenky, M., Sigaroudinia, M., Zhao, J., Li, L., Carles, A., Delaney, A., Tam, A., Kamoh, B., Cho, S., et al. (2015). Epigenetic and transcriptional determinants of the human breast. Nat. Commun. *6*, ncomms7351.

Gillespie, M.A., Le Grand, F., Scime, A., Kuang, S., von Maltzahn, J., Seale, V., Cuenda, A., Ranish, J.A., and Rudnicki, M.A. (2009). p38-gamma-dependent gene silencing restricts entry into the myogenic differentiation program. J. Cell Biol. *187*, 991.

Giry-Laterrière, M., Cherpin, O., Kim, Y.-S., Jensen, J., and Salmon, P. (2011). Polyswitch Lentivectors: "All-in-One" Lentiviral Vectors for Drug-Inducible Gene Expression, Live Selection, and Recombination Cloning. Hum. Gene Ther. *22*, 1255–1267.

Glaser, S., Schaft, J., Lubitz, S., Vintersten, K., van der Hoeven, F., Tufteland, K.R., Aasland, R., Anastassiadis, K., Ang, S.-L., and Stewart, A.F. (2006). Multiple epigenetic maintenance factors implicated by the loss of Mll2 in mouse development. Dev. Camb. Engl. *133*, 1423–1432.

Goulding, M., Lumsden, A., and Paquette, A.J. (1994). Regulation of Pax-3 expression in the dermomyotome and its role in muscle development. Development *120*, 957–971.

Grembecka, J., He, S., Shi, A., Purohit, T., Muntean, A.G., Sorenson, R.J., Showalter, H.D., Murai, M.J., Belcher, A.M., Hartley, T., et al. (2012). Menin-MLL inhibitors reverse oncogenic activity of MLL fusion proteins in leukemia. Nat. Chem. Biol. *8*, 277–284.

Gros, J., Manceau, M., Thome, V., and Marcelle, C. (2005). A common somitic origin for embryonic muscle progenitors and satellite cells. Nature *435*, 954–958.

Gu, W., Gaeta, X., Sahakyan, A., Chan, A.B., Hong, C.S., Kim, R., Braas, D., Plath, K., Lowry, W.E., and Christofk, H.R. (2016). Glycolytic Metabolism Plays a Functional Role in Regulating Human Pluripotent Stem Cell State. Cell Stem Cell *19*, 476–490.

Guenther, M.G., Jenner, R.G., Chevalier, B., Nakamura, T., Croce, C.M., Canaani, E., and Young, R.A. (2005). Global and Hox-specific roles for the MLL1 methyltransferase. Proc. Natl. Acad. Sci. U. S. A. *102*, 8603–8608.

Günther, S., Kim, J., Kostin, S., Lepper, C., Fan, C.-M., and Braun, T. (2013). Myf5-Positive Satellite Cells Contribute to Pax7-Dependent Long-Term Maintenance of Adult Muscle Stem Cells. Cell Stem Cell *13*, 590–601.

Gustafsson, M.V., Zheng, X., Pereira, T., Gradin, K., Jin, S., Lundkvist, J., Ruas, J.L., Poellinger, L., Lendahl, U., and Bondesson, M. (2005). Hypoxia Requires Notch Signaling to Maintain the Undifferentiated Cell State. Dev. Cell *9*, 617–628.

Guttridge, D.C., Mayo, M.W., Madrid, L.V., Wang, C.-Y., and Jr, A.S.B. (2000). NF-κB-Induced Loss of MyoD Messenger RNA: Possible Role in Muscle Decay and Cachexia. Science *289*, 2363–2366.

Hansen, K.H., Bracken, A.P., Pasini, D., Dietrich, N., Gehani, S.S., Monrad, A., Rappsilber, J., Lerdrup, M., and Helin, K. (2008). A model for transmission of the H3K27me3 epigenetic mark. Nat Cell Biol *10*, 1291–1300.

Hasty, P., Bradley, A., Morris, J.H., Edmondson, D.G., Venuti, J.M., Olson, E.N., and Klein, W.H. (1993). Muscle deficiency and neonatal death in mice with a targeted mutation in the myogenin gene. Nature *364*, 501–506.

Hermann, A., Goyal, R., and Jeltsch, A. (2004). The Dnmt1 DNA-(cytosine-C5)-methyltransferase Methylates DNA Processively with High Preference for Hemimethylated Target Sites. J. Biol. Chem. *279*, 48350–48359.

Herz, H.-M., Mohan, M., Garruss, A.S., Liang, K., Takahashi, Y., Mickey, K., Voets, O., Verrijzer, C.P., and Shilatifard, A. (2012). Enhancer-associated H3K4 monomethylation by Trithorax-related, the Drosophila homolog of mammalian Mll3/Mll4. Genes Dev. *26*, 2604–2620.

Hess, J.L. (2004). MLL: a histone methyltransferase disrupted in leukemia. Trends Mol. Med. *10*, 500–507.

Hess, J.L., Yu, B.D., Li, B., Hanson, R., and Korsmeyer, S.J. (1997). Defects in yolk sac hematopoiesis in Mll-null embryos. Blood *90*, 1799–1806.

Himeda, C.L., Barro, M.V., and Emerson Jr., C.P. (2013). Pax3 synergizes with Gli2 and Zic1 in transactivating the Myf5 epaxial somite enhancer. Dev. Biol. *383*, 7–14.

Hino, S., Kishida, S., Michiue, T., Fukui, A., Sakamoto, I., Takada, S., Asashima, M., and Kikuchi, A. (2001). Inhibition of the Wnt Signaling Pathway by Idax, a Novel Dvl-Binding Protein. Mol. Cell. Biol. *21*, 330–342.

Hofmann, M., Schuster-Gossler, K., Watabe-Rudolph, M., Aulehla, A., Herrmann, B.G., and Gossler, A. (2004). WNT signaling, in synergy with T/TBX6, controls Notch signaling by regulating Dll1 expression in the presomitic mesoderm of mouse embryos. Genes Dev. *18*, 2712–2717.

Hu, D., Gao, X., Morgan, M.A., Herz, H.-M., Smith, E.R., and Shilatifard, A. (2013). The MLL3/MLL4 Branches of the COMPASS Family Function as Major Histone H3K4 Monomethylases at Enhancers. Mol. Cell. Biol. *33*, 4745–4754.

Hutcheson, D.A., Zhao, J., Merrell, A., Haldar, M., and Kardon, G. (2009). Embryonic and fetal limb myogenic cells are derived from developmentally distinct progenitors and have different requirements for beta-catenin. Genes Dev. *23*, 997–1013.

Huxley, H.E. (1969). The Mechanism of Muscular Contraction. Science *164*, 1356–1366.

Huxley, A.F., and Niedergerke, R. (1954). Structural changes in muscle during contraction; interference microscopy of living muscle fibres. Nature *173*, 971–973.

Intlekofer, A.M., Dematteo, R.G., Venneti, S., Finley, L.W.S., Lu, C., Judkins, A.R., Rustenburg, A.S., Grinaway, P.B., Chodera, J.D., Cross, J.R., et al. (2015). Hypoxia Induces Production of L-2-Hydroxyglutarate. Cell Metab. *22*, 304–311.

Ishibashi, J., Perry, R.L., Asakura, A., and RUDNICKI, M.A. (2005). MyoD induces myogenic differentiation through cooperation of its NH2- and COOH-terminal regions. J Cell Biol *171*, 471–482.

Itoh, K., Brott, B.K., Bae, G.-U., Ratcliffe, M.J., and Sokol, S.Y. (2005). Nuclear localization is required for Dishevelled function in Wnt/beta-catenin signaling. J. Biol. *4*, 3.

Janke, R., Dodson, A.E., and Rine, J. (2015). Metabolism and Epigenetics. Annu. Rev. Cell Dev. Biol. *31*, 473–496.

Jones, P.L., Jan Veenstra, G.C., Wade, P.A., Vermaak, D., Kass, S.U., Landsberger, N., Strouboulis, J., and Wolffe, A.P. (1998). Methylated DNA and MeCP2 recruit histone deacetylase to repress transcription. Nat. Genet. *19*, 187–191.

Jordan, H.E. (1920). Studies on striped muscle structure. VI. The comparative histology of the leg and wing muscle of the wasp, with special reference to the phenomenon of stripe reversal during contraction and to the genetic relation between contraction bands and intercalated discs. Am. J. Anat. *27*, 1–67.

Joshi, A.A., and Struhl, K. (2005). Eaf3 Chromodomain Interaction with Methylated H3-K36 Links Histone Deacetylation to Pol II Elongation. Mol. Cell *20*, 971–978.

Juan, A.H., Kumar, R.M., Marx, J.G., Young, R.A., and Sartorelli, V. (2009). Mir-214-Dependent Regulation of the Polycomb Protein Ezh2 in Skeletal Muscle and Embryonic Stem Cells. Mol. Cell *36*, 61–74.

Juan, A.H., Derfoul, A., Feng, X., Ryall, J.G., Dell'Orso, S., Pasut, A., Zare, H., Simone, J.M., Rudnicki, M.A., and Sartorelli, V. (2011). Polycomb EZH2 controls self-renewal and safeguards the transcriptional identity of skeletal muscle stem cells. Genes Dev. *25*, 789–794.

Jude, C.D., Climer, L., Xu, D., Artinger, E., Fisher, J.K., and Ernst, P. (2007). Unique and independent roles for MLL in adult hematopoietic stem cells and progenitors. Cell Stem Cell *1*, 324–337.

Kanisicak, O., Mendez, J.J., Yamamoto, S., Yamamoto, M., and Goldhamer, D.J. (2009). Progenitors of skeletal muscle satellite cells express the muscle determination gene, MyoD. Dev. Biol. *332*, 131–141.

Kassar-Duchossoy, L., Gayraud-Morel, B., Gomès, D., Rocancourt, D., Buckingham, M., Shinin, V., and Tajbakhsh, S. (2004). Mrf4 determines skeletal muscle identity in Myf5:Myod double-mutant mice. Nature *431*, 466–471.

Kassar-Duchossoy, L., Giacone, E., Gayraud-Morel, B., Jory, A., Gomès, D., and Tajbakhsh, S. (2005). Pax3/Pax7 mark a novel population of primitive myogenic cells during development. Genes Dev. *19*, 1426–1431.

Kaufman, M.H. (1992). The Atlas of Mouse Development (Academic Press).

Kawabe, Y., Wang, Y.X., McKinnell, I.W., Bedford, M.T., and Rudnicki, M.A. (2012). Carm1 Regulates Pax7 Transcriptional Activity through MLL1/2 Recruitment during Asymmetric Satellite Stem Cell Divisions. Cell Stem Cell *11*, 333–345.

Kebede, A.F., Schneider, R., and Daujat, S. (2015). Novel types and sites of histone modifications emerge as players in the transcriptional regulation contest. FEBS J. *282*, 1658–1674.

Kelly, A.M., and Zacks, S.I. (1969). The Histogenesis of Rat Intercostal Muscle. J. Cell Biol. *42*, 135–153.

Keogh, M.-C., Kurdistani, S.K., Morris, S.A., Ahn, S.H., Podolny, V., Collins, S.R., Schuldiner, M., Chin, K., Punna, T., Thompson, N.J., et al. (2005). Cotranscriptional Set2 Methylation of Histone H3 Lysine 36 Recruits a Repressive Rpd3 Complex. Cell *123*, 593–605.

Kizer, K.O., Phatnani, H.P., Shibata, Y., Hall, H., Greenleaf, A.L., and Strahl, B.D. (2005). A Novel Domain in Set2 Mediates RNA Polymerase II Interaction and Couples Histone H3 K36 Methylation with Transcript Elongation. Mol. Cell. Biol. *25*, 3305–3316.

Klose, R.J., and Bird, A.P. (2006). Genomic DNA methylation: the mark and its mediators. Trends Biochem. Sci. *31*, 89–97.

Ko, M., Huang, Y., Jankowska, A.M., Pape, U.J., Tahiliani, M., Bandukwala, H.S., An, J., Lamperti, E.D., Koh, K.P., Ganetzky, R., et al. (2010). Impaired hydroxylation of 5-methylcytosine in myeloid cancers with mutant TET2. Nature *468*, 839–843.

Ko, M., An, J., Bandukwala, H.S., Chavez, L., Äijö, T., Pastor, W.A., Segal, M.F., Li, H., Koh, K.P., Lähdesmäki, H., et al. (2013). Modulation of TET2 expression and 5-methylcytosine oxidation by the CXXC domain protein IDAX. Nature *497*, 122–126.

Kolasinska-Zwierz, P., Down, T., Latorre, I., Liu, T., Liu, X.S., and Ahringer, J. (2009). Differential chromatin marking of introns and expressed exons by H3K36me3. Nat. Genet. *41*, 376–381.

Kondrashov, N., Pusic, A., Stumpf, C.R., Shimizu, K., Hsieh, A.C., Xue, S., Ishijima, J., Shiroishi, T., and Barna, M. (2011). Ribosome-Mediated Specificity in Hox mRNA Translation and Vertebrate Tissue Patterning. Cell *145*, 383–397.

Konieczny, S.F., and Emerson, C.P.J. (1984). 5-azacytidine induction of stable mesodermal stem cell lineages from 10T1/2 cells: Evidence for regulatory genes controlling determination. Cell *38*, 791–800.

Kornberg, R.D. (1974). Chromatin Structure: A Repeating Unit of Histones and DNA. Science *184*, 868–871.

Krogan, N.J., Kim, M., Tong, A., Golshani, A., Cagney, G., Canadien, V., Richards, D.P., Beattie, B.K., Emili, A., Boone, C., et al. (2003). Methylation of Histone H3 by Set2 in Saccharomyces cerevisiae Is Linked to Transcriptional Elongation by RNA Polymerase II. Mol. Cell. Biol. *23*, 4207–4218.

Kuang, S., Chargé, S.B., Seale, P., Huh, M., and Rudnicki, M.A. (2006). Distinct roles for Pax7 and Pax3 in adult regenerative myogenesis. J. Cell Biol. *172*, 103–113.

Kuang, S., Kuroda, K., Le Grand, F., and Rudnicki, M.A. (2007). Asymmetric self-renewal and commitment of satellite stem cells in muscle. Cell *129*, 999–1010.

Lassar, A.B., Paterson, B.M., and Weintraub, H. (1986). Transfection of a DNA locus that mediates the conversion of 10T12 fibroblasts to myoblasts. Cell *47*, 649–656.

Lawrence, M., Daujat, S., and Schneider, R. (2016). Lateral Thinking: How Histone Modifications Regulate Gene Expression. Trends Genet. *32*, 42–56.

Le Grand, F., Jones, A.E., Seale, V., Scimè, A., and RUDNICKI, M.A. (2009). Wnt7a Activates the Planar Cell Polarity Pathway to Drive the Symmetric Expansion of Satellite Stem Cells. Cell Stem Cell *4*, 535–547.

Lee, H., Habas, R., and Abate-Shen, C. (2004). Msx1 Cooperates with Histone H1b for Inhibition of Transcription and Myogenesis. Science *304*, 1675–1678.

Lee, T.I., Jenner, R.G., Boyer, L.A., Guenther, M.G., Levine, S.S., Kumar, R.M., Chevalier, B., Johnstone, S.E., Cole, M.F., Isono, K., et al. (2006). Control of Developmental Regulators by Polycomb in Human Embryonic Stem Cells. Cell *125*, 301–313.

Leeuwenhoek, M., and Sprengell, D. (1720). Observations upon the Membranes Enclosing the Fasciculi of Fibres, into Which a Muscle is Divided. By Mr. Leeuwenhoek, F. R. S. Translated by Dr. Sprengell, F. R. S. Philos. Trans. 1683-1775 *31*, 129–134.

Lepper, C., Conway, S.J., and Fan, C.-M. (2009). Adult satellite cells and embryonic muscle progenitors have distinct genetic requirements. Nature *460*, 627–631.

Lepper, C., Partridge, T.A., and Fan, C.-M. (2011). An absolute requirement for Pax7-positive satellite cells in acute injury-induced skeletal muscle regeneration. Development *138*, 3639–3646.

Li, H., Ilin, S., Wang, W., Duncan, E.M., Wysocka, J., Allis, C.D., and Patel, D.J. (2006). Molecular basis for site-specific read-out of histone H3K4me3 by the BPTF PHD finger of NURF. Nature *442*, 91–95.

Li, J.-Y., Chai, B., Zhang, W., Wu, X., Zhang, C., Fritze, D., Xia, Z., Patterson, C., and Mulholland, M.W. (2011). Ankyrin repeat and SOCS box containing protein 4 (Asb-4) colocalizes with insulin receptor substrate 4 (IRS4) in the hypothalamic neurons and mediates IRS4 degradation. BMC Neurosci. *12*, 95.

Li, X., Zhu, L., Chen, X., and Fan, M. (2007). Effects of hypoxia on proliferation and differentiation of myoblasts. Med. Hypotheses *69*, 629–636.

Liang, G., Lin, J.C.Y., Wei, V., Yoo, C., Cheng, J.C., Nguyen, C.T., Weisenberger, D.J., Egger, G., Takai, D., Gonzales, F.A., et al. (2004). Distinct localization of histone H3 acetylation and H3-K4 methylation to the transcription start sites in the human genome. Proc. Natl. Acad. Sci. U. S. A. *101*, 7357–7362.

Lim, D.A., Huang, Y.-C., Swigut, T., Mirick, A.L., Garcia-Verdugo, J.M., Wysocka, J., Ernst, P., and Alvarez-Buylla, A. (2009). Chromatin remodelling factor Mll1 is essential for neurogenesis from postnatal neural stem cells. Nature *458*, 529–533.

Liu, W., Wen, Y., Bi, P., Lai, X., Liu, X.S., Liu, X., and Kuang, S. (2012). Hypoxia promotes satellite cell self-renewal and enhances the efficiency of myoblast transplantation. Development *139*, 2857–2865.

Lucarelli, M., Fuso, A., Strom, R., and Scarpa, S. (2001). The Dynamics of Myogenin Site-specific Demethylation Is Strongly Correlated with Its Expression and with Muscle Differentiation. J. Biol. Chem. *276*, 7500–7506.

Luger, K., Mäder, A.W., Richmond, R.K., Sargent, D.F., and Richmond, T.J. (1997). Crystal structure of the nucleosome core particle at 2.8 Å resolution. Nature *389*, 251–260.

Mal, A., and Harter, M.L. (2003). MyoD is functionally linked to the silencing of a muscle-specific regulatory gene prior to skeletal myogenesis. Proc. Natl. Acad. Sci. *100*, 1735–1739.

Maltzahn, J. von, Bentzinger, C.F., and Rudnicki, M.A. (2011). Wnt7a-Fzd7 signalling directly activates the Akt/mTOR anabolic growth pathway in skeletal muscle. Nat. Cell Biol. *14*, 186–191.

von Maltzahn, J., Jones, A.E., Parks, R.J., and Rudnicki, M.A. (2013a). Pax7 is critical for the normal function of satellite cells in adult skeletal muscle. Proc. Natl. Acad. Sci. *110*, 16474–16479.

von Maltzahn, J., Zinoviev, R., Chang, N.C., Bentzinger, C.F., and Rudnicki, M.A. (2013b). A truncated Wnt7a retains full biological activity in skeletal muscle. Nat. Commun. *4*.

Mansouri, A., Stoykova, A., Torres, M., and Gruss, P. (1996). Dysgenesis of cephalic neural crest derivatives in Pax7−/− mutant mice. Development *122*, 831–838.

Margueron, R., Justin, N., Ohno, K., Sharpe, M.L., Son, J., Drury III, W.J., Voigt, P., Martin, S.R., Taylor, W.R., De Marco, V., et al. (2009). Role of the polycomb protein EED in the propagation of repressive histone marks. Nature *461*, 762–767.

Marmorstein, R., and Zhou, M.-M. (2014). Writers and Readers of Histone Acetylation: Structure, Mechanism, and Inhibition. Cold Spring Harb. Perspect. Biol. *6*, a018762.

Maroto, M., Reshef, R., Münsterberg, A.E., Koester, S., Goulding, M., and Lassar, A.B. (1997). Ectopic Pax-3 Activates MyoD and Myf-5 Expression in Embryonic Mesoderm and Neural Tissue. Cell *89*, 139–148.

Marson, A., Levine, S.S., Cole, M.F., Frampton, G.M., Brambrink, T., Johnstone, S., Guenther, M.G., Johnston, W.K., Wernig, M., Newman, J., et al. (2008). Connecting microRNA Genes to the Core Transcriptional Regulatory Circuitry of Embryonic Stem Cells. Cell *134*, 521–533.

Mauro, A. (1961). Satellite cell of skeletal muscle fibers. J. Biophys. Biochem. Cytol. *9*, 493–495.

McKinnell, I.W., and Rudnicki, M.A. (2004). Molecular mechanisms of muscle atrophy. Cell *119*, 907–910.

McKinnell, I.W., Ishibashi, J., Le Grand, F., Punch, V.G.J., Addicks, G.C., Greenblatt, J.F., Dilworth, F.J., and Rudnicki, M.A. (2008). Pax7 activates myogenic genes by recruitment of a histone methyltransferase complex. Nat Cell Biol *10*, 77–84.

McMahon, K.A., Hiew, S.Y.L., Hadjur, S., Veiga-Fernandes, H., Menzel, U., Price, A.J., Kioussis, D., Williams, O., and Brady, H.J.M. (2007). Mll has a critical role in fetal and adult hematopoietic stem cell self-renewal. Cell Stem Cell *1*, 338–345.

Meissner, A., Mikkelsen, T.S., Gu, H., Wernig, M., Hanna, J., Sivachenko, A., Zhang, X., Bernstein, B.E., Nusbaum, C., Jaffe, D.B., et al. (2008). Genome-scale DNA methylation maps of pluripotent and differentiated cells. Nature *454*, 766–770.

Milne, T.A., Briggs, S.D., Brock, H.W., Martin, M.E., Gibbs, D., Allis, C.D., and Hess, J.L. (2002). MLL targets SET domain methyltransferase activity to Hox gene promoters. Mol. Cell *10*, 1107–1117.

Milne, T.A., Dou, Y., Martin, M.E., Brock, H.W., Roeder, R.G., and Hess, J.L. (2005). MLL associates specifically with a subset of transcriptionally active target genes. Proc. Natl. Acad. Sci. U. S. A. *102*, 14765–14770.

Milne, T.A., Kim, J., Wang, G.G., Stadler, S.C., Basrur, V., Whitcomb, S.J., Wang, Z., Ruthenburg, A.J., Elenitoba-Johnson, K.S.J., Roeder, R.G., et al. (2010). Multiple Interactions Recruit MLL1 and MLL1 Fusion Proteins to the HOXA9 Locus in Leukemogenesis. Mol. Cell *38*, 853–863.

Miner, J.H., and Wold, B. (1990). Herculin, a fourth member of the MyoD family of myogenic regulatory genes. Proc. Natl. Acad. Sci. *87*, 1089–1093.

Mishra, B.P., Zaffuto, K.M., Artinger, E.L., Org, T., Mikkola, H.K.A., Cheng, C., Djabali, M., and Ernst, P. (2014). The Histone Methyltransferase Activity of MLL1 Is Dispensable for Hematopoiesis and Leukemogenesis. Cell Rep. *7*, 1239–1247.

Miyata, K., Miyata, T., Nakabayashi, K., Okamura, K., Naito, M., Kawai, T., Takada, S., Kato, K., Miyamoto, S., Hata, K., et al. (2015). DNA methylation analysis of human myoblasts during in vitro myogenic differentiation: de novo methylation of promoters of muscle-related genes and its involvement in transcriptional down-regulation. Hum. Mol. Genet. *24*, 410–423.

Montarras, D., Morgan, J., Collins, C., Relaix, F., Zaffran, S., Cumano, A., Partridge, T., and Buckingham, M. (2005). Direct Isolation of Satellite Cells for Skeletal Muscle Regeneration. Science *309*, 2064–2067.

Morselli, M., Pastor, W.A., Montanini, B., Nee, K., Ferrari, R., Fu, K., Bonora, G., Rubbi, L., Clark, A.T., Ottonello, S., et al. (2015). In vivo targeting of de novo DNA methylation by histone modifications in yeast and mouse. ELife *4*, e06205.

Müller, J., Hart, C.M., Francis, N.J., Vargas, M.L., Sengupta, A., Wild, B., Miller, E.L., O'Connor, M.B., Kingston, R.E., and Simon, J.A. (2002). Histone Methyltransferase Activity of a Drosophila Polycomb Group Repressor Complex. Cell *111*, 197–208.

Nabeshima, Y., Hanaoka, K., Hayasaka, M., Esuml, E., Li, S., Nonaka, I., and Nabeshima, Y. (1993). Myogenin gene disruption results in perinatal lethality because of severe muscle defect. Nature *364*, 532–535.

Naito, M., Mori, M., Inagawa, M., Miyata, K., Hashimoto, N., Tanaka, S., and Asahara, H. (2016). Dnmt3a Regulates Proliferation of Muscle Satellite Cells via p57Kip2. PLoS Genet. *12*, e1006167.

Nan, X., Ng, H.-H., Johnson, C.A., Laherty, C.D., Turner, B.M., Eisenman, R.N., and Bird, A. (1998). Transcriptional repression by the methyl-CpG-binding protein MeCP2 involves a histone deacetylase complex. Nature *393*, 386–389.

Neri, F., Rapelli, S., Krepelova, A., Incarnato, D., Parlato, C., Basile, G., Maldotti, M., Anselmi, F., and Oliviero, S. (2017). Intragenic DNA methylation prevents spurious transcription initiation. Nature *543*, 72–77.

Oikawa, Y., Omori, R., Nishii, T., Ishida, Y., Kawaichi, M., and Matsuda, E. (2011). The methyl-CpG-binding protein CIBZ suppresses myogenic differentiation by directly inhibiting myogenin expression. Cell Res. *21*, 1578–1590.

Okano, M., Bell, D.W., Haber, D.A., and Li, E. (1999). DNA Methyltransferases Dnmt3a and Dnmt3b Are Essential for De Novo Methylation and Mammalian Development. Cell *99*, 247–257.

Ooi, S.K.T., Qiu, C., Bernstein, E., Li, K., Jia, D., Yang, Z., Erdjument-Bromage, H., Tempst, P., Lin, S.P., and Allis, C.D. (2007). DNMT3L connects unmethylated lysine 4 of histone H3 to de novo methylation of DNA. Nature *448*, 714–717.

Otani, J., Nankumo, T., Arita, K., Inamoto, S., Ariyoshi, M., and Shirakawa, M. (2009). Structural basis for recognition of H3K4 methylation status by the DNA methyltransferase 3A ATRX–DNMT3–DNMT3L domain. EMBO Rep. *10*, 1235–1241.

Ott, M.-O., Bober, E., Lyons, G., Arnold, H., and Buckingham, M. (1991). Early expression of the myogenic regulatory gene, myf-5, in precursor cells of skeletal muscle in the mouse embryo. Development *111*, 1097–1107.

Palacios, D., Summerbell, D., Rigby, P.W.J., and Boyes, J. (2010a). Interplay between DNA Methylation and Transcription Factor Availability: Implications for Developmental Activation of the Mouse Myogenin Gene. Mol. Cell. Biol. *30*, 3805–3815.

Palacios, D., Mozzetta, C., Consalvi, S., Caretti, G., Saccone, V., Proserpio, V., Marquez, V.E., Valente, S., Mai, A., Forcales, S.V., et al. (2010b). TNF/p38[alpha]/Polycomb Signaling to Pax7 Locus in Satellite Cells Links Inflammation to the Epigenetic Control of Muscle Regeneration. Cell Stem Cell *7*, 455–469.

Pallafacchina, G., FranÃ§ois, S., Regnault, B., Czarny, B., Dive, V., Cumano, A., Montarras, D., and Buckingham, M. (2010). An adult tissue-specific stem cell in its niche: A gene profiling analysis of in vivo quiescent and activated muscle satellite cells. Stem Cell Res. *4*, 77–91.

Pan, B., Chao, H., Chen, B., Zhang, L., Li, L., Sun, X., and Shen, W. (2011). DNA methylation of germ-cell-specific basic helix-loop-helix (HLH) transcription factors, Sohlh2 and Figlα during gametogenesis. Mol. Hum. Reprod. *17*, 550–561.

Parker, M.H., Seale, P., and Rudnicki, M.A. (2003). Looking back to the embryo: defining transcriptional networks in adult myogenesis. Nat. Rev. Genet. *4*, 497–507.

Parmar, K., Mauch, P., Vergilio, J.-A., Sackstein, R., and Down, J.D. (2007). Distribution of hematopoietic stem cells in the bone marrow according to regional hypoxia. Proc. Natl. Acad. Sci. *104*, 5431–5436.

Pasut, A., Oleynik, P., and Rudnicki, M.A. (2012). Isolation of Muscle Stem Cells by Fluorescence Activated Cell Sorting Cytometry. In Myogenesis, J.X. DiMario, ed. (Totowa, NJ: Humana Press), pp. 53–64.

Patapoutian, A., Yoon, J.K., Miner, J.H., Wang, S., Stark, K., and Wold, B. (1995). Disruption of the mouse MRF4 gene identifies multiple waves of myogenesis in the myotome. Development *121*, 3347–3358.

Peng, M., Yin, N., Chhangawala, S., Xu, K., Leslie, C.S., and Li, M.O. (2016). Aerobic glycolysis promotes T helper 1 cell differentiation through an epigenetic mechanism. Science *354*, 481–484.

Porpiglia, E., Samusik, N., Van Ho, A.T., Cosgrove, B.D., Mai, T., Davis, K.L., Jager, A., Nolan, G.P., Bendall, S.C., Fantl, W.J., et al. (2017). High-resolution myogenic lineage mapping by single-cell mass cytometry. Nat. Cell Biol. *19*, 558–567.

Pourquié, O. (2003). The Segmentation Clock: Converting Embryonic Time into Spatial Pattern. Science *301*, 328–330.

Rando, T.A., and Blau, H.M. (1994). Primary mouse myoblast purification, characterization, and transplantation for cell-mediated gene therapy. J. Cell Biol. *125*, 1275–1287.

Rasmussen, K.D., and Helin, K. (2016). Role of TET enzymes in DNA methylation, development, and cancer. Genes Dev. *30*, 733–750.

Rawls, A., Valdez, M.R., Zhang, W., Richardson, J., Klein, W.H., and Olson, E.N. (1998). Overlapping functions of the myogenic bHLH genes MRF4 and MyoD revealed in double mutant mice. Development *125*, 2349–2358.

Relaix, F., Rocancourt, D., Mansouri, A., and Buckingham, M. (2004). Divergent functions of murine Pax3 and Pax7 in limb muscle development. Genes Dev. *18*, 1088–1105.

Relaix, F., Rocancourt, D., Mansouri, A., and Buckingham, M. (2005). A Pax3/Pax7-dependent population of skeletal muscle progenitor cells. Nature *435*, 948–953.

Relaix, F., Montarras, D., Zaffran, S., Gayraud-Morel, B., Rocancourt, D., Tajbakhsh, S., Mansouri, A., Cumano, A., and Buckingham, M. (2006). Pax3 and Pax7 have distinct and overlapping functions in adult muscle progenitor cells. J. Cell Biol. *172*, 91.

Relaix, F., Demignon, J., Laclef, C., Pujol, J., Santolini, M., Niro, C., Lagha, M., Rocancourt, D., Buckingham, M., and Maire, P. (2013). Six Homeoproteins Directly

Activate Myod Expression in the Gene Regulatory Networks That Control Early Myogenesis. PLOS Genet. *9*, e1003425.

Rhodes, S.J., and Konieczny, S.F. (1989). Identification of MRF4: a new member of the muscle regulatory factor gene family. Genes Dev. *3*, 2050–2061.

Rolfe, D.F., and Brown, G.C. (1997). Cellular energy utilization and molecular origin of standard metabolic rate in mammals. Physiol. Rev. *77*, 731–758.

Rollet, A. (1884). Untersuchungen uber den Bau der quergestreiften Muskelfasern. I. Theil (Denkschriften der Akademie der Wissenschaften.Math.Natw.Kl.).

Rollet, A. (1885). Untersuchungen uber den Bau der quergestreiften Muskelfasern. II. Theil (Denkschriften der Akademie der Wissenschaften.Math.Natw.Kl.).

Rudnicki, M.A., Braun, T., Hinuma, S., and Jaenisch, R. (1992). Inactivation of MyoD in mice leads to up-regulation of the myogenic HLH gene Myf-5 and results in apparently normal muscle development. Cell *71*, 383–390.

Rudnicki, M.A., Schnegelsberg, P.N., Stead, R.H., Braun, T., Arnold, H.H., and Jaenisch, R. (1993). MyoD or Myf-5 is required for the formation of skeletal muscle. Cell *75*, 1351–1359.

Rudnicki, M.A., Le Grand, F., McKinnell, I., and Kuang, S. (2009). The Molecular Regulation of Muscle Stem Cell Function. Cold Spring Harb. Symp. Quant. Biol.

Ryall, J.G., Dell'Orso, S., Derfoul, A., Juan, A., Zare, H., Feng, X., Clermont, D., Koulnis, M., Gutierrez-Cruz, G., Fulco, M., et al. (2015a). The NAD+-Dependent SIRT1 Deacetylase Translates a Metabolic Switch into Regulatory Epigenetics in Skeletal Muscle Stem Cells. Cell Stem Cell *16*, 171–183.

Ryall, J.G., Cliff, T., Dalton, S., and Sartorelli, V. (2015b). Metabolic Reprogramming of Stem Cell Epigenetics. Cell Stem Cell *17*, 651–662.

Sacco, A., Doyonnas, R., Kraft, P., Vitorovic, S., and Blau, H.M. (2008). Self-renewal and expansion of single transplanted muscle stem cells. Nature *456*, 502–506.

Sambasivan, R., Yao, R., Kissenpfennig, A., Wittenberghe, L.V., Paldi, A., Gayraud-Morel, B., Guenou, H., Malissen, B., Tajbakhsh, S., and Galy, A. (2011a). Pax7-expressing satellite cells are indispensable for adult skeletal muscle regeneration. Development *138*, 3647–3656.

Sambasivan, R., Kuratani, S., and Tajbakhsh, S. (2011b). An eye on the head: the development and evolution of craniofacial muscles. Development *138*, 2401–2415.

Schafer, K., and Braun, T. (1999). Early specification of limb muscle precursor cells by the homeobox gene Lbx1h. Nat Genet *23*, 213–216.

Schafer, B.W., Czerny, T., Bernasconi, M., Genini, M., and Busslinger, M. (1994). Molecular cloning and characterization of a human PAX-7 cDNA expressed in normal and neoplastic myocytes. Nucleic Acids Res. *22*, 4574.

Schienda, J., Engleka, K.A., Jun, S., Hansen, M.S., Epstein, J.A., Tabin, C.J., Kunkel, L.M., and Kardon, G. (2006). Somitic origin of limb muscle satellite and side population cells. Proc. Natl. Acad. Sci. U. S. A. *103*, 945–950.

Schübeler, D. (2015). Function and information content of DNA methylation. Nature *517*, 321–326.

Seale, P., Sabourin, L.A., Girgis-Gabardo, A., Mansouri, A., Gruss, P., and Rudnicki, M.A. (2000). Pax7 is required for the specification of myogenic satellite cells. Cell *102*, 777–786.

Seale, P., Ishibashi, J., Scimè, A., and Rudnicki, M.A. (2004). Pax7 is necessary and sufficient for the myogenic specification of CD45+:Sca1+ stem cells from injured muscle. PLoS Biol. *2*, E130.

Seale, P., Bjork, B., Yang, W., Kajimura, S., Chin, S., Kuang, S., Scime, A., Devarakonda, S., Conroe, H.M., Erdjument-Bromage, H., et al. (2008). PRDM16 controls a brown fat/skeletal muscle switch. Nature *454*, 961–967.

Seenundun, S., Rampalli, S., Liu, Q.-C., Aziz, A., Palii, C., Hong, S., Blais, A., Brand, M., Ge, K., and Dilworth, F.J. (2010). UTX mediates demethylation of H3K27me3 at muscle-specific genes during myogenesis. EMBO J *29*, 1401–1411.

Seibler, J., Zevnik, B., Küter-Luks, B., Andreas, S., Kern, H., Hennek, T., Rode, A., Heimann, C., Faust, N., Kauselmann, G., et al. (2003). Rapid generation of inducible mouse mutants. Nucleic Acids Res. *31*, e12–e12.

Sen, P., Shah, P.P., Nativio, R., and Berger, S.L. (2016). Epigenetic Mechanisms of Longevity and Aging. Cell *166*, 822–839.

Seto, E., and Yoshida, M. (2014). Erasers of Histone Acetylation: The Histone Deacetylase Enzymes. Cold Spring Harb. Perspect. Biol. *6*, a018713.

Sharma, U., and Rando, O.J. (2017). Metabolic Inputs into the Epigenome. Cell Metab. *25*, 544–558.

Shea, K.L., Xiang, W., LaPorta, V.S., Licht, J.D., Keller, C., Basson, M.A., and Brack, A.S. (2010). Sprouty1 Regulates Reversible Quiescence of a Self-Renewing Adult Muscle Stem Cell Pool during Regeneration. Cell Stem Cell *6*, 117–129.

Sherrington, C.S. (1922). Some aspects of animal mechanism. Science *56*, 345.

Shi, Z., and Barna, M. (2015). Translating the Genome in Time and Space: Specialized Ribosomes, RNA Regulons, and RNA-Binding Proteins. Annu. Rev. Cell Dev. Biol. *31*, 31–54.

Shilatifard, A. (2012). The COMPASS Family of Histone H3K4 Methylases: Mechanisms of Regulation in Development and Disease Pathogenesis. Annu. Rev. Biochem. *81*, 65–95.

Simsek, T., Kocabas, F., Zheng, J., DeBerardinis, R.J., Mahmoud, A.I., Olson, E.N., Schneider, J.W., Zhang, C.C., and Sadek, H.A. (2010). The Distinct Metabolic Profile of Hematopoietic Stem Cells Reflects Their Location in a Hypoxic Niche. Cell Stem Cell *7*, 380–390.

Sinha, M., Jang, Y.C., Oh, J., Khong, D., Wu, E.Y., Manohar, R., Miller, C., Regalado, S.G., Loffredo, F.S., Pancoast, J.R., et al. (2014). Restoring Systemic GDF11 Levels Reverses Age-Related Dysfunction in Mouse Skeletal Muscle. Science *344*, 649–652.

Smallwood, A., Estève, P.-O., Pradhan, S., and Carey, M. (2007). Functional cooperation between HP1 and DNMT1 mediates gene silencing. Genes Dev. *21*, 1169–1178.

Smith, Z.D., and Meissner, A. (2013). DNA methylation: roles in mammalian development. Nat. Rev. Genet. *14*, 204–220.

Snow, M.H. (1977). Myogenic cell formation in regenerating rat skeletal muscle injured by mincing II. An autoradiographic study. Anat. Rec. *188*, 201–217.

Snow, M.H. (1978). An autoradiographic study of satellite cell differentiation into regenerating myotubes following transplantation of muscles in young rats. Cell Tissue Res. *186*, 535–540.

Soleimani, V.D., Punch, V.G., Kawabe, Y., Jones, A.E., Palidwor, G.A., Porter, C.J., Cross, J.W., Carvajal, J.J., Kockx, C.E.M., van IJcken, W.F.J., et al. (2012). Transcriptional Dominance of Pax7 in Adult Myogenesis Is Due to High-Affinity Recognition of Homeodomain Motifs. Dev. Cell *22*, 1208–1220.

Soneoka, Y., Cannon, P.M., Ramsdale, E.E., Griffiths, J.C., Romano, G., Kingsman, S.M., and Kingsman, A.J. (1995). A transient three-plasmid expression system for the production of high titer retroviral vectors. Nucleic Acids Res. *23*, 628–633.

Song, S.J., Poliseno, L., Song, M.S., Ala, U., Webster, K., Ng, C., Beringer, G., Brikbak, N.J., Yuan, X., Cantley, L.C., et al. (2013a). MicroRNA-Antagonism Regulates Breast Cancer Stemness and Metastasis via TET-Family-Dependent Chromatin Remodeling. Cell *154*, 311–324.

Song, S.J., Ito, K., Ala, U., Kats, L., Webster, K., Sun, S.M., Jongen-Lavrencic, M., Manova-Todorova, K., Teruya-Feldstein, J., Avigan, D.E., et al. (2013b). The Oncogenic MicroRNA miR-22 Targets the TET2 Tumor Suppressor to Promote Hematopoietic Stem Cell Self-Renewal and Transformation. Cell Stem Cell *13*, 87–101.

Squire, J.M. (1975). Muscle filament structure and muscle contraction. Annu. Rev. Biophys. Bioeng. *4*, 137–163.

Su, X., Wellen, K.E., and Rabinowitz, J.D. (2016). Metabolic control of methylation and acetylation. Curr. Opin. Chem. Biol. *30*, 52–60.

Suda, T., Takubo, K., and Semenza, G.L. (2011). Metabolic Regulation of Hematopoietic Stem Cells in the Hypoxic Niche. Cell Stem Cell *9*, 298–310.

Sun, J., Zhao, Y., McGreal, R., Cohen-Tayar, Y., Rockowitz, S., Wilczek, C., Ashery-Padan, R., Shechter, D., Zheng, D., and Cvekl, A. (2016). Pax6 associates with H3K4-specific histone methyltransferases Mll1, Mll2, and Set1a and regulates H3K4 methylation at promoters and enhancers. Epigenetics Chromatin *9*, 37.

Sved, J., and Bird, A. (1990). The expected equilibrium of the CpG dinucleotide in vertebrate genomes under a mutation model. Proc. Natl. Acad. Sci. *87*, 4692–4696.

Tahiliani, M., Koh, K.P., Shen, Y., Pastor, W.A., Bandukwala, H., Brudno, Y., Agarwal, S., Iyer, L.M., Liu, D.R., Aravind, L., et al. (2009). Conversion of 5-Methylcytosine to 5-Hydroxymethylcytosine in Mammalian DNA by MLL Partner TET1. Science *324*, 930–935.

Tajbakhsh, S., and Buckingham, M. (1999). 6 The Birth of Muscle Progenitor Cells in the Mouse: Spatiotemporal Considerations. In Current Topics in Developmental Biology, C.P. Ordahl, ed. (Academic Press), pp. 225–268.

Tajbakhsh, S., Rocancourt, D., Cossu, G., and Buckingham, M. (1997). Redefining the Genetic Hierarchies Controlling Skeletal Myogenesis: Pax-3 and Myf-5 Act Upstream of MyoD. Cell *89*, 127–138.

Talbert, P.B., and Henikoff, S. (2006). Spreading of silent chromatin: inaction at a distance. Nat Rev Genet *7*, 793–803.

Taylor, S.M., and Jones, P.A. (1979). Multiple new phenotypes induced in 10T1/2 and 3T3 cells treated with 5-azacytidine. Cell *17*, 771–779.

Terranova, R., Agherbi, H., Boned, A., Meresse, S., and Djabali, M. (2006). Histone and DNA methylation defects at Hox genes in mice expressing a SET domain-truncated form of Mll. Proc. Natl. Acad. Sci. U. S. A. *103*, 6629–6634.

Thomson, J.P., Skene, P.J., Selfridge, J., Clouaire, T., Guy, J., Webb, S., Kerr, A.R.W., Deaton, A., Andrews, R., James, K.D., et al. (2010). CpG islands influence chromatin structure via the CpG-binding protein Cfp1. Nature *464*, 1082–1086.

Tian, Y., Garcia, G., Bian, Q., Steffen, K.K., Joe, L., Wolff, S., Meyer, B.J., and Dillin, A. (2016). Mitochondrial Stress Induces Chromatin Reorganization to Promote Longevity and UPRmt. Cell *165*, 1197–1208.

Tiffin, N., Williams, R.D., Shipley, J., and Pritchard-Jones, K. (2003). PAX7 expression in embryonal rhabdomyosarcoma suggests an origin in muscle satellite cells. Br. J. Cancer *89*, 327–332.

Toit, A.D. (2012). Chromatin: Defining heterochromatin. Nat. Rev. Mol. Cell Biol. *13*, 684–685.

Tremblay, P., Dietrich, S., Mericskay, M., Schubert, F.R., Li, Z., and Paulin, D. (1998). A Crucial Role for Pax 3 in the Development of the Hypaxial Musculature and the Long-Range Migration of Muscle Precursors. Dev. Biol. *203*, 49–61.

Urbani, L., Piccoli, M., Franzin, C., Pozzobon, M., and Coppi, P.D. (2012). Hypoxia Increases Mouse Satellite Cell Clone Proliferation Maintaining both In Vitro and In Vivo Heterogeneity and Myogenic Potential. PLOS ONE *7*, e49860.

Valinluck, V., Tsai, H.-H., Rogstad, D.K., Burdzy, A., Bird, A., and Sowers, L.C. (2004). Oxidative damage to methyl-CpG sequences inhibits the binding of the methyl-CpG binding domain (MBD) of methyl-CpG binding protein 2 (MeCP2). Nucleic Acids Res. *32*, 4100–4108.

Vasyutina, E., and Birchmeier, C. (2006). The development of migrating muscle precursor cells. Anat. Embryol. (Berl.) *211*, 37.

Veratti, E. (1902). Richerche sulle fine struttura della fibra muscolare striata. Mem. Inst Lomb Cl Sci Mat E Nat 87–133.

Waddington, C.H. (1947). Organisers And Genes (University Press ; Cambridge).

Waddington, C.H. (1956). Principles of embryology (University Press ; Cambridge).

Wang, P., Lin, C., Smith, E.R., Guo, H., Sanderson, B.W., Wu, M., Gogol, M., Alexander, T., Seidel, C., Wiedemann, L.M., et al. (2009a). Global Analysis of H3K4 Methylation Defines MLL Family Member Targets and Points to a Role for MLL1-Mediated H3K4 Methylation in the Regulation of Transcriptional Initiation by RNA Polymerase II. Mol Cell Biol *29*, 6074–6085.

Wang, Z., Zang, C., Cui, K., Schones, D.E., Barski, A., Peng, W., and Zhao, K. (2009b). Genome-wide Mapping of HATs and HDACs Reveals Distinct Functions in Active and Inactive Genes. Cell *138*, 1019–1031.

Warburg, O. (1956). On the Origin of Cancer Cells. Science *123*, 309–314.

Wellen, K.E., Hatzivassiliou, G., Sachdeva, U.M., Bui, T.V., Cross, J.R., and Thompson, C.B. (2009). ATP-Citrate Lyase Links Cellular Metabolism to Histone Acetylation. Science *324*, 1076–1080.

Wen, H., Li, Y., Xi, Y., Jiang, S., Stratton, S., Peng, D., Tanaka, K., Ren, Y., Xia, Z., Wu, J., et al. (2014). ZMYND11 links histone H3.3K36me3 to transcription elongation and tumour suppression. Nature *508*, 263–268.

Wheeler, R. (2007). File:Nucleosome 1KX5 colour coded.png.

Wittenberg, J.B. (1970). Myoglobin-facilitated oxygen diffusion: role of myoglobin in oxygen entry into muscle. Physiol. Rev. *50*, 559–636.

Wood, W.M., Etemad, S., Yamamoto, M., and Goldhamer, D.J. (2013). MyoD-expressing progenitors are essential for skeletal myogenesis and satellite cell development. Dev. Biol. *384*, 114–127.

Woodhouse, S., Pugazhendhi, D., Brien, P., and Pell, J.M. (2013). Ezh2 maintains a key phase of muscle satellite cell expansion but does not regulate terminal differentiation. J. Cell Sci. *126*, 565–579.

Wright, W.E., Sassoon, D.A., and Lin, V.K. (1989). Myogenin, a factor regulating myogenesis, has a domain homologous to MyoD. Cell *56*, 607–617.

Wu, H., and Zhang, Y. (2014). Reversing DNA Methylation: Mechanisms, Genomics, and Biological Functions. Cell *156*, 45–68.

Wu, M., Wang, P.F., Lee, J.S., Martin-Brown, S., Florens, L., Washburn, M., and Shilatifard, A. (2008). Molecular regulation of H3K4 trimethylation by Wdr82, a component of human Set1/COMPASS. Mol. Cell. Biol. *28*, 7337–7344.

Xu, H.E., Rould, M.A., Xu, W., Epstein, J.A., Maas, R.L., and Pabo, C.O. (1999). Crystal structure of the human Pax6 paired domain–DNA complex reveals specific roles for the linker region and carboxy-terminal subdomain in DNA binding. Genes Dev. *13*, 1263–1275.

Xue, S., Tian, S., Fujii, K., Kladwang, W., Das, R., and Barna, M. (2015). RNA regulons in Hox 5′ UTRs confer ribosome specificity to gene regulation. Nature *517*, 33–38.

Yaffe, D., and Saxel, O. (1977). Serial passaging and differentiation of myogenic cells isolated from dystrophic mouse muscle. Nature *270*, 725–727.

Yagi, H., Deguchi, K., Aono, A., Tani, Y., Kishimoto, T., and Komori, T. (1998). Growth disturbance in fetal liver hematopoiesis of Mll-mutant mice. Blood *92*, 108.

Yang, J.-H., Song, Y., Seol, J.-H., Park, J.Y., Yang, Y.-J., Han, J.-W., Youn, H.-D., and Cho, E.-J. (2011). Myogenic transcriptional activation of MyoD mediated by replication-independent histone deposition. Proc. Natl. Acad. Sci. *108*, 85–90.

Yin, H., Pasut, A., Soleimani, V.D., Bentzinger, C.F., Antoun, G., Thorn, S., Seale, P., Fernando, P., van IJcken, W., Grosveld, F., et al. (2013a). MicroRNA-133 Controls

Brown Adipose Determination in Skeletal Muscle Satellite Cells by Targeting Prdm16. Cell Metab. *17*, 210–224.

Yin, H., Price, F., and Rudnicki, M.A. (2013b). Satellite Cells and the Muscle Stem Cell Niche. Physiol. Rev. *93*, 23–67.

Yokoyama, A., Ficara, F., Murphy, M.J., Meisel, C., Hatanaka, C., Kitabayashi, I., and Cleary, M.L. (2013). MLL Becomes Functional through Intra-Molecular Interaction Not by Proteolytic Processing. PLOS ONE *8*, e73649.

Yu, B.D., Hess, J.L., Horning, S.E., Brown, G.A., and Korsmeyer, S.J. (1995). Altered Hox expression and segmental identity in Mll-mutant mice. Nature *378*, 505–508.

Yu, B.D., Hanson, R.D., Hess, J.L., Horning, S.E., and Korsmeyer, S.J. (1998). MLL, a mammalian trithorax-group gene, functions as a transcriptional maintenance factor in morphogenesis. Proc. Natl. Acad. Sci. U. S. A. *95*, 10632–10636.

Yun, Z., Lin, Q., and Giaccia, A.J. (2005). Adaptive Myogenesis under Hypoxia. Mol. Cell. Biol. *25*, 3040–3055.

Zacharias, A.L., Lewandoski, M., Rudnicki, M.A., and Gage, P.J. (2011). Pitx2 is an upstream activator of extraocular myogenesis and survival. Dev. Biol. *349*, 395–405.

Zammit, P.S., Golding, J.P., Nagata, Y., Hudon, V., Partridge, T.A., and Beauchamp, J.R. (2004). Muscle satellite cells adopt divergent fates: a mechanism for self-renewal? J. Cell Biol. *166*, 347–357.

Zhang, C.L., McKinsey, T.A., and Olson, E.N. (2002). Association of Class II Histone Deacetylases with Heterochromatin Protein 1: Potential Role for Histone Methylation in Control of Muscle Differentiation. Mol. Cell. Biol. *22*, 7302–7312.

Zhang, H., Gayen, S., Xiong, J., Zhou, B., Shanmugam, A.K., Sun, Y., Karatas, H., Liu, L., Rao, R.C., Wang, S., et al. (2016a). MLL1 Inhibition Reprograms Epiblast Stem Cells to Naive Pluripotency. Cell Stem Cell *18*, 481–494.

Zhang, H., Ryu, D., Wu, Y., Gariani, K., Wang, X., Luan, P., D'Amico, D., Ropelle, E.R., Lutolf, M.P., Aebersold, R., et al. (2016b). NAD+ repletion improves mitochondrial and stem cell function and enhances life span in mice. Science aaf2693.

Zhang, W., Behringer, R.R., and Olson, E.N. (1995). Inactivation of the myogenic bHLH gene MRF4 results in up-regulation of myogenin and rib anomalies. Genes Dev. *9*, 1388–1399.

Zhao, X., Han, X., Chew, J., Liu, J., Chiu, K., Choo, A., Orlov, Y., Sung, W., Shahab, A., and Kuznetsov, V. (2007). Whole-Genome Mapping of Histone H3 Lys4 and 27 Trimethylations Reveals Distinct Genomic Compartments in Human Embryonic Stem Cells. Cell Stem Cell *1*, 286–298.

Zhong, X., Wang, Q.-Q., Li, J.-W., Zhang, Y.-M., An, X.-R., and Hou, J. (2017). Ten-Eleven Translocation-2 (Tet2) Is Involved in Myogenic Differentiation of Skeletal Myoblast Cells in Vitro. Sci. Rep. *7*, 43539.

Zhu, H., Wang, G., and Qian, J. (2016). Transcription factors as readers and effectors of DNA methylation. Nat. Rev. Genet. *17*, 551–565.

Ziller, M.J., Gu, H., Müller, F., Donaghey, J., Tsai, L.T.-Y., Kohlbacher, O., De Jager, P.L., Rosen, E.D., Bennett, D.A., Bernstein, B.E., et al. (2013). Charting a dynamic DNA methylation landscape of the human genome. Nature *advance online publication*.

Appendix A

Table S1. Primers for gene expression analysis

Gene	Forward	Reverse
Asb4	CCATCCTCTGTGCCAAGCAGTTGG	GCGTTCATGCTATCCACGATGGCC
Dlx1	CTACATCAGTTCCGTGCAGTCCTACC	CTTTGCCGTTAAAGCGCACCTCG
Dlx2	CAGCTACGACCTGGGCTACACC	CTGGAGTAGATGGTGCGTGGTTTCC
Fgfr4	GCCGATACCTCTGCCTGGCC	GGTGCTTGCTGTGGGTAGACATGACC
Hoxc10	AGACCGCAGACTCCAGTCC	TCCAATTCCAGCGTCTGGTG
Lbx1	GAGCTCGCCAGCAAGACCTTTAAGG	GTAGATCTGGTGGTTGGTGAAGGCC
MLL1	ATCGGCACCAACCTGCGC	TTTGGTCTCTGATTTGTTTAGAGGG
MLL2	TCCGAGGAGGAGGAGTTTCAGG	TCGTCTTATGCTTGCGGCCC
MLL3	GCTTTCAACTCTGCTGCTGGAAGC	AATGGCACTGCCAGAAAGCTGC
MLL4	CAGACCTTCCCATTCTGTGTATCGG	TTGTGATGCGTCCTCCTTGGG
Myf5	CACCAACCCTAACCAGAGACTCCC	GCTGTTACATTCAGGCATGCCG
MyHC IIa	GACCAGATCTTCCCCATGAA	TAAGGGTTGACGGTGACACA
MyoD	CATGATGGATTACAGCGGCCC	TCTGTGTCGCTTAGGGATGCCC
myog	GCAATGCACTGGAGTTCG	ACGATGGACGTAAGGGAGTG
Pax7	CGACTCTGGATTCGTCTCC	GGCCTTGGCCAAGAGGG
Set1a	CATCTTCCTTTGGCCAGTTCACC	CGGCGAGAAAAAGAATCTTGATAGC
Setib	TGACGAAGATGACAACGAAGCCG	CAGAACTTTCACTGGAGGATGAGGA
Six1	AGGGAGAAACGGGAGCTGGC	GACCGAGTTCTGGTCTGGACTTTGG
Six2	CTTCAAGGAGAAGAGCCGCAGC	CTTCTCATCCTCGGAACTGCCTAGC
Six4	CAAGGAGCTCTACAAGCAGAATCGC	TAGAGAGGCTGAGGTTGGTGACGC
Pax7 exon 1-1	GAAGACGCCAAGAGGTTTATC	CAGGGGGAAGCCGGTG
Pax7 exon 1-2	CGACTCTGGATTCGTCTCC	GGCCTTGGCCAAGAGGG
Pax7 exon 2-2	GGTCAATCAGCTTGGTGGG	GATATCGGCACAGAATCTTGG

Pax7 exon 2-3	TCCGTCACAAGATAGTGGAAATGGC	TTTCCCAGCTGAACATCCCGG
Pax7 exon 4-5	GACAAGAAAGAAGAAGATGGCG	GCTGCTTGCGCTTCAGGG
Pax7 exon 5-6	CGCAGTCGGACCACGTTC	CTGCTTACGCCAGCGGG
Pax7 exon 7-8	TCTCCAGCTACTCTGACAGC	GATGGAGAAGTCGGCCTGG
Pax7 exon 9-9	GCATCCTGCAGTGACCTCC	ACTCAGAGGTCAAGGACTCC

Table S2. Primers for ChIP qPCR

Gene and Loci	Forward	Reverse
Pax7 -0.2	CGCAAGGCGCAGCTGGG	GGGAGGAGTGGAAGGTGG
Pax7 +0.6	GTCCCTCAAAGTCGGGATGG	GCGGGAAATAAGGCACTATGC
Pax7 +1.1	GGGTGCGGGAGGATGGG	TTCGCCTCTGTCTAATTCGGG
Pax7 +11.5	AAATCTAATCAAGGCAGAACGCG	CTTGGAATCCCGGTCTCGC
Pax7 +11.7	GCCAAACGAAAGGATGTGGG	CGCTTGGAAACTGGATTTGGG
IGH	GCCGATCAGAACCAGAACAACTGC	TGGTGGGGCTGGACAGAGTGTTTC
Myf5 -6.4	GATGCAATCCTCCTGCGTGG	AAGACTGCTGGAGGCTGAGG
Myf5 -3.5	CAAAATATACGTAACTCAGTCTGGG	CATATCAATTGCACACAGAATCTGG
Myf5 +0.2	CCTGCTTCTCTGAAGGATGG	CGAAGGCTGCTACTCTTGGC
Myf5 +0.4	CCAGGCTGGCCACTGCC	CTTGGTTGACCTTCTTCAGGC
Myf5 +1.1	GGGCGCATTGCTGCGGG	CAGCACTGATCTAGGAAGGG
Myf5 +1.7	CTTTTGCTTGAAATATTACCAGGG	CTTGTGGTGCCCTTTAAACCC
Myf5 +4.9	CTGTTTACCCAATAGCCTACC	TATGCTGCCTTGCCTGCCC

Table S3. Primers for meDIP qPCR

Gene and Loci	Forward	Reverse
Myf5 TSS	CTAATAACGCCCAGCTACAGGG	GAGCTCCCGGAGTTTGGG
Myf5 +450	GGCCACTGCCTCATGTGGG	CTTGGTTGACCTTCTTCAGGCG
Myf5 +3600	ATGCCCTCAGCCTCTAAGGTGC	GTTGAGAGGCACAGGCAGGG
Pax7	CGTGGACTCCGCTGACC	CTGTTGTGTCAGAGAAGAGTGG
Sohlh2	TTGCACAGGCGTCAGATGGG	CAAGGCTCTACTACGCATGGG
NeuroD6	TACAGATTGCCAGTGAGACCC	GCACTGATCATCTGGCATCCC

Table S4. Cloning and subcloning primers

pHAN-Asb4	Asb4 BamHI Fwd	caaggatccccgaggatggacggcatcac
	Asb4 Stop EcoRI Rev	gcagaattcttagtaaatgattccctctggctcc
pHAN-Fgfr4	Fgfr4 BglII Fwd	caaagatctatgtggctgctcttggccc
	Fgfr4 MfeI Rev	gcacaattgtcatgtcgtctgcgagtcagag
pHAN-Six2	Six2 BamHI Fwd 2	caaggatccgccaccATGtccatgctgccc
	Six2 Stop EcoRI Rev 2	gcagaattcCTAggagcccaggtccacaagg
pHAN-Dlx1	Dlx1 BamHI Fwd	caaggatccgaagagatgaccatgaccaccatgcc
	Dlx1 Stop EcoRI Rev	gcagaattctcacatcagttgaggctgctgcatagc
pHAN-Lbx1	Lbx1 BamHI Fwd	caaggatccgccgagatgacttccaaggagg
	Lbx1 Stop EcoRI Rev	gcagaattctcaatcgtccacgtcgatctcttcatcttcc
pCLX-Pax7	Pax7start attB1	ACAAGTTTGTACAAAAAAGCAGGCTatggcggcgctgccc
	Pax7stop attB2	ACCCAGCTTTCTTGTACAAAGTGGTccctagtaggcttgtccc

Table S5. List of small interfering RNAs

MLL1-1	Sense	AGAAGAGUAAGAGUCUCAAACAG[dA][dC]
MLL1-1	Antisense	ACUCUUUCUCAUUCUCAGAGUUUGUCUG
MLL1-2	Sense	GGAGUUCAGCGAUGAUAUUGUGA[dA][dG]
MLL1-2	Antisense	AACCUCAAGUCGCUACUAUAACACUUC
MLL1-3	Sense	GGCAACGACCAUGUAAUAAUGUU[dT][dC]
MLL1-3	Antisense	ACCCGUUGCUGGUACAUUAUUACAAAG
MLL2-1	Sense	GGAGUACACGGCUGCCAAACGGA[dG][dT]
MLL2-1	Antisense	UGCCUCAUGUGCCGACGGUUUGCCUCA
MLL2-2	Sense	AGCAGUAGUGUUAGCAGAAGCGG[dC][dT]
MLL2-2	Antisense	GUUCGUCAUCACAAUCGUCUUCGCCGA
MLL2-3	Sense	GAAGUGUGACCAGAUAGAGGCU[dC][dG]
MLL2-3	Antisense	GGCCUUCACACUGUUCUAUCUCCGACG
MLL3-1	Sense	GGAACCGGAGCUGUUGUAU[dT][dT]
MLL3-1	Antisense	AUACAACAGUCUUAAUUCC[dT][dT]
MLL3-2	Sense	CAGCUAUGAGGUUAGUAAU[dT][dT]
MLL3-2	Antisense	AUUACUAACCUCAUAGCUG[dT][dT]
MLL3-3	Sense	CAAUUAAUCCCUUCCGUCA[dT][dT]
MLL3-3	Antisense	UGACGGAAGGGAUUCCUUG[dT][dT]
MLL4-1	Sense	CUAAGGAGCUGUCCUUGUU[dT][dT]
MLL4-1	Antisense	AACAAGGACAGCUCCUUAG[dT][dT]
MLL4-2	Sense	CAGACAAGUUUGUUCUAAU[dT][dT]
MLL4-2	Antisense	AUUAGAACAAACUUGUCUG[dT][dT]
MLL4-3	Sense	CUCUAGAUGGGACUGGACA[dT][dT]
MLL4-3	Antisense	UGUCCAGUCCCAUCUAGAG[dT][dT]
SET1A-1	Sense	GUUCUAUAUUGGACAGAUA[dT][dT]
SET1A-1	Antisense	UAUCUGUCCAAUAUAGAAC[dT][dT]
SET1A-2	Sense	CACACAAUCACCAACCUAA[dT][dT]
SET1A-2	Antisense	UUAGGUUGGUGAUUGUGUG[dT][dT]
SET1A-3	Sense	CGAUUUGGCCGGAGCCGUA[dT][dT]
SET1A-3	Antisense	UACGGCUCCGGCCAAAUCG[dT][dT]
SET1B-1	Sense	GCCUUCAACCUCUGUGGAU[dT][dT]
SET1B-1	Antisense	AUCCACAGAGGUUGAAGGC[dT][dT]
SET1B-2	Sense	CCCAGAAGAAGAUCGUCAU[dT][dT]
SET1B-2	Antisense	AUGACUAUCUUCUUCUGGG[dT][dT]
SET1B-3	Sense	GGAUGUCAGCCGUAGCCCA[dT][dT]
SET1B-3	Antisense	UGGGCUACGGCUGACAUCC[dT][dT]
Negative Ctrl	Sense	CUUCCUCUCUUUCUCUCCCUUG[dG][dA]
Negative Ctrl	Antisense	UCACAAGGGAGAGAAAGAGAGGAAGGA

Table S6. List of antibodies

Species and Antigen	Source	Identifier
Mouse anti Pax7	DSHB, Kawakami	Pax7
Mouse anti Tubulin (clone DM1A)	Sigma	T9026
Mouse anti GAPDH	UBC AbLab	GA1R
Mouse anti Myosin Heavy Chain	DSHB	MF20
Mouse anti meCpG (clone 33D3)	Millipore	MABE146
Mouse anti dystrophin (clone DY4/6D3)	Leica Microsystems	DYS1-CE
Rabbit anti-myogenin	Santa Cruz	sc-576
Rabbit anti-Myf5	Abcam	ab125301
Rabbit anti H3K4me3	Abcam	ab8580
Rabbit anti H3K27me3	Abcam	ab6002
Normal Rabbit IgG	Millipore	12-370
Normal Mouse anti IgG	Millipore	12-371
Rabbit anti Mouse IgG	Jackson Labs	315-005-008
Mouse anti MLL1	Millipore	05-764
APC mouse anti-integrin alpha7 (clone R2F2)	UBC AbLab	67-0010-10
PE mouse anti-Sca1 (clone D7)	BD Biosciences	553108
PE mouse anti-CD45 (clone 30-F11)	BD Biosciences	12-0451-83
PE mouse anti-CD31 (clone 390)	BD Biosciences	12-0311-81
PE mouse anti-CD11b (clone M1/70)	BD Biosciences	12-0112-81

Table S7. Affymetrix data for all probes with greater than two fold change.

Affymetrix data for all probes with greater than two fold change between control and *Mll1* KO myoblasts. Affymetrix signal for control myoblast RNA is (**Affy4957**). Affymetrix signal for *Mll1* KO myoblast RNA is (**Affy4958B**). All probe sets are designated by gene symbol, if applicable, and by chromosomal location by chromosome number (**Ch**), strand (**Str**), and loci (**start** and **stop** of region targeted by probes). Subtraction of Affymetrix signal for *Mll1* KO myoblast RNA from Affymetrix signal for control myoblast RNA was used to determine difference between signals (**Difference**). **Fold change** is the log2 transformation of the absolute difference value with "–" designating that gene expression is lower in *Mll1* KO and "+" designating that gene expression is higher in *Mll1* KO.

Probe Set ID	Affy#4957	Affy#4958	Gene Symbol	Ch	Str	Start	Stop	Difference	Fold Change	
10372226	9.50906	6.140067	Myf5	chr10	-	106919964	106923190	3.369	–	10.332
10536324	9.992788	7.123243	Asb4	chr6	+	5333386	5383022	2.870	–	7.308
10508719	9.174999	7.029644	---	chr4	+	131865380	131865515	2.145	–	4.424
10516906	10.47735	8.488178	---	chr4	-	131908237	131908441	1.989	–	3.970
10516908	10.3898	8.470442	---	chr4	-	131908690	131908894	1.919	–	3.783
10453394	9.201182	7.668017	Six2	chr17	-	86083608	86087594	1.533	–	2.894
10458762	8.112397	6.605179	---	chr18	-	45445487	45445762	1.507	–	2.843
10402512	10.08959	8.691132	---	chr12	-	106269287	106269559	1.398	–	2.636
10382104	10.58623	9.196234	---	chr11	+	106362307	106362376	1.390	–	2.621
10472809	9.002811	7.741342	Dlx1	chr2	+	71367502	71372038	1.261	–	2.397
10405380	9.001039	7.771609	Fgfr4	chr13	+	55254001	55270120	1.229	–	2.345
10584524	4.651093	3.447046	---	chr9	+	39858175	39860601	1.204	–	2.304
10373610	7.643711	6.461029	Olfr767	chr10	-	128516088	128517017	1.183	–	2.270
10468046	7.972652	6.823596	Lbx1	chr19	-	45308135	45309815	1.149	–	2.218
10492169	6.588424	5.459296	Mab21l1	chr3	+	55586434	55588923	1.129	–	2.187
10392825	7.766903	6.667329	OTTMUSG00000003606	chr11	-	114882003	114909644	1.100	–	2.143
10392834	7.575061	6.488804	OTTMUSG00000003606	chr11	-	114892800	114898969	1.086	–	2.123
10455813	8.913897	7.836621	Lmnb1	chr18	+	56867518	56913078	1.077	–	2.110
10502949	9.626022	8.5723	---	chr3	-	153574574	153574654	1.054	–	2.076
10453049	8.68536	7.635813	Cdc42ep3	chr17	-	79733067	79754431	1.050	–	2.070
10375055	5.488249	4.44293	F830116E18Rik	chr11	+	32186964	32187912	1.045	–	2.064
10505917	8.115001	7.074561	---	chr4	+	90704591	90704964	1.040	–	2.057
10360745	9.035222	8.000598	Lbr	chr1	-	183745447	183772492	1.035	–	2.049
10489503	4.140586	3.108337	Wfdc6a	chr2	-	164405020	164410677	1.032	–	2.045
10425046	7.269979	6.247836	LOC626711	chr15	+	77532463	77533052	1.022	–	2.031
10515090	8.026818	7.01997	Cdkn2c	chr4	-	109333481	109338280	1.007	–	2.010
10517486	4.442112	3.437992	---	chr4	-	136164963	136165720	1.004	–	2.006
10459227	5.203088	4.199553	---	chr18	-	61808850	61808912	1.004	–	2.005
10404061	10.60837	9.605441	Hist1h2bb	chr13	+	23838603	23839393	1.003	–	2.004
10522895	3.987588	4.989783	Csn3	chr5	+	88354632	88361570	-1.002	+	2.003
10365344	5.197994	6.200439	Tcp11l2	chr10	+	84039692	84077104	-1.002	+	2.003
10481518	6.041405	7.044753	Ptges	chr2	-	30744991	30758817	-1.003	+	2.005
10450038	6.609109	7.61375	Angptl4	chr17	-	33910695	33918520	-1.005	+	2.006
10498576	8.456583	9.463669	Lxn	chr3	-	67261919	67268265	-1.007	+	2.010
10350473	4.561762	5.569593	B3galt2	chr1	+	145487873	145496960	-1.008	+	2.011
10456171	4.211409	5.220606	Spink10	chr18	+	62708565	62821042	-1.009	+	2.013
10576189	5.423725	6.432957	---	chr8	+	125407494	125407686	-1.009	+	2.013
10569504	8.275231	9.284623	Tnfrsf23	chr7	-	150851712	150871777	-1.009	+	2.013
10577641	7.008813	8.021966	1810011O10Rik	chr8	-	25548087	25549418	-1.013	+	2.018
10532313	3.92497	4.938361	AB010352 // AB010352	chr5	-	110475251	110475505	-1.013	+	2.019
10501063	6.506387	7.523302	Cd53	chr3	-	106562839	106592970	-1.017	+	2.024
10598073	7.825447	8.843273	---	chrM	-	3772	3842	-1.018	+	2.025
10409314	5.844322	6.863218	Msx2	chr13	-	53562250	53568443	-1.019	+	2.026
10465580	7.437877	8.456903	Nudt22	chr19	-	7067508	7070527	-1.019	+	2.027
10404036	7.306263	8.330848	Hist1h2bg	chr13	+	23663265	23663891	-1.025	+	2.034
10569008	5.812182	6.838784	Cox8b	chr7	-	148084841	148086322	-1.027	+	2.037
10553477	7.13808	8.166965	Ano5	chr7	+	58766399	58854079	-1.029	+	2.040
10374777	4.338007	5.367937	Efemp1	chr11	+	28753204	28826743	-1.030	+	2.042
10473125	6.186704	7.217612	Itga4	chr2	+	79095583	79173271	-1.031	+	2.043
10587231	4.517818	5.54995	Bmp5	chr9	+	75623172	75746824	-1.032	+	2.045
10499854	8.175922	9.209099	S100a1	chr3	-	90314956	90318314	-1.033	+	2.047
10362442	4.899306	5.932651	Trdn	chr10	+	33157524	33157553	-1.033	+	2.047
10559667	5.725666	6.76074	Il11	chr7	-	4724657	4729627	-1.035	+	2.049
10435704	7.495303	8.531247	Cd80	chr16	+	38459013	38487015	-1.036	+	2.050
10360418	5.590205	6.628416	Rgs7	chr1	-	176989218	177422631	-1.038	+	2.054
10371188	6.279467	7.318119	Brunol5	chr10	-	80924969	80945440	-1.039	+	2.054

Probe Set ID	Affy#4957	Affy#4958	Gene Symbol	Ch	Str	Start	Stop	Difference	Fold Change	
10466800	5.625351	6.665284	Pgm5	chr19	-	24752751	24936332	-1.040	+	2.056
10452516	6.248374	7.288579	Ankrd12	chr17	-	66316841	66426386	-1.040	+	2.057
10594963	3.892929	4.933532	Unc13c	chr9	-	73476956	73477041	-1.041	+	2.057
10593449	7.980424	9.022433	Layn	chr9	-	50865411	50885159	-1.042	+	2.059
10463476	5.544312	6.588754	Kazald1	chr19	+	45150629	45153772	-1.044	+	2.063
10363224	9.212885	10.25774	Fabp7	chr10	+	57504729	57508257	-1.045	+	2.063
10407742	7.603036	8.649387	Actn2	chr13	-	12361693	12432999	-1.046	+	2.065
10591544	7.060644	8.107084	Yipf2	chr9	-	21393126	21397216	-1.046	+	2.065
10349661	5.43122	6.478277	5430435G22Rik	chr1	+	133585272	133610045	-1.047	+	2.066
10446756	8.177116	9.224277	Ypel5	chr17	+	73186044	73200535	-1.047	+	2.066
10478383	5.59033	6.638142	R3hdml	chr2	+	163318238	163328180	-1.048	+	2.067
10420274	6.019894	7.06842	Gzmd	chr14	-	56748417	56751445	-1.049	+	2.068
10419082	5.910537	6.959893	5730469M10Rik	chr14	-	41807024	41827064	-1.049	+	2.070
10519886	5.305504	6.355359	Sema3c	chr5	+	17080634	17236088	-1.050	+	2.070
10511136	7.833059	8.884542	B930041F14Rik	chr4	+	155068451	155070590	-1.051	+	2.073
10504902	7.94158	8.993618	Murc	chr4	+	48676386	48686371	-1.052	+	2.073
10577388	4.410193	5.464351	---	chr8_ra	-	374283	381170	-1.054	+	2.077
10443690	6.042903	7.097919	Glp1r	chr17	+	31038812	31073478	-1.055	+	2.078
10455461	5.25282	6.308047	Myot	chr18	+	44493728	44515382	-1.055	+	2.078
10450982	6.540763	7.597281	Gpr115	chr17	-	42793840	42842149	-1.057	+	2.080
10588691	6.571939	7.628955	Hyal1	chr9	+	107479283	107482478	-1.057	+	2.081
10481186	5.955968	7.013576	Sardh	chr2	-	27043917	27102332	-1.058	+	2.081
10532669	7.08238	8.140575	2900026A02Rik	chr5	-	113517970	113592311	-1.058	+	2.082
10598032	8.969702	10.0291	---	chrM	+	3845	3913	-1.059	+	2.084
10433032	7.816449	8.876762	Atf7	chr15	-	102359067	102359456	-1.060	+	2.085
10444778	6.759569	7.819968	---	chr17	+	35384120	35384195	-1.060	+	2.086
10363455	8.400932	9.461855	Pcbd1	chr10	+	60552107	60557070	-1.061	+	2.086
10513692	7.920468	8.98175	Whrn	chr4	-	63075944	63156985	-1.061	+	2.087
10535053	6.660993	7.723067	Prkar1b	chr5	-	139493260	139605653	-1.062	+	2.088
10500204	8.369267	9.434324	Ecm1	chr3	-	95538072	95543485	-1.065	+	2.092
10512265	6.603569	7.668793	2310028H24Rik	chr4	-	41465962	41516542	-1.065	+	2.092
10578574	5.122635	6.188232	Stox2	chr8	-	48271293	48437702	-1.066	+	2.093
10549760	7.671782	8.739617	Zfp580	chr7	+	5003140	5005325	-1.068	+	2.096
10384223	10.49612	11.56402	Igfbp3	chr11	-	7106089	7113926	-1.068	+	2.096
10545502	3.737301	4.805241	Dnahc6	chr6	-	73041981	73073880	-1.068	+	2.096
10490302	5.11896	6.18846	2810021G02Rik	chr2	-	177804256	177804603	-1.070	+	2.099
10560945	6.485631	7.555481	Grik5	chr7	-	25794868	25857317	-1.070	+	2.099
10539135	8.725011	9.796184	Capg	chr6	+	72494433	72512974	-1.071	+	2.101
10570855	6.659373	7.731126	Plat	chr8	+	23868219	23893316	-1.072	+	2.102
10472400	3.229571	4.305926	Scn2a1	chr2	+	65581122	65581175	-1.076	+	2.109
10554574	6.274218	7.352812	Tm6sf1	chr7	+	89003887	89028957	-1.079	+	2.112
10390117	7.127118	8.206507	Itga3	chr11	-	94905789	94938115	-1.079	+	2.113
10507101	5.538962	6.622499	Gm12824	chr4	+	114252893	114272572	-1.084	+	2.119
10497077	4.081289	5.165212	---	chr3	+	157207243	157207313	-1.084	+	2.120
10517609	7.609082	8.693123	Cda	chr4	-	137894443	137923875	-1.084	+	2.120
10530536	4.784023	5.868137	Tec	chr5	-	73146973	73259722	-1.084	+	2.120
10455123	4.769114	5.853268	Pcdhb19	chr18	+	37656652	37661365	-1.084	+	2.120
10533462	5.369191	6.453345	Rad9b	chr5	-	122775407	122804204	-1.084	+	2.120
10538658	4.545394	5.630378	Herc3	chr6	+	58781883	58870394	-1.085	+	2.121
10507479	7.627172	8.712904	Tmem53	chr4	+	116924594	116941187	-1.086	+	2.122
10484371	7.687429	8.773941	Calcrl	chr2	-	84170783	84265424	-1.087	+	2.124
10347669	6.710557	7.798742	Inha	chr1	+	75503652	75506929	-1.088	+	2.126
10389581	5.869934	6.960133	Ypel2	chr11	-	86749927	86807264	-1.090	+	2.129
10376765	5.180132	6.272154	Aldh3a1	chr11	+	61022247	61031916	-1.092	+	2.132
10393573	7.294281	8.387157	Lgals3bp	chr11	-	118254063	118263273	-1.093	+	2.133
10607619	5.721589	6.815344	Cdkl5	chrX	-	157222410	157432609	-1.094	+	2.134
10544150	5.798718	6.893033	Jhdm1d	chr6	-	39092309	39156633	-1.094	+	2.135

Probe Set ID	Affy#4957	Affy#4958	Gene Symbol	Ch	Str	Start	Stop	Difference	Fold Change	
10485070	6.872813	7.968844	Mdk	chr2	-	91769805	91772439	-1.096	+	2.138
10385776	6.787421	7.88405	Tcf7	chr11	-	52066106	52096681	-1.097	+	2.139
10545484	3.646303	4.745493	Dnahc6	chr6	-	72967603	73010297	-1.099	+	2.142
10531274	5.872826	6.972691	Btc	chr5	-	91786287	91831939	-1.100	+	2.143
10471294	6.331949	7.438686	Ppapdc3	chr2	+	31951171	31966340	-1.107	+	2.154
10475866	6.883944	7.992426	Bcl2l11	chr2	+	127951774	127988283	-1.108	+	2.156
10464688	5.639225	6.750284	Ankrd13d	chr19	-	4270180	4283137	-1.111	+	2.160
10357965	8.708781	9.81989	Lgr6	chr1	-	136882930	137001853	-1.111	+	2.160
10412882	5.465538	6.576778	Thrb	chr14	+	18758162	18870600	-1.111	+	2.160
10375245	6.619215	7.731165	Gabrb2	chr11	+	42233259	42442530	-1.112	+	2.161
10595979	5.932551	7.046961	Mras	chr9	-	99286225	99286571	-1.114	+	2.165
10449955	7.062243	8.177891	Cyp4f13	chr17	-	33061614	33084315	-1.116	+	2.167
10491952	5.287574	6.403863	Mgst2	chr3	+	51465115	51486597	-1.116	+	2.168
10572527	3.759655	4.877024	---	chr8	+	73611708	73665197	-1.117	+	2.170
10362426	3.072543	4.194377	Trdn	chr10	+	33054788	33054820	-1.122	+	2.176
10445293	4.823937	5.946786	Pla2g7	chr17	+	43705400	43749150	-1.123	+	2.178
10605181	4.334481	5.460711	Renbp	chrX	-	71167460	71176157	-1.126	+	2.183
10601878	6.46655	7.593493	Tceal1	chrX	+	133242571	133244412	-1.127	+	2.184
10410931	9.243387	10.37383	Vcan	chr13	-	89796661	89881923	-1.130	+	2.189
10360235	5.997584	7.128764	Casq1	chr1	-	174140028	174149972	-1.131	+	2.190
10579341	8.582829	9.716358	Mpv17l2	chr8	-	73282548	73284829	-1.134	+	2.194
10399478	6.820171	7.955743	Lpin1	chr12	-	16542763	16617772	-1.136	+	2.197
10477637	7.653535	8.790674	Map1lc3a	chr2	+	155096422	155103808	-1.137	+	2.199
10573344	5.975161	7.112478	---	chr8	+	86732571	86732657	-1.137	+	2.200
10499870	7.078136	8.218407	Lor	chr3	-	91884193	91887064	-1.140	+	2.204
10469609	6.81984	7.96214	Gm13375	chr2	+	20891520	20891834	-1.142	+	2.207
10481175	8.907806	10.05042	Tmem8c	chr2	-	26917156	26927681	-1.143	+	2.208
10398859	7.626647	8.769471	Adssl1	chr12	+	113858300	113879569	-1.143	+	2.208
10465089	6.266174	7.412189	Snx32	chr19	-	5495274	5510489	-1.146	+	2.213
10442321	8.092546	9.23901	Hcfc1r1	chr17	+	23810575	23812491	-1.146	+	2.214
10415074	7.038472	8.190404	Rem2	chr14	+	55094937	55099271	-1.152	+	2.222
10530100	5.236913	6.389963	Arap2	chr5	-	62993687	63157325	-1.153	+	2.224
10437210	5.463298	6.61983	Bace2	chr16	+	97578369	97660619	-1.157	+	2.229
10530560	5.698916	6.859873	Slain2	chr5	-	73357047	73365941	-1.161	+	2.236
10372891	6.136662	7.2981	Srgap1	chr10	-	121222221	121484364	-1.161	+	2.237
10540509	5.611744	6.776957	Grm7	chr6	+	110595592	111517224	-1.165	+	2.243
10394593	3.82838	4.9939	Fam49a	chr12	+	12268983	12383169	-1.166	+	2.243
10564237	4.282814	5.450445	Gm9801	chr7	-	69239392	69354365	-1.168	+	2.246
10472562	7.143448	8.311676	Kbtbd10	chr2	+	69508264	69521653	-1.168	+	2.247
10349980	7.310884	8.484089	Mybph	chr1	+	136090025	136097809	-1.173	+	2.255
10593316	5.638709	6.811919	---	chr9	-	49338736	49339005	-1.173	+	2.255
10447084	6.05368	7.227299	Galm	chr17	+	80526811	80584440	-1.174	+	2.256
10375443	4.838541	6.016963	Havcr2	chr11	+	46268437	46294757	-1.178	+	2.263
10579812	6.091125	7.271385	Ednra	chr8	-	80186928	80248351	-1.180	+	2.266
10474223	5.171867	6.354717	Cd59b	chr2	+	103910023	103931347	-1.183	+	2.270
10553057	6.411014	7.597041	Mamstr	chr7	+	52895347	52901138	-1.186	+	2.275
10538150	7.987373	9.174746	Tmem176a	chr6	+	48791508	48797047	-1.187	+	2.277
10494804	6.598847	7.787487	Casq2	chr3	+	101890433	101950437	-1.189	+	2.279
10424119	8.015501	9.204212	Nov	chr15	+	54577477	54585319	-1.189	+	2.279
10393098	8.263634	9.455034	Wbp2	chr11	-	115939887	115948286	-1.191	+	2.284
10398366	5.152876	6.345175	---	chr12	+	110895335	110895406	-1.192	+	2.285
10350742	4.477824	5.670505	Rnasel	chr1	+	155600060	155609471	-1.193	+	2.286
10607183	4.355291	5.550844	Lhfpl1	chrX	-	141724902	141783493	-1.196	+	2.290
10576332	5.828691	7.02545	Tubb3	chr8	+	125932663	125945976	-1.197	+	2.292
10575693	8.049362	9.248941	Vat1l	chr8	+	116729530	116897971	-1.200	+	2.297
10574572	4.688929	5.895408	2210023G05Rik	chr8	+	107485640	107493433	-1.206	+	2.308
10487722	6.340213	7.546943	Slc4a11	chr2	-	130509850	130522447	-1.207	+	2.308

Probe Set ID	Affy#4957	Affy#4958	Gene Symbol	Ch	Str	Start	Stop	Difference	Fold Change
10355500	9.428188	10.63564	Igfbp5	chr1	-	72904610	72921439	-1.207	+ 2.309
10545086	5.018376	6.230706	Snca	chr6	-	60681566	60779849	-1.212	+ 2.317
10543785	6.012906	7.230957	AB041803	chr6	-	31115511	31168433	-1.218	+ 2.326
10350149	7.427479	8.647919	Tnni1	chr1	+	137696016	137707564	-1.220	+ 2.330
10406407	6.856459	8.077772	Arrdc3	chr13	+	81022673	81035303	-1.221	+ 2.332
10485580	5.247802	6.470709	Cstf3	chr2	-	104504327	104504668	-1.223	+ 2.334
10420616	6.177564	7.401219	Sgcg	chr14	-	61839896	61877327	-1.224	+ 2.335
10382341	5.561581	6.785259	Sstr2	chr11	+	113485571	113486950	-1.224	+ 2.335
10574027	9.304008	10.52806	Mt1	chr8	+	96703111	96704227	-1.224	+ 2.336
10373400	6.590897	7.81523	Myl6b	chr10	-	127931213	127935741	-1.224	+ 2.336
10355259	10.19594	11.42048	Myl1	chr1	-	66970872	66991606	-1.225	+ 2.337
10460582	8.70678	9.934497	AI837181	chr19	+	5425157	5427319	-1.228	+ 2.342
10355214	9.670338	10.90236	Idh1	chr1	-	65205202	65225688	-1.232	+ 2.349
10492136	6.008771	7.243943	Dclk1	chr3	+	55046501	55340600	-1.235	+ 2.354
10492396	3.646333	4.881552	Vmn2r1	chr3	+	63885564	63909380	-1.235	+ 2.354
10455112	5.33536	6.572248	Pcdhb17	chr18	+	37644449	37649108	-1.237	+ 2.357
10377087	6.616099	7.857905	Myh1	chr11	+	67013604	67038079	-1.242	+ 2.365
10488060	6.593852	7.842034	Jag1	chr2	-	136907194	136942431	-1.248	+ 2.375
10397346	6.024742	7.285225	Fos	chr12	+	86814851	86818219	-1.260	+ 2.396
10399465	5.611926	6.873725	Fam84a	chr12	-	14154404	14158844	-1.262	+ 2.398
10607738	7.269715	8.532794	Car5b	chrX	-	160416297	160465929	-1.263	+ 2.400
10352905	5.959479	7.222745	Cd34	chr1	+	196765080	196787475	-1.263	+ 2.400
10383799	9.179474	10.44382	Tcn2	chr11	-	3817193	3831586	-1.264	+ 2.402
10476633	6.413778	7.679217	Pcsk2	chr2	+	143371915	143642022	-1.265	+ 2.404
10562192	6.534295	7.802324	Fxyd5	chr7	-	31817749	31827148	-1.268	+ 2.408
10368585	5.114255	6.383695	Nkain2	chr10	-	31409125	32609654	-1.269	+ 2.411
10461237	7.392924	8.662835	Bscl2	chr19	+	8912219	8923157	-1.270	+ 2.411
10494978	4.012097	5.282103	Ptpn22	chr3	+	103664215	103716634	-1.270	+ 2.412
10350630	5.054349	6.326858	Fam129a	chr1	+	153418605	153566472	-1.273	+ 2.416
10540472	5.157282	6.430528	Bhlhe40	chr6	+	108610623	108616919	-1.273	+ 2.417
10421950	5.806486	7.081148	Dach1	chr14	-	98186065	98568762	-1.275	+ 2.419
10378855	4.755744	6.039499	Ssh2	chr11	+	77272411	77272566	-1.284	+ 2.435
10564169	3.499583	4.783574	Snord116	chr7	-	66948590	66948683	-1.284	+ 2.435
10399581	4.297109	5.582669	3110053B16Rik	chr12	-	20879998	20882774	-1.286	+ 2.438
10503083	3.126937	4.417444	---	chr3	-	159579222	159579325	-1.291	+ 2.446
10442493	7.298545	8.593251	---	chr17	+	24665421	24665498	-1.295	+ 2.453
10509901	7.22796	8.523116	Mfap2	chr4	+	140566596	140578815	-1.295	+ 2.454
10363082	4.725973	6.024072	Lilrb4	chr10	+	51210781	51216419	-1.298	+ 2.459
10475643	4.802058	6.100687	Fgf7	chr2	+	125860520	125916264	-1.299	+ 2.460
10579054	4.049881	5.352196	---	chr8	-	71970394	71977295	-1.302	+ 2.466
10495625	4.627947	5.930658	Dpyd	chr3	+	118265094	119135842	-1.303	+ 2.467
10578572	4.938651	6.242646	Stox2	chr8	-	48269751	48269962	-1.304	+ 2.469
10445338	6.853261	8.161985	Enpp5	chr17	+	44215818	44223508	-1.309	+ 2.477
10574023	9.993347	11.30631	Mt2	chr8	+	96696684	96697464	-1.313	+ 2.485
10360377	6.171252	7.485382	AI607873	chr1	-	175662412	175671878	-1.314	+ 2.487
10567095	5.004596	6.323728	Calca	chr7	-	121775005	121779809	-1.319	+ 2.495
10399632	5.068986	6.390436	F630048H11Rik	chr12	-	21407255	21407434	-1.321	+ 2.499
10408870	7.891671	9.21408	Tbc1d7	chr13	-	43247113	43266728	-1.322	+ 2.501
10488459	5.100185	6.425987	Zfp442	chr2	-	150232855	150277218	-1.326	+ 2.507
10375259	5.389659	6.71996	Gabrb2	chr11	+	42443147	42444166	-1.330	+ 2.515
10555389	5.693841	7.024486	Ucp2	chr7	+	107641867	107650682	-1.331	+ 2.515
10572398	6.412824	7.745865	Crlf1	chr8	+	73017055	73027980	-1.333	+ 2.519
10428594	7.497439	8.834893	Samd12	chr15	-	53293356	53733991	-1.337	+ 2.527
10398362	4.907564	6.25458	Rian	chr12	+	110892837	110892908	-1.347	+ 2.544
10391103	8.210878	9.558716	Jup	chr11	-	100231933	100259057	-1.348	+ 2.545
10466712	5.475159	6.825529	Mamdc2	chr19	-	23377099	23522842	-1.350	+ 2.550
10350341	4.581821	5.932589	---	chr1	+	139863216	139863295	-1.351	+ 2.550

Probe Set ID	Affy#4957	Affy#4958	Gene Symbol	Ch	Str	Start	Stop	Difference	Fold Change	
10587241	5.011549	6.364657	Hmgcll1	chr9	+	75862784	75984157	-1.353	+	2.555
10387816	8.847227	10.20518	Rnasek	chr11	-	70051626	70053348	-1.358	+	2.563
10598083	5.978298	7.338946	---	chrM	-	6870	6938	-1.361	+	2.568
10606868	3.979655	5.340747	Bex1	chrX	-	132748511	132750052	-1.361	+	2.569
10406736	4.988636	6.354113	F2rl2	chr13	+	96466875	96472694	-1.365	+	2.577
10602198	4.256696	5.624238	Pak3	chrX	+	139953254	140226396	-1.368	+	2.580
10519693	6.177935	7.548845	Sema3d	chr5	+	12383556	12587058	-1.371	+	2.586
10378568	7.748999	9.121149	---	chr11	+	75277218	75277312	-1.372	+	2.589
10369835	5.112184	6.485285	Phyhipl	chr10	-	70020434	70062025	-1.373	+	2.590
10511363	4.199297	5.572886	Penk	chr4	-	4060680	4065592	-1.374	+	2.591
10413609	7.416295	8.791428	Mustn1	chr14	+	31692726	31694794	-1.375	+	2.594
10579060	3.956074	5.335804	---	chr8	-	72039802	72046711	-1.380	+	2.602
10570634	4.020444	5.400175	---	chr8	+	19732704	19778328	-1.380	+	2.602
10360053	5.540534	6.923231	Pcp4l1	chr1	-	173103395	173126370	-1.383	+	2.608
10360684	8.839058	10.22482	Ephx1	chr1	-	182919687	182947652	-1.386	+	2.613
10387536	6.079151	7.469858	Cd68	chr11	-	69477715	69479629	-1.391	+	2.622
10366391	4.688375	6.089067	Kcnc2	chr10	+	111708177	111903360	-1.401	+	2.640
10362428	5.319759	6.730185	Trdn	chr10	+	33054943	33054972	-1.410	+	2.658
10581643	3.685222	5.096867	---	chr8	-	112364488	112364589	-1.412	+	2.660
10406504	7.240526	8.671928	Edil3	chr13	+	88961035	89462466	-1.431	+	2.697
10498309	7.589257	9.020823	Pfn2	chr3	-	57645817	57651459	-1.432	+	2.697
10551185	8.333713	9.767529	Tgfb1	chr7	+	26472021	26490096	-1.434	+	2.702
10406434	6.251102	7.687067	Mef2c	chr13	+	83643194	83804078	-1.436	+	2.706
10455118	5.10132	6.541336	Pcdhb18	chr18	+	37649119	37654159	-1.440	+	2.713
10489569	6.620033	8.063806	Pltp	chr2	-	164665018	164683208	-1.444	+	2.720
10423520	6.664839	8.108758	Sema5a	chr15	+	32174858	32626085	-1.444	+	2.721
10356172	5.241571	6.688103	5033414K04Rik	chr1	-	84032873	84281166	-1.447	+	2.726
10593499	7.860085	9.308029	AI593442	chr9	-	52482515	52487542	-1.448	+	2.728
10390519	5.276951	6.725047	Plxdc1	chr11	-	97784552	97847694	-1.448	+	2.728
10474229	7.365619	8.827966	Cd59a	chr2	+	103936010	103955506	-1.462	+	2.756
10514865	5.835969	7.318453	Acot11	chr4	-	106417185	106477595	-1.482	+	2.794
10588263	6.306283	7.793289	Slco2a1	chr9	+	102910817	102998332	-1.487	+	2.803
10598626	8.514295	10.01234	Tspan7	chrX	+	10062242	10173732	-1.498	+	2.825
10362420	6.957051	8.455552	Trdn	chr10	+	33024843	33024896	-1.499	+	2.825
10367400	5.077469	6.576036	Mmp19	chr10	+	128228029	128236534	-1.499	+	2.826
10569020	4.610604	6.117103	Ifitm6	chr7	-	148201605	148202807	-1.506	+	2.841
10495206	4.010797	5.518306	Slc16a4	chr3	+	107094210	107115033	-1.508	+	2.843
10516735	6.115337	7.630589	Tinagl1	chr4	-	129841698	129852366	-1.515	+	2.858
10530854	3.475939	4.996843	Tecrl	chr5	-	83707173	83784220	-1.521	+	2.870
10574220	7.525798	9.048911	Cx3cl1	chr8	+	97296080	97306327	-1.523	+	2.874
10395553	6.371159	7.899692	Nrcam	chr12	+	45429971	45702951	-1.529	+	2.885
10347910	7.617661	9.147254	Fbxo36	chr1	+	84836430	84897059	-1.530	+	2.887
10599736	6.268203	7.8097	Fhl1	chrX	+	53984964	54046523	-1.541	+	2.911
10414065	4.625596	6.171126	Anxa8	chr14	+	34899168	34913757	-1.546	+	2.919
10571567	5.471869	7.027132	Sorbs2	chr8	+	46743646	46913259	-1.555	+	2.939
10425623	6.545571	8.112786	Csdc2	chr15	+	81767325	81781371	-1.567	+	2.963
10607562	4.084398	5.653052	Cnksr2	chrX	-	154259500	154481042	-1.569	+	2.966
10429515	6.805371	8.375483	Lynx1	chr15	-	74578286	74583418	-1.570	+	2.969
10416181	6.410188	7.981171	Stc1	chr14	+	69647261	69659785	-1.571	+	2.971
10362434	6.566591	8.145917	Trdn	chr10	+	33083784	33083828	-1.579	+	2.988
10399470	6.66954	8.255434	Trib2	chr12	-	15798531	15823591	-1.586	+	3.002
10471058	4.918163	6.514638	Cstad	chr2	+	30450564	30464465	-1.596	+	3.024
10470959	6.717234	8.317843	Phyhd1	chr2	+	30121723	30137668	-1.601	+	3.033
10349157	7.571865	9.173019	Serpinb2	chr1	+	109408000	109422175	-1.601	+	3.034
10362404	5.894933	7.509027	Trdn	chr10	+	32803346	32953798	-1.614	+	3.061
10374083	6.781013	8.399744	Aebp1	chr11	+	5761877	5772093	-1.619	+	3.071
10602756	6.111297	7.741792	Smpx	chrX	+	154137050	154190523	-1.630	+	3.096

Probe Set ID	Affy#4957	Affy#4958	Gene Symbol	Ch	Str	Start	Stop	Difference	Fold Change	
10345869	7.201254	8.834314	Tmem182	chr1	+	40862611	40911849	-1.633	+	3.102
10521678	4.833516	6.518277	Cd38	chr5	+	44260089	44303613	-1.685	+	3.215
10375261	4.620177	6.314641	Gabrb2	chr11	+	42444978	42446074	-1.694	+	3.237
10582882	5.374961	7.070806	---	chr9	+	3000922	3002330	-1.696	+	3.240
10355893	5.50865	7.218594	Epha4	chr1	-	77363760	77511663	-1.710	+	3.271
10361887	4.28353	6.003712	Perp	chr10	+	18564877	18576884	-1.720	+	3.295
10488678	4.846503	6.573872	Dusp15	chr2	-	152768927	152777141	-1.727	+	3.311
10362436	2.953922	4.687053	Trdn	chr10	+	33118901	33118951	-1.733	+	3.324
10582890	3.599812	5.353887	---	chr9	+	3017408	3021593	-1.754	+	3.373
10455108	5.281404	7.041821	Pcdhb16	chr18	+	37637494	37642438	-1.760	+	3.388
10401607	7.505562	9.275286	Pgf	chr12	-	86507591	86518235	-1.770	+	3.410
10485948	7.677663	9.461566	Grem1	chr2	-	113588727	113598803	-1.784	+	3.444
10564165	3.811993	5.619032	Snord116	chr7	-	66936425	66936518	-1.807	+	3.499
10398326	6.476895	8.297792	Meg3	chr12	+	110783828	110799933	-1.821	+	3.533
10559649	6.248113	8.076605	Cox6b2	chr7	-	4703396	4704696	-1.828	+	3.552
10499545	5.86432	7.697175	Efna3	chr3	-	89118873	89126801	-1.833	+	3.562
10351477	5.168446	7.01437	Sh2d1b1	chr1	+	172207451	172216900	-1.846	+	3.595
10598071	5.881231	7.728978	---	chrM	+	15289	15355	-1.848	+	3.599
10564177	3.71069	5.558528	Snord116	chr7	-	67009126	67009219	-1.848	+	3.600
10564207	3.7341	5.600611	Snord116	chr7	-	67047099	67047192	-1.867	+	3.646
10564205	3.7341	5.600611	Snord116	chr7	-	67044573	67044666	-1.867	+	3.646
10564201	3.7341	5.600611	Snord116	chr7	-	67039506	67039599	-1.867	+	3.646
10564199	3.7341	5.600611	Snord116	chr7	-	67036997	67037090	-1.867	+	3.646
10564197	3.7341	5.600611	Snord116	chr7	-	67034479	67034572	-1.867	+	3.646
10564195	3.7341	5.600611	Snord116	chr7	-	67031943	67032036	-1.867	+	3.646
10564193	3.7341	5.600611	Snord116	chr7	-	67029385	67029478	-1.867	+	3.646
10564191	3.7341	5.600611	Snord116	chr7	-	67026875	67026968	-1.867	+	3.646
10564189	3.7341	5.600611	Snord116	chr7	-	67024345	67024438	-1.867	+	3.646
10564187	3.7341	5.600611	Snord116	chr7	-	67021819	67021912	-1.867	+	3.646
10564185	3.7341	5.600611	Snord116	chr7	-	67019266	67019359	-1.867	+	3.646
10564181	3.7341	5.600611	Snord116	chr7	-	67014216	67014309	-1.867	+	3.646
10564179	3.7341	5.600611	Snord116	chr7	-	67011674	67011767	-1.867	+	3.646
10564175	3.7341	5.600611	Snord116	chr7	-	67006617	67006710	-1.867	+	3.646
10564173	3.7341	5.600611	Snord116	chr7	-	67004100	67004193	-1.867	+	3.646
10564171	3.7341	5.600611	Snord116	chr7	-	66951114	66951207	-1.867	+	3.646
10564167	3.7341	5.600611	Snord116	chr7	-	66938956	66939049	-1.867	+	3.646
10564163	3.7341	5.600611	Snord116	chr7	-	66933879	66933972	-1.867	+	3.646
10564161	3.7341	5.600611	Snord116	chr7	-	66931358	66931451	-1.867	+	3.646
10564183	3.830935	5.718995	Snord116	chr7	-	67016750	67016843	-1.888	+	3.701
10607486	7.461979	9.378599	Ptchd1	chrX	-	152008084	152057868	-1.917	+	3.775
10532784	5.490762	7.409569	Svop	chr5	-	114476919	114541389	-1.919	+	3.781
10490913	8.773073	10.70783	Car3	chr3	+	14863509	14872532	-1.935	+	3.823
10522208	6.31834	8.2936	Uchl1	chr5	+	67067480	67078473	-1.975	+	3.932
10582899	3.566993	5.545332	---	chr9	+	3025417	3033289	-1.978	+	3.940
10523977	5.871083	7.859464	Gm10419	chr5	+	108801991	108802245	-1.988	+	3.968
10363070	5.425472	7.41727	Gp49a	chr10	+	51200464	51206115	-1.992	+	3.977
10564159	3.745838	5.804091	Snord116	chr7	-	66928831	66928924	-2.058	+	4.165
10393662	8.680485	10.74622	Nptx1	chr11	-	119400686	119409139	-2.066	+	4.186
10427075	6.186533	8.263538	Krt18	chr15	+	101858656	101862452	-2.077	+	4.219
10362418	2.624788	4.707305	Trdn	chr10	+	32977893	32977946	-2.083	+	4.235
10598079	3.350952	5.501249	---	chrM	-	5192	5257	-2.150	+	4.439
10603182	5.006048	7.181795	Arhgap6	chrX	+	165233031	165742757	-2.176	+	4.518
10429564	6.549048	8.73065	Ly6a	chr15	-	74825307	74828334	-2.182	+	4.537
10368175	5.569779	7.774895	Pde7b	chr10	-	20117810	20444884	-2.205	+	4.611
10481272	6.745091	8.952412	1700007K13Rik	chr2	-	28317521	28321852	-2.207	+	4.618
10475517	5.248662	7.458022	AA467197	chr2	+	122463623	122466823	-2.209	+	4.625
10477986	7.147294	9.396242	Nnat	chr2	+	157385846	157388253	-2.249	+	4.753

Probe Set ID	Affy#4957	Affy#4958	Gene Symbol	Ch	Str	Start	Stop	Difference	Fold	Change
10587799	3.252012	5.506307	Plscr2	chr9	+	92170558	92192573	-2.254	+	4.771
10362422	5.643956	7.928473	Trdn	chr10	+	33041111	33041140	-2.285	+	4.872
10598081	6.060302	8.363274	---	chrM	-	5260	5326	-2.303	+	4.935
10607484	3.55119	6.014849	Ptchd1	chrX	-	152006450	152006623	-2.464	+	5.516
10362424	3.004738	5.468565	Trdn	chr10	+	33052242	33052271	-2.464	+	5.517
10407435	3.710092	6.204081	Akr1c18	chr13	-	4131861	4149877	-2.494	+	5.633
10485357	8.956623	11.45296	---	chr2	-	98506704	98507458	-2.496	+	5.643
10362896	7.972126	10.4983	Cd24a	chr10	+	43298975	43304073	-2.526	+	5.760
10492798	6.411643	8.95393	Sfrp2	chr3	+	83570243	83578608	-2.542	+	5.825
10398354	5.585559	8.18994	---	chr12	+	110869284	110869358	-2.604	+	6.081
10398319	6.699174	9.369679	Dlk1	chr12	+	110691433	110698901	-2.671	+	6.367
10598077	4.667285	7.355573	---	chrM	-	5089	5159	-2.688	+	6.445
10582896	3.215914	6.046844	---	chr9	+	3023547	3025218	-2.831	+	7.115
10490818	5.017569	7.892159	Stmn2	chr3	+	8509527	8561606	-2.875	+	7.334
10365482	5.602189	8.591475	Timp3	chr10	+	85763282	85812253	-2.989	+	7.941
10354374	5.840495	8.868592	Slc40a1	chr1	-	45964929	45982408	-3.028	+	8.157
10582916	3.041129	6.114406	---	chr9	+	3034599	3035805	-3.073	+	8.417
10582888	4.199297	7.488643	---	chr9	+	3013140	3014344	-3.289	+	9.777
10598075	4.413004	7.835132	---	chrM	-	5018	5086	-3.422	+	10.719

Appendix B

Contribution of co-authors. Gregory C. Addicks built the constructs for Figure 2f, and performed the experiments for Figure 2g and 2h.

nature cell biology

Pax7 activates myogenic genes by recruitment of a histone methyltransferase complex

Iain W. McKinnell[1,4], Jeff Ishibashi[1,4], Fabien Le Grand[1], Vincent G. J. Punch[1], Gregory C. Addicks[1], Jack F. Greenblatt[2], F. Jeffrey Dilworth[1] and Michael A. Rudnicki[1,3]

Satellite cells purified from adult skeletal muscle can participate extensively in muscle regeneration and can also re-populate the satellite cell pool, suggesting that they have direct therapeutic potential for treating degenerative muscle diseases[1,2]. The paired-box transcription factor Pax7 is required for satellite cells to generate committed myogenic progenitors[3]. In this study we undertook a multi-level approach to define the role of Pax7 in satellite cell function. Using comparative microarray analysis, we identified several novel and strongly regulated targets; in particular, we identified *Myf5* as a gene whose expression was regulated by Pax7. Using siRNA, fluorescence-activated cell sorting (FACS) and chromatin immunoprecipitation (ChIP) studies we confirmed that *Myf5* is directly regulated by Pax7 in myoblasts derived from satellite cells. Tandem affinity purification (TAP) and mass spectrometry were used to purify Pax7 together with its co-factors. This revealed that Pax7 associates with the Wdr5–Ash2L–MLL2 histone methyltransferase (HMT) complex that directs methylation of histone H3 lysine 4 (H3K4, refs 4–10). Binding of the Pax7–HMT complex to Myf5 resulted in H3K4 tri-methylation of surrounding chromatin. Thus, Pax7 induces chromatin modifications that stimulate transcriptional activation of target genes to regulate entry into the myogenic developmental programme.

Satellite cells arise from a population of muscle progenitor cells that originate in the central domain of the dermomyotome. These progenitors express the paired-box transcription factors Pax3 and Pax7 (refs 11, 12), and although neither their emergence nor their maintenance requires Pax3 function[13], recent studies have demonstrated that Pax7 is uniquely indispensable for these cells[14]. In the absence of Pax7, satellite cells die and thus fail to re-populate their niche[11,14,15]. Pax7, is therefore essential for the formation and maintenance of a population of functional satellite cells. Analysis of the physiological functions of Pax7 has been hindered by relatively weak *trans*-activation properties resulting from *cis*-repression[16]. Consequently, the mechanisms by which Pax7 activates downstream target genes remain unclear. To address this problem, we used a comparative microarray approach to globally identify Pax7 myogenic targets and we propose that the regulation of those genes by Pax7 is intimately related to the protein complexes with which it interacts.

Pools of C2C12 myoblasts were infected with retrovirus expressing either mouse Pax7–FLAG, or a control virus expressing only the puromycin resistance gene (Puro). As expected, persistent Pax7 expression resulted in the maintenance of a proliferative phenotype and inhibition of differentiation[17] (Supplementary Information, Fig. S1). Total RNA was harvested to generate probes for hybridization to Affymetrix GeneChip microarrays; 43 genes were up-regulated by Pax7–FLAG, including several that exhibited striking changes in expression (Table 1). Real-time PCR analysis confirmed that the candidate transcripts were increased in response to Pax7 (Fig. 1a). Pax7 and Pax3 are very closely related proteins; however, Pax7 and Pax3 differed significantly in their abilities to regulate the target genes that were identified. When expressed in C2C12 myoblasts, the levels of each target were substantially increased by Pax7–FLAG whereas Pax3–FLAG had either no effect (*PlagL1*; *Syne2*) or only modest effects (*Cipar1*; *Lix1*; *Mest*; *Trim54*) (Fig. 1a). To further assess the specificity and responsiveness of these genes, 10T1/2 fibroblast cells were transfected with Pax7–FLAG, Pax3–FLAG or Puro control Despite the non-muscle environment of these cells, the levels of all the candidate genes tested, with the exception of *Mest*, were increased by Pax7 and they were more responsive to Pax7 than to Pax3 (Fig. 1b), confirming the observations made in C2C12 myoblasts. This is consistent with the phenotypic observations that Pax7 and Pax3 have divergent, non-redundant functions during both embryonic[14] and post-natal[15] myogenesis.

The most significant target identified in our microarray study was the gene for the myogenic regulatory factor Myf5, one of two well-established primary master regulators of skeletal muscle commitment (Myf5) and differentiation (MyoD) in satellite cells[1,18,19]. This suggests a direct link between Pax7 and myogenic commitment of adult myoblasts. *Myf5* expression was increased by Pax7–FLAG, as shown by microarray analysis (2.2-fold; Table 1) and real-time PCR (~3-fold; data not

[1]Sprott Centre for Stem Cell Research, Ottawa Health Research Institute, 501 Smyth Road, Ottawa, Ontario, Canada K1H 8L6 and Department of Medicine, University of Ottawa, 501 Smyth Road, Ottawa, Ontario, Canada K1H 8L6. [2]Banting and Best Department of Medical Research, University of Toronto, 112 College Street, Ontario, Canada M5G 1L6.
[3]Correspondence should be addressed to M.A.R. (e-mail: mrudnicki@ohri.ca). [4]These authors contributed equally to this work.

Received 4 June 2007; accepted 5 November 2007; published online 9 December 2007; DOI: 10.1038/ncb1671

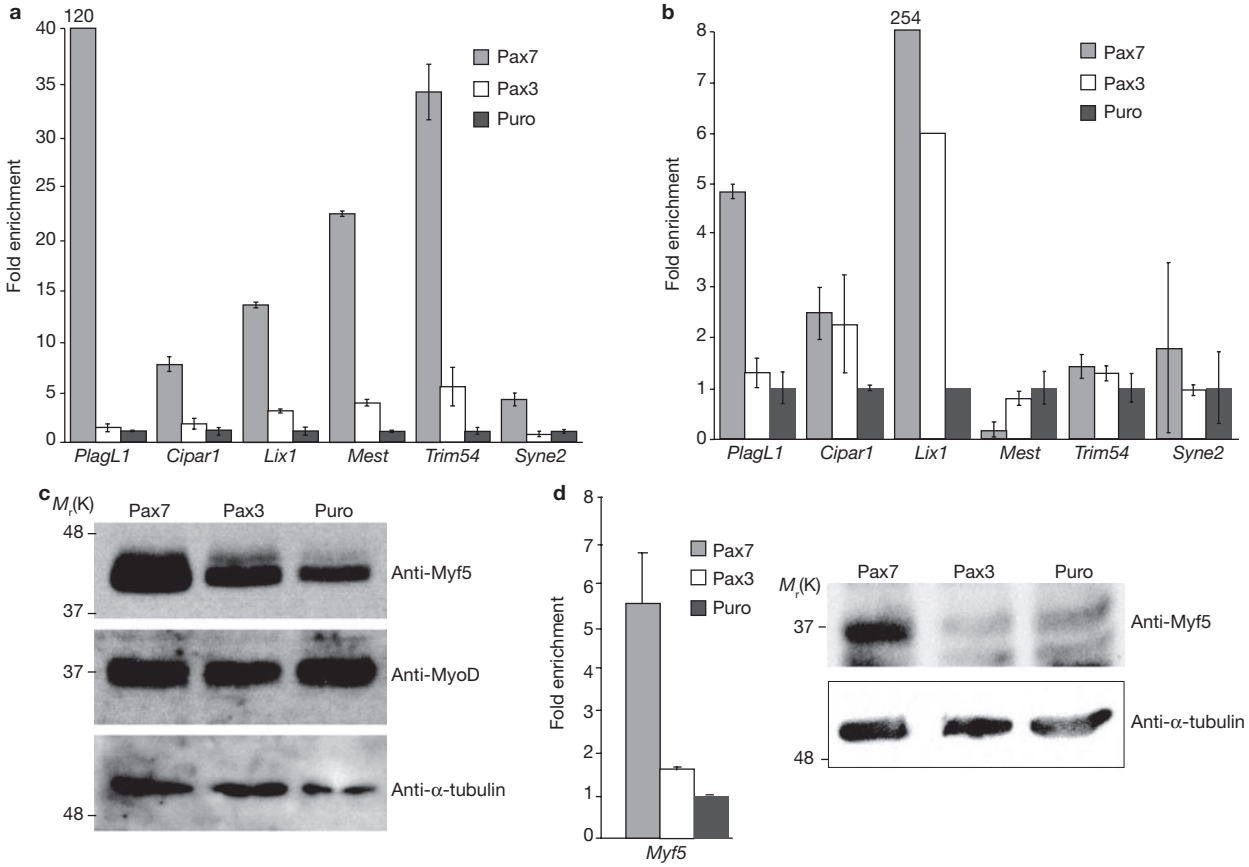

Figure 1 Candidate target genes are specifically activated by Pax7 in C2C12 myoblasts and are only weakly responsive to Pax3. (**a**) Pax7 strongly activated *PlagL1*, *Cipar1*, *Lix1*, *Mest* and *Trim54* in C2C12 myoblasts whereas Pax3 was far less effective. *Syne2* was only weakly increased by Pax7. Expression was normalized to *GAPDH* transcript levels and is shown relative to the empty-vector (Puro) controls. (**b**) *PlagL1*, and particularly *Lix1*, were both strongly induced by Pax7 in non-muscle 10T1/2 fibroblasts but were weakly induced or unresponsive to Pax3. *Cipar, Trim54* and *Syne2* transcripts are also increased by Pax7 in 10T1/2 cells. (**c**) Myf5 protein levels were also increased by Pax7–FLAG and Pax3–FLAG expression in C2C12 myoblasts whereas MyoD protein levels remained unaffected; α-tubulin was included as a control. (**d**) Real-time PCR and western blot analysis demonstrated that Myf5 RNA and protein, respectively, were increased in 10T1/2 cells expressing Pax7-FLAG (error bars are s.e.m.). Full-length scans of western blot data can be found in Supplementary Information, Fig. S4.

shown). Importantly, changes in Myf5 protein levels were consistent with the observed increases in mRNA levels. Expression of Pax7–FLAG in C2C12 cells resulted in a dramatic increase in Myf5 protein compared with the Puro control (Fig. 1c). An exaggerated change in Myf5 protein versus mRNA levels has been reported previously in *MyoD*$^{-/-}$ myoblasts[20]. As shown for previously described targets, Pax3-induced levels of Myf5 protein were substantially lower than those induced by Pax7 in C2C12 myoblasts; in contrast, *MyoD* levels were unaffected by Pax3 or Pax7 (Fig. 1c). 10T1/2 fibroblasts are capable of myogenic differentiation in the presence of exogenous Myf5 or MyoD. Remarkably, Pax7 expression in 10T1/2 cells resulted in the induction of Myf5 at both RNA and protein levels (Fig. 1d), whereas Pax3 produced no detectable change. This indicates that Pax7 readily stimulates Myf5 transcription in both muscle and non-muscle cell lines and provides a molecular connection between Pax7 and myogenic commitment.

To test our hypothesis that Pax7 activates target genes by recruiting regulatory complexes to these loci, proteins interacting with Pax7 were purified using a 6x-histidine–TEV (tobacco etch virus) cleavage–3xFLAG tandem affinity purification (TAP) tag fused to the carboxy (C)-terminus of full-length mouse Pax7 (Fig. 2a). This construct (Pax7–CTAP), or the tag alone (HisFLAG–tag) control, was expressed in C2C12 myoblasts. The Pax7–CTAP protein migrated at the predicted size; showed no sign of degradation; was amenable to cleavage by TEV protease and was detected by western-blot analysis of the final eluate (Fig. 2b).

We performed large-scale TAPs to identify interacting proteins via MALDI–TOF (matrix-assisted laser desorption ionisation-time of flight) mass spectrometry of silver-stained SDS–PAGE bands (Fig. 2c). A complex mixture of largely uncharacterized, interacting proteins was identified, together with the target protein Pax7. Of particular interest, one of the Pax7-associated proteins identified was the WD40-domain-containing protein Wdr5. The observation that Pax7 was co-isolated with Wdr5 is intriguing given that Wdr5, the trithorax-group protein Ash2L, and RbBP5 are the three common components of histone methyltransferase (HMT) complexes that methylate histone H3 at lysine 4 (H3K4, refs 4–10, 21). Extensive biochemical and structural studies have revealed that Wdr5 is a crucial component of HMT complexes because it associates directly with the amino acid tail of histone H3 (refs 4, 22–25), whereas Ash2L, RbBP5 and Wdr5 together create the core structural platform for subsequent protein complex assembly[4]. This suggests that Pax7 interacts with a core component of the complex, namely Wdr5, to recruit HMT complexes to target promoters for inscription of epigenetic modifications.

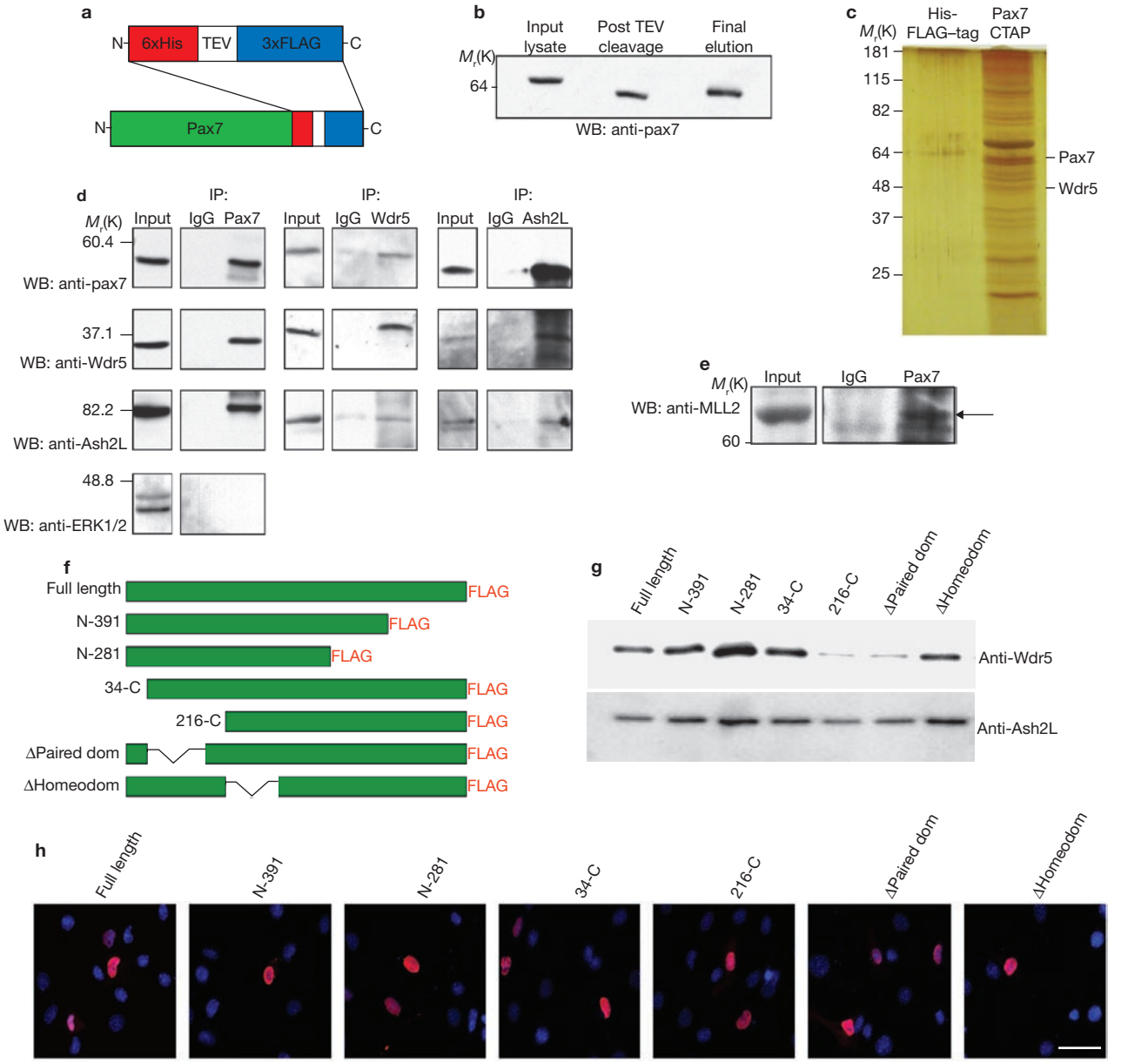

Figure 2 Identification of Pax7-interacting co-factors. (**a**) A TAP tag, consisting of six histidine and three FLAG epitopes, separated by a TEV cleavage site, was fused to the C-terminus of Pax7 to create a Pax7–CTAP (His–TEV–FLAG) construct. A construct expressing only the tag (referred to as HisFLAG-tag) was used as a negative control. (**b**) High yield purification of the Pax7–CTAP protein as shown by detection of the fusion protein in the initial cell lysate, in the eluate following TEV cleavage, and in the final elution from Ni^{+}-resin. (**c**) TAP of Pax7–CTAP- compared with HisFLAG-tag-associated proteins from C2C12 cells. Protein matches were generated from multiple data sets and were identified following MALDI–TOF (analysed via Mascot). Pax7–CTAP-interacting proteins were compared with those identified in HisFLAG-tag purifications to unequivocally identify those that were Pax7-specific (versus those that represented contaminants). (**d**) Pax7 co-immunoprecipitated with Wdr5 and Ash2L, two conserved units of a HMT complex. As a negative control, the Pax7-immunoprecipitate was also probed with an antibody to a non-native-Pax7 interacting nuclear protein, ERK1/2. (**e**) Co-purification of Pax7 and MLL2 immunoprecipitated from primary myoblast nuclear extract. (**f**) Pax7-deletion constructs used to map Pax7 binding to the HMT complex. (**g**) Loss of the paired domain was observed to almost entirely abolish binding between Pax7 and Wdr5. (**h**) Pax7–FLAG truncations where observed to localize to the nucleus (DAPI-blue, Pax7–FLAG deletion constructs-red, scale bar = 20 μm). Full length scans of western blot data can be found in Supplementary Information, Fig. S4.

We used nuclear extracts from satellite cell-derived primary myoblasts to validate the Wdr5 interaction in an endogenous setting and to determine whether native Pax7 associates with the other core components of HMT complexes. Using antibodies to the endogenous Pax7, Wdr5 and Ash2L proteins, reciprocal co-immunoprecipitation analysis revealed that antibodies reactive with Pax7 specifically co-precipitated Wdr5 and Ash2L (versus IgG controls). In addition, antibodies reactive with Wdr5 co-precipitated Pax7 and Ash2L, and antibodies reactive with Ash2L co-precipitated Pax7 and Wdr5 (Fig. 2d). These results support the assertion that the three proteins are found in the same complex. We also performed control western blots with α-Erk1/2, a nuclear protein present in abundance in many protein complexes. The failure to detect Erk1/2 in Pax7-immunoprecipitates demonstrated the specificity of the observed interactions. Together, these data confirm that in primary myoblasts Wdr5

Table 1 Pax7-induced increases in expression in C2C12 myoblasts

Symbol	GID	Fold	Name	RLT-PCR
Plagl1	**NM_009538**	**385.0**	**[1]Pleiomorphic adenoma gene-like 1**	**135.8**
Lix1	**NM_025681**	**12.3**	**Limb expression 1 homolog (chicken)**	**34.8**
Syne2	**BF582734**	**11.3**	**Synaptic nuclear envelope 2**	**2.2**
Cipar1	**AK008716**	**8.1**	**Castration-induced prostatic apoptosis-related 1**	**166.6**
Trim54	**NM_021447**	**7.2**	**Tripartite motif-containing 54**	**4.1**
Il13ra1	NM_133990	5.4	[2]Interleukin 13 receptor, alpha 1	–
Mest	**NM_008590**	**5.0**	**Mesoderm specific transcript**	**17.9**
Peg3	NM_008817	4.6	[2]Paternally expressed 3	–
3110001A13Rik	NM_025626	4.6	[3]RIKEN cDNA 3110001A13 gene	–
Ahr	NM_013464	4.4	Aryl-hydrocarbon receptor	–
Npnt	NM_033525	4.1	[2]Nephronectin	–
Ltb4dh	NM_025968	4.1	Leukotriene B4 12-hydroxydehydrogenase	–
Msln	NM_018857	4.1	mesothelin	–
C1qtnf3	NM_030888	3.8	C1q and tumour necrosis factor related protein 3	–
–	BB369191	3.7	Sim. to mouse pentylenetetrazol-related mRNA	–
Pparg	NM_011146	3.4	Peroxisome proliferator activated receptor gamma	–
Cd24a	NM_009846	3.1	[2]CD24a antigen	–
Pkia	NM_008862	3.0	[2]Protein kinase inhibitor, alpha	–
Nqo1	NM_008706	2.9	NAD(P)H dehydrogenase, quinone 1	–
Marcks	NM_008538	2.6	[3]Myristoylated alanine-rich protein kinase C substrate	–
Gch1	NM_008102	2.6	GTP cyclohydrolase 1	–
Cdh11	NM_009866	2.6	Cadherin 11	–
Myo1d	NM_177390	2.5	Myosin ID	–
Cxcr4	NM_009911	2.5	Chemokine (C-X-C motif) receptor 4	–
Crlf1	NM_018827	2.5	Cytokine receptor-like factor 1	–
Sema3e	NM_011348	2.4	Semaphorin 3E	–
Mdfic	NM_175088	2.4	MyoD family inhibitor domain-containing	–
Ass1	NM_007494	2.4	Argininosuccinate synthetase 1	–
Id3	NM_008321	2.4	Inhibitor of DNA binding 3	–
Ppap2a2	NM_008903	2.3	[2]Phosphatidic acid phosphatase 2a isoform 2	–
Myf5	**NM_008656**	**2.2**	**Myogenic factor 5**	**3.0**
Cdh2	NM_007664	2.2	Cadherin 2 (N-cadherin)	–
Depdc6	NM_145470	2.2	DEP domain containing 6	–
Prss23	NM_029614	2.2	[2]Protease, serine, 23	–
Id2	NM_010496	2.1	Inhibitor of DNA binding 2	–
Emb	NM_010330	2.1	Embigin	–
Rnf128	NM_023270	2.1	[2]Ring finger protein 128	–
Rnh1	NM_145135	2.1	Ribonuclease/angiogenin inhibitor 1	–
Olfm1	NM_019498	2.1	Olfactomedin 1	–
–	BG069607	2.1	–	–
Tob1	NM_009427	2.1	Transducer of ErbB-2.1	–
Atp11a	NM_015804	2.1	ATPase, class VI, type 11A	–
2210409B22Rik	BM207133	2.0	RIKEN cDNA 2210409B22 gene	–

Pax7–FLAG samples were stringently compared with Puro samples to derive sets of candidate Pax7-regulated genes. *PlagL1* was not detected in Puro samples but was highly expressed in Pax7–FLAG samples. Others that were also considerably increased included *Lix1* (12-fold); *Syne2* (11-fold); *Cipar1* (8-fold); *Trim54* (7-fold); and *Mest* (5-fold).
[1]Signal was very low and called Absent in control. [2]Mean fold change for two distinct probesets directed at the same transcript. [3]Mean fold change for 3 distinct probesets directed at the same transcript. Bold lines indicate those used for real-time PCR validation

and Ash2L interact with Pax7, and support an association of Pax7 with a HMT complex. To identify the methyltransferase responsible for this activity, we performed co-immunoprecipitation with Pax7 and probed for the members of the mixed-lineage leukaemia (MLL) family of HMTs. The MLL proteins are obvious candidates for this activity because of their known association with the Wdr5–Ash2L–RbBP5 core complex[21]. Indeed, Pax7 interacted with MLL2 (Fig. 2e) but not MLL1 (data not shown), indicating that MLL2 is a specific HMT recruited to this complex.

To further investigate these interactions we produced Pax7–FLAG constructs that contained amino (N)- and C-termini truncations, and specific deletions of the Pax7 paired-domain or homeodomain (Fig. 2f). Deletion of the paired-domain of Pax7, whether following truncation of a significant portion of the N-terminus or a more subtle deletion of only the paired-domain, resulted in near complete abolition of Wdr5 binding to Pax7 (a moderate decrease in binding was observed with Ash2L). In contrast, the effect of deleting the homeodomain appeared to be negligible (Fig. 2g). To ensure that these effects did not result from a failure of the constructs to enter the correct cellular compartment, we performed immunocytochemistry and noted that all of the Pax7–FLAG deletion constructs were localized to the nucleus (Fig. 2h). Given that the paired-domain is involved in the DNA-binding activity of Pax7, this result suggests that DNA binding may be required for the Pax7–HMT complex to form and/or remain bound.

To directly confirm that the Pax7–Wdr5–Ash2L–MLL2 complex possesses methyltransferase activity, we incubated Pax7 immunocomplexes (from primary myoblast nuclear extracts) with core histones in the presence of the tritiated methyl-donor S-adenosyl-methionine (SAM). Histones incubated with the Pax7–immunoprecipitated complex showed an elevated level of tritium incorporation (>1,000 c.p.m.) compared with the IgG control, demonstrating that the Pax7–immunocomplex indeed possesses HMT activity. Histones incubated with immunoprecipitates from primary myotubes (which do not express Pax7) showed no incorporation of SAM above baseline levels of activity (a representative experiment is shown in Fig. 3a).

Modifications of the histone tail significantly influence the nature of gene expression[26]. Methylation of H3K4 marks chromatin in a conformation permissive for transcription, while trimethylated H3K4 is restricted to the 5′ promoter and coding regions and is considered to be a definitive marker of active genes[27–30]. To test the prediction that the Pax7-Wdr5–Ash2L–MLL2 complex specifically directs methylation of H3K4, we repeated the previous experiment and performed SDS–PAGE on the samples. Coomassie staining and fluorography indicated that methyltransferase activity is indeed directed against H3 (Fig. 3b). Using H3K4 modification-specific antibodies, we observed that the Pax7 complex mediated trimethylation and (to a markedly lesser extent) dimethylation of H3K4 (Fig. 3c). These modifications are indicative of active or transcriptionally permissive chromatin[27]. In contrast, western blots with antibodies specific for dimethylated H3K9 (a marker of repressed chromatin[31]) showed no increases over background levels in the presence of the Pax7 complex (data not shown).

These data demonstrate that Pax7 recruits a protein complex capable of methylating H3K4. As such, we predicted that Pax7 physically associates with sites of open chromatin that are methylated on H3K4. To test this, we performed immunoprecipitations using methylation-specific antibodies and probed western blots for the presence of Pax7. Pax7 was observed to associate strongly with regions of dimethylated H3K4, and, to a lesser extent, with trimethylated H3K4 (Fig. 3d). No association of Pax7 with dimethylated H3K9 was observed (Fig. 3d).

Intriguingly, certain structural data show that Wdr5 binds directly to the H3 tail with an affinity not affected by the state of lysine-4 methylation[22,23], although other data indicate a preference for dimethylated H3K4[24,25]. In neither case is the question addressed of how the HMT complex is recruited to specific target genes. This function must be conferred by the unique component(s) of the overall complex, such as a site-specific transcriptional activator, rather than any of the three core elements[21,22,25]. Our data indicate that Pax7 provides the missing selective

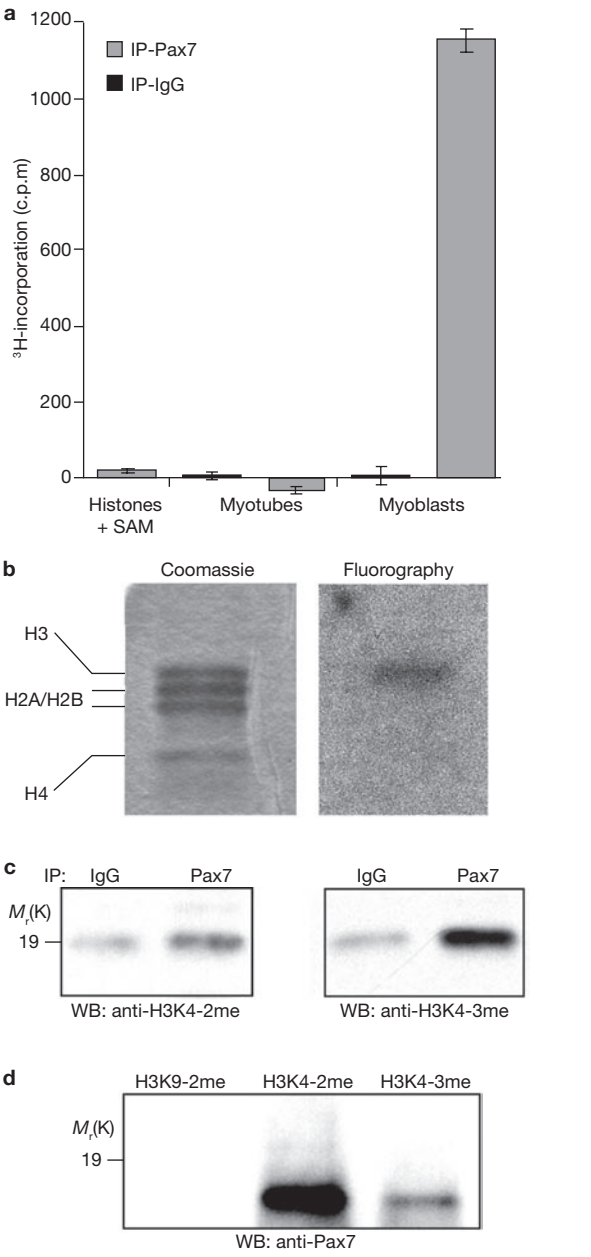

Figure 3 Pax7 immunocomplex has HMT activity and associates with sites of H3K4 methylation. (**a**) Pax7 or IgG immunoprecipitates from differentiated myotubes (Pax7 negative) or primary myoblasts were incubated with core histones and ^{3}H-SAM. Pax7 immunocomplexes from primary myoblasts were consistently observed to induce a markedly higher level of histone methylation than IgG controls (error bars represent s.e.m.). (**b**) Fluorography of histones incubated with Pax7 immunocomplexes from primary myoblasts indicated that the methyltransferase activity associated with the Pax7 immunocomplex were directed at histone H3. (**c**) Western blot analysis with antisera directed against dimethylated H3K4 (H3K42me) and trimethylated H3K4 (H3K43me) indicate that histones incubated with the Pax7 immunocomplexes show a markedly increased level of H3K43me, with a concurrent but lesser increase in H3K42me. (**d**) IP-western blot analysis revealed that Pax7 was highly associated with chromatin isolated from primary myoblasts using antisera reactive with H3K42me and H3K43me, but not at all with chromatin isolated with antisera reactive with dimethylated H3K9. Full-length scans of western blot data can be found in Supplementary Information, Fig. S4.

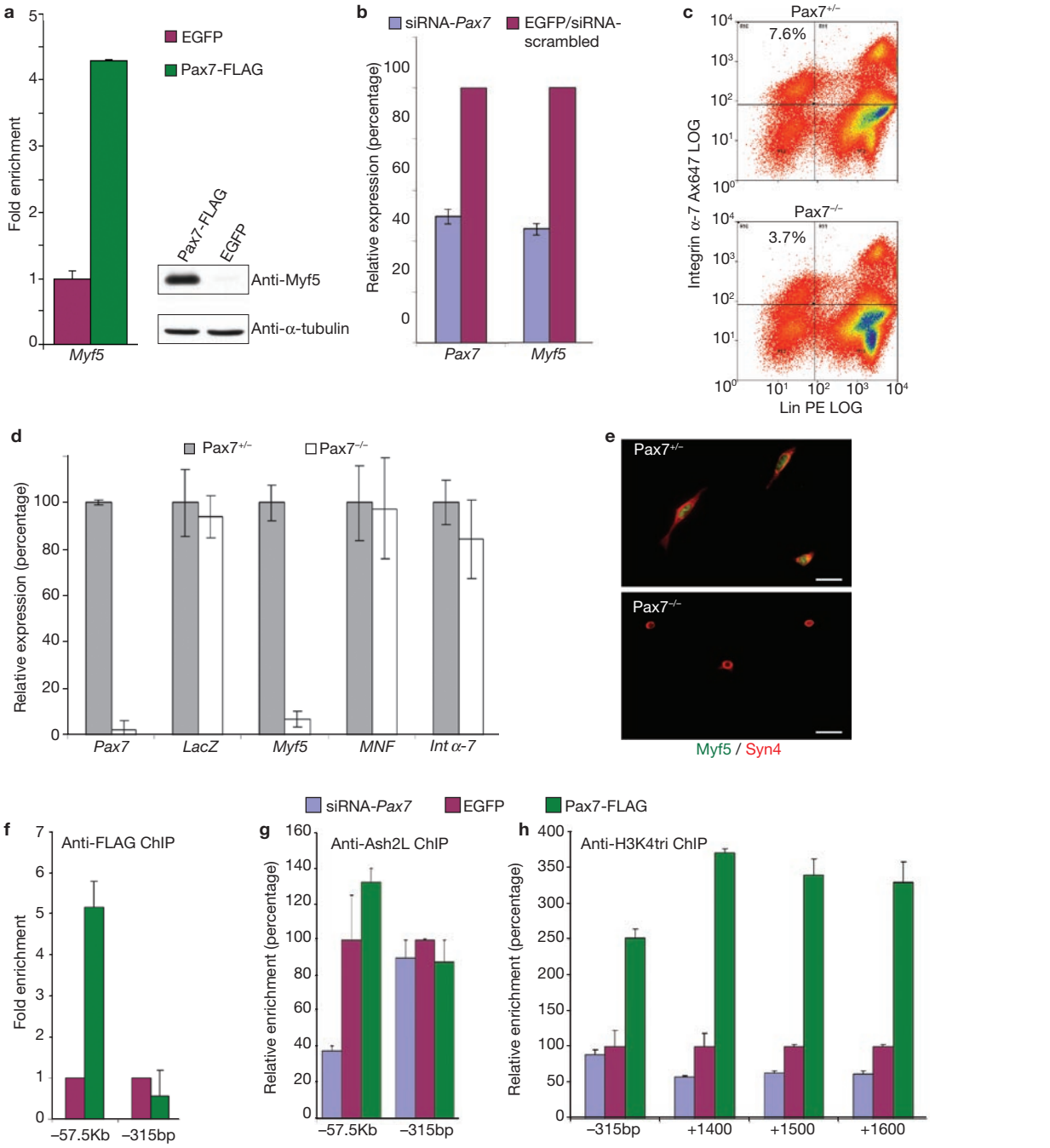

Figure 4 Pax7 regulates *Myf5* expression directly in satellite cell-derived myoblasts. (**a**) Over-expression of Pax7 resulted in elevated levels of *Myf5* RNA and protein. (**b**) siRNA knockdown of *Pax7* in satellite cell-derived myoblasts results in concurrent knockdown of *Myf5* expression. (**c**) FACS sorted satellite cells (Integrin α-7+; Lin: CD31–, CD45–, CD11–, Sca1–) from Pax7$^{-/-}$ mice show complete absence of Myf5 expression via both (**d**) RNA (n = 3 animals per group, P =: 2.9 x 10^{-5} for Pax7 and 1.7 x 10^{-5}, for Myf5), and (**e**) immunofluorescence (sorted cells were cultured for 16 h before being fixed and stained for Myf5–Syndecan4, Syndecan4-red, (Syn4) Myf5-green (Myf5), scale bar = 20 μm). Expression of *LacZ* was assayed as the *Pax7* knockout was created via the insertion of a *LacZ* sequence into the Pax7 locus and as such all satellite cells should be expressing LacZ in place of Pax7. (**f**, **g**) ChIP demonstrated that Pax7 was bound directly to the –57.5 kb region of Myf5 in complex with Ash2L (**f**) and in a site-specific manner (**g**). The downstream –315 bp loci, which does not contain a binding site and hence did not show any enrichment, is shown for comparison purposes. (**h**) Antisera directed against H3K4 trimethylation ChIP demonstrated that, accordingly, the coding region of *Myf5* showed a marked increase in activation as measured by trimethylation of H3K4 (error bars are s.e.m.). Full-length scans of western blot data can be found in Supplementary Information, Fig. S4.

function that targets HMT complexes to specific genes while remaining consistent with either model of Wdr5 function.

To directly examine the effect of Pax7 on myogenic commitment, we focused on the Pax7 regulation of *Myf5* in satellite cells. We proposed that *Myf5* would be regulated by Pax7 in satellite cells, would be bound by Pax7 and HMT–complex proteins and would exhibit an altered methylation status. Expression of Pax7–FLAG in satellite cell-derived myoblasts produced a large increase in *Myf5* RNA expression, with an exaggerated change at the

protein level (Fig. 4a), consistent with our observations in C2C12 myoblasts and those of other groups[20]. Accordingly, when we knocked down *Pax7* expression by 50% using siRNA, *Myf5* expression was reduced to approximately 40% of that observed in the scrambled siRNA control cells (Fig. 4b), demonstrating that *Myf5* expression is responsive to Pax7 in satellite cell-derived myoblasts. To test this *in vivo,* we sorted satellite cells from *Pax7*-null mice. These mice possess reduced numbers of satellite cells (3.7% –/– versus 7.6% +/– Fig. 4c), and were previously shown to have a severely impaired ability to regenerate damaged muscle and maintain viable satellite cell populations[3,11–13,15]. However, we were able to obtain sufficient numbers of satellite cells from four-week old pups to examine the expression level of *Myf5*. Initially we examined the levels of *LacZ*, and two key markers of satellite cells, myocyte nuclear factor and integrin-α7. Expression was equivalent between the heterozygous and homozygous-null populations of cells, indicating that we were indeed sorting satellite cells from the mutant. Strikingly, *Myf5* was absent from *Pax7*-null satellite cells (Fig. 4d). Immunocytochemistry of the sorted cells revealed that the $Pax7^{-/-}$ cells maintained a rounded, non-activated, non-myogenic phenotype (Fig. 4e). Thus, Pax7 is required for the expression of *Myf5* and the commitment of satellite cells to the myogenic lineage.

A Pax3-paired-domain binding site (~57.5 kb upstream of the transcriptional start) that activates the *Myf5* gene in primary myoblasts was recently defined[32,33]. Chromatin immunoprecipitations (performed from Pax7–FLAG and EGFP control satellite cell-derived myoblasts using α-FLAG) revealed that this site is bound by Pax7 (Fig. 4f). To test our model of Pax7 recruiting a HMT complex, we performed ChIP using anti-Ash2L antibodies from three satellite cell-derived myoblast populations: Pax7–FLAG, EGFP control, and siRNA–*Pax7* knockdown cells. This revealed that, in the presence of high Pax7 (Pax7–FLAG), Ash2L levels on the –57.7 Myf5 promoter were increased by more than 125% compared with controls (EGFP); however, reduced Pax7 levels in myoblasts (siRNA–*Pax7*) decreased Ash2L binding to this region to 40% of that seen in the controls (Fig. 4g), demonstrating a Pax7-dependent recruitment of the HMT complex to this region.

In keeping with the hypothesis that the recruitment of this complex results in downstream trimethylation of the coding region and gene activation, we performed ChIP experiments using an anti-H3K4 trimethylation antibody. Accordingly, and despite the fact that Myf5 is already activated in myoblasts, H3K4 trimethylation in the immediate 5′ and coding regions of *Myf5* in myoblasts with ectopic Pax7 expression (Pax7–FLAG) was increased by 250–300% above that seen in EGFP cells, consistent with a propagation of the methylation signal by the HMT complex downstream from the Pax7 binding site. Significantly, in myoblasts where Pax7 expression (and Myf5, Fig. 4b) was reduced (siRNA–*Pax7*), the level of H3K4 trimethylation was markedly diminished (Fig. 4h).

Taken together, our data support a model whereby specific binding of Pax7 to dimethylated-H3K4 regulatory elements in target genes leads to the recruitment of HMT core complexes, strong H3K4 trimethylation around their transcription start site, and ensuing activation of gene expression. This is consistent with structural data showing an interaction between the Wdr5–Ash2L core complex and histone H3 (refs 21–25), and answers the question of how this generic complex is recruited to specific genes. It also corroborates other genomic data[27–29] indicating that recruitment of this complex and subsequent trimethylation of the 5′ promoter and coding regions result in target gene activation. Finally, it defines a specific role and molecular mechanism for Pax7 in myogenic stem cells[1–3,11–16] in regulating *Myf5* and other target genes. Together, these experiments indicate that Pax7 enforces satellite cell commitment by recruiting a HMT complex to *Myf5*, resulting in transcriptional activation. Notably, Pax-family genes are essential for the embryonic specification of diverse tissues; thus, Pax recruitment of HMT complexes could be a conserved mechanism for seeding lineage-specific gene-expression programmes during development. □

METHODS

Generation of cell lines. C2C12 myoblasts and 10T1/2 fibroblasts were cultured in DMEM with 10% fetal calf serum and 1% penicillin/streptomycin. Primary myoblasts were isolated from adult C57BL/6 mice and cultured using two previously described methods[1,20]. Pax7– or Pax3–FLAG were cloned into the pHAN backbone (with puromycin resistance driven from a distinct SV40 promoter). Control virus expressed puromycin-resistance alone. Additionally, full-length mouse Pax7d was fused in-frame to a C-terminal TAP tag and cloned into the pBRIT retroviral plasmid to make pBRIT–Pax7–CTAP (Fig. 2a). A plasmid comprising only the TAP tag was used as a control. Retrovirus was produced by transient co-transfection as described[19]; or using Lipofectamine 2000 (Invitrogen, Burlington, Canada) into Phoenix-Eco cells (a gift from the Nolan lab, Stanford University Medical Center, CA). Viral supernatant containing 8 μg ml^{-1} polybrene was used to infect C2C12 cells. Stable lines were created by antibiotic selection (1.0–1.5 μg ml^{-1} puromycin; Sigma).

Microarray analysis. Triplicate pools of C2C12 cells stably infected with retrovirus expressing Pax7d, or with empty-control retrovirus were produced. Total RNA was purified from cultured cells using the RNeasy Mini kit (Qiagen, Mississauga, Canada) according to the manufacturer's instructions. Samples were hybridized to MOE430A GeneChips (Affymetrix, Santa Clara, CA) at the Ottawa Genome Centre (Ontario, Canada) and analysed as previously described[19]. Criteria used to derive Tables 1 and S1 included: log-fold change of greater than one (that is, 2-fold cut-off); significant change (Increase or Marginal Increase call); detectable expression above background (non-Absent call) for the higher signal, and consistency between replicate samples. Raw microarray data is available from the Gene Expression Omnibus, National Center for Biotechnology Information (http://www.ncbi.nlm.nih.gov/geo/) under series accession no. GSE3224 (GSM72628, -30, -32, -34...6).

Primers. PCR primers for all RT- and real-time PCR were designed using the online Primer3 software (http://frodo.wi.mit.edu/cgi-bin/primer3/primer3_www.cgi). All primer sequence specifications are provided in Supplementary Information, Table S2.

Real-time RT-PCR. Total RNA was isolated as described for microarray samples and used as a template for first-strand reverse transcription (RT) using the RNA PCR Core kit (Perkin Elmer, Woodbridge, Canada) with random hexamer primers. SYBR Green real-time PCR reactions were performed in duplicate using an MX4000 PCR machine (Stratagene, La Jolla, CA) with fold-change normalized against GAPDH β-Actin, or tubulin. Primer specificity was validated by denaturation curve analysis (55–94 °C) and direct sequencing of the PCR products. Amplification-curve plotting and calculation of cycle threshold (C_t) values were performed using the MX4000 software (v4.20; Stratagene), with further calculations performed using Microsoft Excel. Each experiment was performed independently on at least two occasions.

Tandem affinity purification. Whole cell extracts were prepared from Pax7–CTAP and HisFLAG–tag C2C12 cells, corresponding to approximately 200 × 100 mm plates. Cells were homogenized in 10 mM Tris-Cl pH 7.9, 0.1 M NaCl, 1.5 mM $MgCl_2$, 0.18% NP-40, on ice. One volume of 50 mM Tris-Cl pH 7.9, 0.6 M NaCl, 1.5 mM $MgCl_2$, 25% glycerol was then added, and the mixture was homogenized again before being treated with benzonase nuclease (Novagen, San Diego, CA) for 30 min at 4 °C. The lysate was centrifuged, dialysed against 10 mM Tris-Cl pH 7.9, 0.1 M NaCl, 0.1 mM EDTA, 10% glycerol and cleared by centrifugation. Pax7–CTAP or HisFLAG-tag complexes were immunoprecipitated with M2-agarose (Sigma, St Louis, MO) at 4 °C then eluted with TEV protease (Invitrogen) and FLAG peptide (Sigma) in 20 mM Tris-Cl pH 7.9, 0.1 M NaCl, 0.1 mM EDTA, 0.1% NP40. The eluate was incubated with ProBond resin (Invitrogen) and complexes eluted with 100 mM EDTA, dialysed against 10 mM Tris-Cl pH 7.9, 0.1 M NaCl, 0.1 mM EDTA, 10% glycerol and concentrated on a Centricon column (Amicon, Oakville, Canada).

Mass spectrometry. Samples processed for MALDI-TOF were subjected to SDS–PAGE and silver-stained as described previously[34]. Bands were excised directly from the gel and analysed at the Ottawa Genome Centre. MALDI-MS/MS spectra were acquired using a QSTAR XL tandem mass spectrometer (ABI/Sciex, Concord, Canada) with a MALDI-2 source, α-Cyano-4-hydroxycinnamic acid (Agilent, Palo Alto, CA) matrix and Analyst QS version 1.1, build 9865. Spectra were searched against the NCBI database using Mascot daemon version 2.0.5 on an in-house Mascot server version 2.0.04.

Co-immunoprecipitation analysis. Mouse primary myoblasts were used for immunoprecipitation analysis. For differentiation protocols, cells were maintained for 7 days in DMEM + 2% horse serum. Nuclear extracts were produced as follows: cells were re-suspended in hypotonic lysis buffer (10 mM Hepes pH 7.6, 1.5 mM $MgCl_2$, 10 mM KCl, 0.5 mM DTT and protease inhibitors), lysed using a 27-gauge needle and the nuclei collected by centrifugation. Nuclei were re-suspended in 20 mM Hepes pH 7.6, 1.5 mM $MgCl_2$, 420 mM NaCl, 2 mM DTT, 0.2 mM EDTA, 25% glycerol, plus protease inhibitors, and lysed using a 27-gauge needle. The nuclear suspension was agitated for 60 min at 4 °C, cleared by centrifugation, and adjusted to 20 mM Hepes pH 7.6, 1.5 mM $MgCl_2$, 150 mM NaCl, 2 mM DTT, 0.2 mM EDTA, 20% glycerol, plus protease inhibitors, for subsequent use. Primary antibodies (concentrated α-Pax7 hybridoma supernatant, Developmental Studies Hybridoma Bank, University of Iowa; α-Wdr5, kindly donated by Winship Herr (Université de Lausanne, Switzerland); α-Ash2L, kindly donated by Marjorie Brand (Sprott Centre for Stem Cell Research, Ottawa, Canada); control normal IgG, (Upstate, Lake Placid, NY) were either incubated at a concentration of 1–2 μg 500 μg^{-1} nuclear extract overnight at 4 °C, before being collected with Protein G/A; or alternatively, were cross-linked to Protein G/A via DMP before incubation with nuclear extract. Immuno-complexes were washed and subjected to SDS–PAGE and western blotting with the antibodies listed above and α-Erk1/2 (Chemicon, Temecula, CA).

HMT activity assay. Mouse primary myoblast nuclear extracts were immunoprecipitated with α-Pax7 or control IgG as described above and incubated with 2 μg core histones (Upstate) in the presence of ^{3}H-adenosyl-L-methionine (PerkinElmer), for 60 mins at 30 °C, spotted onto P81 phosphocellulose squares (Upstate), and read in a Beckman LS 6500 scintillation counter. Counts per minute for the α-Pax7 immunoprecipitations were normalized against the background counts observed with the IgG immunoprecipitations. Three independent experiments were performed and each sample was read in triplicate. In complementary experiments the HMT assay samples were subjected to SDS–PAGE and treated in one of two ways: (1) Gels were stained in 0.25% Coomassie Brilliant Blue R250, 50% methanol, 10% acetic acid; de-stained in 50% methanol, 10% acetic acid, amplified with Enlightning (NEN Life Sciences, Boston, MA), dried and exposed for fluorography; (2) Gels were transferred to nitrocellulose membrane and subjected to western blotting with antibodies raised against dimethylated H3K4, trimethylated H3K4 and dimethylated H3K9 (Upstate).

ChIP analysis. Pax7–FLAG, Ash2L and H3K4 trimethyl protein-DNA complexes were crosslinked with 1% formaldehyde and sonicated. Processing of samples was performed according to the ChIP kit manufacturer's protocols (Upstate). DNA was recovered using PCR purification columns (Invitrogen). The immunoprecipitated DNA was subjected to real-time PCR assays with each primer pair, and normalized against primers for GAPDH as a control locus representing a control fragment that was immunoprecipitated non-specifically to produce robust and reproducible results. This strategy is validated by noting that, for example, Pax7–FLAG samples showed little or no enrichment at flanking loci.

Each DNA sample was analysed by real-time PCR in triplicate, in at least two independent experiments. PCR specificity was validated by denaturation curve analysis and direct sequencing of the products.

Additional methods. Information on western blots, Pax-7 domain deletion construction, histone pull-down assays, FACS of satellite cells, siRNA transfection and immunocytochemistry is available in Supplementary Information S5.

ACKNOWLEDGEMENTS

The authors are indebted to Doug Borris and Murray Smith for mass spectrometry analysis; Jeff Baker and Joyce Li for technical assistance; and to Marjorie Brand, Jennifer McCann, Mark Gillespie and Dave Picketts for critical input. This work was supported by grants to M.A.R. from the National Institutes of Health, the HHMI, the Canadian Institutes of Health Research, the Muscular Dystrophy Association and the CRC Program.

Published online at http://www.nature.com/naturecellbiology/
Reprints and permissions information is available online at http://npg.nature.com/reprintsandpermissions/

1. Kuang, S., Kuroda, K., Le Grand, F. & Rudnicki, M. A. Asymmetric self-renewal and commitment of satellite stem cells in muscle. *Cell* **129,** 999–1010 (2007).
2. Montarras, D. *et al.* Direct isolation of satellite cells for skeletal muscle regeneration. *Science* **309,** 2064–2067 (2005).
3. Seale, P. *et al.* Pax7 is required for the specification of myogenic satellite cells. *Cell* **102,** 777–786. (2000).
4. Steward, M. M. *et al.* Molecular regulation of H3K4 trimethylation by ASH2L, a shared subunit of MLL complexes. *Nature Struct. Mol. Biol.* **13,** 852–854 (2006).
5. Wysocka, J., Myers, M. P., Laherty, C. D., Eisenman, R. N. & Herr, W. Human Sin3 deacetylase and trithorax-related Set1/Ash2 histone H3-K4 methyltransferase are tethered together selectively by the cell-proliferation factor HCF-1. *Genes Dev.* **17,** 896–911 (2003).
6. Roguev, A. *et al.* The Saccharomyces cerevisiae Set1 complex includes an Ash2 homologue and methylates histone 3 lysine 4. *Embo J.* **20,** 7137–7148 (2001).
7. Yokoyama, A. *et al.* Leukemia proto-oncoprotein MLL forms a SET1-like histone methyltransferase complex with menin to regulate Hox gene expression. *Mol. Cell. Biol.* **24,** 5639–5649 (2004).
8. Milne, T. A. *et al.* MLL associates specifically with a subset of transcriptionally active target genes. *Proc. Natl Acad. Sci. USA* **102,** 14765–14770 (2005).
9. Milne, T. A. *et al.* Menin and MLL cooperatively regulate expression of cyclin-dependent kinase inhibitors. *Proc. Natl Acad. Sci. USA* **102,** 749–754 (2005).
10. Hughes, C. M. *et al.* Menin associates with a trithorax family histone methyltransferase complex and with the hoxc8 locus. *Mol. Cell* **13,** 587–597 (2004).
11. Relaix, F., Rocancourt, D., Mansouri, A. & Buckingham, M. A Pax3/Pax7-dependent population of skeletal muscle progenitor cells. *Nature* **435,** 948–953 (2005).
12. Gros, J., Manceau, M., Thome, V. & Marcelle, C. A common somitic origin for embryonic muscle progenitors and satellite cells. *Nature* **435,** 954–958 (2005).
13. Kassar-Duchossoy, L. *et al.* Pax3/Pax7 mark a novel population of primitive myogenic cells during development. *Genes Dev.* **19,** 1426–1431 (2005).
14. Relaix, F. *et al.* Pax3 and Pax7 have distinct and overlapping functions in adult muscle progenitor cells. *J. Cell Biol.* **172,** 91–102 (2006).
15. Kuang, S., Charge, S. B., Seale, P., Huh, M. & Rudnicki, M. A. Distinct roles for Pax7 and Pax3 in adult regenerative myogenesis. *J. Cell Biol.* **172,** 103–113 (2006).
16. Bennicelli, J. L., Advani, S., Schafer, B. W. & Barr, F. G. PAX3 and PAX7 exhibit conserved cis-acting transcription repression domains and utilize a common gain of function mechanism in alveolar rhabdomyosarcoma. *Oncogene* **18,** 4348–4356. (1999).
17. Zammit, P. S. *et al.* Muscle satellite cells adopt divergent fates: a mechanism for self-renewal? *J. Cell Biol.* **166,** 347–357 (2004).
18. Berkes, C. A. & Tapscott, S. J. MyoD and the transcriptional control of myogenesis. *Semin. Cell Dev. Biol.* **16,** 585–595 (2005).
19. Ishibashi, J., Perry, R. L., Asakura, A. & Rudnicki, M. A. MyoD induces myogenic differentiation through cooperation of its NH2- and COOH-terminal regions. *J. Cell Biol.* **171,** 471–482 (2005).
20. Sabourin, L. A., Girgis-Gabardo, A., Seale, P., Asakura, A. & Rudnicki, M. A. Reduced differentiation potential of primary MyoD–/– myogenic cells derived from adult skeletal muscle. *J. Cell. Biol.* **144,** 631–643 (1999).
21. Dou, Y. *et al.* Regulation of MLL1 H3K4 methyltransferase activity by its core components. *Nature Struct. Mol. Biol.* **13,** 713–719 (2006).
22. Ruthenburg, A. J. *et al.* Histone H3 recognition and presentation by the WDR5 module of the MLL1 complex. *Nature Struct. Mol. Biol.* **13,** 704–712 (2006).
23. Couture, J. F., Collazo, E. & Trievel, R. C. Molecular recognition of histone H3 by the WD40 protein WDR5. *Nature Struct. Mol. Biol.* **13,** 698–703 (2006).
24. Han, Z. *et al.* Structural basis for the specific recognition of methylated histone H3 lysine 4 by the WD-40 protein WDR5. *Mol. Cell* **22,** 137–144 (2006).
25. Wysocka, J. *et al.* WDR5 associates with histone H3 methylated at K4 and is essential for H3 K4 methylation and vertebrate development. *Cell* **121,** 859–872 (2005).
26. Martin, C. & Zhang, Y. The diverse functions of histone lysine methylation. *Nature Rev. Mol. Cell Biol.* **6,** 838–849 (2005).
27. Bernstein, B. E. *et al.* Methylation of histone H3 Lys 4 in coding regions of active genes. *Proc. Natl Acad. Sci. USA* **99,** 8695–700 (2002).
28. Liang, G. *et al.* Distinct localization of histone H3 acetylation and H3-K4 methylation to the transcription start sites in the human genome. *Proc. Natl Acad. Sci. USA* **101,** 7357–7362 (2004).
29. Santos-Rosa, H. *et al.* Active genes are tri-methylated at K4 of histone H3. *Nature* **419,** 407–411 (2002).
30. Bernstein, B. E. *et al.* Genomic maps and comparative analysis of histone modifications in human and mouse. *Cell* **120,** 169–181 (2005).
31. Rea, S. *et al.* Regulation of chromatin structure by site-specific histone H3 methyltransferases. *Nature* **406,** 593–599 (2000).
32. Bajard, L. *et al.* A novel genetic hierarchy functions during hypaxial myogenesis: Pax3 directly activates Myf5 in muscle progenitor cells in the limb. *Genes Dev.* **20,** 2450–2464 (2006).
33. Buchberger, A., Freitag, D. & Arnold, H. H. A homeo-paired domain-binding motif directs Myf5 expression in progenitor cells of limb muscle. *Development* **134,** 1171–1180 (2007).
34. Shevchenko, A., Wilm, M., Vorm, O. & Mann, M. Mass spectrometric sequencing of proteins silver-stained polyacrylamide gels. *Anal. Chem.* **68**, 850–858 (1996).

a

Pax7 induced decreases in expression in C2C12 myoblasts

Symbol	GID	Fold	Name
Igfbp2	NM_008342	-6.4	insulin-like growth factor binding protein 2
Fbln2	NM_007992	-3.7	fibulin 2
Tnnt2	NM_011619	-3.3	[1]troponin T2, cardiac
Ctgf	NM_010217	-3.2	connective tissue growth factor
Timp3	NM_011595	-2.6	[2]tissue inhibitor of metalloproteinase 3
Serpine1	NM_008871	-2.6	serine (or cysteine) proteinase inhibitor, E1
Csrp2	NM_007792	-2.6	cysteine and glycine-rich protein 2
4732435N03Rik	AV371987	-2.5	RIKEN cDNA 4732435N03 gene
Lox	NM_010728	-2.5	[1]lysyl oxidase
Aqp1	NM_007472	-2.5	aquaporin 1
Serpinb9b	NM_011452	-2.4	serine (or cysteine) proteinase inhibitor, B9b
Thbs2	NM_011581	-2.4	thrombospondin 2
Col6a3	NM_009935	-2.4	procollagen, type VI, alpha 3
Tubb3	NM_023279	-2.3	tubulin, beta 3
Tspan9	NM_175414	-2.3	tetraspanin 9
Hbegf	NM_010415	-2.3	heparin-binding EGF-like growth factor
Hspb1	NM_013560	-2.2	[1]heat shock protein 1
Sgpp1	NM_030750	-2.2	sphingosine-1-phosphate phosphatase 1
Ankrd1	NM_013468	-2.1	ankyrin repeat domain 1 (cardiac muscle)
Ccl2	NM_011333	-2.1	chemokine (C-C motif) ligand 2
Fhl1	NM_010211	-2.1	four and a half LIM domains 1
Anxa3	NM_013470	-2.0	annexin A3
Akap12	NM_031185	-2.0	A kinase (PRKA) anchor protein (gravin) 12
Actb	NM_007393	-2.0	actin, beta, cytoplasmic
Cst6	NM_028623	-2.0	cystatin E/M
Tm4sf1	NM_008536	-2.0	transmembrane 4 superfamily member 1

[1] mean fold change for 2 distinct probesets in Table S1 directed at the same transcript
[2] mean fold change for 3 distinct probesets in Table S1 directed at the same transcript

b

Pax7 inhibits C2C12 differentiation

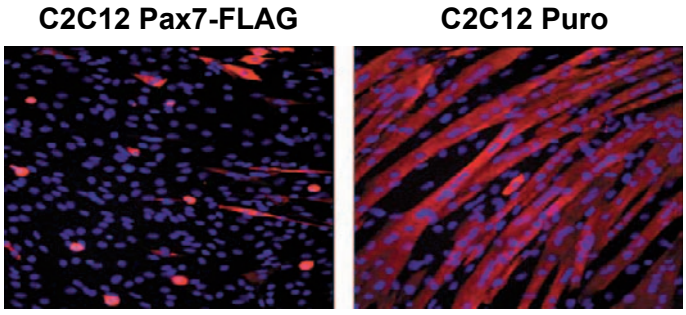

Figure S1 (**a**) Pax7 induced decreases in expression in C2C12 myoblasts. Only one gene was down-regulated by greater than 4-fold (*IGFBP2*, 6.5-fold) of the 26 genes that decreased. (**b**) Stable over-expression of Pax7 effectively inhibited myogenic differentiation compared to empty-vector control (puro) as assayed by expression of myosin heavy-chain and myoblast fusion. Myosin heavy chain-red, DAPI-blue.

Primer sequences used for RT and ChIP real-time PCR

RT Target	Product		Strand Sequence (5'→ 3')
β-actin - NM_007393	167 bp	F	accctgtgctgctcacc
		R	tccggagtccatcacaat
Cipar - NM_145562	141 bp	F	ttggtcagacccaggaaact
		R	caatgggactgttggtgaac
GAPDH - NM_008084	228 bp	F	tcggtgtgaacggatttg
		R	ggtctcgctcctggaaga
Integrin–α7 - NM_008398	67 bp	F	tatgcgctcagaagagctga
		R	tggcgttcaaagaagtaggg
LacZ	135 bp	F	aacgtgacctatcccattacg
		R	aacgccatcaaaaataattcg
Lix1 - NM_025681	288 bp	F	gcagcagaaagccaccttt
		R	gggtcatccgcatcatct
Mest - NM_008590	370 bp	F	gcaacctggtcatcgaca
		R	tgatggccaggacctctt
MNF - NM_199068	246 bp	F	gatctccggagcctcgtc
		R	gatcagctgcgcataggagt
Myf5 - NM_008656	85 bp	F	acagcagctttgacagcatc
		R	aagcaatccaagctggacac
MyoD- NM_010866	86 bp	F	cgctccaactgctctgatg
		R	tagtaggcggtgtcgtagcc
Pax7 - NM_011039	328 bp	F	gctaccagtacagccagtatg
		R	gtcactaagcatgggtagatg
PlagL1 - NM_009538	98 bp	F	ccactaccacagccacagat
		R	tgctgctgaggttgcagt
Syne2 - BF582734	269 bp	F	acccgggtcagctctttt
		R	gccaacagctcaaccaga
Trim54 - NM_021447	342 bp	F	agcggaacctgctagtgg
		R	tctgtctgcggctgttgt
ChIP Target	**Location**		**Strand Sequence (5'→ 3')**
Myf5	-57.5 kb	F	tgtggctctctctccgtatg
		R	aatacagacatgcaggcttcac
	-315 bp	F	aatgtcttgctaccgtgctg
		R	ctggtccctttgacgctaat
	+1.4 kb	F	gagttaggggctggtatga
		R	tcaaagctgctgttctttcg
	+1.5 kb	F	acagcagctttgacagcatc
		R	ggacagactgccatgactga
	+1.6 kb	F	atggcagtctgtccttcaaa
		R	gcgtgtatgctggtctgtct

Figure S2 (**a**) Primer sequences used for RT- and ChIP real-time PCR.

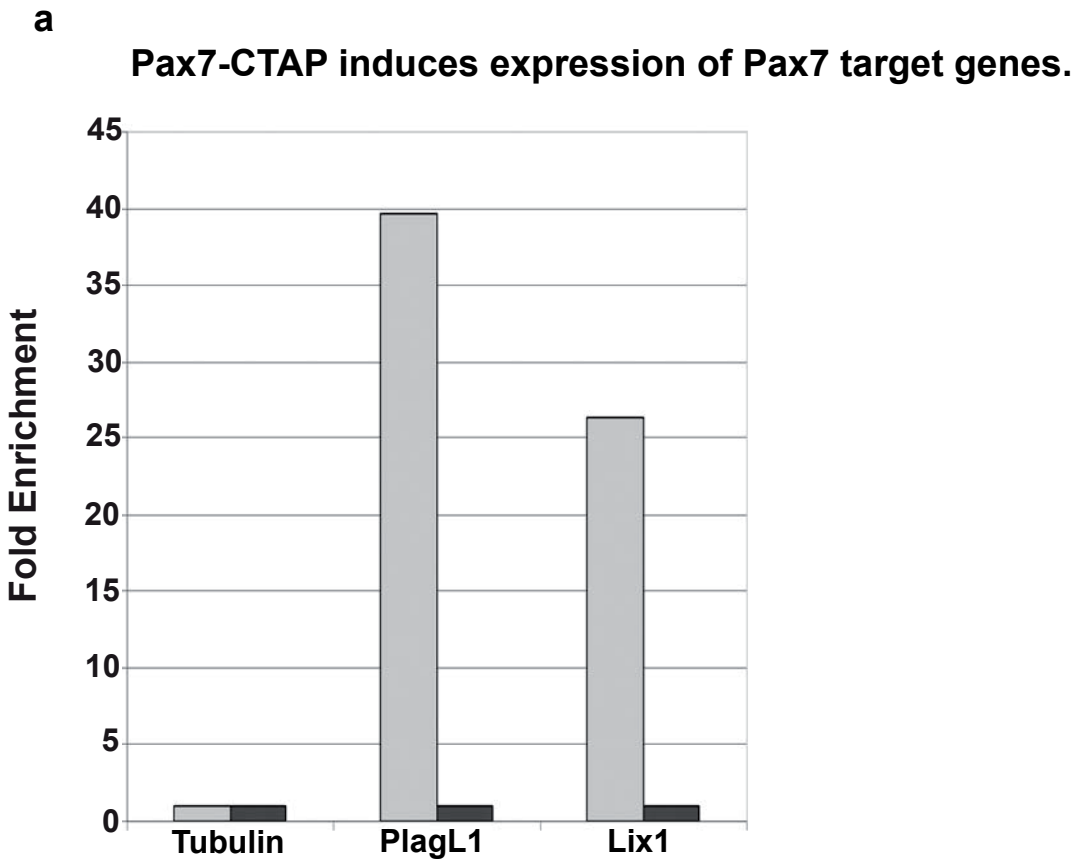

Figure S3 (**a**) Activation of Pax7 target gene expression by the Pax7-CTAP construct. The addition of the 50aa tag to Pax7 did not compromise its ability to induce target gene expression by real-time PCR analysis as compared to HisFLAG controls. Expression of PlagL1 and Lix1 (normalized to level of tubulin expression) are shown as examples.

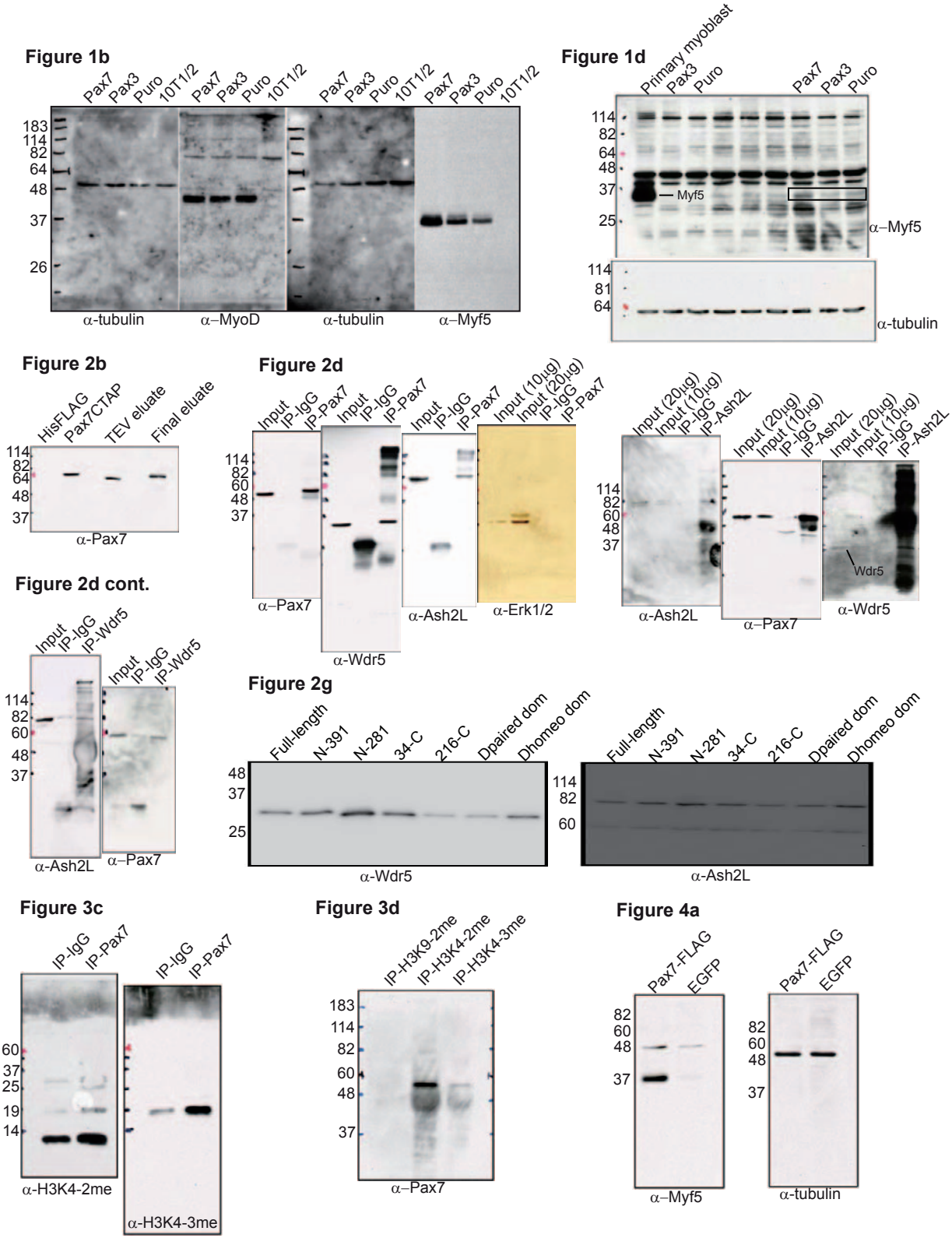

Figure S4 Full scans of key Western blot data presented in Figures 1-4.

Supplementary Information S5: Materials and methods.

Western Blots: Total protein was harvested in RIPA lysis buffer, subjected to SDS-PAGE, and electroblotted onto Immobilon-P membrane (Millipore). Membranes were probed with primary antibody and HRP-conjugated secondary antibody in blocking solution. Target proteins were visualized by ECL (Amersham-Pharmacia) with Biomax XAR film (Kodak). Primary antibodies used were: anti-FLAG (M2; Sigma); anti-Myf5 (C-20; Santa Cruz); anti-MyoD (C-20; Santa-Cruz); anti-Pax7 (hybridoma supernatant; DSHB); anti-α-tubulin (Sigma). Secondary antibodies were HRP-conjugated anti-mouse and anti-rabbit (Biorad).

Pax7 Domain-Deletion Construction: All constructs were made by PCR amplification of the desired regions. 5' primers contained a BamHI site followed by GCC ACC ATG. 3' primers contained a XhoI site. The stop codon in the full length construct was deleted allowing read through to the FLAG tag. In constructs containing internally deleted regions, internal primers contained EcoRI sites which were used to fuse two PCR products. All PCR products were inserted into pBrit-LoxP-HA-FLAG cut with BamHI and XhoI resulting in the exclusion of the HA tag. Constructs were verified by sequencing.

Histone Pull-down Assay: Whole cell extract was obtained from mouse primary myoblasts as described above and histones were immunoprecipitated with antibodies raised against H3K4^{2me}, H3K4^{3me} and H3K9^{2me} (Upstate). Immuno-complexes were washed, treated to SDS-PAGE, and Western blotted with α-Pax7 antibody (DSHB).

Fluorescent Activated Cell Sorting (FACS) of Satellite Cells:

Satellite cells were sorted from 4 week old Pax7-heterozygous (+/-) and knock-out (-/-) pups, as previously described[1]. RNA was extracted via MicroRNA kit (Qiagen) following manufacturers protocols, and subjected to RT and Real-time PCR as described above. An Independent samples two-tailed t-test was used to statistically analyze the difference in gene expression.

siRNA Transfection: Annealed siRNA duplexes specific to Pax7 (#156692 (Ambion) 5' GGUAACAUCCCAGCUUUACtt (s)), or a scrambled control (AAGTAAGCTGATGAAAGACTG) were transfected into primary myoblasts at a concentration of 40nM using Lipofectamine 2000 (Invitrogen) according to manufacturers protocols.

Immunocytochemistry: Cells were fixed and stained and images captured as previously described[15] using α-Myf5 (C-20; Santa Cruz), α-Sydecan4 (a gift from Brad Olwin) and α-FLAG (M2-Sigma) antibodies.